



Grand Canyon National Park

Geologic Resources Inventory Report

Natural Resource Report NPS/NRSS/GRD/NRR—2020/2195





The production of this document cost \$25,046, including costs associated with data collection, processing, analysis, and subsequent authoring, editing, and publication.

ON THE COVER

Muted sunrise from Cape Royal, North Rim, Grand Canyon National Park
National Park Service photograph by Michael Quinn (https://www.flickr.com/photos/grand_canyon_nps/9346181170/in/album-72157625927050687/, accessed 05 October 2017).

THIS PAGE

Rafters running Lava Falls Rapid in Grand Canyon National Park. National Park Service photograph by Mark Lellouch (https://www.flickr.com/photos/grand_canyon_nps/8451166801/in/album-72157626635172217/, accessed 05 October 2017).

Grand Canyon National Park

Geologic Resources Inventory Report

Natural Resource Report NPS/NRSS/GRD/NRR—2020/2195

John P. Graham

Colorado State University Research Associate
National Park Service Geologic Resources Inventory
Geologic Resources Division
PO Box 25287
Denver, CO 80225

November 2020

U.S. Department of the Interior
National Park Service
Natural Resource Stewardship and Science
Fort Collins, Colorado

The National Park Service, Natural Resource Stewardship and Science office in Fort Collins, Colorado, publishes a range of reports that address natural resource topics. These reports are of interest and applicability to a broad audience in the National Park Service and others in natural resource management, including scientists, conservation and environmental constituencies, and the public.

The Natural Resource Report Series is used to disseminate comprehensive information and analysis about natural resources and related topics concerning lands managed by the National Park Service. The series supports the advancement of science, informed decision-making, and the achievement of the National Park Service mission. The series also provides a forum for presenting more lengthy results that may not be accepted by publications with page limitations.

All manuscripts in the series receive the appropriate level of peer review to ensure that the information is scientifically credible, technically accurate, appropriately written for the intended audience, and designed and published in a professional manner. This report received informal peer review by subject-matter experts who were not directly involved in the collection, analysis, or reporting of the data.

Views, statements, findings, conclusions, recommendations, and data in this report do not necessarily reflect views and policies of the National Park Service, U.S. Department of the Interior. Mention of trade names or commercial products does not constitute endorsement or recommendation for use by the U.S. Government.

This report is available from the [Geologic Resources Inventory publications site](#) and the [Natural Resource Report publication series site](#). If you have difficulty accessing information in this publication, particularly if using assistive technology, please email irma@nps.gov.

Please cite this publication as:

Graham, J. P. 2020. Grand Canyon National Park: Geologic resources inventory report. Natural Resource Report NPS/NRSS/GRD/NRR—2020/2195. National Park Service, Fort Collins, Colorado. <https://doi.org/10.36967/nrr-2279886>

Contents

Executive Summary	ix
Products and Acknowledgments	xiii
GRI Products	xiii
Acknowledgments	xiii
Geologic Heritage, Setting, and Significance	1
Geologic Heritage	1
Park Significance and Fundamental Geologic Resources	1
Geologic Setting.....	3
Exploration and Geologic Study of the Grand Canyon	15
Geologic Features and Processes	19
Landscape	19
Sedimentary Rock and Features.....	25
Igneous Rock and Features.....	37
Granite Gorge Metamorphic Rock and Features	50
Paleontological Resources	54
Caves, Karst, and Springs.....	62
Unusual Minerals	68
Breccia Pipes and Ore Deposits	72
Unconformities.....	72
Folds and Faults.....	77
Features in Side Canyons.....	82
Desert Varnish	82
Geomorphic Features and Unconsolidated Deposits.....	84
Geologic Type Sections	91
Geologic Resource Management Issues	93
Geologic Resource Management Assistance	93
Climate Change and Water Supply	94
Flash Floods and Debris Flows.....	97
Restoring and Monitoring Colorado River Sediment Load	100
Slope Movement Hazards.....	102
Cave and Karst Inventory, Monitoring, and Protection	106
Trans-Canyon Pipeline Replacement.....	111
Paleontological Resource Inventory, Monitoring, and Protection.....	111
Earthquakes.....	112
Abandoned Mineral Lands	114
Uranium Mining.....	117
Hydrocarbon Exploration	122
Lake Mead Delta.....	122
Geologic History	123
Paleoproterozoic Era (2.5 billion–1.6 billion years ago): Magma, Metamorphism, and Deformation.....	123
Mesoproterozoic Era (1.6 billion–1.0 billion years ago): Coastal Environments Dominate North America’s Southern Margin	124
Neoproterozoic Era (1.0 billion–541 million years ago): Extensional Tectonics, Glaciation, and Climate Change	126
Paleozoic Era (541 million–252 million years ago): Tectonics, Transgressions, and Assembling Pangea.....	128
Mesozoic Era (252 million–66 million years ago): Disassembling Pangea, Ergs, and an Inland Sea	133
Cenozoic Era (66 million years–present day): Crustal Extension and Carving the Grand Canyon	136
Geologic Map Data	143
Geologic Maps.....	143
Source Maps	143
GRI GIS Data	144
GRI Map Posters	144
Use Constraints.....	144
Literature Cited	145

Additional References 167
 Geology of National Park Service Areas 167
 NPS Resource Management Guidance and Documents..... 167
 Climate Change Resources 167
 Geological Surveys and Societies 167
 US Geological Survey Reference Tools 167
Appendix A: Scoping Participants 169
Appendix B: Geologic Resource Laws, Regulations, and Policies..... 171

Figures

Figure 1. Photograph of Zoroaster and Brahma temples.....	xiv
Figure 2. Map of Grand Canyon National Park.....	2
Figure 3. Physiographic provinces of the western United States.....	4
Figure 4. Generalized map of the area surrounding the Grand Canyon and west-to-east cross section of the area north of the Grand Canyon.	5
Figure 5. Geologic time scale.	6
Figure 6. Cross section diagram of the Grand Staircase sedimentary sequence.	14
Figure 7. Schematic illustrations of fault types.	16
Figure 8. Annotated photograph of the Grandview–Phantom monocline.....	16
Figure 9. Stages in the formation of a monocline in the Grand Canyon region.	18
Figure 10. Photograph from the South Rim of the historic Yavapai Observation Station.....	20
Figure 11. Photograph of the Redwall Limestone and Temple Butte Formation.....	20
Figure 12. Photographs of Vulcan's Throne.....	21
Figure 13. Photograph of the Grand Canyon from Toroweap Overlook.	21
Figure 14. Photograph of Bright Angel Canyon and Bright Angel Trail.	22
Figure 15. Photograph of cross-bedding in the Coconino Sandstone.....	23
Figure 16. Photographs of fossilized vertebrate tracks in the Coconino Sandstone.....	23
Figure 17. Photograph of Zoroaster Granite.....	24
Figure 18. Photograph of the Vishnu Schist.....	24
Figure 19. Photograph of Crystal Rapid.	25
Figure 20. Photographs of some sedimentary rock types found within Grand Canyon National Park.....	27
Figure 21. Photograph of cliffs composed of Tapeats Sandstone.....	28
Figure 22. Photograph of mudcracks in the Hakatai Sandstone.....	31
Figure 23. Photographs of Hermit Formation fossils.....	32
Figure 24. Photograph of ripple marks in the Hakatai Shale (Yh).	32
Figure 25. Photographs of modern and ancient oolites.....	33
Figure 26. Photograph of stromatolites in the Mesoproterozoic Bass Formation (Yb).....	34
Figure 27. Photograph of fossil worm trails in the Bright Angel Shale, Tonto Plateau.....	34
Figure 28. Photographs of invertebrate fossils in Paleozoic limestones, Grand Canyon National Park.....	35
Figure 29. Photographs of sedimentary features that signal a change in sea level.....	36
Figure 30. Photograph of a dike intruded into the layered sedimentary rock of the Hakatai Shale (Yh) at Hance Creek.....	37
Figure 31. Photographs of igneous rock compositional endmembers, granite and basalt, in Grand Canyon National Park.....	39
Figure 32. Simplified geologic map showing the distribution of Tertiary and Quaternary basaltic volcanism.....	42
Figure 33. Location and age of lava dams in Grand Canyon.....	44
Figure 34. Annotated photograph of Vulcan's Anvil, the 177-mile remnant, and the High Remnant.....	46
Figure 35. Annotated photograph of the Buried Canyon flow sequence.....	47
Figure 36. Annotated photograph showing the stratigraphic relationships between the Whitmore and Upper Black Ledge lava flows.....	47
Figure 37. Photographs of cooling structures within a lava dam.....	48
Figure 38. Conceptual model of lava dam failure.....	49
Figure 39. Historic photograph of Vulcan's Forge at RM 178.....	50
Figure 40. Photograph of metasedimentary rocks of the Vishnu Schist in Grand Canyon National Park.....	51
Figure 41. Plate tectonic model for the addition of crust to the southern margin of Laurentia.....	53
Figure 42. Photograph of 20,000-year-old giant ground sloth dung in a cave in Grand Canyon National Park.....	60
Figure 43. Photograph of a Harrington's Mountain Goat cranium with horns and sheaths and teeth discovered in the caves in Grand Canyon National Park.....	61
Figure 44. Photograph of an entrance to a cave in the Redwall Limestone, Grand Canyon National Park.....	62
Figure 45. Map showing the cave density in the greater Grand Canyon landscape assessment area.....	64
Figure 46. Hydro-stratigraphic schematic profile of the aquifer system in Grand Canyon National Park.....	64
Figure 47. Locations of four dye injection sites, flow paths, and the 29 receptor sites on the Kaibab Plateau.....	66
Figure 48. Photograph of speleothems of gypsum.....	68
Figure 49. Photograph of talmessite from the Gold Hill Mine, western Utah.....	70
Figure 50. Photograph of grandviewite from Grandview Mine, Grand Canyon National Park.....	70

Figure 51. Photograph of minerals from the Grandview Mine.....	72
Figure 52. Breccia pipes in Grand Canyon National Park.	73
Figure 53. Illustration showing the three types of unconformities.	74
Figure 54. Annotated photograph showing an angular unconformity.	75
Figure 55. Annotated photograph of the view from Lipan Point, Desert View Drive, East Rim, Grand Canyon National Park.	76
Figure 56. Annotated photograph of Precambrian and Paleozoic faults.	77
Figure 57. Segment of a west–east geologic cross-section showing normal faulting on the Hurricane Fault.	81
Figure 58. Simplified drainage network map of eastern Grand Canyon.....	83
Figure 59. Photograph shot in October 2012 of a dory maneuvering in Hance Rapid.	85
Figure 60. Photograph of Phantom Ranch boat beach.	85
Figure 61. Photograph of the alluvial fan at the mouth of Clear Creek, RM 87.....	86
Figure 62. Schematic diagram of the pool-debris fan-rapid-eddy complex on the Colorado River in Grand Canyon.	88
Figure 63. Photograph of a rockslide as seen from Hopi Point.....	89
Figure 64. Photograph of the waterfall emerging from Deer Spring.	90
Figure 65. Effects of global climate change on the southwestern United States.....	95
Figure 66. Photograph of Grand Canyon’s trail crew rebuilding a wall.	97
Figure 67. Photographs of Indian Gardens mule corral following the 2004 flash flood on Bright Angel Trail.....	98
Figure 68. Aerial photograph of the 1995 debris fan at Lava Falls Rapid.....	98
Figure 69. Photograph of a sandbar on the Colorado River deposited by the 2008 controlled flood.....	101
Figure 70. Photograph of the rockslide that closed Tanner Trail in October 2004.	102
Figure 71. Photograph of potential rockfall hazards in the Box, North Kaibab Trail.....	103
Figure 72. Rockfall data collected along the North Kaibab Trail within Grand Canyon National Park.	104
Figure 73. Photograph of a small rockfall that caused a serious injury in 2012.	105
Figure 74. Chart illustrating the potential seasonal influence on mass movement events in the park.	106
Figure 75. Photograph of delicate speleothems.	107
Figure 76. Photograph of fossils in a cave.....	107
Figure 77. Generalized hydrogeologic cross-section of the Coconino Plateau.....	109
Figure 78. Photograph of water gushing from a break in the Trans-Canyon Pipeline.	111
Figure 79. Photographs of vandalism of paleontological resources in Grand Canyon National Park.....	113
Figure 80. Photograph of the installation of Grandview Mine bat gates in 2009.....	117
Figure 81. Map showing land ownership in northwestern Arizona and the three Segregation Areas withdrawn from mining in 2012.	118
Figure 82. NASA photograph of the delta being formed where the Colorado River enters Lake Mead.....	122
Figure 83. Proterozoic Eon paleogeographic maps of southwestern North America.	124
Figure 84. Paleozoic Era paleogeographic maps of North America.	129
Figure 85. Paleogeographic map of Pangea.	134
Figure 86. Mesozoic Era paleogeographic maps of North America.....	135
Figure 87. Schematic contrasting the subduction angles of the Sevier Orogeny and Laramide Orogeny.	136
Figure 88. Cenozoic Era paleogeographic and present-day maps of North America.....	138

Tables

Table 1. Stratigraphic column of Cenozoic Era units mapped within Grand Canyon National Park.....	7
Table 2. Stratigraphic column of Mesozoic Era units mapped within Grand Canyon National Park.	8
Table 3. Stratigraphic column of Paleozoic Era units mapped within Grand Canyon National Park.	9
Table 4. Stratigraphic column of Proterozoic Eon units mapped within Grand Canyon National Park.....	11
Table 5. Sedimentary rock classification and characteristics.	26
Table 6. Sedimentary rock features identified in Grand Canyon National Park.	28
Table 7. Igneous rock classification for igneous rocks exposed in Grand Canyon National Park.	38
Table 8. Precambrian plutons and dike swarms of the Zoroaster Plutonic Complex in Granite Gorge.	40
Table 9. Lava dams in western Grand Canyon National Park.....	44
Table 10. General classification of regional metamorphic rocks.....	51
Table 11. Tectonic blocks and shear zones in Granite Gorge.	52
Table 12. Precambrian, Paleozoic, and Mesozoic fossils found in Grand Canyon National Park.....	55
Table 13. Cenozoic fossils found in caves in Grand Canyon National Park.	57
Table 14. Rock type, unit, location, and physical properties of unusual minerals found in the park.	69
Table 15. Documented minerals and associated commodities from abandoned mines in the Grand Canyon National Park area.....	71
Table 16. Fault offsets on major normal faults in Precambrian and Paleozoic units, Grand Canyon.....	78
Table 17. Side canyons and morphological divisions in Grand Canyon National Park.	83
Table 18. Designated type sections in Grand Canyon National Park.	91
Table 19. Abandoned mines in Grand Canyon National Park.	115
Table 20. Examples of uranium concentrations in the Grand Canyon area.	120
Table 21. Incision rates of the Colorado River over the last 1 million years.....	139
2001 Scoping Meeting Participants	169
2015 Conference Call Participants	169

Executive Summary

The Geologic Resources Inventory (GRI) provides geologic map data and pertinent geologic information to support resource management and science-informed decision making in more than 270 natural resource parks throughout the National Park System. The GRI is one of 12 inventories funded by the National Park Service (NPS) Inventory and Monitoring Program. The Geologic Resources Division of the NPS Natural Resource Stewardship and Science Directorate administers the GRI.

This report synthesizes discussions from a scoping meeting held in 2001 and a follow-up conference call in 2015 (see Appendix A). Chapters of this report discuss the geologic setting, distinctive geologic features and processes within Grand Canyon National Park, highlight geologic issues facing resource managers, describe the geologic history leading to the present-day landscape, and provide information about the previously completed GRI map data. Posters illustrate these data.

Each year, over 4.5 million visitors experience the iconic landscape of Grand Canyon National Park either from the canyon rim, the park trails, or from the river. The serenity found in slot canyons or in the 4,931 km² (1,904 mi²) portion of the park managed as wilderness contrasts dramatically with the dynamic rapids that, for many visitors, define the Colorado River and Grand Canyon. Established in 1919, Grand Canyon National Park is not only a keystone in the national park system but also a World Heritage Site and one of the seven natural wonders of the world.

To form Grand Canyon, the Colorado River incised sedimentary rock strata and bedrock of the southwestern Colorado Plateau, a physiographic province that includes a vast tableland of plateaus, basins, and steep-walled canyons carved by the Colorado River and its tributaries. Flowing 1.6 km (1 mi) below the canyon rim, the Colorado River meanders past sheer cliffs and step-like ledges and slopes that represent nearly 2 billion years of Earth history. The western portion of Grand Canyon National Park lies in the transition zone between the Colorado Plateau and the Basin and Range Province to the west. The many geologic features associated with the two physiographic provinces and the processes responsible for them, along with paleontological and cave resources, are fundamental geologic resources in the park.

In addition, Grand Canyon National Park preserves evidence of at least 12,000 years of human occupation. As part of America's geologic heritage, the Grand Canyon remains entwined with, and inseparable from, our country's history and culture. Geologic features enrich aesthetic, artistic, cultural, ecological, economic, educational, recreational, and scientific values.

The geologic features in the park document an exceptional diversity of depositional environments, tectonic deformation, ancient animal and plant life,

rise and fall of sea levels, the complex interaction of groundwater and rock, and the transformative power of the Colorado River. The geologic features and processes described in this report include:

- **Landscape.** Grand Canyon National Park offers an exceptional landscape of iconic geologic features that include mesas, buttes, spires, slot canyons, volcanic cones, rock strata, and geomorphic features associated with the Colorado River corridor. These landscape features may be viewed from three general perspectives: from the rim, along the trails, and from the Colorado River.
- **Sedimentary Rock and Features.** Preservation of sedimentary features such as ripple marks, cross-bedding, and rain drop impressions, combined with sedimentary rock type, characterize six general depositional environments recognized in the Grand Canyon region: 1) eolian, 2) mass wasting, 3) fluvial-floodplain, 4) intertidal-to-marginal marine, 5) subtidal-to-nearshore, and 6) marine.
- **Igneous Rock and Features.** The Grand Canyon documents many episodes of igneous intrusions and volcanic eruptions. Precambrian igneous intrusions, known collectively as the Zoroaster Plutonic Complex, form the nearly 2-billion-year-old "basement" upon which the other geologic units were deposited. Volcanic eruptions spread magma onto the neighboring plateaus as well as cascading over the cliff edge to form lava falls and temporary lava dams.
- **Granite Gorge Metamorphic Rock and Features.** Metamorphic rocks in Granite Gorge document tectonic events that sutured microplates to the southern margin of the pre-North American continent from approximately 1.8 billion years ago to 1.6 billion years ago. Metamorphic minerals provide

estimates of pressures and temperatures associated with crustal conditions during metamorphism.

- **Paleontological Resources.** The sedimentary rocks and caves in Grand Canyon contain a variety of fossil remains (e.g., shells, bone, leaves, trackways, and dung) that help determine the relative ages of rock units, the evolution of various taxa, and the depositional environments in which these ancient organisms lived or were entombed.
- **Caves, Karst, and Springs.** Grand Canyon National Park contains more karst area than any other NPS unit except Everglades National Park. Speleothems (cave features), some of which are quite delicate and fragile, document the complex cave formation process in Grand Canyon. Mineral deposits, significant archeological remains, and important biological systems, including bat habitat, connect these caves to past and present human and animal occupation and to the region's intricate hydrologic system. Thousands of caves in the Mississippian Redwall Limestone help document the evolution of Paleozoic and Cenozoic karst landscape in the Grand Canyon region.
- **Unusual Minerals.** An eclectic variety of rare and unusual minerals are found in the park, especially in the Redwall Limestone caves. Many of these minerals are connected to the canyon's groundwater system, and many are associated with the breccia pipes and ore bodies found in Grand Canyon.
- **Breccia Pipes and Ore Deposits.** The vertical columns of brecciated rock known as breccia pipes served as conduits for groundwater containing high-grade uranium ore, sulphides of copper, lead, zinc, and silver, and a variety of other metals. Breccia pipes sparked the mining activity in Grand Canyon in the late 19th century.
- **Unconformities.** Unconformities represent strata that are missing from the geologic record. These gaps represent episodes of erosion or non-deposition, and in Grand Canyon, they document tectonic episodes, sea level fluctuations, and the accretion of land masses that formed the pre-North American continent. The Great Unconformity, first recognized by John Wesley Powell, is an especially significant unconformity documenting Precambrian episodes of metamorphism, tectonic compression and mountain-building, deformation, uplift, erosion, and deposition.
- **Folds and Faults.** Folds and faults have deformed the igneous, metamorphic, and sedimentary rocks in the Grand Canyon. Tectonic compression resulted in reverse faults, which are responsible for most of the monoclines on the Colorado Plateau, while extension pulled apart the crust, generating normal

faulting. Many of the ancient Precambrian faults have been reactivated throughout geologic time. Movement occurred on the north-south trending Toroweap and Hurricane faults from about 2 million to 3 million years ago, and these faults remain active. Fault movement has influenced the incision rate of the Colorado River.

- **Features in Side Canyons.** Folds, faults, and regional stratigraphic dip influenced the location and morphology of narrow side canyons, which expose details of both deformation and depositional events.
- **Desert Varnish.** Common to arid regions, the red-to-black surface coating on the Coconino Sandstone results from iron and manganese solutions interacting with microorganisms.
- **Geomorphic Features and Unconsolidated Deposits.** Pools, rapids, debris flows and fans, river terraces, sand dunes and sand sheet deposits, slope movements (landslides), travertine deposits, and waterfalls represent recent processes that have acted throughout geologic time.
- **Geologic Type Sections.** Grand Canyon National Park preserves an extraordinary amount of type localities, significant areas where rock strata were originally described. Preservation of these type sections protects an exceptional geologic heritage.

The geologic landscape of Grand Canyon National Park also includes geologic management issues. Geologic resource management issues identified during the GRI scoping meeting, the follow-up conference call, and geologic literature include:

- **Climate Change and Water Supply.** Global climate change may be the most comprehensive issue facing the park resource managers. Alterations such as increased temperature and drought coupled with decreased precipitation may trigger a cascading effect that negatively impacts water resources and the ecosystems these resources support.
- **Flash Floods and Debris Flows.** Flash floods may damage infrastructure and threaten visitor safety, but they also contribute needed sediment to the Colorado River corridor. Earlier rain-on-snow events, predicted by climate change models, may increase the frequency of debris flows.
- **Restoring and Monitoring Colorado River Sediment Load.** Glen Canyon Dam dramatically altered the sediment load entering Grand Canyon. Controlled floods attempt to redistribute sediment through the canyon to maintain beaches, riparian habitat, and dune fields. Current monitoring of sediment input helps to assess different components of the Colorado River ecosystem, such as fish habitat, sand bars, and canyon constriction.

- Slope Movement Hazards. Like flash floods, slope movements (e.g., landslides) also have the potential to damage infrastructure and threaten visitor safety. Cliffs undercut by erosion may collapse and generate landslides. Using GPS and photodocumentation combined with rock type and surface faults may allow resource managers to monitor potential mass movement locations.
- Cave and Karst Inventory, Monitoring, and Protection. Addressing human impacts to the caves, preserving archeological artifacts and fossils found in the caves, and understanding cave hydrology are priorities for park management. Except for Cave of the Domes, the caves in Grand Canyon National Park are closed to visitors without permits. However, vandalism still occurs. Ongoing research documents the association of the sinkholes in the karst landscape of the Kaibab Plateau with springs, caves, and groundwater flow and recharge to the Redwall-Muav aquifer and Roaring Springs, the sole water source for visitors and permanent residents. Working with the GRD, the park is in the process of developing a cave and karst management program, which is a monumental task for a park containing thousands of caves and sinkholes.
- Trans-Canyon Pipeline Replacement. Installed between 1965 and 1970, the Trans-Canyon Pipeline (TCP) delivers water from Roaring Springs to both the north and south rims. Debris flows, flash floods, slope movements, or other geologic processes rupture the pipeline, requiring repairs from a few to a few dozen times per year. Replacement costs exceed the park's total yearly budget. A long-term solution to replace the pipeline is needed.
- Paleontological Resource Inventory, Monitoring, and Protection. The park's exceptionally diverse fossil record is recognized as a fundamental resource. The 2009 Paleontological Resources Preservation Act subjects all paleontological resources to science-informed inventory, monitoring, protection, and interpretation. Since 2001, the park has been developing and implementing a paleontological inventory and monitoring program. In 2019, the NPS Geologic Resources Division (GRD) coordinated a multidisciplinary paleontological resource inventory for Grand Canyon National Park.
- Earthquakes. Although large magnitude earthquakes rarely affect northwestern Arizona, the Grand Canyon region remains seismically active. Swarms of small magnitude earthquakes appear to be more common than previously thought. In general, the earthquakes occur on north-south trending normal faults associated with the boundary between the Colorado Plateau and the Basin and Range province.
- Abandoned Mineral Lands (AML). Grand Canyon National Park contains dozens of AML sites that are remnants of past mining activity. AML sites pose a variety of resource management issues such as visitor and staff safety and environmental quality of air, water, and soil. These sites require an accurate inventory for efficient resource management. The abandoned mining sites have been evaluated with regards to mitigation needs. Some sites contain important mineral resources, while others include uranium contamination.
- Uranium Mining. Although mining is not allowed in the park, past uranium mining has raised concerns regarding the degradation of the park's water resources and employee/visitor safety. Since 2012, the US Geological Survey (USGS) has been conducting scientific investigations to better understand the potential contamination from uranium-mining.
- Hydrocarbon Exploration. The Walcott (**Zkw**) and Awatubi (**Zka**) Members of the Kwagunt Formation contain hydrocarbons, and in 1906, the first oil well was drilled in the region. That well, like all the others that have been drilled in the region, did not encounter economic quantities of oil or gas.
- Lake Mead Delta. Drought has decreased the lake levels in Lake Mead, expanding the delta forming where the Colorado River enters the lake. Delta growth may alter riparian environments and may influence archaeological sites. However, the severity of this issue is unknown.

This GRI report was written for resource managers to support science-informed planning, programming, and decision making. The report may also be useful for interpretation. The report was prepared using available geologic information, and the NPS Geologic Resources Division conducted no new fieldwork in association with its preparation. The report is supported by GRI GIS data compiled from eight geologic maps published by the US Geological Survey. Those maps represent many decades of research and field work within and surrounding Grand Canyon National Park.

Products and Acknowledgments

The NPS Geologic Resources Division partners with the Colorado State University Department of Geosciences to produce GRI products. The US Geological Survey developed the source maps and, along with NPS staff, reviewed GRI content. This chapter describes GRI products and acknowledges contributors to this report.

GRI Products

The GRI team undertakes three tasks for each park in the Inventory and Monitoring program: (1) conduct a scoping meeting and provide a summary document, (2) provide digital geologic map data in a geographic information system (GIS) format, and (3) provide a GRI report (this document). These products are designed and written for nongeoscientists.

Scoping meetings bring together park staff and geologic experts to review and assess available geologic maps, develop a geologic mapping plan, and discuss geologic features (fig. 1), processes, and resource management issues that should be addressed in the GRI report. Following the scoping meeting, the GRI map team converts the geologic maps identified in the mapping plan to GIS data in accordance with the GRI data model. After the map is completed, the GRI report team uses these data, as well as the scoping summary and additional research, to prepare the GRI report. The GRI team conducts no new field work in association with their products.

The compilation and use of natural resource information by park managers is called for in the 1998 National Parks Omnibus Management Act (§ 204), 2006 National Park Service Management Policies, and the Natural Resources Inventory and Monitoring Guideline (NPS-75). The “Additional References” chapter and Appendix B provide links to these and other resource management documents and information.

Additional information regarding the GRI, including contact information, is available at <http://go.nps.gov/gri>.

Acknowledgments

Additional thanks to: Vincent Santucci (NPS) for providing fossil photos; Vincent Santucci, Justin Tweet, and Ben Tobin for their insightful comments and references to current literature; George Billingsley for his years of mapping the Grand Canyon and for his help with understanding the stratigraphy during the scoping session; and Trista Thornberry-Ehrlich (Colorado State University) for producing some of the graphics in this report.

Review

Jason Kenworthy (NPS Geologic Resources Division)
Vincent Santucci (NPS Geologic Resources Division)
Justin Tweet (NPS Geologic Resources Division)
George Billingsley (USGS, retired)
Ben Tobin (NPS Grand Canyon National Park)
Mark Nebel (NPS Grand Canyon National Park)

Editing

Michael Barthelmes (Colorado State University)

Report Formatting and Distribution

Rebecca Port (NPS Geologic Resources Division)

Source Maps

Billingsley (2000) (USGS)
Billingsley and Priest (2013) (USGS)
Billingsley and Wellmeyer (2004) (USGS)
Billingsley et al. (2006a, b; 2007; 2008; 2012) (USGS)

GRI GIS Data Production

Derek Witt (Colorado State University)
Jim Chappell (Colorado State University)
James Winter (Colorado State University)
Stephanie O’Meara (Colorado State University)

GRI Map Poster Design

Chase Winters (Colorado State University)
Dalton Meyer (Colorado State University)
Jake Suri (Colorado State University)

GRI Map Poster Review

Georgia Hybels (Colorado State University)
Rebecca Port (NPS Geologic Resources Division)
Michael Barthelmes (Colorado State University)
Chelsea Bitting (NPS Geologic Resources Division)
Jason Kenworthy (NPS Geologic Resources Division)



Figure 1. Photograph of Zoroaster and Brahma temples.
Zoroaster and Brahma temples as seen from Mormon Flats on the South Kaibab Trail, Grand Canyon National Park. NPS photograph by Michael Quinn, available online at the park's Flickr site (https://www.flickr.com/photos/grand_canyon_nps/collections/).

Geologic Heritage, Setting, and Significance

This chapter describes the regional geologic setting of Grand Canyon National Park and summarizes connections among geologic resources, other park resources, and park stories.

Geologic Heritage

In his 1903 speech at the South Rim of the Grand Canyon, Theodore Roosevelt asserted,

In the Grand Canyon, Arizona has a natural wonder which, so far as I know, is in kind absolutely unparalleled throughout the rest of the world. I want to ask you to do one thing. . .keep this great wonder of nature as it now is. . .Leave it as it is. You cannot improve on it. The ages have been at work on it, and man can only mar it. (Roosevelt 1905, p. 369-370)

Revered as one of Earth's seven natural wonders of the world, the Grand Canyon contains an exceptional diversity of natural resources, and the park is recognized as an extraordinary geological heritage (geoheritage) site. America's geoheritage encompasses the geologic features, landforms, and landscapes that played, and continue to play, an integral part in shaping our country's history and culture. As in so many of our national parks, the geologic features in Grand Canyon National Park inspire a sense of awe and wonder (fig. 1), and the preservation of these features enriches a full range of values including aesthetic, artistic, cultural, ecological, economic, educational, recreational, and scientific. The importance and significance of preserving geoheritage sites may be explored on the National Park Service's (NPS) America's Geoheritage website (<https://www.nps.gov/subjects/geology/americas-geoheritage.htm>) and in America's Geologic Heritage: An Invitation to Leadership (National Park Service and American Geosciences Institute 2015).

The American landscape of mountains, plateaus, plains, volcanoes, glaciers, canyons, and beaches is one of the most diverse on Earth. The layers of rock in Grand Canyon span roughly 40% of Earth's history. The ebb and flow of entire continents, the rise and erosion of mountain ranges, and the evolution of life is documented in the rocks that form the cliffs, plateaus, and canyon walls.

Park Significance and Fundamental Geologic Resources

Stated in the park's foundation document,

Grand Canyon is one of the planet's most iconic geologic landscapes. Grand Canyon National Park preserves a wide range of geologic resources including bedrock geology with exposures of rocks ranging from 1,840 to 270 million years old; diverse paleontological resources; surficial deposits; a complex neotectonic and erosional history; and Pliocene to Holocene volcanic deposits. The Colorado River established its course through Grand Canyon within the last six million years, and likely evolved from pre-existing drainages to its current course. Geologic processes, including erosional processes on hill slopes and in tributaries, and active tectonism continue to shape the canyon today. The geologic record in Grand Canyon is an important scientific chronicle largely responsible for its inspirational scenery. (NPS 2010, p. 10)

Summarized in the foundation document, the purpose of the park is to:

- Preserve and protect Grand Canyon's unique geologic, paleontologic, and other natural and cultural features for the benefit and enjoyment of the visiting public
- Provide the public opportunity to experience Grand Canyon's outstanding natural and cultural features, including natural quiet and exceptional scenic vistas
- Protect and interpret Grand Canyon's extraordinary scientific and natural values (NPS 2010, p. 1)

Established in 1919, the park currently encompasses 4,931 km² (1,904 mi²) beyond the canyon rim, 94% of which is managed as wilderness (fig. 2). While the park offers a vast array of geologic features, ecosystem, and microhabitats, it also offers the opportunity to explore at least 12,000 years of human history. A spiritual site for many native people, the canyon also contains historic

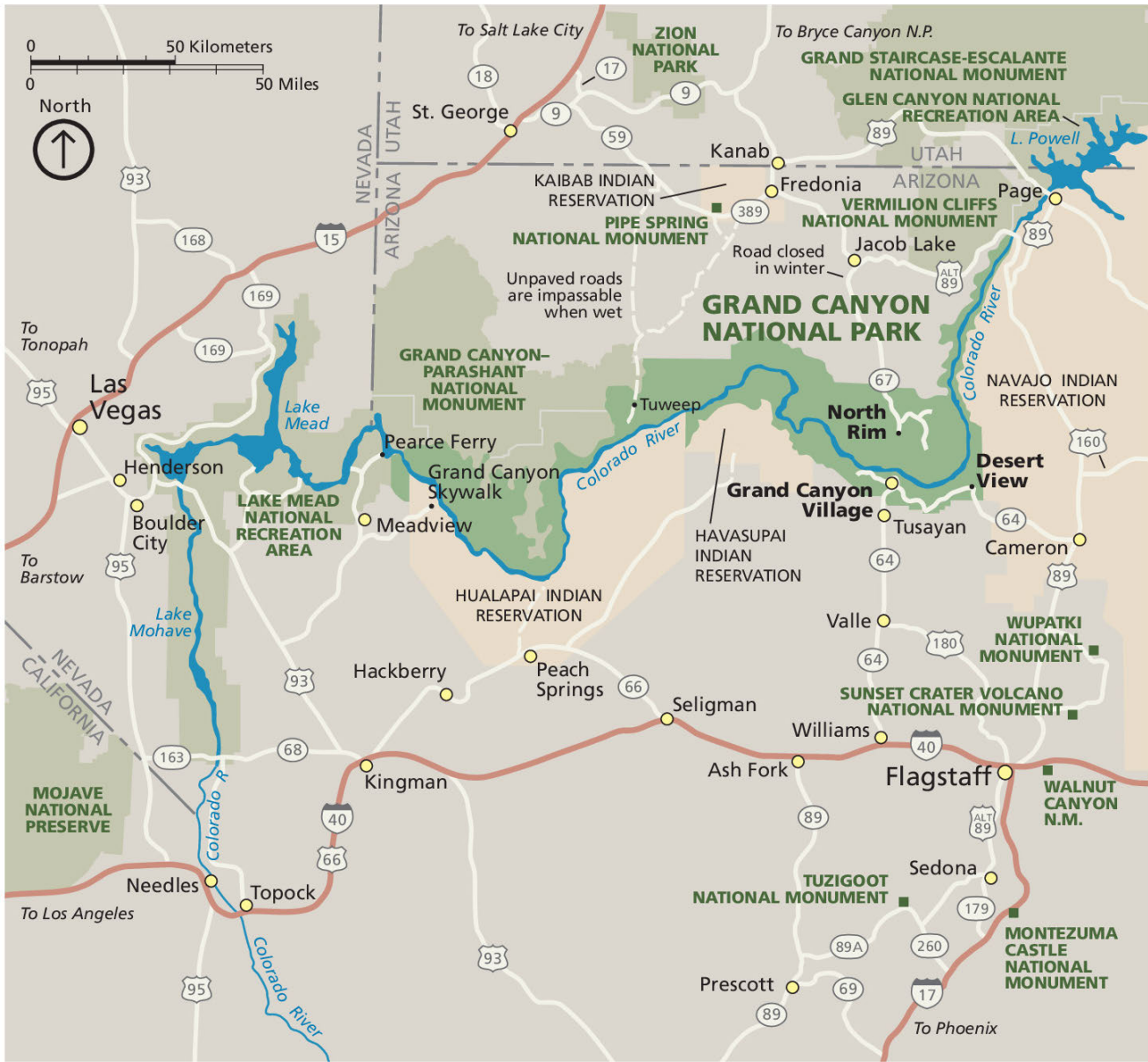


Figure 2. Map of Grand Canyon National Park

The park is located in northwestern Arizona, where the Colorado River carves and flows through the Grand Canyon. The park is bordered downstream by Lake Mead National Recreation Area (to the west) and upstream (to the northeast) by Glen Canyon National Recreation Area. NPS map, available at <https://www.nps.gov/subjects/hfc/index.htm>.

remnants of Euro-American exploration and discovery. Today, the magnificent vistas and natural setting preserved in Grand Canyon National Park inspire a “variety of emotional, intellectual, artistic, and spiritual impressions” for the over 4.5 million annual visitors (NPS 2010, p. 2).

Designated a UNESCO World Heritage Site in 1979, the park also contains three National Historic Landmark Districts and four National Historic Landmarks (NPS 2010). The Arizona National Scenic Trail, part of

the National Trails System, traverses Grand Canyon National Park. The Kaibab Squirrel National Natural Landmark straddles the border between the park and the Kaibab National Forest. About 10% of the natural landmark lies within the park. In addition, park staff manages seven Research Natural Areas (RNAs). RNAs are sites “set aside permanently and managed exclusively for approved nonmanipulative research,” that is, research that does not alter the existing natural conditions (NPS 2010, p. 6).

Fundamental resources are defined as resources and values critical to achieving the park's purpose (NPS 2010). The 2010 foundation document identified the following fundamental resources and values as relevant to Grand Canyon National Park:

- Geologic Features and Processes
- Biodiversity and Natural Processes
- Visitor Experience in an Outstanding Natural Landscape
- Water Resources
- Human History

Within the Geologic Features and Processes category, the primary fundamental resources include geologic features, geologic processes, paleontological resources, and cave resources. These resources are discussed in this report. Because geology and water are so intimately connected, water resources, such as waterfalls, groundwater, and cave formation, are also addressed.

The geologic landscape establishes a framework upon which the other fundamental resources are based. Flora and fauna biodiversity are dependent on the geological substrate as is a quality visitor experience. Author and non-scientist Anais Nin (1971, p. 207–208) captured what many visitors feel when they first witness the exceptional geological landscape of Grand Canyon when she visited the canyon in 1947:

The earth-red canyons, layered in geological strata, rising to a height of awesome proportions, peak after peak. The work of a myth, a force beyond our grasp, silencing human beings, evoking religions and gods unknown. Temples, pyramids, tombs, palaces. The colors in a wide range of sepias, reds, maroons, silvered at the top by light.

Standing there stunned by the mass of colors changing in the light, we heard a subtle vibration, a faint symphony of sounds. It was the wind, traveling through changing depths and heights, affected by curves, towers, heights, abysses, issuing prolonged musical whispers.

If one has lost in the city the sense of nature, its greatness and vastness, if one has lost awe, wonder, or faith, the Grand Canyon reinstates this vision of immensity and beauty.

Geologic Setting

Grand Canyon National Park lies primarily within the Colorado Plateau, a 340,000 km² (131,000 mi²) physiographic province that includes parts of Arizona, Utah, Colorado, and New Mexico (fig. 3). The semi-arid Colorado Plateau is a vast tableland of plateaus, basins, and steep-walled canyons defined by the Colorado River and its tributaries.

The western portion of the park lies in the transition zone between the Colorado Plateau and the Basin and Range Province and borders Lake Mead National Recreation Area (fig. 3). Noted for its arid conditions and its characteristic topography of north–south trending mountain ranges (horsts) separated by relatively flat basins (grabens), the Basin and Range is a globally unique landscape that extends from Mexico to southern Oregon and Idaho.

From Lake Powell (Glen Canyon National Recreation Area) to Lake Mead (Lake Mead National Recreation Area), the Colorado River flows through the Grand Canyon past six local plateaus and two low-lying platforms (fig. 4). Marble Canyon bisects the Marble Platform on the east end of Grand Canyon National Park, and the Sanup Platform at the western end of the park separates the Shivwits Plateau from the north–south-trending Grand Wash Fault.

The Colorado River drains a land surface of 632,000 km² (244,000 mi²). As the Colorado River flows through the canyon, it drops about 620 m (2,000 ft) in elevation. Between Lees Ferry (mile 0) and Diamond Creek (mile 225), 525 tributaries drain into the Colorado River and periodically yield debris flows (Webb et al. 2003). Debris flows are responsible for the debris fans, rapids, and sand bars in the river. Debris fans, fan-shaped features formed where debris flows enter the river, remain relatively stable until the next debris flow. The river removes most of the debris flow sediment, especially the mud, silt, and sand, but boulders and cobbles are not immediately transported downstream, resulting in rapids. Sand bars are relatively unstable, changing with fluctuations in flow, largely determined by the discharge of water from the Glen Canyon Dam (Webb et al. 2000, 2003).

The strata exposed by the Colorado River represent six geologic eras, from the Paleoproterozoic Era to the Cenozoic Era. The approximately 1.5 km (0.9 mi) of rock strata exposed in the Grand Canyon spans nearly 2 billion years of the Earth's 4.6-billion-year history (fig. 5). Erosion has carved a vast array of temple-like buttes, spires, and mesas in a gorge that spans a width of 0.5–30 km (0.3–19 mi). The Colorado River twists and turns for 445 km (277 mi) through the park.

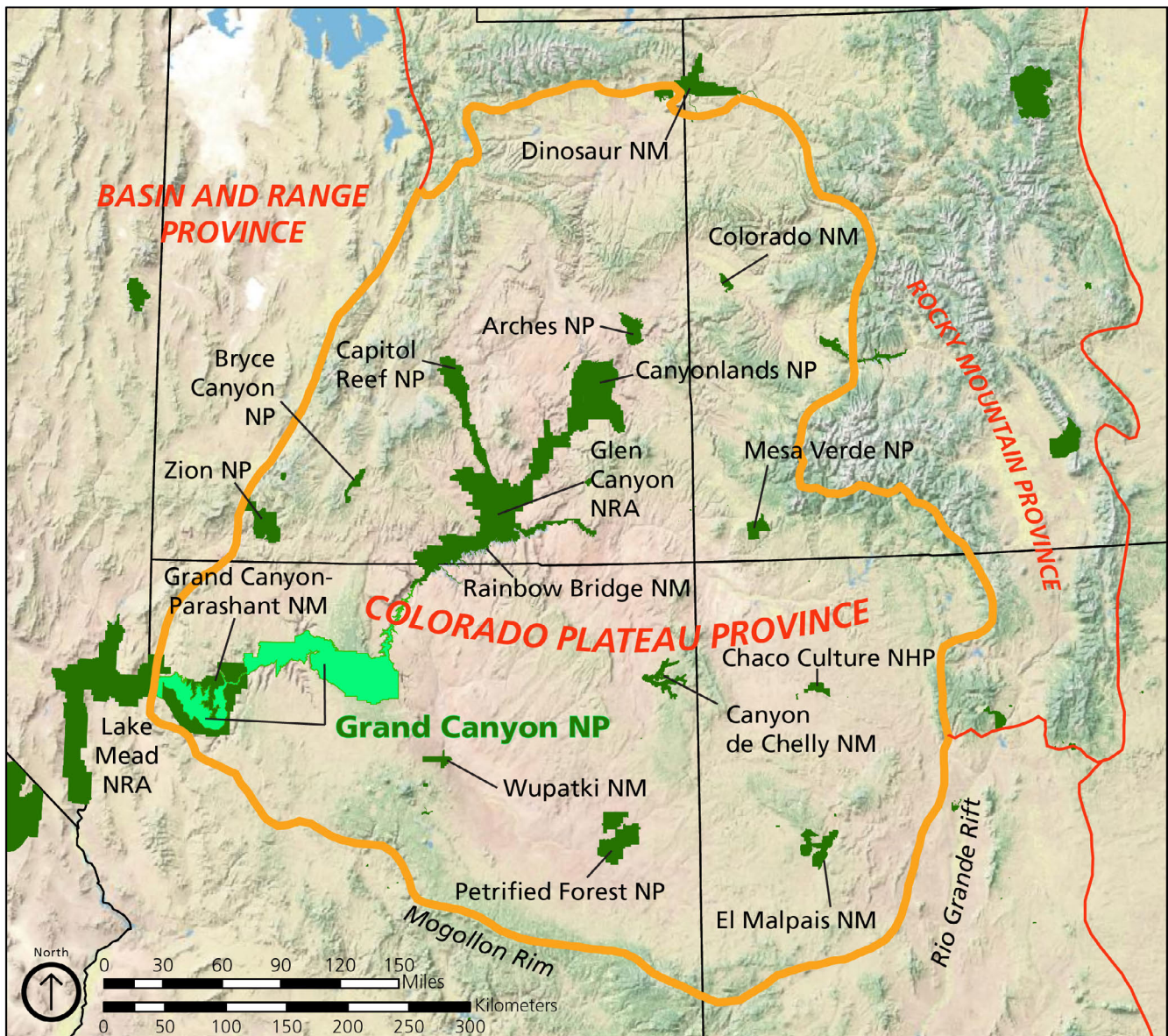


Figure 3. Physiographic provinces of the western United States. Grand Canyon National Park lies within the transition zone between the Colorado Plateau and the Basin and Range provinces. Green areas are units managed by the National Park Service, some units are labelled. Compiled by Jason Kenworthy and Philip Reiker (NPS Geologic Resources Division) from ESRI Arc Image Service, National Geographic Society TOPO Imagery.

Cenozoic deposits in the park reflect the most recent geologic processes that carved the current landscape and include fluvial terrace-gravel and alluvial fan deposits, landslide deposits, basalts of Neogene and Quaternary age, important travertine deposits, and sediments in caves (table 1). Research on the Colorado River terraces and terraces associated with tributaries to the Colorado River has led to greater understanding of the history and evolution of the Grand Canyon. About 5–6 million years ago, in the early Pliocene epoch, the swift-flowing Colorado River began carving its present course through sedimentary rock strata of the

southwestern Colorado Plateau. By early Pleistocene time, the Colorado River had excavated the Grand Canyon to within 15 m (50 ft) of its present depth.

The abundant volcanic deposits in the Miocene Epoch (table 1) record a tectonic regime shift in which previous tectonic compression along the western margin of North America transitioned into tectonic extension, which pulled apart the crust, resulting in the Basin and Range Province. The youngest volcanic rock in the area is about 1,000 years old (Fenton 1998; Billingsley 2000b).

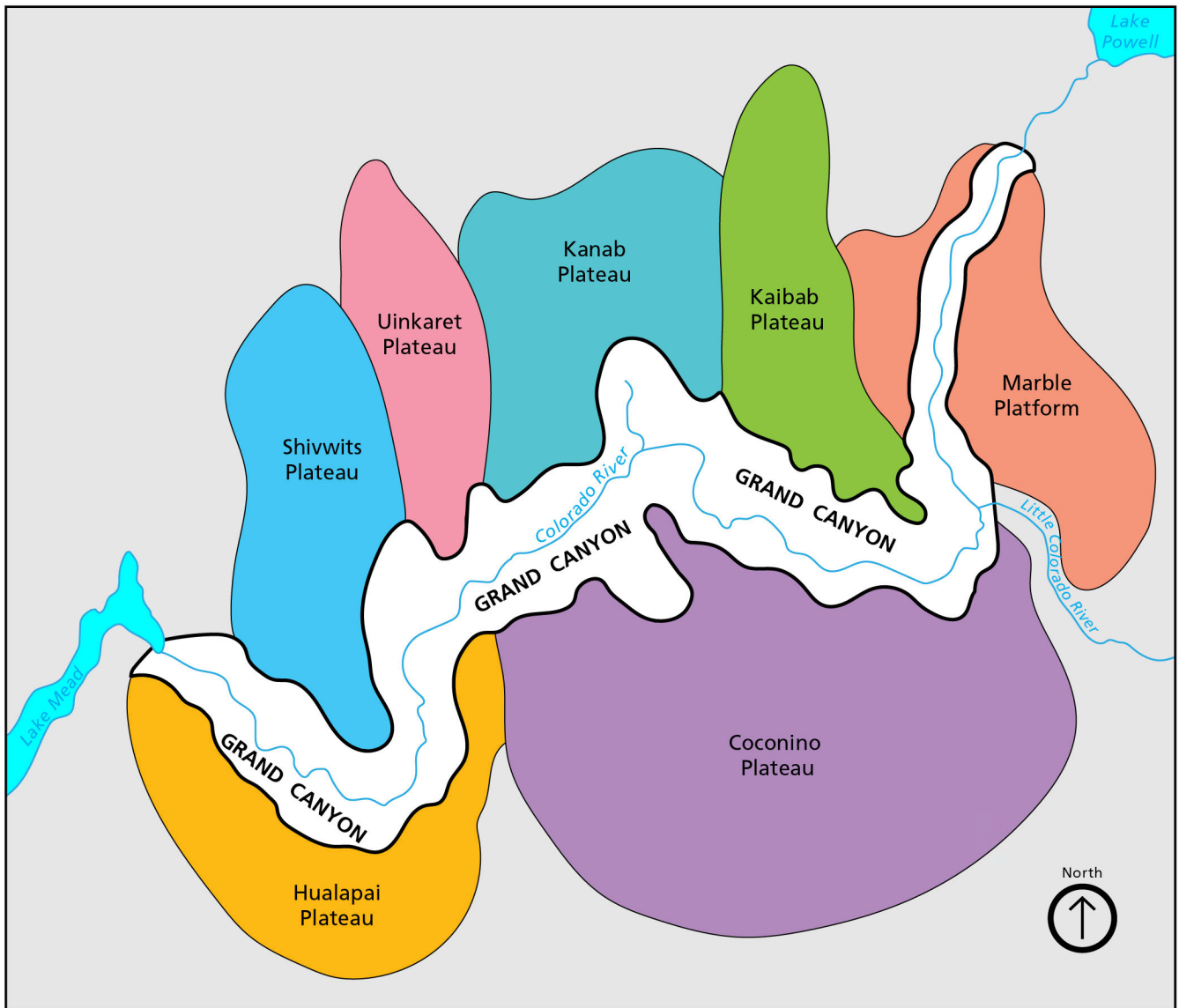


Figure 4. Generalized map of the area surrounding the Grand Canyon and west-to-east cross section of the area north of the Grand Canyon. Plateaus on the diagram are sub-basins within the Colorado Plateau physiographic province. Arrows on the cross section indicate direction of movement on the fault planes. Map by Trista Thornberry-Ehrlich (Colorado State University), modified from Beus and Morales (2003, figures 1.2 and 1.3).

Eon	Era	Period	Epoch	MYA	Life Forms	North American Events								
Phanerozoic	Cenozoic (CZ)	Quaternary (Q)	Holocene (H)	0.01	Age of Mammals	Extinction of large mammals and birds Modern humans	Ice age glaciations; glacial outburst floods							
			Pleistocene (PE)											
		Tertiary (T)	Neogene (N)	Pliocene (PL)				2.6	Age of Reptiles	Placental mammals	Laramide Orogeny (W) Western Interior Seaway (W)			
				Miocene (MI)				5.3						
			Paleogene (PG)	Oligocene (OL)				23.0				Age of Amphibians	Early flowering plants	Sevier Orogeny (W)
		Eocene (E)		33.9										
		Paleocene (EP)						56.0	Age of Fishes	Dinosaurs diverse and abundant	Nevadan Orogeny (W) Elko Orogeny (W)			
								66.0						
		Mesozoic (MZ)	Cretaceous (K)					145.0	Age of Invertebrates	First land plants Mass extinction Primitive fish Trilobite maximum Rise of corals Early shelled organisms	Laramide Orogeny (W) Western Interior Seaway (W)			
								201.3						
	Jurassic (J)			251.9	Age of Reptiles	Dinosaurs diverse and abundant	Nevadan Orogeny (W) Elko Orogeny (W)							
				251.9										
	Paleozoic (PZ)		Triassic (TR)		251.9	Age of Amphibians	First dinosaurs; first mammals Flying reptiles	Breakup of Pangaea begins Sonoma Orogeny (W)						
					251.9									
			Permian (P)		298.9							Age of Amphibians	Coal-forming swamps Sharks abundant First reptiles	Supercontinent Pangaea intact Ouachita Orogeny (S) Alleghany (Appalachian) Orogeny (E) Ancestral Rocky Mountains (W)
					323.2									
			Pennsylvanian (PN)		323.2							Age of Fishes	First amphibians First forests (evergreens)	Antler Orogeny (W) Acadian Orogeny (E-NE)
					358.9									
	Mississippian (M)		419.2	Age of Fishes	First land plants Mass extinction	Taconic Orogeny (E-NE)								
			443.8											
	Devonian (D)		485.4	Age of Fishes	First amphibians First forests (evergreens)	Taconic Orogeny (E-NE)								
			485.4											
	Proterozoic	Neoproterozoic Era	Ediacaran Pd.	635	Age of Invertebrates	Complex multicelled organisms	Supercontinent rifted apart Formation of early supercontinent Grenville Orogeny (E)							
			Cryogenian Pd.	720										
Tonian Pd.			1000											
Stenian Pd.			1200											
Mesoproterozoic Era		Ectasian Pd.	1400	Age of Invertebrates				Simple multicelled organisms	Mazatal Orogeny Yavapai Orogeny Trans Hudson Orogeny					
		Calymmian Pd.	1600											
		Statherian Pd.	1800											
Paleoproterozoic Era		Orosirian Pd.	2050	Age of Invertebrates				Early bacteria and algae (stromatolites)	Oldest known Earth rocks					
		Rhyacian Pd.	2300											
		Siderian Pd.	2500											
Precambrian (PC, W, X, Y, Z)	Archean Eon		4000	Age of Invertebrates	Origin of life	Formation of Earth's crust								
			4600											
	Hadean Eon		4600	Age of Invertebrates	Formation of the Earth									
		4600												

Figure 5. Geologic time scale.

The divisions of the geologic time scale are organized stratigraphically, with the oldest divisions at the bottom and the youngest at the top. Time periods representing strata mapped in Grand Canyon National Park area are in green. GRI map abbreviations for each time division are in parentheses. Compass directions in parentheses indicate the regional locations of events. Boundary ages are millions of years ago (MYA). Pd. = "Period." Note the time scale is not proportional. National Park Service graphic using dates from the International Commission on Stratigraphy (<http://www.stratigraphy.org/index.php/ics-chart-timescale>).

Table 1. Stratigraphic column of Cenozoic Era units mapped within Grand Canyon National Park.

In tables 1–4, detailed lithologic descriptions are available in the GRI GIS data and in the many references. References for radiometric ages of igneous rocks are available in the GRI map information document (grca_geology.pdf). In tables 1–4, age ranges are from the International Commission of Stratigraphy 2018 age chart (fig. 3); Mya: million years ago; river miles refer to miles from Lees Ferry. The stratigraphic columns in tables 1–4 are a compilation of the GIS source maps, Dehler et al. (2017), and Karlstrom et al. (2018).

Period	Epoch (mya)	Map Unit (map symbol)	Lithology and Thickness
Quaternary	Holocene (present–0.01)	Unconsolidated deposits (Qs, Qf, Qd, Qg1, Qtgr, Qa1, Qa2, Qay, Qps)	Various amounts of clay, silt, sand, pebbles, cobbles, and boulders deposited by water and wind.
	Holocene and Pleistocene	Unconsolidated deposits (Qgy, Qg2, Qg3, Qr, Qa3, Qv, Qtr, Ql) and Travertine (Qt)	River terrace, alluvial fan, and landslide deposits. Travertine associated with springs and seeps.
	Pleistocene (0.01–2.6)	Uinkaret Plateau intrusive rocks (Qi), pyroclastic deposits (Qp), and basalt flows (Qb)	Basalt south of Mount Trumbull. Basalt flowed over TRm, Pk, and Pt . ~100,000–200,000 years old.
	Pleistocene	Basalt flows (Qb)	Age: 220,000–770,000 years.
	Pleistocene	Basalt dikes and necks (Qidn)	Age: 407,000–780,000 years.
	Pleistocene	Tuckup Canyon Basalt (Qtid, Qtp, Qtb)	Intrusive dikes (Qtid), pyroclastic deposits (Qtp), and basalt flows (Qtb). Basalt ~760,000 years.
	Pleistocene	Hancock Knolls Basalt (Qhp, Qhb)	Pyroclastic deposits (Qhp) and basalt flows (Qhb).
	Pleistocene	Pyroclastic deposits (Qpyr)	Basalt cinders, ribbons, and bombs.
	Pleistocene	Basalt flows along the Colorado River (Qbcr)	Basalt. One flow is known as the Black Ledge flow.
	Pleistocene and Pliocene	Terrace gravel deposits (QTg4, QTga)	Silt, sand, well-rounded quartzite pebbles, cobbles, and boulders.
Neogene	Pliocene (2.6–5.3)	Basalt of Mount Emma (Teb)	Basalt flows with plagioclase laths.
	Pliocene	Whitmore dike swarm, basalt flow (Twb)	Basalt on informal “Whitmore Hill.”
	Pliocene	Gravel and sedimentary deposits (Tgs)	Mudstone, sandstone, and pebbles.
	Miocene (5.3–23)	Shivwits Plateau igneous rocks (Tsi, Tsb)	Intrusive rocks (Tsi) and basalt flows (Tsb).
	Miocene	Dikes of Colorado River Mile 202 (T2i)	Basalt ~5.76 million years.
	Miocene	Parashant Canyon dikes and Hundred and Ninetysix Mile Creek (Tp6i)	Basalt dikes (6.3 million years) intrude Cambrian–Permian rocks.
	Miocene	Snap Point Basalt and Garrett intrusive dikes (Tsgi) and basalt flows (Tsgb)	Indicate a shallower and narrower Grand Canyon 9 million years ago.
	Miocene	227-Mile Intrusive (T227i)	Basalt ~13.5 million years.
	Miocene	Grand Wash Trough sedimentary deposits (Tgl, Tgg)	Interbedded limestone (Tgl), siltstone, and gypsum (Tgg).
	Miocene	Hualapai Plateau igneous rocks (Tv, Ti)	Basalt and rhyolite ash flows. Age: 18.5 million–19.9 million years.
Paleogene	Oligocene (23–33)	Regional Unconformity from Upper Triassic to lower Miocene epochs	At least 214 million years of missing sedimentary record in the park.
	Eocene (33–56)	Regional Unconformity from Upper Triassic to lower Miocene epochs	At least 214 million years of missing sedimentary record in the park.
	Paleocene (56–66)	Regional Unconformity from Upper Triassic to lower Miocene epochs	At least 214 million years of missing sedimentary record in the park.

In a geologic sense, erosion is the great equalizer. At one time, approximately 1,200 m (4,000 ft) of Mesozoic rock units rose above the present canyon rim. Uplift and erosion in the Cenozoic Era removed nearly all of it from the Grand Canyon region (Price 1999; Huntoon 2003; Morales 2003). Today, remnants of Mesozoic formations (table 2) provide evidence of near-shore shallow marine environments, fluvial systems, and vast eolian dunes that once swept back and forth across the Colorado Plateau. The National Parks on the Colorado Plateau preserve many of these ancient environments. For example, Zion National Park (Graham 2006) and Glen Canyon National Recreation Area (Graham 2016) contain excellent exposures of extensive Mesozoic sand dunes (fig. 3).

Cenozoic lava flows cover and thereby preserve Mesozoic strata both north and south of the Grand Canyon. South of Grand Canyon Village, basalt flows

have been deposited over Moenkopi and Chinle formations at Red Butte. North of the canyon, Mesozoic strata are preserved under Neogene and Quaternary basalt flows on the Shivwits, Uinkaret, and Kanab plateaus or concealed beneath Quaternary alluvium and landslide deposits (Billingsley 2000b; Billingsley and Wellmeyer 2004).

Paleozoic strata (table 3) represent a wide variety of depositional environments that record multiple transgressions (sea level rise) and regressions (sea level lowering), orogenies (mountain-building episodes), development of coastal sand dunes, karst topography, caves, river channels and floodplains, and erosional interludes that leveled highlands. A major unconformity, part of John Wesley's Great Unconformity, separates Cambrian Period strata from the underlying Precambrian rocks in the Grand Canyon (table 3).

Table 2. Stratigraphic column of Mesozoic Era units mapped within Grand Canyon National Park.

Regional unconformities are discussed in the "Geologic Features and Processes" section of the report.

Period	Epoch (mya)	Map Unit (map symbol)	Lithology and Thickness	
Cretaceous	Upper to Lower (66–145)	Regional Unconformity from Upper Triassic to lower Miocene epochs	At least 214 million years of missing sedimentary record in the park.	
Jurassic	Upper to Lower (145–201)	Regional Unconformity from Upper Triassic to lower Miocene epochs	At least 214 million years of missing sedimentary record in the park.	
Triassic	Upper (201–237)	Regional Unconformity from Upper Triassic to lower Miocene epochs	At least 214 million years of missing sedimentary record in the park.	
		Chinle Formation Shinarump Member (TRcs)	Sandstone and conglomerate. Thickness: 18–60 m (60–220 ft).	
	Middle (237–247)	Regional Unconformity	Regional Unconformity	
	Lower (247–252)		Moenkopi Formation Undivided (TRm)	Overall thickness: 152 m (500 ft).
			Moenkopi Formation informal upper red member (TRmu)	Reddish-brown claystone, siltstone, sandstone. Thickness: 0–37 m (0–120 ft).
			Moenkopi Formation Shnabkaib Member (TRms)	Cliff-forming dolomite, sandstone, and siltstone. Thickness: 0–30 m (0–100 ft).
			Moenkopi Formation Wupatki Member (TRmw)	Mudstone, siltstone, and sandstone. Thickness: 9–26 m (30–85 ft).
	Moenkopi Formation lower members, undivided (TRmlm)	Mudstone, siltstone, and sandstone. Thickness: 114–122 m (375–400 ft).		
	Regional Unconformity from uppermost Lower Permian to Lower Triassic epochs	Approximately 50 million years of missing sedimentary record		

Limestones in the 270 million-year-old Kaibab Formation (map unit **Pk**), the youngest Paleozoic unit exposed in Grand Canyon National Park, support the rim of the Grand Canyon north and east of the Colorado River and the surfaces of the Shivwits, Uinkaret, Kanab, and Coconino Plateaus. The Laramide

Orogeny in the Late Cretaceous–Paleogene uplifted the region and subsequent erosion removed the Kaibab Formation from the southern part of the Shivwits Plateau so that the underlying Toroweap Formation (**Pt**) now forms the canyon rim in that area (table 3; Billingsley 2000b; Billingsley and Wellmeyer 2004).

Table 3. Stratigraphic column of Paleozoic Era units mapped within Grand Canyon National Park.

Following compilation of the GRI GIS data in 2013, the age of the Sixtymile Formation (**Zs***) was revised to Cambrian from Precambrian (Neoproterozoic) as per Karlstrom et al. (2018). That change is reflected on this table and throughout the report, however, as of 2019 the GRI GIS data retains the “Zs” map symbol. The symbol may change to “Cs” if GRI GIS data are updated in the future.

Period	Epoch (mya)	Map Unit (map symbol)	Lithology and Thickness
Permian	Upper (252–259)	Regional Unconformity from Lower Permian to Lower Triassic epochs	Approximately 50 million years of missing sedimentary record.
	Middle (259–272)	Regional Unconformity from Lower Permian to Lower Triassic epochs	Approximately 50 million years of missing sedimentary record.
	Lower (272–299)	Regional Unconformity from Lower Permian to Lower Triassic epochs	Approximately 50 million years of missing sedimentary record.
		Kaibab Formation (Pk)	Calcareous sandstone, gypsum, and sandy limestone.
		Kaibab Formation Harrisburg Member (Pkh)	Ledge- and slope-forming, siltstone, sandstone, and limestone. Thickness: 25–37 m (80–120 ft).
		Kaibab Formation Fossil Mountain Member (Pkf)	Fossiliferous limestone and dolomite. Thickness: 48–70 m (160–230 ft).
		Toroweap Formation (Pt)	Three members (below). Thickness: 60–76 m (200–250 ft).
		Toroweap Formation Woods Ranch Member (Ptw)	Slope-forming siltstone, gypsum, sandstone, and limestone. Thickness: 30–55 m (100–180 ft).
		Toroweap Formation Brady Canyon and Seligman Members, undivided (Ptb)	Brady Canyon: limestone with chert nodules. Thickness: 6–9 m (20–30 ft). Seligman: dolomite, sandstone, gypsum. Thickness: 3–6 m (10–20 ft).
		Coconino Sandstone (Pc)	Cliff-forming sandstone. Fossil trackways. Thickness: 9–122 m (30–400 ft).
		Hermit Formation (Ph)	Siltstone and sandstone. Thickness: 158–195 m (520–640 ft).
		Supai Group Esplanade Sandstone (Pe)	Cliff-forming sandstone. Thickness: 107–122 m (350–400 ft).
	Supai Group Esplanade Sandstone and Pakoon Limestone, undivided (Pep)	Esplanade Sandstone: see above Pakoon Limestone: fossiliferous limestone. Thickness: 107–137 m (350–450 ft).	
Pennsylvanian to Mississippian	Penn. to Upper Miss. (299–331)	Supai Group Wescogame, Manakacha, and Watahomigi Formations (PNMs)	Mudstone, siltstone, sandstone, sandy limestone, basal conglomerate, undivided. Wescogame thickness: 34–40 m (110–130 ft). Manakacha thickness: 53 m (175 ft). Watahomigi thickness: 30–37 m (100–120 ft).
Mississippian	Upper	Surprise Canyon Formation (Ms)	Siltstone, sandstone, limestone, dolomite, and basal conglomerate. Thickness: 0–122 m (0–400 ft).
	Upper and Lower (323–359)	Redwall Limestone (Mr)	Cliff-forming, fossiliferous limestone and dolomite. Thickness: 152–167 m (500–550 ft).

Table 3, continued. Stratigraphic column of Paleozoic Era units mapped within Grand Canyon National Park.

Period	Epoch (mya)	Map Unit (map symbol)	Lithology and Thickness
Devonian	Upper and Middle (359–393)	Temple Butte Formation (Dtb)	Dolomite, sandstone, mudstone, and limestone. Thickness: 24–106 m (80–350 ft).
	Lower (393–419)	Regional Unconformity	Regional Unconformity
Silurian	Upper to Lower (419–444)	Regional Unconformity	Regional Unconformity
Ordovician	Upper to Lower (444–485)	Regional Unconformity	Regional Unconformity
Cambrian	Upper (485–501)	Regional Unconformity	Regional Unconformity
	Middle (501–513)	Tonto Group Muav Limestone (Cm)	Limestone, dolomite, mudstone. Thickness: 97–115 m (320–380 ft).
	Middle	Tonto Group Bright Angel Shale (Cba)	Shale, siltstone, and sandstone. Thickness: 60–90 m (200–300 ft).
	Middle and Lower (501–541)	Tonto Group Tapeats Sandstone (Ct)	Sandstone and conglomerate. Thickness: 0–91 m (0–300 ft).
	Middle and Lower	Tonto Group Sixtymile Formation (Zs*)	Siltstone, sandstones, black shale surrounding slumped dolomite blocks. To the west, separated from Ct by the Great Unconformity. To the east, laterally equivalent to Tonto Group. Age: 527 million–509 million years. Thickness: 196 ft (60 m).
	Lower (513–541)	Part of Powell’s Great Unconformity.	Where Ct directly overlies Xv , as much as 1,200 million years of stratigraphic record is missing.

During his pioneering exploration of the canyon in 1869, John Wesley Powell recognized that an extraordinary gap in the stratigraphic record occurred between the Middle to Late Proterozoic formations of the Grand Canyon Supergroup and the underlying granitic rocks of the Zoroaster Plutonic Complex (table 4; Vince Santucci, NPS, senior paleontologist, written communication, 30 August 2018; Powell 1875; Karlstrom and Timmons 2012). Subsequent radiometric age data has proved Powell correct. For example, in locations where the Cambrian Tapeats Sandstone (**Ct**) overlies the metamorphic rocks of the Statherian (Paleoproterozoic) Vishnu Schist (**Xv**), as much as 1.2 billion years of stratigraphic record is missing (table 4). This equates to nearly 26% of Earth’s history.

Above Powell’s Great Unconformity, the 2,100 m (6,800 ft) sequence of Neoproterozoic rocks and Mesoproterozoic rocks preserve an exceptional assemblage of late Precambrian Era fossils. Grand Canyon National Park contains the only exposures in the southwestern United States of the younger Chuar Group strata that unconformably overlie the Unkar Group (table 4; Ford and Dehler 2003).

The contact between the Nankoweap Formation (**Yzn**), the lowermost unit of the Chuar Group, and the Cardenas Basalt (**Yc**), the uppermost unit of the Unkar Group, represents at least 300 million years of missing sedimentary record in the park. The siltstones and sandstones of the Nankoweap Formation were deposited following tectonic uplift that raised and tilted the eastern Grand Canyon region toward the northeast, exposing the Cardenas Basalt to erosion (Hendricks and Stevenson 2003).

The Cardenas Basalt, an outpouring of lava more than 300 m (1,000 ft) thick, caps the shallow marine and nonmarine sedimentary rocks of the Dox Formation of the Unkar Group (table 4). The Bass Formation (**Yb**), the lowermost unit of the Unkar Group, records a major west-to-east transgression followed by a regression in the Grand Canyon area (Hendricks and Stevenson 2003). The major sea level rise flooded a region that had also been tilted and exposed to erosion. The contact between clastic rocks of the Bass Formation and the granitic rocks of the Zoroaster Plutonic Complex represents an extraordinary gap in the stratigraphic record of approximately 500 million years (table 4).

Table 4. Stratigraphic column of Proterozoic Eon units mapped within Grand Canyon National Park.

The unconformities in this table are the most significant hiatuses in the Grand Canyon region and are discussed in the “Geologic Features and Processes” section. Following compilation of the GRI GIS data in 2013, the age of the Nankoweap Formation (**YZn***) was determined to be 782 mya (Dehler et al. 2017), placing it in the Neoproterozoic rather than spanning the Neoproterozoic and latest Mesoproterozoic. That change is reflected on this table and throughout the report, however, as of 2019 the GRI GIS data retains the “**YZn**” map symbol. The symbol may change to “**Zn**” if GRI GIS data are updated in the future.

Age (mya)	Map Unit (map symbol)	Lithology, Age, and Thickness
Neoproterozoic Era Ediacaran Period (541–635)	Part of Powell’s Great Unconformity.	Where Ct directly overlies Xv , as much as 1,200 million years of stratigraphic record is missing.
Neoproterozoic Era Cryogenian Period (635–720)	Part of Powell’s Great Unconformity.	Where Ct directly overlies Xv , as much as 1,200 million years of stratigraphic record is missing.
	Grand Canyon Supergroup Chuar Group Kwagunt Formation: Walcott Member (Zkw)	Mudstone, sandstone, brecciated dolomite, sandstone. Age: ~742 million years. Thickness: 255 m (838 ft).
	Grand Canyon Supergroup Chuar Group Kwagunt Formation: Awatubi Member (Zka)	Mudstone, siltstone, sandstone with macroalgal fossil, <i>Chuarina circularis</i> . Age: 764 ± 16 million years. Thickness: 252–344 m (823–1,128 ft).
	Grand Canyon Supergroup Chuar Group Kwagunt Formation: Carbon Butte Member (Zkcb)	Sandstone, mudstone, and siltstone. Sedimentary features. Thickness: 34–68 m (112–223 ft).
	Grand Canyon Supergroup Chuar Group Galeros Formation: Duppa Member (Zgd)	Shale and siltstone. Thickness: 174–625 m (571–2,050 ft).
	Grand Canyon Supergroup Chuar Group Galeros Formation: Carbon Canyon Member (Zgcc)	Mudstone, siltstone, and sandstone. Stromatolites. Sedimentary features. Thickness: 471 m (1,546 ft).
	Grand Canyon Supergroup Chuar Group Galeros Formation: Jupiter Member (Zgj)	Mudstone, siltstone, sandstone, and dolomite. Sedimentary features. Thickness: 264–462 m (868–1,516 ft).
	Grand Canyon Supergroup Chuar Group Galeros Formation: Tanner Member (Zgt)	Siltstone, sandstone, and dolomite. Age: ~800 million years. Thickness: 6–24 m (20–80 ft).
Neoproterozoic Era Tonian Period (720–1000)	Grand Canyon Supergroup Chuar Group Nankoweap Formation (YZn*)	Siltstone and sandstone. Age: ~782 million years. Thickness: 100 m (300 ft).
	Regional Unconformity	At least 300 million years of missing sedimentary record in the park.

Table 4, continued. Stratigraphic column of Proterozoic Eon units mapped within Grand Canyon National Park.

Age (mya)	Map Unit (map symbol)	Lithology, Age, and Thickness
Mesoproterozoic Era Stenian Period (1,000–1,200)	Regional Unconformity	At least 300 million years of missing sedimentary record in the park
	Grand Canyon Supergroup Unkar Group Cardenas Basalt (Yc)	Massive basalt flows, basaltic andesite, sandstone beds. Age: ~1,070 million years.
	Grand Canyon Supergroup Unkar Group Unnamed diabase sills and dikes (Yi)	Intrudes all units of the Unkar Group below the Cardenas Lava.
	Grand Canyon Supergroup Unkar Group Dox Formation, undivided (Yd)	Upper part removed by erosion. Exposed thickness: ~60 m (200 ft).
	Grand Canyon Supergroup Unkar Group Dox Formation: Ochoa Point Member (Ydo)	Mudstone and sandstone. Thickness: 76–91 m (250–300 ft).
	Grand Canyon Supergroup Unkar Group Dox Formation: Comanche Point Member (Ydc)	Mudstone and siltstone. Thickness: 155 m (508 ft).
	Grand Canyon Supergroup Unkar Group Dox Formation: Solomon Temple Member (Yds)	Mudstone, siltstone, and sandstone. Thickness: 280 m (920 ft).
	Grand Canyon Supergroup Unkar Group Dox Formation: Escalante Creek Member (Yde)	Sandstone with minor shale and mudstone. Thickness: 390 m (1,278 ft).
	Grand Canyon Supergroup Unkar Group Shinumo Quartzite (Ys)	Cliff-forming sandstone and quartzite. Thickness: 345 m (1,132 ft).
	Grand Canyon Supergroup Unkar Group Hakatai Shale (Yh)	Shale (lower); sandstone (upper). Thickness: 137–300 m (448–981 ft).
Mesoproterozoic Era Ectasian Period (1,200–1,400)	Grand Canyon Supergroup Unkar Group Bass Formation (Yb)	Dolomite with sandstone, siltstone, volcanic ash, breccias and conglomerates. Age: ~1,254 million years. Thickness: 60–100 m (196–327 ft).
	The Greatest Angular Unconformity	As much as 500 million years of missing sedimentary record.
Mesoproterozoic Era Calymmian Period (1,400–1,600)	The Greatest Angular Unconformity	As much as 500 million years of missing sedimentary record.

Table 4, continued. Stratigraphic column of Proterozoic Eon units mapped within Grand Canyon National Park.

Age (mya)	Map Unit (map symbol)	Lithology, Age, and Thickness
Paleoproterozoic Era Statherian Period (1,600–1,800) (~1,700)	The Greatest Angular Unconformity	As much as 500 million years of missing sedimentary record.
	Zoroaster Plutonic Complex Young granite and pegmatite (Yg)	Granite and pegmatite. Age: ~1,400 million years.
	Zoroaster Plutonic Complex Granite (Xg)	Pegmatite and granitic intrusions. Age: 1,685 million–1,680 million years.
	Zoroaster Plutonic Complex Granite, granitic pegmatite and aplite (Xgr)	Granitic rocks emplaced coincident with peak metamorphism. Age: ~1,700 million–1,680 million years.
	Zoroaster Plutonic Complex Granodiorite-gabbro-diorite and granodiorite complexes (Xgd)	Composition suggests probable volcanic arc origin. Age: 1,740 million–1,710 million years.
	Zoroaster Plutonic Complex Ultramafic rocks (Xum)	Supracrustal rocks deposited on crustal basement rocks.
	Zoroaster Plutonic Complex Diorite, gabbro, and anorthosite (Xdg)	Age: ~1,740 million–1,720 million years.
	Granite Gorge Metamorphic Suite Schist (Xs)	Quartz-mica and pelitic schist.
	Granite Gorge Metamorphic Suite Vishnu Schist (Xv)	Schist. Age: ~1,750 million years.
	Granite Gorge Metamorphic Suite Rama Schist and Gneiss (Xr)	Strongly foliated schist and gneiss. Age: 1,750 million years.
	Granite Gorge Metamorphic Suite Brahma Schist (Xbr)	Schist with amphibole, hornblende, and biotite. Age: ~1,750 million years.
	Granite Gorge Metamorphic Suite Mafic metavolcanic rocks (Xm)	Schist and amphibolite with biotite and garnet. Equivalent to Xbr .
	Granite Gorge Metamorphic Suite Orthoamphibole schist (Xo)	Regolith (weathered detritus) eroded from older plutonic rocks.
Granite Gorge Metamorphic Suite Carbonate and chert (Xc)	Carbonate rock and chert nodules within Xo .	
Paleoproterozoic Era Orosirian Period (1,800–2,050)	Zoroaster Plutonic Complex Elves Chasm Pluton (Xec)	Oldest plutonic rocks. Tonalite and quartz diorite. Substantially older than other dated rocks in the Inner Gorge. Age: 1,840 million years.

Vishnu basement rocks comprise the oldest rocks in the park. Exposed in the Inner Gorge, the metamorphic rocks of the 1.84-billion-year-old Elves Chasm Pluton (**Xec**) form the very basement of the North American continent (Karlstrom et al. 2003). In Granite Gorge, 1.75 billion–1.68 billion-year-old metamorphosed sedimentary and volcanic rocks of the Granite Gorge Metamorphic Suite, which include the Vishnu (**Xv**), Brahma (**Xbr**), and Rama (**Xr**) Schists, and the rest of the Zoroaster Plutonic Complex overlie the Elves Chasm Gneiss (Price 1999; Beus and Morales 2003; Karlstrom et al. 2003).

North of the Grand Canyon, the topography of the Colorado Plateau consists of a series of alternating cliffs and flat plateaus that have been eroded in Mesozoic and Cenozoic strata (fig. 6). These erosional steps are referred to as the Grand Staircase and inspired the name for the Grand Staircase-Escalante National Monument, northeast of Grand Canyon National Park. The Chocolate Cliffs, named for the reddish-brown mudstone of the Lower Triassic Moenkopi Formation (**TRm**), form the first line of cliffs in the Grand Staircase north of the Grand Canyon. The fluvial sandstones and conglomerates of the Shinarump Member of the Upper Triassic Chinle Formation (**TRcs**) cap the cliffs (fig. 6;

BRYCE CANYON NATIONAL PARK CEDAR BREAKS NATIONAL MONUMENT

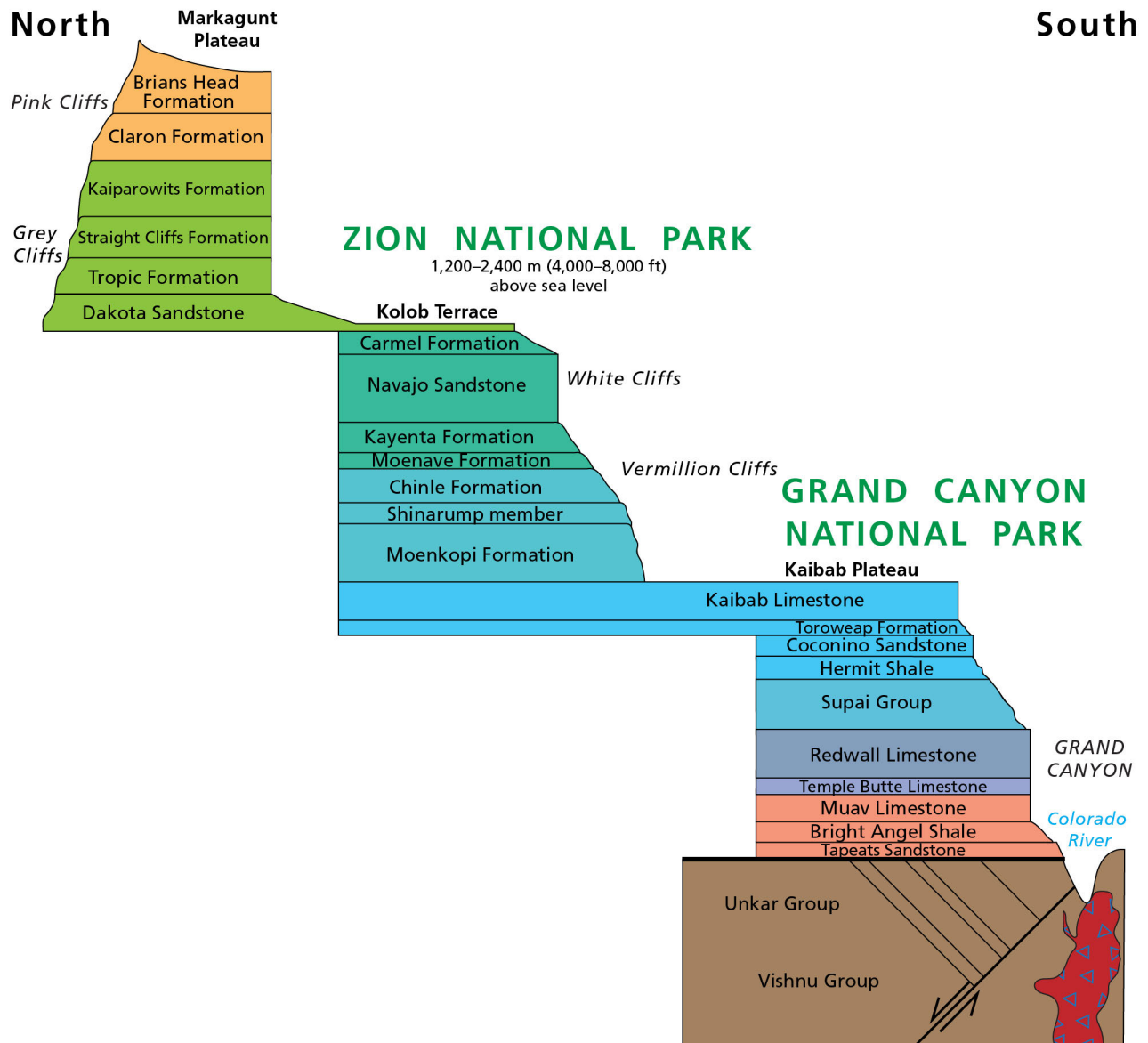


Figure 6. Cross section diagram of the Grand Staircase sedimentary sequence. North of Grand Canyon National Park consists of a series of alternating cliffs and plateaus that increase in elevation. Cliffs consist of rocks that resist erosion. Slopes form from more easily eroded strata. The Chocolate Cliffs, composed of the Moenkopi Formation, form the first erosional step north of Grand Canyon.

Morales 2003). In Grand Canyon National Park, Triassic strata are primarily exposed in the northernmost section of the park, south of Lees Ferry (Billingsley and Priest 2013). The erosional steps of the Grand Staircase continue northward into Zion National Park and Bryce Canyon National Park (fig. 6; Morales 2003; see the GRI reports by Thornberry-Ehrlich 2005 and Graham 2006).

The stairstep topography of the Grand Canyon resulted from differential erosion of the Paleozoic rocks. Typically, limestone, dolomite, and sandstone in arid and semi-arid climates erode very slowly compared to siltstone and shale, and in the Grand Canyon, these lithologies form cliffs while more easily eroded units form slopes. For example, slopes of the Cambrian Bright Angel Shale (**Cba**) separate the cliff-forming

sandstones of the underlying Tapeats Sandstone (**Ct**) from the overlying Muav Limestone (**Cm**).

The region south of Grand Canyon National Park does not have a general name like the Grand Staircase. The Kaibab Formation (**Pk**) caps the northern border of the vast Coconino Plateau (fig. 4) in the central and eastern portion of the Grand Canyon (Morales 2003). East of the South Rim's Desert View overlook, the Kaibab Formation is overlain by the Moenkopi Formation (**TRm**), which is capped by a resistant layer of Cenozoic volcanic rock (table 1). Triassic rocks are also preserved on the Marble Platform (fig. 4).

Faults and folds modify the landscape of the Colorado Plateau, including the Grand Canyon region (see the "Geologic Features and Processes" section). Because they are planes of weakness, faults have been reactivated throughout the geologic history of the canyon, especially during the past 60 million years. For example, Precambrian reverse faults, resulting from tectonic compression, have been transformed into normal faults because of more recent tectonic extension (fig. 7). The GRD GIS data include major faults, anticlines (convex folds), synclines (concave folds), and monoclines (one-limbed folds).

Monoclines are one of the signature characteristics of the Colorado Plateau (fig. 8). The monoclines in the Grand Canyon region began forming about 60 million years ago, during the Laramide Orogeny (Huntoon 2003). West–east compression deformed the Paleozoic and Mesozoic sedimentary rock layers, folding them over reactivated Precambrian faults (fig. 9). About 15 million years ago, during the Miocene Epoch, crustal extension transformed reverse faults into normal faults, accentuating the tilt of the sedimentary layers (fig. 9; Huntoon 2003).

The monoclines trend north–south, but are sinuous, often branching into segments that form an echelon patterns (see poster sheets 2 and 3). For example, the Hurricane monocline bifurcates into two parallel branches (Huntoon 2003). The East Kaibab monocline is the longest monocline in the region, extending north–south for approximately 300 km (190 mi) (Huntoon 2003). East–west spacing between monoclines ranges from 11 to 50 km (7 to 30 mi).

The morphology of side canyons branching from the main Grand Canyon reflects various combinations of stratigraphic and structural (folds and faults) controls, as well as surface and groundwater hydrology (Potochnik and Reynolds 2003). The side canyons thus offer excellent exposures of geologic features associated with tectonic deformation of the strata (see the "Geologic Features and Processes" section).

Exploration and Geologic Study of the Grand Canyon

Archeologists continue to discover evidence of the first humans to experience the Grand Canyon. Only a very small part of Grand Canyon National Park has been surveyed for archeological sites. Within the surveyed part of the park, over 3,500 known archeological sites exist. Details on the archeological resources, people, and cultures associated with the Grand Canyon are available on the park websites (<https://www.nps.gov/grca/learn/historyculture/arch.htm>; <https://www.nps.gov/grca/learn/historyculture/people.htm>) and the Arizona State University partner site (<http://grcahistory.org/>).

Ancestral Puebloans or Hisatsinom ("people who lived here long ago") occupied the area but abandoned the canyon, along with many other sites on the Colorado Plateau, about 700 years ago. Occupation patterns in the Grand Canyon are closely tied to climatic changes. In the recent past, Paiute, Hualapai, Navajo, and Hopi peoples built communities in the surrounding plateaus. The Havasu Village, in the western part of the park, may be one of the oldest, continuously occupied settlements in the conterminous United States. The Hopi Mesas, which are east of the park on the Navajo Reservation, contain the oldest continuously occupied village.

The first Europeans viewed the canyon in 1540 when Hopi guides led thirteen Spaniards who were looking for the fabled lost cities of gold to the South Rim. They were unable to reach the river and over the next three centuries, only two visits to the region by Europeans have been reliably recorded (Beus and Morales 2003).

Jules Marcou in 1856 and John Strong Newberry in 1861 were among the first geologists to explore the Grand Canyon and describe the region's Paleozoic strata. Newberry, a prominent 19th century geologist, traveled with Lieutenant Joseph Ives, who was exploring the lower Colorado River as a possible steamboat route. Ives was discouraged by the canyon, and in contrast to those who find the Grand Canyon magnificent, he reported that no other whites would probably visit such a "profitless locality" (Beus and Morales 2003).

Newberry became a staunch supporter of Major John Wesley Powell and wrote letters of recommendation to Congress encouraging financial support for Powell's exploration of the Grand Canyon (Stegner 1954). On 24 May 1869, John Wesley Powell, who had lost an arm at the Battle of Shiloh, left Green River, Wyoming, with four boats and a party of nine men. On 30 August, six men emerged from the Grand Canyon at the mouth of the Virgin River at what is today the north end of Lake Mead. Fearing that running the rest of the river was impossible, three of the explorers left the party at

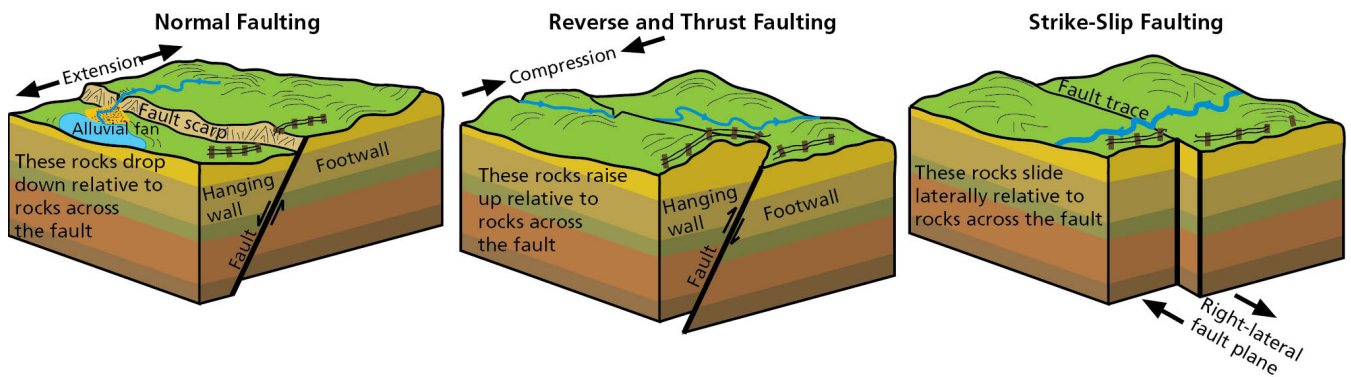


Figure 7. Schematic illustrations of fault types.

Footwalls are below the fault plane and hanging walls are above. In a normal fault, crustal extension (pulling apart) moves the hanging wall down relative to the footwall. In a reverse fault, crustal compression moves the hanging wall up relative to the footwall. A thrust fault is a reverse fault but has a dip angle of less than 45°. In a strike-slip fault, the relative direction of movement of the opposing plate is lateral. When movement across the fault is to the right, it is a right-lateral (dextral) fault, as illustrated above. When movement is to the left, it is a left-lateral (sinistral) fault. A strike-slip fault between two plate boundaries is called a transform fault. In the Grand Canyon region, thrust faults resulting from the Late Cretaceous Laramide Orogeny became normal faults during Miocene crustal extension. Graphic by Trista Thornberry-Ehrlich (Colorado State University).



Figure 8. Annotated photograph of the Grandview–Phantom monocline.

Photograph of the Grandview–Phantom monocline in the Grand Canyon viewed facing northwest from the Grandview Trail south of Horeshoe Mesa. Black arrows show movement direction along the plane of the fault (thick black line). Public domain photograph by James Stuby (user: Jstuby) available at https://commons.wikimedia.org/wiki/File:Grandview-Phantom_Monocline.jpg (accessed 16 June 2016).

Separation Rapid, climbed out of the canyon, and were murdered on the plateau (Stegner 1954).

Powell became a national hero, led a second Green and Colorado River expedition, and in 1881, became the second director of the fledgling US Geological Survey (USGS), an organization he helped establish.

Powell's interest in advancing geologic exploration of the West led to funding for a small group of outstanding geologists through the turn of the nineteenth century. These scientists included G. K. Gilbert, who was the first to apply formal rock unit names to the Grand Canyon rocks; C. E. Dutton, who wrote the first monograph on the geology and geologic history of the Grand Canyon; A. R. Marvine, a member of the USGS West of the 100th Meridian; and C. D. Walcott, who described both the Paleozoic and Precambrian rocks in the Grand Canyon's central and eastern sections (Dutton 1882; Gilbert 1874, 1875a, 1875b, 1877; Marvine 1874; Walcott 1880, 1883, 1889, 1890, 1892, 1894, 1899, 1910, 1918, 1920).

Edwin D. McKee became a premier research scientist of Grand Canyon geology in the twentieth century. McKee, who was the park naturalist for Grand Canyon National Park from 1929 to 1940, worked on the geology exhibits at the Yavapai Point Trailside Museum, which was built in 1928 on the South Rim of the Grand Canyon and re-dedicated in 2007 as the Yavapai Museum of Geology, and joined the faculty at the University of Arizona from 1942–1953 before continuing his illustrious career with the USGS. McKee authored or coauthored five monographs on various Paleozoic rock units of the canyon between 1931 and 1982. His seminal work provided the foundation to our present understanding of the stratigraphy and age of the Grand Canyon rocks (McKee 1932, 1933a, 1933b, 1937, 1938, 1939, 1944, 1945, 1947, 1963, 1974, 1975, 1976, 1979, 1982; McKee and Breed 1969; McKee and Gutschick 1969; McKee and McKee 1972; McKee and Nobel 1974, 1976; McKee and Resser 1945; McKee and Schenk 1942; McKee et al. 1967, 1968, 1971).

Miners began exploring the canyon in the late 19th century (see the “Geologic Features and Processes” section). The Grandview Mine, located 900 m (3,000 ft) below the South Rim, produced copper and uranium from 1893 to 1916 (Anthony et al. 1995). In 1893, prospector Daniel Hogan constructed a precarious trail consisting of ropes, wooden ladders, and toe steps 340 m (1,000 ft) below the South Rim and opened the Orphan Mine, reportedly named because Hogan grew up in an orphanage (Chenoweth 1986; Weinberger 2005). After 30 years of unrewarding mining, Hogan turned to tourism, as did the owners of the Grandview Mine and many other early Grand Canyon prospectors.

After Powell's journey down the Colorado River, Senator Benjamin Harrison unsuccessfully introduced a bill in 1887 to establish a national park in the Grand Canyon. As president, Harrison managed to establish the Grand Canyon Forest Preserve, which still left the area open to mining and logging.

Following a visit to the Grand Canyon in 1903, President Theodore Roosevelt was so impressed with the scenery and scientific potential that he established Grand Canyon National Monument in 1908 through the authority within the Antiquities Act (1906). In 1919, the monument was redesignated as a national park.

Two years before the monument was established, however, President Roosevelt gave Hogan, who was a member of Roosevelt's Rough Riders, ownership of 8 ha (20 ac) of the Grand Canyon, including 2 ha (4 ac) above the rim. The Orphan Mine remained unproductive until 1951 when prospectors discovered uranium in the stockpiles on the rim of the canyon. Uranium from the Orphan Mine soon helped fuel the Cold War.

Uranium produced from the Orphan Mine was four times higher than all other US sources. From 1956 to 1969, the Orphan Mine produced 495,107 tons of uranium oxide ore, almost 3,500 tons of copper, 1.6 tons of vanadium oxide, and 3.3 tons of silver, making it one of the most productive mines in the Southwest (Chenoweth 1986; Weinberger 2005).

The Orphan Mine closed in 1969 because of equipment failure, increased fuel costs, and decreased demand for uranium. A law signed by President John F. Kennedy in 1962 transferred ownership of the Orphan Mine to the National Park Service (Weinberger 2005).

Since Powell's trip down the Colorado River, several generations of geologists have worked at unraveling the last 2 billion years of Earth history from evidence exposed in the Grand Canyon. Decades of geological field work by George Billingsley culminated in a series of geologic maps that included the entire canyon (Billingsley 1974, 1989, 2000a, 2000b, 2003; Billingsley and Workman 2000; Billingsley and Wellmeyer 2004; Billingsley and Priest 2013; Billingsley et al. 1999, 2006a, 2006b, 2007, 2008, 2012). The Billingsley maps became the source maps for the GRI GIS map, which is the first digital, seamless, compiled geologic map of the Grand Canyon and surrounding area. Designation of Grand Canyon National Park as a World Heritage Site came in 1979 because of the stunning landscape, labyrinthine topography, myriad geologic features, vast geologic record, and diverse ecosystems.

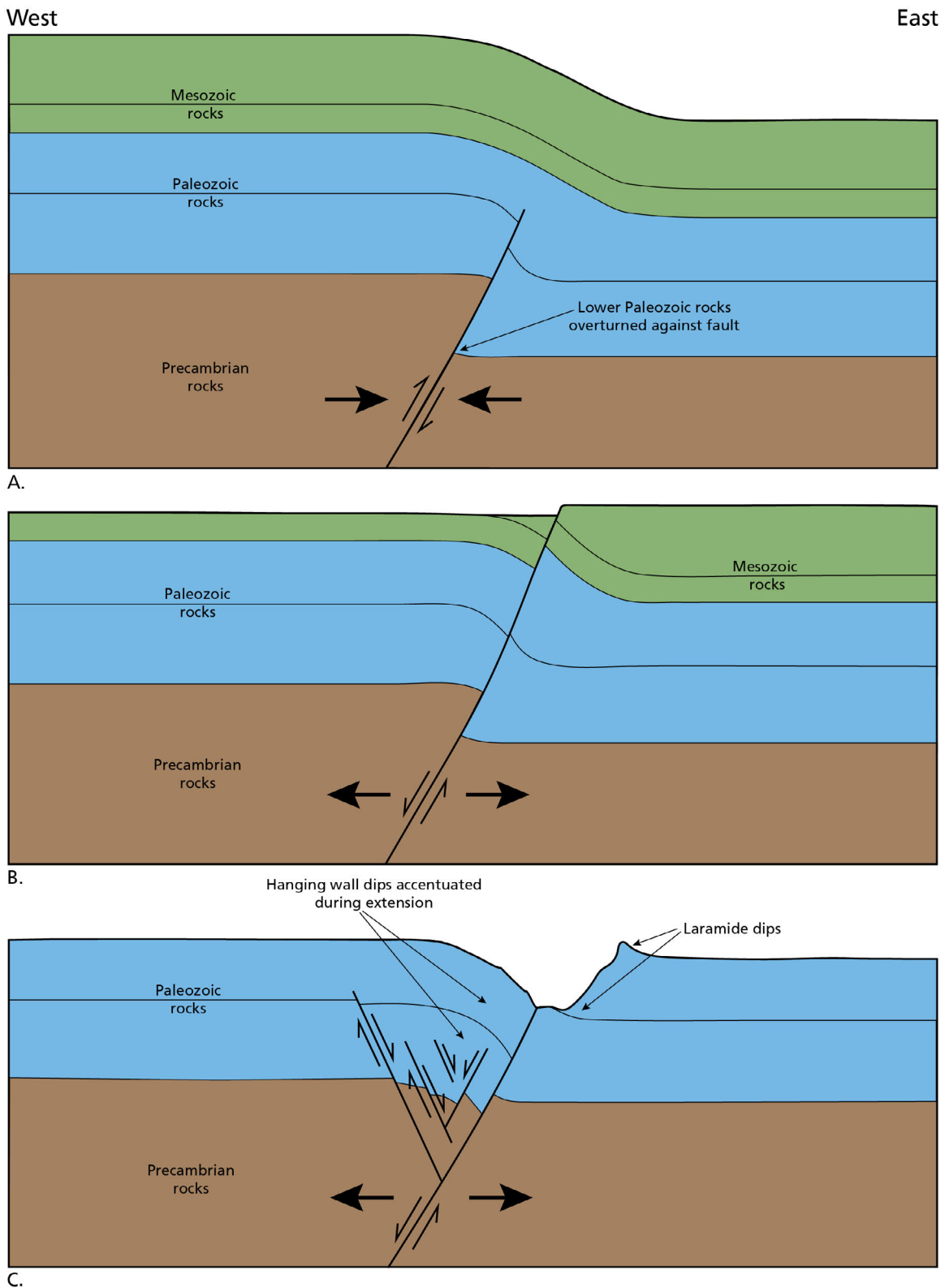


Figure 9. Stages in the formation of a monocline in the Grand Canyon region. (A) Sedimentary rock layers fold over a reactivated Precambrian normal fault. (B) Normal faulting in the Cenozoic offsets the stratigraphic layers. Erosion has removed some of the layers. (C) Continued extension of the crust generates a zone of normal faults. Schematic by Trista Thornberry-Ehrlich (Colorado State University), modified from Huntoon (2003, fig. 14.5).

Geologic Features and Processes

These geologic features and processes are significant to Grand Canyon National Park's landscape and history.

During the 2001 scoping meeting held at Grand Canyon National Park (National Park Service 2001) and the November 2015 conference call, participants (see Appendix A) identified the following geologic features and processes in the park:

- Landscape
- Sedimentary Rock and Features
- Igneous Rock and Features
- Granite Gorge Metamorphic Rock and Features
- Paleontological Resources
- Caves, Karst, and Springs
- Unusual Minerals
- Breccia Pipes and Ore Deposits
- Unconformities
- Folds and Faults
- Features in Side Canyons
- Desert Varnish
- Geomorphic Features and Unconsolidated Deposits
- Geologic Type Sections

According to the Grand Canyon National Park foundation document, geologic features, geologic processes, paleontological resources, and cave resources are fundamental resources (NPS 2010).

Landscape

From the vast panoramas viewed from the canyon rim to the roaring rapids of the Colorado River, Grand Canyon National Park offers an exceptional landscape filled with a myriad of iconic geologic features. Visitors approach the Grand Canyon from three general directions: (1) the canyon rim, (2) trails, and (3) the Colorado River. Each of these perspectives provides opportunity to view features of varying scale and age.

Features Viewed from the Rim

Colorful bluffs, mesas, buttes, spires, canyons, and a myriad of other spectacular landscape features dominate the view from the North and South Rims in Grand Canyon National Park. These features characterize the Colorado Plateau and differ from one another primarily in area. A plateau is usually higher and more extensive than a mesa, which is more extensive than a butte. Smaller yet are the temple-like spires, such as Zoroaster and Brama temples (fig. 1). Part of the greater Colorado Plateau, Grand Canyon National Park

includes six smaller plateaus within its borders (fig. 4). Persistent erosion whittled some of the original plateaus and mesas into buttes and spires.

Overlooks along the rims of the Grand Canyon also offer superb views of the series of cliffs, ledges, and slopes that form the stairstep topography of the canyon walls (fig. 10). For example, slopes formed in the less erosion resistant Hermit Formation (**Ph**) separate cliffs composed of resistant Coconino (**Pc**) and Esplanade (**Pe**) sandstones. In the Cambrian Tonto Group, slopes of Bright Angel Shale (**Cba**) are sandwiched between the cliffs of Muav Limestone (**Cm**) and Tapeats Sandstone (**Ct**). Smaller erosional steps formed in units containing alternating layers of sandstone, siltstone, limestone, and shale, such as the Mississippian Surprise Canyon Formation (**Ms**) and the Pennsylvanian Wescogame Formation (**PNMs**; table 1).

The transition from resistant rock units to less resistant units often reflect a change in ancient depositional environments and relative sea levels, as well as a change in lithology. For example, the slope-forming fossiliferous mudstone of the Bright Angel Shale (**Cba**) represents a relative sea level rise that allowed a shallow, muddy marine environment to inundate the previous sandy, coastal environment of the Tapeats Sandstone (**Ct**). The well-circulated, open marine environments of the cliff-forming Redwall Limestone (**Mr**) also represent transgression of the sea over the more restricted, shallow marine, ledge- and slope-forming Temple Butte Formation (**Dtb**) (fig. 11). See the “Sedimentary Rocks” section for more information about lithology and original depositional environment.

In western Grand Canyon, volcanic features seen from the rim include hardened basaltic lava flows that once cascaded over the rim of the canyon to form lava dams during the last million years and volcanic cinder cones, like Vulcan's Throne near Toroweap Overlook, that punctuate the landscape of the North Rim (fig. 12; poster sheet 2; Hamblin 2003). Basalt that erupted onto the Uinkaret Plateau (**Qb**) flowed over Moenkopi (**TRm**), Kaibab (**Pk**), and Toroweap (**Pt**) formations about 100,000–200,000 years ago. The Tuckup Canyon Basalt (**Qtb**) erupted about 760,000 years ago and today clings to canyon walls of the Supai Group (**Pe**, **PNMs**). The solidified basaltic magma formed lava falls frozen in time (fig. 12). See the “Igneous Rocks” section for more information about volcanoes and other rocks that formed from molten material.



Figure 10. Photograph from the South Rim of the historic Yavapai Observation Station. The station is now called the Yavapai Geology Museum. More erosion-resistant strata form cliffs and benches; strata less resistant to erosion form slopes. Inside the museum, exhibits include explanations of the rock layers, the uplift of the Grand Canyon, and the carving of the Grand Canyon. NPS photograph by Michael Quinn, available at https://www.flickr.com/photos/grand_canyon_nps/5446830720/in/album-72157626052533148/.

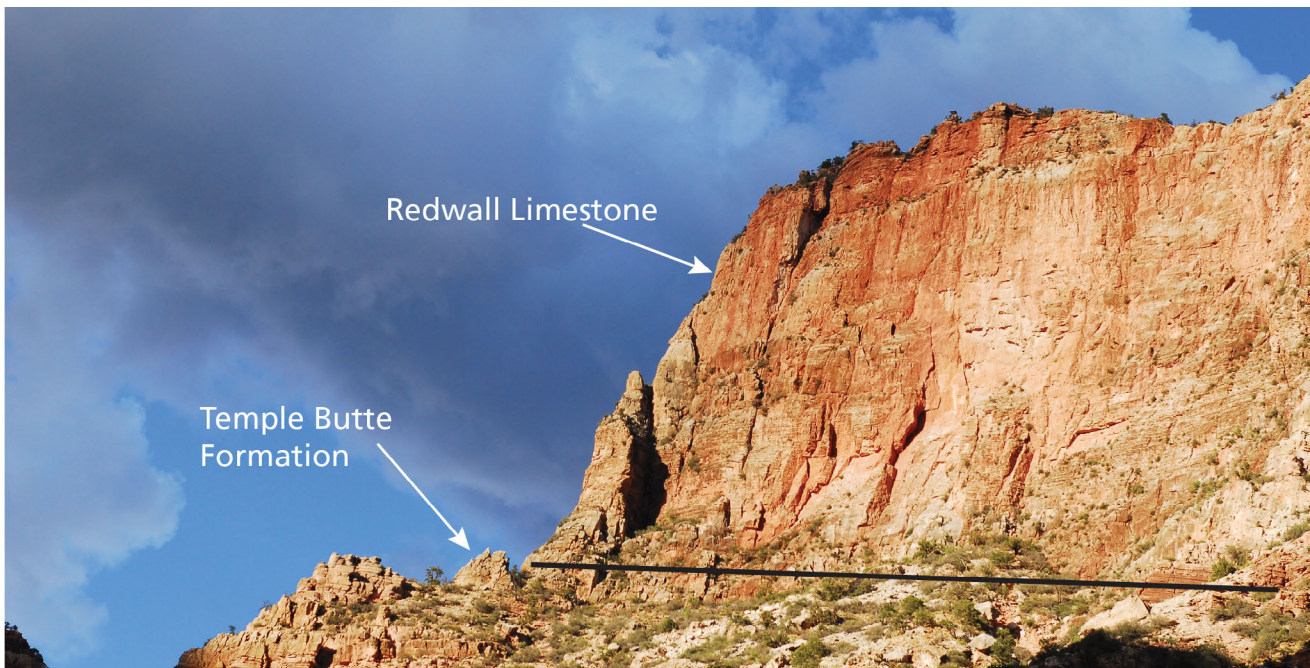


Figure 11. Photograph of the Redwall Limestone and Temple Butte Formation. A cliff of Redwall Limestone overlies a slope composed of the Temple Butte Formation. The Redwall Limestone represents a sea level rise that inundated the shallow marine mudstone, sandstone, and dolomite of the Temple Butte Formation. Upon lithification, the marine carbonates of the Redwall Limestone became more resistant to erosion than did the mixed lithologies of the Temple Butte Formation. NPS photograph by Kristen M. Caldron, available at https://www.flickr.com/photos/grand_canyon_nps/7706752936/in/album-72157630889521118/.

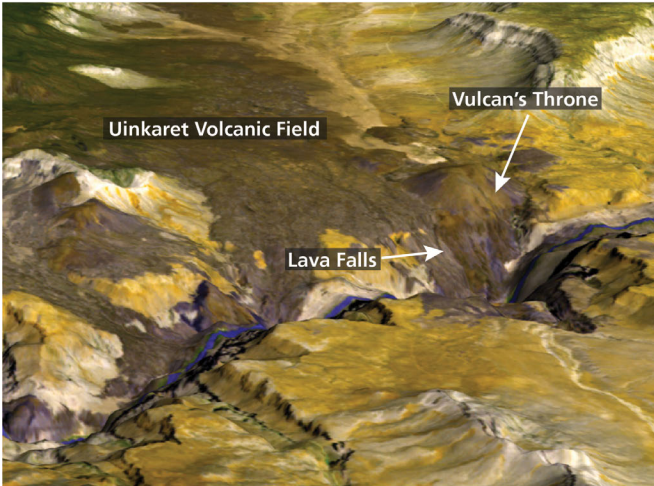


Figure 12. Photographs of Vulcan's Throne. About 73,000 years ago, basalt lava flows from Vulcan's Throne and other volcanic vents in the Uinkaret volcanic field spilled over the rim of the Grand Canyon and dammed the Colorado River. The lava cooled and solidified in situ, resulting in the lava falls that capture the initial flow patterns. Top photograph by Dale Nations, Northern Arizona University, available at <https://azgs.arizona.edu/photo/vulcans-throne-uinkaret-volcanic-field-north-rim-grand-canyon>. Bottom image courtesy of NASA Earth Observatory, available at https://eoimages.gsfc.nasa.gov/images/imagerecords/7000/7521/grandcanyon_ast_2003123_lrg.jpg.

Although access to Toroweap Overlook is challenging, the overlook offers a rare vertical view from the rim to the Colorado River (fig. 13). At 880 m (2,900 ft) above the river and less than 1.6 km (1 mi) across the canyon to the Hualapai Indian Reservation on the South Rim, Toroweap Point is also one of the narrowest and deepest segments of the Inner Gorge. The Esplanade Sandstone caps the cliff at Toroweap Point, and the light red to pinkish-gray sandstones contrast with the underlying black, basaltic lava flows.

Views along the rim in eastern Grand Canyon offer glimpses of the oldest rocks in the park, which are best viewed from the Colorado River (see below). Exposed in the Inner Gorge, Precambrian metamorphic and igneous rocks provide a record of the growth of the North American continent, especially from 1.8 billion to 1.6 billion years ago.

Overlooks along the rim also offer expanded views of geological structures, such as folds and faults that bend and displace the rock layers. For example, layers of rock at Sinking Ship, a promontory located approximately 3 km (2 mi) east of Grandview Point and visible along East Rim Drive (South Rim), dip gently to the northeast and are an expression of the Grandview Monocline, (fig. 8; map poster sheet 3). A popular trail that begins at the South Rim follows the northeast-southwest trace of another structural feature, the Bright Angel Fault, which formed Bright Angel Canyon (fig. 14).

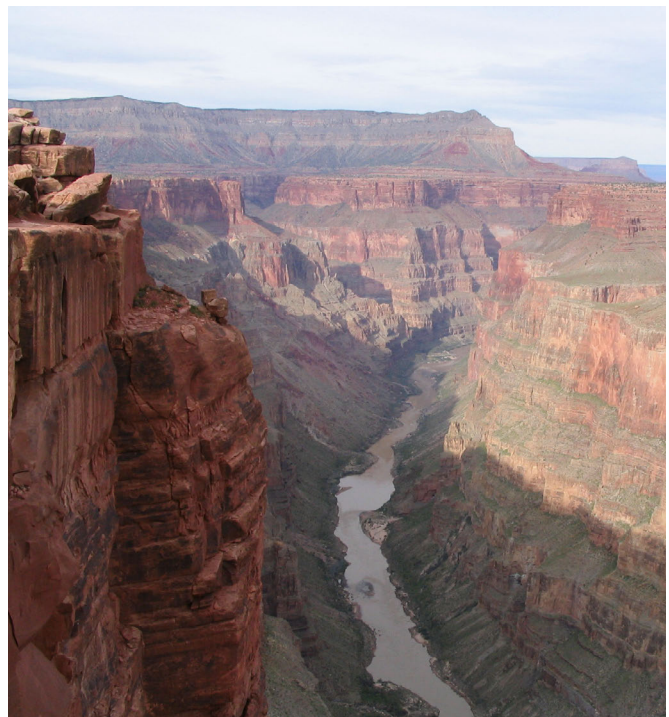


Figure 13. Photograph of the Grand Canyon from Toroweap Overlook. Toroweap Overlook offers the rare view from the rim to the bottom of the canyon and the Colorado River. Photograph by Ken Lund, available at <https://www.flickr.com/photos/kenlund/66044184/in/album-1426070/>, licensed under CC BY-SA 2.0 (<https://creativecommons.org/licenses/by-sa/2.0/>).



Figure 14. Photograph of Bright Angel Canyon and Bright Angel Trail. The Bright Angel Fault (arrow) is responsible for Bright Angel Canyon. Strata on the west wall of the fault (left side of the photograph) are about 50 m (150 ft) higher than the strata on the east side. Hikers (lower right) on this part of the trail are between the first and second tunnels from the trailhead. NPS photograph by Michael Quinn, available at https://www.flickr.com/photos/grand_canyon_nps/6924503615/in/album-72157624199151598/.

Features Viewed along the Trails

The trails expose a detailed geologic history of Earth spanning almost 2 billion years from rim to river. Many sedimentary rock features, such as cross-bedding, ripple marks, and mud cracks are visible from a close inspection of the individual rock layers along the trails (see the “Sedimentary Rock” section). These features are critical to interpreting past depositional environments. For example, the large-scale, sweeping cross-beds in the Coconino Sandstone (**Pc**) preserve an ancient eolian dune field (fig. 15).

Fossil vertebrate tracks (ichnofossils) are also exposed in the Coconino Sandstone along the Hermit Trail and Dripping Springs Trail (fig. 16). Like sedimentary rock features, fossils found in the layers also help identify past environments (paleoenvironments) and past climates (paleoclimate). In contrast to the terrestrial trackways, invertebrate fossils, such as the brachiopods, crinoids, conodonts, and sponges preserved in Paleozoic carbonate strata exposed along the South Kaibab Trail, represent past marine environments. Grand Canyon National Park also preserves excellent examples of stromatolites, the oldest fossils preserved in the park (see the “Paleontological Resources” section). Stromatolites are composed of layers of limy sediment trapped and bound by mats of cyanobacteria (blue-green algae).

Trails in the Inner Gorge traverse Precambrian rocks that represent the very basement of North America in this part of the continent (fig. 17). The rocks formed

under intense heat and pressure beneath thousands of feet of younger sedimentary rocks. Erosion has since exposed these rocks along the Colorado River. In Grand Canyon National Park, hikers get the rare opportunity to rest their feet on rocks that formed as much as 1.7 billion years ago.

Features Viewed from the Colorado River

A view from the Colorado River contrasts nearly 2-billion-year-old rocks with recently deposited sediments (fig. 18). Proterozoic-age Vishnu (**Xv**), Rama (**Xr**), and Brahma (**Xbr**) schists of the Granite Gorge Metamorphic Suite overlie the gneiss of the Elves Chasm pluton (**Xec**). The Elves Chasm pluton, at 1.84 billion years old, is the oldest rock in the park and the oldest in southwestern United States (table 1; fig. 17; see the “Granite Gorge Metamorphic Rocks” section). From the river, the juxtaposition of the Granite Gorge Metamorphic Suite against the tilted strata of the Grand Canyon Supergroup and the relatively horizontal beds of Tapeats Sandstone (**Ct**) can be seen in greater detail than from the rim. Contacts between these rock units form Powell’s Great Unconformity (see the “Unconformities” section).

More recent landscape features seen along the Colorado River include rapids and associated debris fans, eddy pools, and riffles (fig. 19). Boulders attest to the power of flash floods and debris flows (see the “Geomorphic Features” section). Remnants of lava dams exposed for a considerable section of the



Figure 15. Photograph of cross-bedding in the Coconino Sandstone.

The inclined beds (lines in the rock) are foreset beds of ancient sand dunes. The upper and lower contacts of one cross-bed set are marked with green lines. The foreset beds have been truncated by younger sand dunes that migrated across the older dune field. The dark surface stain is desert varnish, explained in the “Desert Varnish” section. NPS photograph by Kristen M. Caldon, available at https://www.flickr.com/photos/grand_canyon_nps/7695154984/in/album-72157628887117233/.

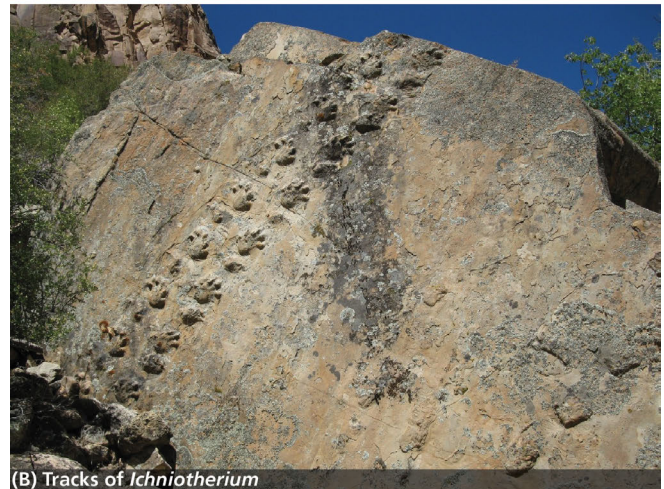
Grand Canyon downstream of the Toroweap area record prolonged eruptions of basalt and subsequent catastrophic outburst floods when the dams failed (fig. 12). Basalt-rich sediments in the river channel remain from these flood events (Hamblin 2003; Fenton et al. 2004; see the “Igneous Rock” section).

Potochnik and Reynolds (2003) describe a wide range of geological features exposed in the side canyons and visible from the river, as well. For example, the narrow cleft of North Canyon at river mile (RM) 20 exposes curved fractures and bedding surfaces in the Esplanade Sandstone (Pe) of the Supai Group. River miles refer to the distance along the Colorado River from Lees Ferry. Downstream from North Canyon, numerous fossils of chambered nautiloids are found in Nautiloid Canyon, a narrow canyon incised into the Redwall Limestone (Mr). Thick purplish lenses of Devonian Temple Butte Limestone (Dtb) exposed between Redwall (Mr) and

Muav (Cm) limestones in Buck Farm Canyon record episodes of marine regression, erosion, and subsequent transgression during the Devonian–Mississippian periods (see “Sedimentary Rocks” section). The gently tilted beds of Tapeats Sandstone (Ct) abruptly bend vertically along a local fold caused by the regional Butte Fault (see the “Folds and Faults” section). The side canyons to the Grand Canyon reveal these and a myriad of other features to river travelers (see the “Side Canyons” section).



(A) Tracks of *Chelichnus*



(B) Tracks of *Ichniotherium*

Figure 16. Photographs of fossilized vertebrate tracks in the Coconino Sandstone.

(A) Tracks of *Chelichnus* found on the Hermit Trail. *Chelichnus* is the most common tetrapod footprint in Coconino ichnoassemblages. NPS photograph by Michael Quinn, available at https://www.flickr.com/photos/grand_canyon_nps/7464100790/in/album-72157628887117233/. (B) In 2013, the tracks of *Ichniotherium* were discovered in a block of Coconino Sandstone along Dripping Springs Trail. These tracks are the geologically youngest record of the ichnogenus. Photograph courtesy of Vincent Santucci, NPS paleontologist.



Figure 17. Photograph of Zoroaster Granite. The basement rocks in Grand Canyon consist of Zoroaster Granite, which formed about 1.8 billion years ago as part of the Elves Chasm pluton (Xec). Minerals in the granite are primarily biotite (flashy surfaces), pink feldspar, dark, tabular hornblende, and gray quartz. NPS photograph by Kristen M. Caldon, available at https://www.flickr.com/photos/grand_canyon_nps/8227983514/in/album-72157628916922939/.

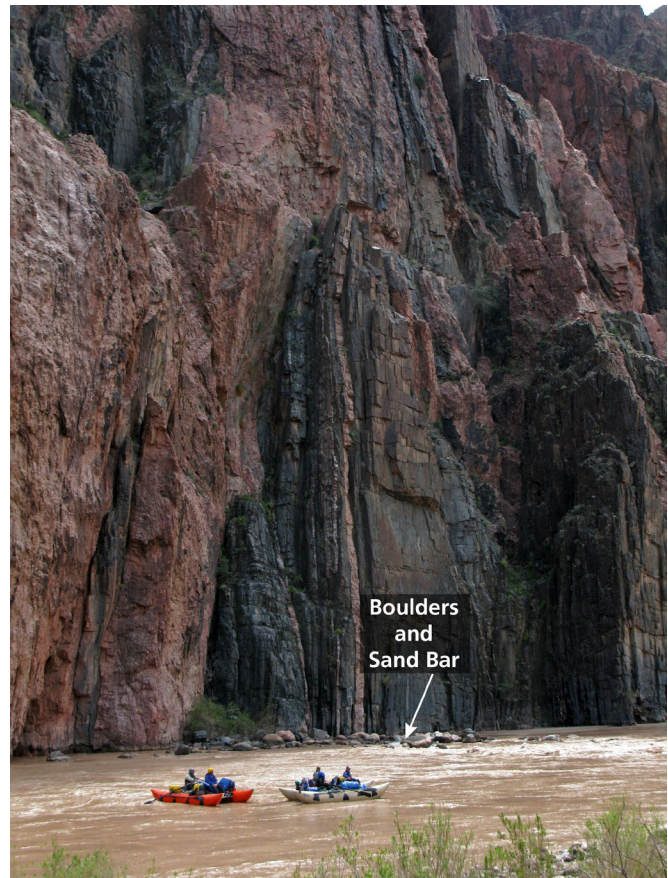


Figure 18. Photograph of the Vishnu Schist. Rafters pass sheer cliffs of Vishnu Schist (Xv) near the confluence of the Colorado River and Bright Angel Creek. About 1.75 billion years ago metamorphism transformed submarine sedimentary rocks into the Vishnu Schist. Recent deposits include the boulders and sand bar at the base of the cliff. The boulders are responsible for the rapids. NPS photograph by Michael Quinn, available at https://www.flickr.com/photos/grand_canyon_nps/6177013790/in/album-72157628916922939/.



Figure 19. Photograph of Crystal Rapid.

Recent geomorphic features include rapids, a debris fan that has constricted the width of the channel, and riffles downstream from the rapids. The debris fan will also cause the depth of the restricted channel to increase. The photograph was taken at low water flows in October 2012. NPS photograph by Kristen M. Caldron, available at https://www.flickr.com/photos/grand_canyon_nps/8241267165/in/album-72157626635172217/.

Sedimentary Rock and Features

John Wesley Powell (1875, p. 212) described the canyon walls as,

a thousand feet of crystalline schists, with dikes of greenstone, and dikes and beds of granite. . .above them we can see beds of hard, vitreous sandstone of many colors, but chiefly dark red.

As Powell noted in 1875, Grand Canyon National Park contains all three of the basic rock types: sedimentary, igneous, and metamorphic. Geologists have developed sophisticated classification schemes for each rock type, but only general classification schemes based on the physical texture of the rock are used in this report. By doing so, the rock type and associated features can be readily identified in the field.

Sedimentary rocks may be classified as clastic, chemical, or organic (table 5). Clastic sedimentary rocks are the products of weathering, erosion, transportation, and deposition of rock fragments called “clasts” (fig. 20). Clasts may consist of inorganic grains, such as sand or clay, and the classification of these rocks is based on grain size. In Grand Canyon National Park, examples of inorganic clastic sedimentary rocks include the Moenkopi Formation (**TRm**), Coconino Sandstone (**Pc**), and Tapeats Sandstone (**Ct**) (fig. 15, 21a). In sedimentary rocks consisting of calcium carbonate, such as the Redwall Limestone (**Mr**) and Kaibab Formation (**Pkh**, **Pkf**), the clasts may be fossil fragments (fig. 20b). In this case, the carbonate sedimentary rock is classified according to the abundance and texture of the fragments (table 5). Chemical sedimentary rocks form when ions, such as calcium and carbonate, precipitate out of water or when freshwater evaporates, leaving salts (table 5). Examples of evaporite deposits include gypsum, found in the Woods Rance Member

Table 5. Sedimentary rock classification and characteristics.

Claystones and siltstones can also be called “mudstone,” or if they break into thin layers, “shale.” Carbonate classification is based on Dunham’s textural classification scheme (Dunham 1962).

Rock Type	Rock Name	Texture and Process of Formation	Park Example (map symbol)
INORGANIC CLASTIC SEDIMENTARY ROCKS*	Conglomerate (rounded clasts) and Breccia (angular clasts)	Cementation of clasts >2 mm (0.08 in) in size. Higher energy environment (e.g. rivers).	Conglomerate: Chinle Formation, Shinarump Member (TRcs) Breccia: Bass Formation (Yb)
	Sandstone	Cementation of clasts 1/16–2 mm (0.0025–0.08 in) in size.	Coconino Sandstone (Pc)
	Siltstone	Cementation of clasts 1/256–1/16 mm (0.00015–0.0025 in) in size.	Moenkopi Formation Wupatki Member (TRmw)
	Claystone	Cementation of clasts <1/256 mm (0.00015 in) in size. Lower energy environment (e.g. floodplains).	Bright Angel Shale (Cba)
CARBONATE CLASTIC SEDIMENTARY ROCKS*	Fossiliferous Limestone	Generic name for carbonate rock containing fossils.	Kaibab Formation (Pkh, Pkf)
	Boundstone	Fossils, fossil fragments, or carbonate mud fragments cemented together during deposition (e. g. reefs).	Rare in the park.
	Grainstone	Grain (e.g., fossil fragments) supported with no carbonate mud. High energy environment. Components cemented together following deposition.	Redwall Limestone Thunder Springs Member (Mr)
	Packstone	Grain (e.g., fossil fragments) supported with some carbonate mud. Lower energy than grainstone. Components cemented together following deposition.	Redwall Limestone Thunder Springs Member (Mr)
	Wackestone	Carbonate mud supported with more than 10% grains and less than 90% carbonate mud. Lower energy than packstone. Components cemented together following deposition.	Kaibab Limestone Fossil Mountain Member (Pkf)
	Mudstone	Carbonate mud supported with less than 10% grains and more than 90% carbonate mud. Lower energy than wackestone. Components cemented together following deposition.	Redwall Limestone Whitmore Wash Member (Mr)
CHEMICAL SEDIMENTARY ROCKS	Limestone (Carbonate Mud)	Generic name. Formed by the precipitation of calcium (Ca) and carbonate (CO_3^{2-}) ions from water (e. g. lakes or marine environments).	Redwall Limestone Moomey Falls Member (Mr)
	Travertine	Precipitation of calcium (Ca) and carbonate (CO_3^{2-}) ions from freshwater (e. g. terrestrial springs).	Travertine deposits (Qt)
	Dolomite	Precipitation of calcium (Ca), magnesium (Mg), and carbonate (CO_3^{2-}) ions from water. Direct precipitation in shallow marine environments or post-depositional alteration by Mg-rich groundwater.	Redwall Limestone Whitmore Wash Member (Mr)
	Chert	Dissolution of siliceous marine skeletons (e.g. sponge spicules) followed by precipitation of microcrystalline silica. Biochemical chert typically forms from marine invertebrates.	Kaibab Limestone Fossil Mountain Member (Pkf)
	Evaporites (i.e., gypsum)	Precipitation of salts to form evaporite minerals. Typical of hot, dry environments.	Toroweap Formation Woods Ranch Member (Ptw)
	Oolite	Precipitation of calcium carbonate in thin spherical layers around an original particle (e.g., fossil fragment) that is rolled back and forth by tides or waves. Typical of warm, shallow marine environments.	Redwall Limestone Horseshoe Mesa Member (Mr)
ORGANIC SEDIMENTARY ROCKS	Coal	Peat (partly decomposed plant matter) is buried, heated, and altered over time. Typical of lagoon, swamp, and marsh environments.	Dakota Sandstone (Kd) (not mapped in the park)

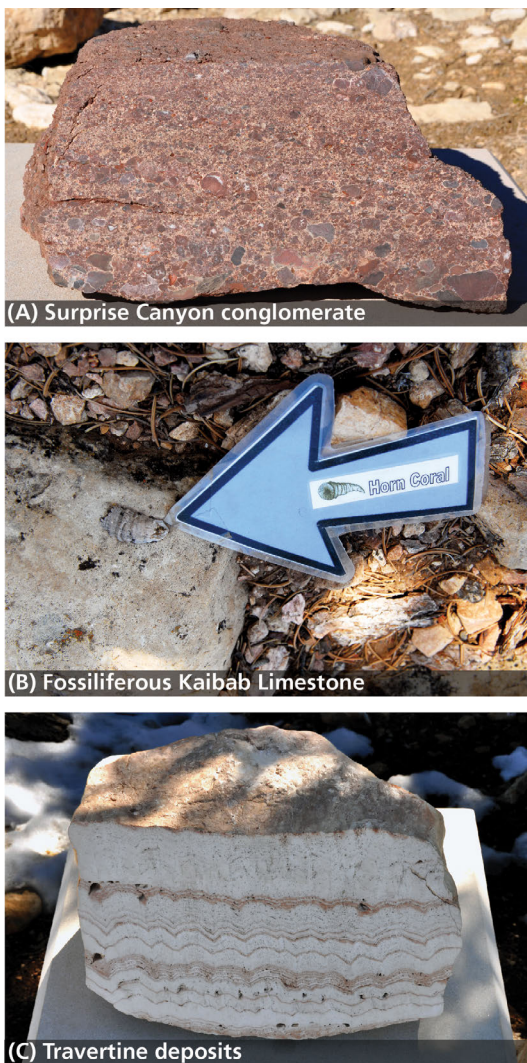


Figure 20. Photographs of some sedimentary rock types found within Grand Canyon National Park. (A) Inorganic clastic sedimentary rocks are represented by the conglomerate of the Surprise Canyon Formation (Ms), which contains pebble-size inorganic clasts. NPS photograph available at https://www.flickr.com/photos/grand_canyon_nps/6529413003/in/album-72157629974795528/. (B) Fossils, such as those found in the Kaibab Formation, form carbonate clastic sedimentary rocks. NPS photograph by Kristen M. Caldon, available at https://www.flickr.com/photos/grand_canyon_nps/7706174560/in/album-72157630888156792/. (C) Precipitation of calcium carbonate, often at the mouth of a hot spring, forms chemical sedimentary rocks such as travertine. NPS photograph available at https://www.flickr.com/photos/grand_canyon_nps/6528738721/in/album-72157629974795528/. (A) and (C) are from the Grand Canyon Trail of Time, an interpretive walking trail that focuses on Grand Canyon’s vistas and rocks.

of the Toroweap Formation (**Ptw**) and travertine in unconsolidated deposits (**Qt**) (fig. 20c). Organic sedimentary rocks are composed of organic remains, such as the plant material that formed the coal beds identified in the Dakota Sandstone (**Kd**), which is present on the Colorado Plateau but not mapped in the park.

A layer of sedimentary rock that has consistent internal characteristics that distinguish it from adjacent layers is known as a “stratum” (plural: “strata”). The strata that form the cliffs and slopes, mesas and buttes, and other prominent landscape features in Grand Canyon National Park are composed primarily of sedimentary rock (fig. 21).

Sedimentary rock features help define the various depositional environments that occupied northern Arizona during the vast span of time represented by the rocks in the Grand Canyon. These features preserved in strata represent the same natural processes that shape the contemporary landscape, a principle in geology known as the Principle of Uniformitarianism. In this report, the features are associated with six general environments of deposition and associated processes (table 6):

- Eolian,
- Mass wasting,
- Fluival-floodplain,
- Intertidal-to-marginal marine,
- Subtidal-to-nearshore, and
- Marine environments.

The abundance, diversity, and type of fossils as sedimentary features contribute to the interpretation of past depositional environments and processes, but fossils also represent a significant fundamental resource in Grand Canyon National Park. They are discussed in the “Paleontological Resources” section.

Eolian Features

Eolian processes refer to wind-blown erosion, transportation, and deposition of sediments (Lancaster 2009). Features created by eolian processes include depositional landforms and deposits such as dunes, loess (wind-blown silt-size sediment), and sand sheets, as well as erosional forms such as desert pavement, yardangs, and ventifacts (see “Glossary”). The NPS Geologic Resources Division Aeolian Resource Monitoring website, go.nps.gov/geomonitoring provides additional information.

As they do today (see the “Geomorphic Features” section), eolian processes in the past winnowed fine-grained clay and silt from accumulations of sand and

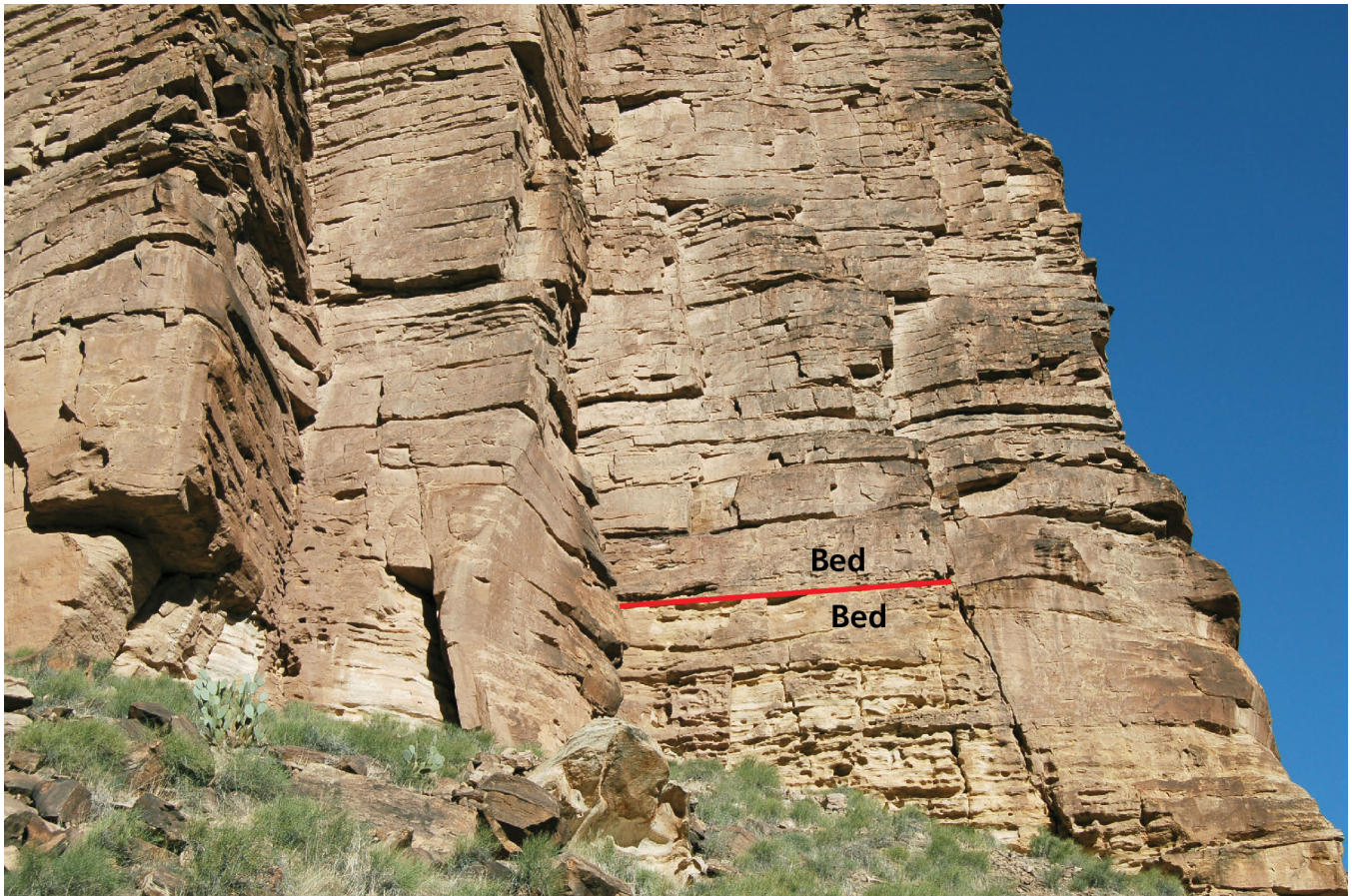


Figure 21. Photograph of cliffs composed of Tapeats Sandstone. Paleozoic strata form most cliffs and slopes in the park. In this photo, the Tapeats Sandstone (Ct) forms a topographic break above slopes of Sixtymile Formation (Zs). Strata are composed of a series of “beds” of various thickness. Two beds, and the contact between them, are highlighted in the diagram. Contacts between beds represent a change in depositional processes (e.g., erosion, fluctuating sea level, migrating river or eolian systems). Modified from NPS photograph by Michael Quinn, available at https://www.flickr.com/photos/grand_canyon_nps/8238194937/in/album-72157630889786616/.

Table 6. Sedimentary rock features identified in Grand Canyon National Park.

Feature		Process/Depositional Environment	Formation (map symbol)
Eolian Features	High-angle cross-bedding and well-sorted sand grains	Wind winnows finer-grained sediment to produce well-sorted migrating sand dunes.	Coconino Sandstone (Pc) Esplanade Sandstone (Pe) Wescogame Formation (PNMs) Manakacha Formation (PNMs)
	Low-relief wind ripple marks in well-sorted sandstone	Secondary wind currents that migrate sand grains across sand dune slopes.	Coconino Sandstone (Pc)
	Amphibian tracks on cross-bedded sandstone surfaces	Terrestrial vertebrate tracks in an arid environment.	Coconino Sandstone (Pc)
Mass Wasting	Boulders, large blocks of rock, breccia, and/or contorted bedding	Mass wasting processes (e. g. slumps, landslides), resulting from earthquakes and fault movement.	Sixtymile Formation (Zs)

Table 6, continued. Sedimentary rock features identified in Grand Canyon National Park.

Feature		Process/Depositional Environment	Formation (map symbol)
Fluvial-Floodplain Features	Interbedding and combinations of reddish-brown mudstone, siltstone, and cross-bedded sandstone (trough and low-angle cross-beds), a basal conglomerate layer, asymmetrical ripple marks, mud cracks, salt crystal casts, raindrop impressions, and thin veins of gypsum	Sandstones and conglomeratic sandstones deposited in fluvial channels form trough-like cross-beds. Asymmetrical ripples indicate unidirectional current flow. Reddish beds, mud cracks, and raindrop impressions indicate subaerial exposure and are common on floodplains and mudflats. Salt crystal casts, mud cracks (desiccation cracks), and gypsum suggest an arid climate.	Chinle Formation (TRcs) Moenkopi Formation (TRmu, TRms, TRmlm, TRmw) Hermit Formation (Ph) Esplanade Sandstone (Pe) Wescogame Formation (PNMs) Surprise Canyon Formation (Ms) Tapeats Sandstone (Ct) Sixtymile Formation (Zs) Kwagunt Formation (Zkcb) Nankoweap Formation (YZn) Dox Formation (Ydo, Yds)
	Vertebrate bones and/or tracks	Terrestrial animal remains	Surprise Canyon Formation (Ms)
	Plant fossils, petrified logs, and/or wood fragments	Terrestrial plant remains	Chinle Formation (TRcs) Hermit Formation (Ph) Supai Group (Pe, PNMs) Surprise Canyon Formation (Ms)
Intertidal/Marginal Marine	Soft-sediment deformation (convolute bedding)	Water-escape features from compaction of semi-consolidated sediment common in floodplains and shallow marine environments. Caused by rapid deposition or tectonic activity.	Kwagunt Formation (Zkcb) Nankoweap Formation (YZn) Dox Formation (Yde) Shinumo Quartzite (Ys)
	Low angle cross-bedded sandstone	Coastal and nearshore environments influenced by wave, tidal, and storm currents.	Kaibab Formation (Pkh) Esplanade Sandstone (Pe) Wescogame Formation (PNMs) Manakacha Formation (PNMs) Shinumo Quartzite (Ys) Hakatai Shale (Yh)
	Planar beds of gypsum, dolomite, and/or calcareous siltstone	Tidal flat, near-shore, supratidal, or restricted marine environments in an arid climate.	Toroweap Formation (Ptw) Temple Butte Formation (Dtb) Galeros Formation (Zgd, Zgcc)
	Interference (herringbone) and/or symmetrical ripple marks, mudcracks, salt casts, and/or raindrop impressions	Tidal and mud flats, beaches, or estuaries dominated by tides and waves that reflect bi-modal flow.	Surprise Canyon Formation (Ms) Tapeats Sandstone (Ct) Kwagunt Formation (Zka, Zkcb) Galeros Formation (Zgcc, Zgj) Dox Formation (Ydc, Yde) Hakatai Shale (Yh) Bass Formation (Yb)
	Cyclic interbeds that include some combination of fossiliferous limestone, algal laminations, fossil fragments (fossil "hash"), cherty limestone, mudstone, gypsum, and/or calcareous sandstone	Alternating near-shore, marine environments representing episodic transgressions (sea level rise) and regressions (sea level fall) in an arid climate.	Kaibab Formation (Pkh, Pkf) Toroweap Formation (Ptw, Ptb)

Table 6, continued. Sedimentary rock features identified in Grand Canyon National Park.

Feature		Process/Depositional Environment	Formation (map symbol)
Subtidal to Nearshore	Cross-bedded sandstone with near-vertical burrows and/or conglomerate-filled channels	Inter- to subtidal channels oriented perpendicular to the shore that eroded into underlying strata and then filled with sediment.	Temple Butte Formation (Dtb) Tapeats Sandstone (Ct)
	Oolitic limestone	Subtidal, shallow marine conditions with high-energy, back-and-forth currents that produce spherical grains (oolites).	Redwall Limestone (Mr) Kwagunt Formation (Zkw)
	Low-angle cross-bedded and ripple-laminated limestone	Shallow marine; nearshore conditions.	Redwall Limestone (Mr)
	Fining- and coarsening-upward conglomerate, cross-bedded sandstone, and mudstone	Subtidal sequences reflecting tidal (fining-upward) and storm (coarsening-upward) processes.	Bright Angel Shale (Cba)
	Ripple-laminated, fossiliferous shale, trace fossils, green siltstone, and/or glauconitic sandstone	Low-energy, subtidal to tidal currents. Green glauconite is a diagnostic mineral of marine depositional environments.	Bright Angel Shale (Cba)
	Flat-pebble conglomerates (disc-like clasts of carbonate mud)	Early cementation of rip-up clasts from tidal flats, tidal channels, or subtidal deposits during storms.	Muav Limestone (Cm)
	Brecciated dolomite, sandy dolomite, laminated dolomite	Shallow subtidal, intertidal, and supratidal environments.	Kwagunt Formation (Zkw) Galeros Formation (Zgt) Bass Formation (Yb)
	Dome-shaped (bioherm) or planer-bedded stromatolites	Subtidal to intertidal to supratidal conditions.	Kwagunt Formation (Zka, Zkw) Galeros Formation (Zgcc, Zgj) Dox Formation (Ydc) Bass Formation (Yb)
	Marine Features	Bottom-dwelling, shallow marine to open marine invertebrate fossils in fine-grained limestone and dolomite	Marine environments ranging from nearshore to subtidal to offshore, open marine and further defined by the abundance and diversity of fossil types; environments are often interlayered due to rise and fall of sea level.
Limestone and cherty limestone		Deep marine environments (below wave base) with normal salinity.	Watahomigi Formation (PNMs) Redwall Limestone (Mr)
Black shales and fossiliferous black shales		Deep marine environments (well below wave base).	Kwagunt Formation (Zka, Zkw) Galeros Formation (Zgt)

rolled and bounced and shaped the remaining well-sorted sand grains into dunes with high-angle foreset (front or lee side) slopes approaching the angle of repose. Ancient sand dunes with high-angle cross-beds of well-sorted sand grains are preserved in the Coconino Sandstone (**Pc**) and the Supai Group (fig. 15; table 6).

Sand dunes in the Permian Coconino Sandstone were part of an enormous sand desert (erg) that extended from Arizona north into Montana (Middleton et al.

2003). The sweeping foreset beds in this Sahara-like desert dip at an average of 25° and are as much as 24 m (80 ft) long, although most are less than 12 m (40 ft) long. In addition to sweeping crossbed sets, features include wind-generated ripple marks on the sloped dune surfaces and fossilized tracks of vertebrates (fig. 16) and insects (spiders) (Middleton et al. 2003). The only exposures of Coconino Sandstone in Grand Canyon National Park occur in Marble Canyon (Billingsley and Priest 2013; map poster sheet 1).

Cross-stratified sandstone units and wind ripples in the Manakacha (**PNMs**) and Wescogame (**PNMs**) formations and the Esplanade Sandstone (**Pe**) are also regarded as eolian deposits (Middleton et al. 2003). However, the heterogeneous lithology of the Supai Group presents a more complex origin to these eolian units compared to the homogeneous Coconino Sandstone (Blakey et al. 1988; Middleton et al. 2003). The sandstone units are not as widespread as the Coconino and this geometry, coupled with the high carbonate content and locally abundant sand-sized marine fossil grains, suggests a more coastal setting. Gypsum deposits in the Esplanade Sandstone support an arid coastal or sabkha environment.

The non-eolian redbeds, conglomerates, limestone, and sandstones in the formations may have originated from several environments, such as fluvial, shoreline, or shallow marine, that impinged on the eolian dune field (Middleton et al. 2003). The Supai Group in Grand Canyon National Park contains features common to all these possible depositional environments that intersected with the coastal dunes (table 6).

Mass Wasting Features

Mass wasting refers to processes associated with slope movements that transfer soil, regolith, and/or rock downslope under the influence of gravity. Soil creep, rockfalls, debris flows, and avalanches are common types of mass wasting processes. Except for debris flows, which result from flash flooding, slope movements are commonly grouped as “landslides.” Slope movements and mass wasting events occur on time scales ranging from seconds to years.

In Sixtymile Canyon, the lower part of the Sixtymile Formation (**Zs**) contains large (10-m [30-ft] scale) gravity slide blocks encased in shale and slump deposits (Ford and Dehler 2003; Timmons et al. 2003). These blocks consist of underlying Chuar Group formations that dislodged and tumbled or slumped down the east limb of the Chuar syncline, a broad trough-shaped fold that developed during the Proterozoic with movement along the Butte Fault, which was reactivated in the Cambrian (table 6; Karlstrom et al. 2018; GRI GIS data; map poster sheet 2).

Processes triggering mass wasting events have been occurring for millions of years. The Sixtymile Formation mass wasting deposits resulted from seismic (earthquake) activity and fault movement that occurred over 500 million years ago during the final breakup of the supercontinent Rodinia (Timmons et al. 2003; Karlstrom et al. 2018). Modern mass wasting events continue to modify the canyon and the channel of

the Colorado River (see the “Geomorphologic Features” section).

Fluvial–Floodplain Features

A combination of sedimentary features document deposition common to river systems (table 6). For example, the Triassic Moenkopi Formation (**TRmu**) contains overbank deposits of fine-grained clay and silt deposited in ancient floodplains adjacent to trough-shaped channels in which coarser material, such as sand grains and pebbles accumulated and solidified into trough cross-bedded sandstone. Grain size becomes an important feature in these mixed environments because transportation of larger clasts requires higher stream energy compared to finer grained sediment. Asymmetrical ripples indicate unidirectional stream flow with the gradual slope on the upstream side.

On the floodplains, desiccation cracks (mudcracks) formed when sediment dried, and delicate raindrop impressions represent precipitation on semi-consolidated sediment (fig. 22). Preservation of more fragile sedimentary features, such as raindrop impressions, usually requires burial by successive flood sediments before disturbance by organisms can occur. Lenses of conglomerate and thin veins of gypsum in the Moenkopi Formation suggest that the fluvial system interacted with possible tidal flats (Morales 2003).



Figure 22. Photograph of mudcracks in the Hakatai Sandstone.

These Precambrian mudcracks record fine-grained sediment deposited in an arid environment. Mudcracks commonly form on floodplains or mudflats. Combined with other sedimentary features, the mudcracks in the Hakatai Sandstone suggest deposition on a coastal mudflat (Hendricks and Stevenson 2003). NPS photograph by Carl Bowman, available at https://www.flickr.com/photos/grand_canyon_nps/8230702894/in/album-72157632128995235/.

Rapid burial by flood sediments or quiet deposition in lakes and lagoons may preserve both plant and animal remains. Vertebrate fossils, plant impressions (fig. 23), petrified logs, and animal tracks are features that identify terrestrial environments, and in Grand Canyon National Park, these features are found with other sedimentary features associated with fluvial–floodplain environments in the Chinle Formation (**TRcs**), Surprise Canyon Formation (**Ms**), and the Hermit Formation (**Ph**) (table 6).

Fluvial features continue to form in the canyon (see the “Geomorphic Features” section); however, the features represented by Mesozoic, Paleozoic, and Precambrian sedimentary rocks record river systems prior to the incision of the Grand Canyon. In narrow canyons with limited areal extent, such as the Grand Canyon, preservation of fluvial features in unconsolidated sediments is very rare.



(A) Impressions of a fern



(B) Dragonfly wing

Figure 23. Photographs of Hermit Formation fossils. (A) is a fern impression and (B) is a dragonfly wing. Terrestrial plant remains, such as the fossil fern, may be preserved in floodplain environments. Photograph (A) by NPS, Michael Quinn, available at https://www.flickr.com/photos/grand_canyon_nps/4749637616/in/album-72157624268517977/. Photograph (B) courtesy of Vincent Santucci, NPS paleontologist.

Intertidal–Marginal Marine Features

Some features found in fluvial environments, such as mudcracks, salt casts, and raindrop impressions, are also found in tidal and mud flats and other marginal marine or nearshore environments (fig. 22; table 6). Ripple marks found in these environments tend to be symmetrical, rather than asymmetrical, with the angle of the slopes on each side of the crest being about equal. Symmetrical ripples suggest a bi-directional flow, as is common with waves on a beach or tidal influences (fig. 24). Low-angle cross-bedded sandstone is also common in coastal environments and reflects processes in tidal channels or shallow streams. In arid climates, evaporation may result in thin beds of gypsum.

Cyclic sequences of fossiliferous limestone, siltstone, sandstone, black organic shale, dolomite, and/or gypsum in the Kaibab (**Pkh** and **Pkf**) and Toroweap (**Ptw** and **Ptb**) formations characterize marginal marine or nearshore depositional environments and represent cycles of transgression and regression.



Figure 24. Photograph of ripple marks in the Hakatai Shale (Yh). The symmetry of these 1,180 million-year-old Precambrian ripples and fine-grained sediment suggests a low-energy, wave-influenced depositional environment such as a coastal mudflat. NPS photograph from the Grand Canyon Trail of Time, an interpretive walking trail that focuses on Grand Canyon’s vistas and rocks, available at https://www.flickr.com/photos/grand_canyon_nps/6529425909/in/album-72157629974795528/.

Soft-sediment deformation features, such as the contorted and convoluted bedding in the upper part of the Shinumo Quartzite (**Ys**), are common in both fluvial and coastal environments. In general, these features result from rapid burial and subsequent compaction of semi-consolidated, water-saturated sediments. With rapid compaction, water is forced

upward and out of the unit, deforming the strata. Rapid sedimentation may result from flooding, storm surges, and tectonic activity, which may generate earthquakes, liquefaction, fault movement, and/or tsunamis. Often, contorted bedding is overlain by undisturbed, relatively horizontal layers, suggesting that the deformed beds characterize a relatively short-lived episode that was followed by a return to previous depositional processes. Commonly, soft-sediment deformation occurs in non-metamorphosed sedimentary rock. In the case of the Shinumo Quartzite, however, the association between metamorphism and soft-sediment deformation is not known.

Subtidal-to-Nearshore Features

Sedimentary features characteristic of marine environments help to differentiate various depths, circulation patterns, and rise and fall of sea level (table 6). For example, cross-bedded sandstone, vertical burrows, and a dearth of fossil material, such as is found in the Temple Butte Formation (**Dtb**) and Tapeats Sandstone (**Ct**), are common features found in subtidal channels that erode and scour the underlying sediments, making the habitat difficult for most organisms. When the channels subsequently fill with sediment, subsurface organisms burrow upward to maintain their surface access. Because subtidal channels are oriented perpendicular to the shore, they can be used to reconstruct the regional coastline. Oolitic limestone, a feature of the Redwall Limestone (**Mr**), characterizes subtidal, warm, shallow marine environments where high velocity currents move clasts back-and-forth along the ocean bottom. Calcium carbonate that precipitates from warm ocean water coats the clasts, and the constant movement shapes the particles into spheres, known as oolites (fig. 25). Oolites form today in the warm seawater along the coastlines of Caribbean islands.

Minerals may also be used to distinguish marine from fresh water environments and deep from shallow water. Glauconite (also known as “green sand”), a constituent of the Bright Angel Shale (**Cba**), only forms in seawater, especially on the continental shelf. Dolomite often precipitates in subtidal, intertidal, and supratidal environments, although it may also form as an alteration product of deep-water limestone. The brecciated, sandy dolomite of the Precambrian formations in Grand Canyon National Park record deposition in shallow, nearshore marine environments (table 6).

The abundance, diversity, and type of fossils also play a significant role in determining marine depositional environments. Today, for example, stromatolites grow in the hypersaline seawater of Shark Bay, Australia. Depending on the depth of the water, stromatolites

form different shapes, from domes and columns in deeper water to planar, horizontal layers in very shallow water. Precambrian stromatolites in the Grand Canyon region record similar shallow, nearshore, subtidal to intertidal to supratidal environments (fig. 26; table 6).

Restricted marine environments often contain a low faunal diversity. Often trace fossils (trails, tracks, or burrows), such as those found in the Bright Angel Shale (**Cba**), are the only recognizable features preserved in the fine clay and silt deposited in these restricted, low-energy, subtidal environments (fig. 27).



Figure 25. Photographs of modern and ancient oolites. (A) Modern oolites from Joulter’s Cay, The Bahamas. Public domain photograph by Mark A. Wilson, Department of Geology, The College of Wooster, available at <https://commons.wikimedia.org/wiki/File:JoultersCayOoids.jpg>. (B) Ooid-rich limestone from the Middle Jurassic Carmel Formation of southern Utah. Public domain photograph by Mark A. Wilson, Department of Geology, The College of Wooster, available at <https://commons.wikimedia.org/wiki/File:OoidSurface01.jpg>.

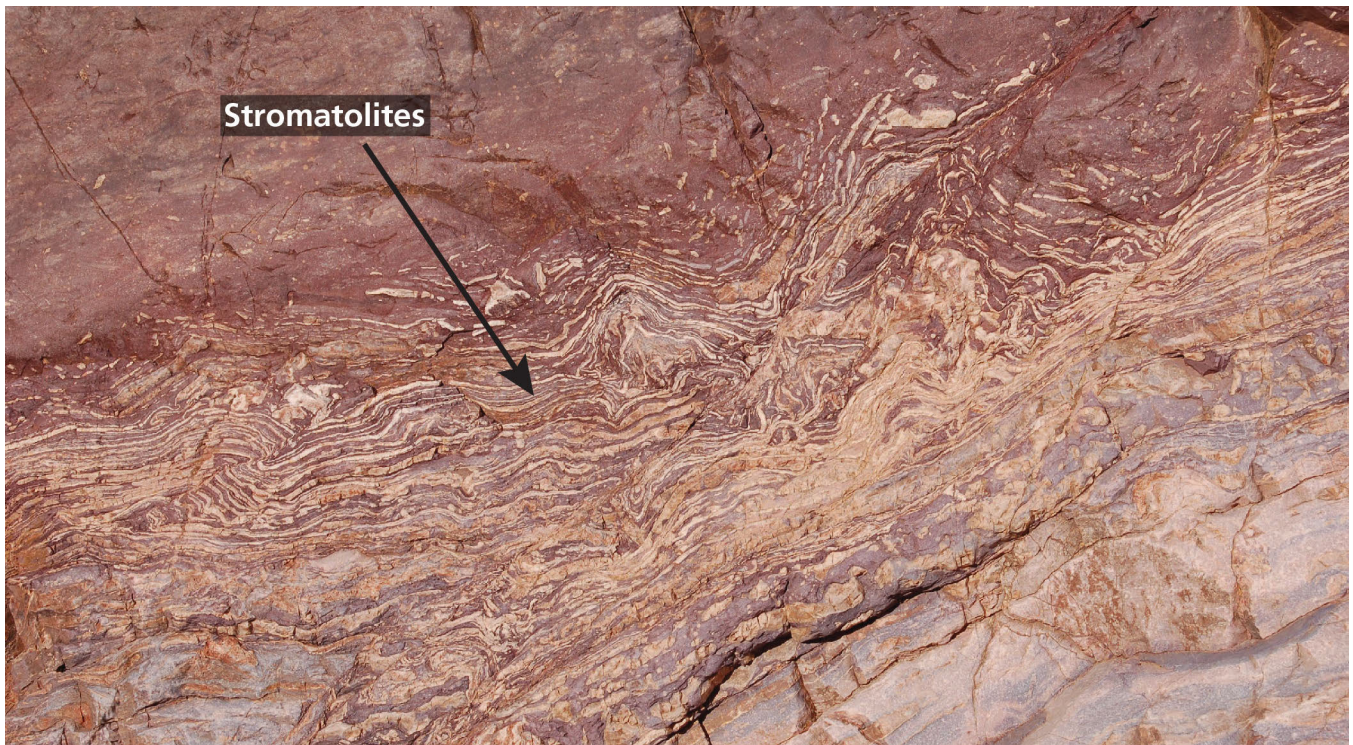


Figure 26. Photograph of stromatolites in the Mesoproterozoic Bass Formation (Yb). Stromatolites are among the oldest fossils in the world. Their presence indicates deposition in a warm, shallow marine environment. NPS photograph by Carl Bowman, available at https://www.flickr.com/photos/grand_canyon_nps/8230702544/in/album-72157632128995235/.



Figure 27. Photograph of fossil worm trails in the Bright Angel Shale, Tonto Plateau. NPS photograph by Michael Quinn, available at https://www.flickr.com/photos/grand_canyon_nps/4748971457/in/album-72157624268517977/.

Marine Features

The abundant and diverse invertebrate fauna found in Paleozoic limestones in Grand Canyon National Park document open, well-circulated marine environments (table 6). The fauna includes brachiopods, bryozoans, crinoids, sponges, and solitary corals such as the horn corals found in the Fossil Mountain Member of the

Kaibab Formation (Pkf) (fig. 20, fig. 28; Hopkins and Thompson 2003). Brachiopods and trilobites, which dominated the Cambrian seas, are the most common invertebrates in the Tonto Group, although sponges, algae, echinoderms, and gastropods have also been found (Middleton and Elliott 2003).



(A) Trilobite in the Bright Angel Shale



(B) Brachiopod in the Redwall Limestone



(C) Bryozoa in the Redwall Limestone



(D) Crinoid column from the Kaibab Limestone

Figure 28. Photographs of invertebrate fossils in Paleozoic limestones, Grand Canyon National Park. (A) Trilobites in the Bright Angel Shale (Cba). (B) Brachiopod in the Redwall Limestone (Mr). (C) Bryozoan in the Redwall Limestone (Mr). (D) Crinoid stems from the Kaibab Limestone (Pk). Trilobites, brachiopods, bryozoans, and crinoids suggest well oxygenated, open marine environments. NPS photographs by Michael Quinn, available at https://www.flickr.com/photos/grand_canyon_nps/sets/72157624268517977.

The widespread distribution of black shales, such as those in the Tanner Member of the Galeros Formation (**Zgt**), narrows the list of potential marine depositional environments. Black shales typically record anoxic environments in which organic matter and clay-sized particles settle through the water column and accumulate on the sea floor, conditions common to deep ocean basins. Black shales in the Tanner Member contain fossils of the small, disc-shaped algae *Chuarina circularis* and are interbedded with thin layers of silt and sand transported into the area during storms (Ford and Dehler 2003). Geologists have interpreted the unit as either a deep marine environment or a sediment-starved basin rich in organic material (Reynolds and Elston 1986; Ford and Dehler 2003). The shallow water features in the overlying Jupiter Member (**Zgj**) and

Carbon Canyon Member (**Zgcc**) (table 6) suggest that the Galeros Formation represents an overall regression (sea level lowering) that took place over 740 million years ago in the Grand Canyon area.

The upper part of the Awatubi Member (**Zka**) and most of the Walcott Member (**Zkw**) of the Kwagunt Formation (**Zk**) include thin-bedded, organic-rich, sulphur-bearing, black shales. The black shales represent an overall transgression (sea level rise) in the region. As sea level rose, *Chuarina*-bearing black shales of the uppermost Awatubi Member (**Zka**) and the younger Walcott Member (**Zkw**) were deposited over the shallow marine features found in the basal Carbon Canyon Member (**Zkcb**) and lower part of the Awatubi Member (fig. 29; Ford and Dehler 2003).

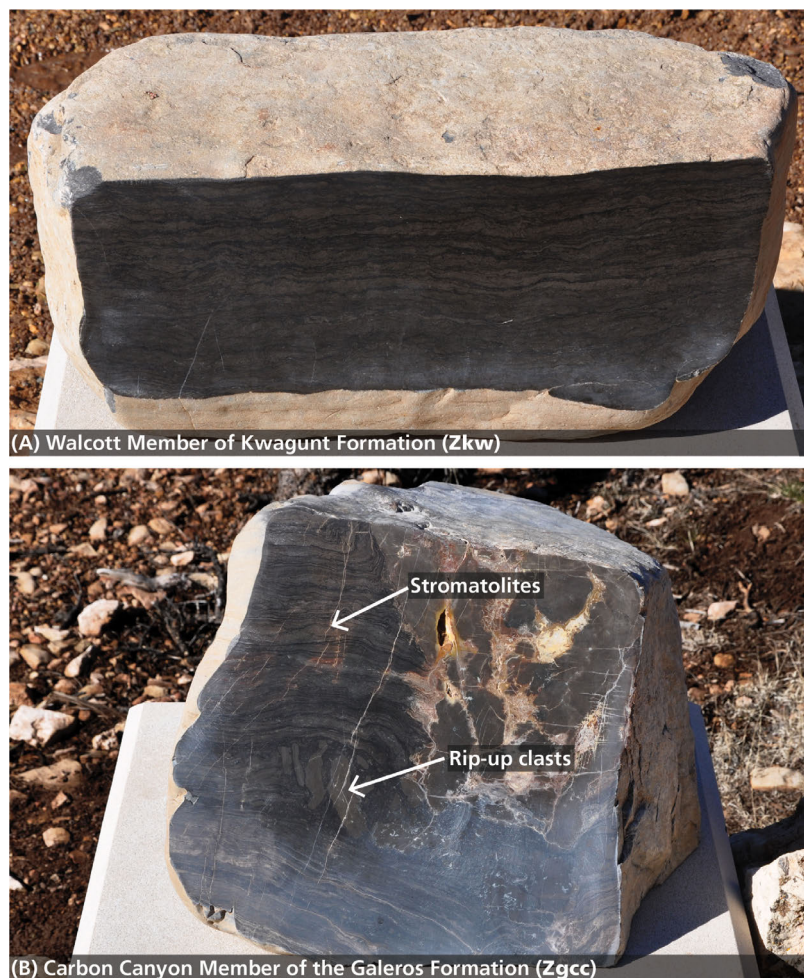


Figure 29. Photographs of sedimentary features that signal a change in sea level. (A) Fine-grained silt and mud that formed the dark shale of the Walcott Member of the Kwagunt Formation (Zkw**) was deposited in a deep marine setting. The relatively horizontal layers reflect deposition in quiet, non-turbulent water. (B) In contrast, the Carbon Canyon Member of the Galeros Formation (**Zgcc**) contains rip-up clasts and stromatolites that suggest shallow marine depositional environments that supported the formation of algal mats and were influenced by waves and/or tides that disturbed the semi-consolidated sediment. NPS photographs by Erin Whitakker from the Trail of Time, available at https://www.flickr.com/photos/grand_canyon_nps/sets/72157629974795528/.**

Lithology, stable carbon isotope ratios, and fossil (plankton) material indicate that the Awatubi and Walcott Members were deposited in either an anaerobic marine basin at depths >150 m (490 ft) or a restricted hypersaline, anaerobic epeiric (shallow) sea (Wiley et al. 1998, 2002). These zones were toxic to benthic organisms so that, upon death, plankton that had been living in the surface aerobic water layer were preserved when they settled to the anaerobic depths of the basin.

In Sixtymile Canyon, which contains the thickest sections of organic-rich layers of both members, the 139 m (456 ft)-thick Awatubi Member contains a minimum of 3 m (10 ft) and a maximum of 108 m (355 ft) of gas-prone source rock potential (Wiley et al. 2002). The 248 m (814 ft)-thick Walcott Member exhibits potential for both oil and gas, containing from 60% to 100% of potential source rock (Wiley et al. 2002).

Igneous Rock and Features

John Wesley Powell (1875, p. 213) remarked

This region of country was fissured, and the rocks displaced so as to form faults, and through the fissures floods of lava were poured, which, on cooling, formed beds of trap, or greenstone. This greenstone was doubtless poured out on the dry land, for it bears evidence of being eroded by rains and streams.

Igneous rocks form by the cooling of molten magma. Magma that cools and solidifies in the subsurface becomes internal, or plutonic, igneous rock. Cooling masses of intrusive magma develop into rock bodies of various sizes, ranging from regional-sized batholiths and slightly smaller plutons, such as those responsible for the Sierra Nevada, to linear rock bodies, such as dikes and sills (fig. 30). Magma, erupting onto the surface as molten lava, cools quickly into external, or volcanic, igneous rock (named for Vulcan, the ancient Roman god of fire).

Classification schemes for igneous rocks vary (table 7). One common classification scheme used in the field to identify igneous rocks focuses on the relative percentages of the minerals quartz, alkali feldspar, and plagioclase present in the rock. Using relative percentages does not require a rigorous chemical analysis of the rock. Igneous rocks containing abundant quartz and feldspar, such as the Precambrian granitic rocks (**Yg**, **Xg**, **Xgr**) and the Tertiary Hualapai Plateau rhyolite (**Tv**), are high in silica (table 7) and typically lighter in color. These rocks are also termed “felsic” igneous rocks, a name derived from their primary minerals feldspar and silica (fig. 31). Darker-colored igneous rocks with less felsic minerals generally have a higher abundance of minerals containing magnesium and iron (ferric), such as pyroxene, olivine, and biotite (fig. 31). These rocks are referred to as “mafic” igneous rocks and include the many Quaternary or Tertiary basalts in the park (table 7).

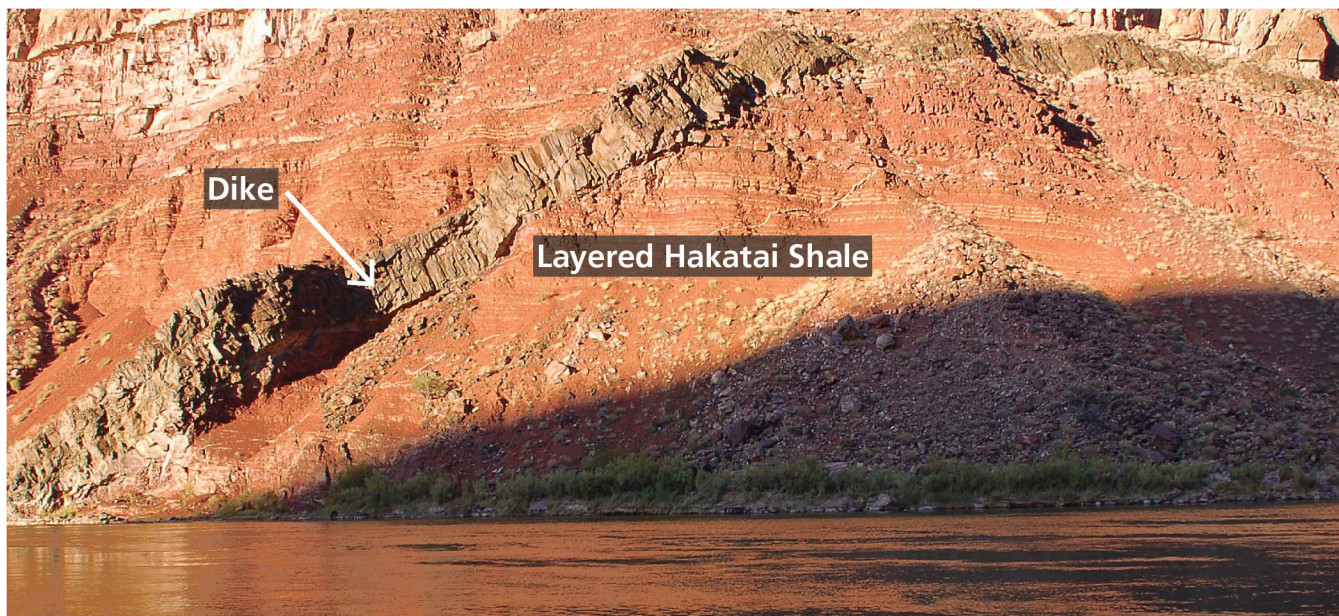


Figure 30. Photograph of a dike intruded into the layered sedimentary rock of the Hakatai Shale (Yh) at Hance Creek.

The dike is composed of gabbro, the plutonic equivalent of basalt. NPS photograph by Carl Bowman, available at https://www.flickr.com/photos/grand_canyon_nps/8229638717/in/album-72157632128995235/.

Table 7. Igneous rock classification for igneous rocks exposed in Grand Canyon National Park.

* Classifications and percentages are based on the Quartz-Alkali Feldspar-Plagioclase (Q-A-P) triangle diagrams (Hyndman 1972).

Igneous Rock Name		Properties*	Unit in Park (map symbol)
External Igneous Rocks (Volcanic)	Rhyolite	Very light color, low density, with >90% quartz. Primary phenocrysts: feldspar, quartz, biotite, hornblende.	Hualapai Plateau rhyolite (Tv) Mount Floyd Volcanic Field (Tri)
	Rhyodacite	Contains >10% quartz and subequal amounts of plagioclase and alkali feldspar. The extrusive equivalent of granodiorite.	Mount Floyd Volcanic Field (Tri)
	Andesite	Blackish-brown or greenish with 5–20% quartz. Primary phenocrysts: plagioclase and biotite.	Dikes of Colorado River Mile 202 (T2i)
	Basalt	Very dark to black, high density, with <5% quartz. Formed from magnesium- and iron-rich magma. Rare phenocrysts of olivine, plagioclase, and pyroxene. Hyaloclastites form when basalt contacts fresh water or shallow salt water, instantly cools, and forms an extensively fractured, completely vitreous (glassy) rock. The extrusive equivalent of gabbro.	Tuckup Canyon Basalt (Qtp, Qtb, Qtid) Basalt of Hancock Knolls (Qhp, Qhb) Basalt dikes and necks (Qidn) Pyroclastic deposits (Qpyr) Basalt flows along the Colorado River (Qbcr) Basalt of Uinkaret Plateau (Qb, Qi) Basalt north of Mount Emma (Teb) Whitmore Dike Swarm (Twb) Shivwits Basalt (Tsi, Tsb) 227-Mile intrusive (T227i) Dikes of Parashant Canyon and Hundred and Ninety-six Mile Creek (Tp6i) Dikes of Colorado River Mile 202 (T2i) Snap Point basalt (Tsgj, Tsgb) Hualapai Plateau basalt (Ti, Tv) Cardenas Basalt (Yc)
Internal Igneous Rocks (Plutonic)	Granite	Light color (white, light gray, pink, yellowish) from dominant minerals quartz (20–60%), potassium feldspar, plagioclase (10–65%), and biotite.	Young granite and pegmatite (Yg) Granite (Xg) Granite, granitic pegmatite, and aplite (Xgr)
	Granodiorite	Light-to-dark gray. Composition like granite but with 65–90% plagioclase.	Granodiorite-gabbro-diorite (Xgd)
	Tonalite	Medium-gray with dark inclusions. Dominant minerals: quartz (20–60%), plagioclase (>90%), hornblende, and biotite.	Elves Chasm pluton (Xec)
	Quartz-diorite	Gray with quartz (5–20%), <5% plagioclase and common biotite, amphiboles and pyroxenes.	Elves Chasm pluton (Xec)
	Diorite	Dark-gray to black dominated by plagioclase (>90%) and little quartz (<5%).	Granodiorite-gabbro-diorite (Xgd) Diorite, gabbro (Xdg)
	Gabbro	Dark-colored with similar composition of basalt. Formed from magnesium- and iron-rich magma.	Unnamed diabase sills and dikes (Yi) Granodiorite-gabbro-diorite (Xgd)

Precambrian Plutonic Rocks

Because they cool slowly within the subsurface, plutonic rocks are coarser-grained than volcanic rocks. Individual minerals are easily recognized (fig. 31). For example, quartz appears gray or translucent, alkali feldspar (orthoclase) appears pink, and plagioclase is the white mineral in the park’s granitic rock units (**Yg, Xg, Xgr**). As the magma body cools slowly, chemical elements have time to combine and form characteristic

crystal shapes. If the minerals grow to be exceptionally large, the rock becomes a “pegmatite” like those found in units **Yg** and **Xgr** (fig. 17). Accessory minerals in plutonic igneous rocks help classify the rock even further (table 7). If biotite and hornblende are plentiful in a granitic rock, for example, the rock will take on a speckled, salt-and-pepper appearance, typical of a granodiorite such as **Xgd**.



Figure 31. Photographs of igneous rock compositional endmembers, granite and basalt, in Grand Canyon National Park.

(A) The minerals quartz and alkali feldspar are responsible for the light-colored, 1.375 billion-year-old Quartermaster granite (included in map unit Yg [Young granite and pegmatite]) in western Grand Canyon. Rhyolite is the volcanic equivalent of granite. **(B)** Iron and manganese provide the dark color to the denser, 1.100 billion-year-old Cardenas Basalt (Yc). Gabbro is the plutonic equivalent of basalt. NPS photographs by Erin Whitakker from the Trail of Time, available at https://www.flickr.com/photos/grand_canyon_nps/sets/72157629974795528/.

Collectively, the plutonic rocks in Grand Canyon National Park are referred to as the Zoroaster Plutonic Complex (table 8). They form the nearly 2-billion-year-old “basement” upon which all the other units were deposited (fig. 17) and have been subdivided into four groups of plutons based on age and tectonic origin: 1) older basement, 2) arc plutons, 3) syncollisional granites (formed at the same time), and 4) post-orogenic granites (Babcock 1990; Karlstrom et al. 2003).

The older basement consists of the 1.84-billion-year-old quartz diorite of the Elves Chasm pluton (**Xec**), the oldest rock known in the southwestern United States (Karlstrom et al. 2003). The geochemistry of the Elves Chasm pluton separates it from younger plutons.

Exposures of the contact between the Elves Chasm pluton and the overlying Granite Gorge Metamorphic Suite (table 1) occur in several places, notably in Walthenberg, 113-mile, and Blacktail canyons.

The arc plutons represent an arc-shaped chain of offshore island volcanoes that developed above a subducting plate, similar to today’s Aleutian Islands or the Japanese Archipelago. The 1.74 billion to 1.71-billion-year-old granodiorite and gabbro-diorite complexes document large magma chambers that were emplaced at a relatively shallow level and fed volcanic eruptions within the island arcs (Karlstrom et al. 2003). The composition of these plutons suggests a comingling of magmas within the magma chambers (table 8).

Table 8. Precambrian plutons and dike swarms of the Zoroaster Plutonic Complex in Granite Gorge.

Modified from Karlstrom et al. (2003, Table 2-1). "Undated" plutons are grouped with nearby plutons that do have radiometric ages.

Category	Pluton and/or Dike Swarm (map symbol)	Age (billions of years)	Composition
Post-Orogenic Granites	Quartermaster Pluton (Yg)	1.375	Coarse-grained granite
Syncollisional Granites	Cottonwood Pegmatite Complex (Xgr)	1.685; 1.680	Granite and granitic pegmatite dikes and sills
	Cremation Pegmatite Complex (Xgr)	1.698	Biotite-muscovite granite and pegmatite
	Bright Angel Pluton	undated	Biotite-muscovite granite and pegmatite
	Phantom Pluton (Xgr)	1.662	Biotite-muscovite granite and pegmatite
	Sapphire Pegmatite Complex	undated	Granite and granitic pegmatite dikes and sills
	Garnet Pegmatite Complex (Xgr)	1.697	Granite and granitic pegmatite dikes and sills
	Travertine Falls Pluton and dike complex (Xgr)	1.704	Medium-grained biotite (+muscovite) granite
	229-mile granite	undated	Medium-grained biotite (+muscovite) granite
	232-mile Pluton and dike complex	undated	Medium-grained biotite (+muscovite) granite
	234-mile Pluton and dike complex	undated	Medium-grained biotite (+muscovite) granite
	237-mile Pluton	undated	Medium-grained biotite (+muscovite) granite
	Separation Pluton	undated	Medium-grained biotite (+muscovite) granite
	Spencer Pluton and dike complex	undated	Medium-grained biotite (+muscovite) granite
	245-mile Pluton (Xgr)	1.720	Granodiorite, tonalite, diorite intruded by Spencer Pluton
Surprise Pluton	undated	Medium-grained biotite and muscovite (garnet) granite	
Arc Plutons	83-mile ultra-mafic	undated	Layered ultramafic rock
	Pipe Creek Pluton (Xgd)	1.74–1.69	Granite to granodiorite
	Tuna Pluton (Xgd)	1.750–1.710	Medium-grained granodiorite
	Horn Creek Pluton (Xgd)	1.713	Medium-grained quartz diorite to tonalite
	Boucher Pluton (Xgd)	1.714	Granodiorite to tonalite
	Ruby Pluton (Xgd)	1.716	Granodiorite, diorite, and gabbro
	Trinity Pluton (Xgd)	1.730	Medium- to coarse-grained granodiorite
	Diamond Creek Pluton (Xgd)	1.736	Granodiorite, tonalite, diorite, and gabbro
	Zoroaster Pluton (Xgd)	1.740	Medium-grained biotite granite to granodiorite
	91-mile ultramafics (Xum?)	Undated	Layered ultramafic rock
	Crystal Pluton	Undated	Granite to granodiorite
Granite Park Mafic Complex	undated	Alternating layers of gabbro, anorthosite, and granodiorite with gabbroic pegmatite	
Older Basement	Elves Chasm Pluton (Xec)	1.841	Tonalite to quartz diorite and granodiorite

The composition, intrusive style, and deformational character of the arc plutons differ from the 1.71 billion to 1.66-billion-year-old syncollisional granites and granitic pegmatites. The syncollisional granites may have formed by partial melting of the lower crust during deformation caused by arc-continent collision. Magma rose along cracks and shear zones and solidified into

dikes or small plutons. In the Upper Granite Gorge, the intrusions consist of medium-grained granite and granitic pegmatite and include Cottonwood, Cremation, Sapphire, and Garnet Canyon complexes (table 8). More massive exposures in the Lower Granite Gorge include Travertine Falls, Separation, and Surprise plutons.

The 1.35-billion-year-old Quartermaster pluton (fig. 31) and related pegmatites in the Lower Granite Gorge represent magmatism that occurred following the main episode of compressional deformation resulting from the collision between what would eventually become the southern margin of the North American craton and the offshore island arc (Karlstrom et al. 2003).

The dike swarms and syncollisional granites in table 8 were emplaced during the main Paleoproterozoic episode of regional deformation and are synchronous with peak regional metamorphism. The heat from the molten magma combined with temperatures at depth to produce the metamorphic minerals found in the schists described below (Karlstrom et al. 2003).

Precambrian intrusive igneous rocks also include Mesoproterozoic sills and dikes composed of diabase, a mafic rock that typically represents shallow intrusive bodies (table 7; linear features layer on the GRI GIS data). A dike cuts across bedding or through an unlayered mass of rock forming a sheet of igneous rock (fig. 30). In contrast, a sill intrudes parallel to bedding. Unnamed diabase sills and dikes (**Yi**) intrude all the formations of the Unkar Group below the Cardenas Lava. About 1.1 billion-year-old diabase dikes and sills (**Ydi**) also intrude granitic rocks from RM 237 to RM 239 (Billingsley et al. 2006b).

In Grand Canyon National Park, the sills are associated with the Bass Formation (**Yb**) and Hakatai Shale (**Yh**). Igneous dikes intrude the Hakatai Shale, Shinumo Quartzite (**Ys**), and Dox Formation (**Yd**) to within a few meters of the Cardenas Lava (Hendricks and Stevenson 2003). In the map area, sills range in thickness from about 20 m (65 ft) in Clear Creek to more than 200 m (655 ft) near Bass Rapids.

Precambrian Volcanic Rocks

Because magma cools rapidly when erupted onto the surface, crystals in volcanic rocks fuse together and become too small to be identified without magnification. In certain cases, however, large minerals grow in the fine-grained groundmass, and these large crystals are called “phenocrysts.” Phenocrysts are present in the Precambrian Brahma Schist (**Xbr**) where interbeds of metamorphosed volcanic rocks contain relatively large crystals of quartz and feldspar.

The Mesoproterozoic Cardenas Basalt (**Yc**) of the Unkar Group (table 1) is the only Precambrian volcanic unit mapped in Grand Canyon National Park (fig. 31; table 7; GRI GIS data). Located in eastern Grand Canyon, the 240–300- m (785–985 ft) thick unit can be divided into a 75–90 m (245–295 ft), bottle-green, highly-weathered and altered lower member and a more massive, less

altered upper member (Hendricks and Stevenson 2003). Alternating layers of the Cardenas Basalt with the slope-forming lower member and the Dox Formation (**Yd**) suggests continuous deposition of the two units, but the unconformity between the Cardenas Basalt and the overlying Nankoweap Formation (**YZn**) indicates that erosion removed an unknown amount of Cardenas Basalt prior to deposition of the Nankoweap.

Cenozoic Volcanic Rocks

Cenozoic Era volcanic events dramatically influenced the landscape of western Grand Canyon National Park. Cenozoic volcanism produced lava dams and associated lake sediments, lava falls, volcanic cones, dikes and sills, and pyroclastic deposits. These features represent complex, dynamic volcanic events that took place on the Colorado Plateau during the Miocene, Pliocene, and Pleistocene epochs (table 1; Billingsley 2000b; Billingsley and Wellmeyer 2004). Volcanic vents are included in the GRI GIS data. Of the 149 vents in the data, 47 are mapped within the park. The GRI GIS data also include basalt flow directions.

Cenozoic volcanic rocks feature a more varied composition than does the Precambrian Cardenas Basalt (table 7). Phenocrysts are common in Cenozoic volcanic units. The Snap Point Basalt (**Tsgi**), for example, contains phenocrysts of augite and olivine. In addition to basalt, volcanic rocks of the Hualapai Plateau (**Tv**) and the Mount Floyd Volcanic Field (**Tri**) contain andesite, rhyodacite, and rhyolite. Rhyolite, in contrast to basalt, contains abundant silica, which determines a magma’s viscosity, or internal friction (table 7). Viscosity influences explosiveness. Thick, high viscous lavas do not allow trapped gases to escape easily and so generate intense, explosive eruptions, such as the 1980 Mount St. Helens eruption and past eruptions of Mount Rainier (see the Geologic Resource Evaluation report by Graham 2005). The rhyolite ash in the volcanic rocks of the Hualapai Plateau was derived from local and distant sources (Billingsley et al. 2006a).

Low-silica lavas, on the other hand, are fluid and spread out in broad, thick sheets up to several kilometers wide. Examples of low-silica, fluid lava flows in the Grand Canyon include the low-silica Neogene basalt flow deposits (table 7). Some of these fluid lava flows cascaded over the rim of the Grand Canyon, forming lava dams that blocked the Colorado River. Solidification of basaltic magma flowing over the canyon rim also formed the spectacular lava falls visible from Vulcan’s Throne (GRI GIS data).

Lava Dams

On 25 August 1869, John Wesley Powell considered the volcanic history of the region:

We have no difficulty as we float along, and I am able to observe the wonderful phenomena connected with this flood of lava. The canyon was doubtless filled to a height of 1,200 to 1,500 feet, perhaps by more than one flood. This would dam the water back; and in cutting through this great lava bed, a new channel has been formed, sometimes on one side, sometimes on the other. . . What a conflict of water and fire there must have been here! Just imagine a river of molten rock running down a river of melted snow. What a seething and boiling of waters; what clouds of steam rolled into the heavens! (quoted in Hamblin 2003, p. 313)

Western Grand Canyon offers one of the best exposed and most iconic lava dam localities worldwide, and yet, after almost 150 years of study, questions remain as to the construction of the lava dams, their longevity,

the lakes that formed upstream, the time it took for sediment to fill the lakes, and the processes by which the dams failed. Many models designed to answer these questions have been proposed in the past (see Hamblin 1994, 2003; Fenton et al. 2002, 2004, 2006; Karlstrom et al. 2007; Crow et al. 2008). However, in 2015, Crow et al. revolutionized the understanding of lava dams in the Grand Canyon with their comprehensive study utilizing data from field observations, $^{40}\text{Ar}/^{39}\text{Ar}$ geochronology, inset and stratigraphic relationships, LiDAR (Light Detection and Ranging)-derived flow heights, paleomagnetism, whole-rock geochemistry, and comparative analysis of historical and modern lava dams (Crow et al. 2015).

According to Crow et al. (2015), basalt flows originated from the Uinkaret volcanic field, centered between the Toroweap and Hurricane faults north of western Grand Canyon (see the GRI GIS data) (fig. 32). The Lava Falls area, Whitmore Wash area, and the region between Lava Falls and Whitmore Wash were impacted by 17 damming events from five episodes of volcanic activity beginning about 830,000 years ago (table 9). Some of the more notable features of the lava dams are listed in table 9.

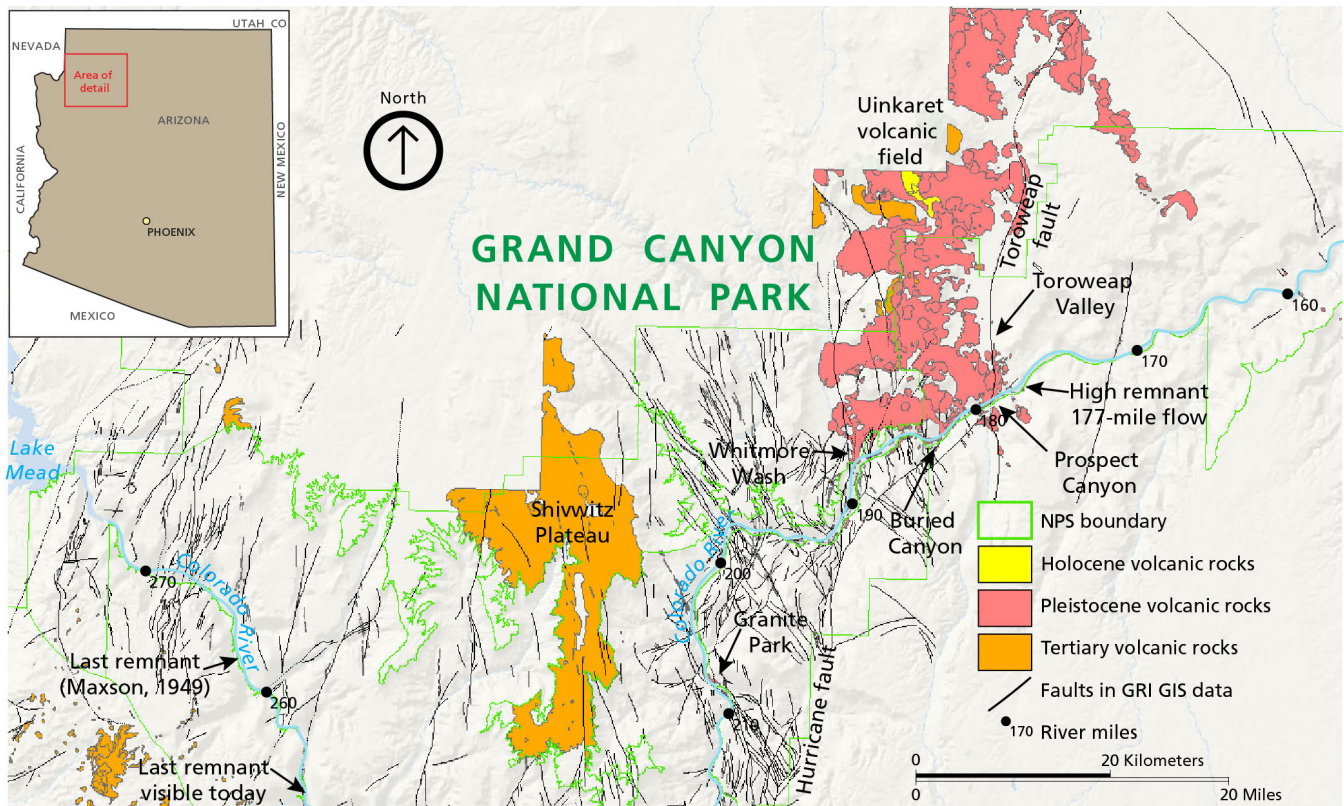


Figure 32. Simplified geologic map showing the distribution of Tertiary and Quaternary basaltic volcanism. Map by Trista Thornberry-Ehrlich (Colorado State University) using GRI GIS data and information in Billingsley (2000a), Billingsley and Wellmeyer (2003), and Billingsley et al. (2006) (Crow et al. 2015, figure 1).

Rates and Ages of Lava Dam Emplacement

Episodes 1–5 of Crow et al. (2015) reflect major refinements of previous flow-remnant correlations and flow stratigraphy based on $^{40}\text{Ar}/^{39}\text{Ar}$ ages and whole-rock geochemistry. The one remnant from episode 1 (900,000–775,000 years ago) now dates the earliest occurrence of Cenozoic volcanism in the canyon at about 830,000 years ago (fig. 33; table 9). In contrast to episode 1, at least ten lava flows cascaded over the canyon rim or from intracanyon eruptions in episode 2 (700,000–400,000 years ago) to produce the most voluminous, highest, and longest lava dams (Crow et al. 2015).

As Hamblin states (1994, 2003), the single flow dams were likely emplaced in a geologically instantaneous time frame, over a period of days or weeks. In contrast to single flow dams however, new age dates and correlations of remnants suggest that the rate of emplacement of multiple flow dams may range from instantaneous to millennia. For example, age data for the three massive flows that resulted in the High Remnant dam indicate that the whole sequence was emplaced quickly about 620,000 years ago (Crow et al. 2015). Unlike the High Remnant flows, the interbeds between the seven eruptive units that formed the Buried Canyon dam contain river gravels and colluvium. In general, colluvium refers to unconsolidated material deposited at the base of a slope, hillside, or cliff by processes such as rainwash, sheetwash, rockfall, slow continuous downslope creep, or a combination of processes. The presence of colluvium suggests that a significant amount of time elapsed between flow events.

Field relations of the High Remnant and Buried Canyon dams also illustrate the complexity of multiple lava flows and the need for precise age data. Without age data, the stratigraphy suggests that the High Remnant flow is younger than Vulcans Anvil and the 177-mile remnant (fig. 34). In fact, the High Remnant flow is one of the oldest flows in the canyon. The Buried Canyon flow preserves multiple lava flows and is the only complete cross section of a lava dam in the Grand Canyon (fig. 35).

A 100,000-year lull in volcanic activity followed the 424,000-year-old Ponderosa flow (table 9). Volcanic activity resumed in the Lava Falls area with the 177-mile flow, the only intracanyon flow of episode 3 (400,000–275,000 years ago) (Crow et al. 2015). Pillow structures, which form when magma interacts with water, mark the base of this lava flow.

Thin lava flows pouring down Whitmore Wash initiated episode 4 (275,000–150,000 years ago) (table 9). The

Lower and Upper Whitmore flows filled the tributary and at least 5.5 km (1.8 mi) of the Grand Canyon (fig. 36). The age data are not precise enough to determine if there is a significant hiatus between the two flows or if they were erupted in quick succession. However, a 2-m (7-ft)-thick lens of colluvium separates the Lower and Upper Whitmore flows at RM 189 and from RM 189.2 to 189.4 (Crow et al. 2015). About 200,000 years ago, multiple lava flows cascaded into the canyon downstream from Lava Falls, forming the Lower Gray Ledge and 180.8-mile lava dams (fig. 36; Crow et al. 2015).

During episode 5 (150,000–75,000 years ago), many lava flows cascaded between the Lava Falls area and Whitmore Wash (fig. 33). Most of the cascades erupted in Toroweap Valley between RM 179 and RM 181 (Crow et al. 2015). One intracanyon flow, the Upper Gray Ledge flow, resulted from these cascades. Lower Gray Ledge and Upper Gray Ledge flows can only be distinguished based on $^{40}\text{Ar}/^{39}\text{Ar}$ ages (table 9).

Lake Development and Sedimentation Rates

In addition to refining flow correlations and stratigraphy, new data from Crow et al. (2015) revised the effectiveness of lava dams at restricting the flow of water and sediment and the rate at which the lakes upstream of the dams filled with water and sediment. Stratigraphic features observed in the field suggest that most, if not all, of the 17 intracanyon flows resulted in lava dams that blocked the Colorado River and produced extensive lakes. For example, rounded river gravels that were deposited 200–260 m (660–850 ft) above the modern river level on top of the Upper Whitmore and Buried Canyon flows require a rise in the Colorado River to that level by lava dams. The lake that would have formed upstream from the 260-m (850-ft)-high Buried Canyon lava dam would have extended to the 760 m (2,500 ft) modern elevation contour, past Phantom Ranch to about RM 80. The reservoir capacity would have been $\sim 5 \text{ km}^3$ (1.2 mi^3) (Crow et al. 2015).

Filling a deep canyon behind a dam, these lakes would have been like today's Lake Mead and Lake Powell (Hamblin 2003). Coarser-grained sediments, such as sand and gravel, would have formed deltas, like the current Hite delta in Glen Canyon National Recreation Area, where the Colorado River enters the lake. Turbidity (density) currents would have transported finer-grained sediment into the deeper parts of the lake. Extensive beaches probably would not have formed along the shorelines. Rather, like the shoreline of Lake Powell, steep cliffs, mass wasting deposits, and downslope movement of colluvium would have marked the lake margins (Hamblin 2003).

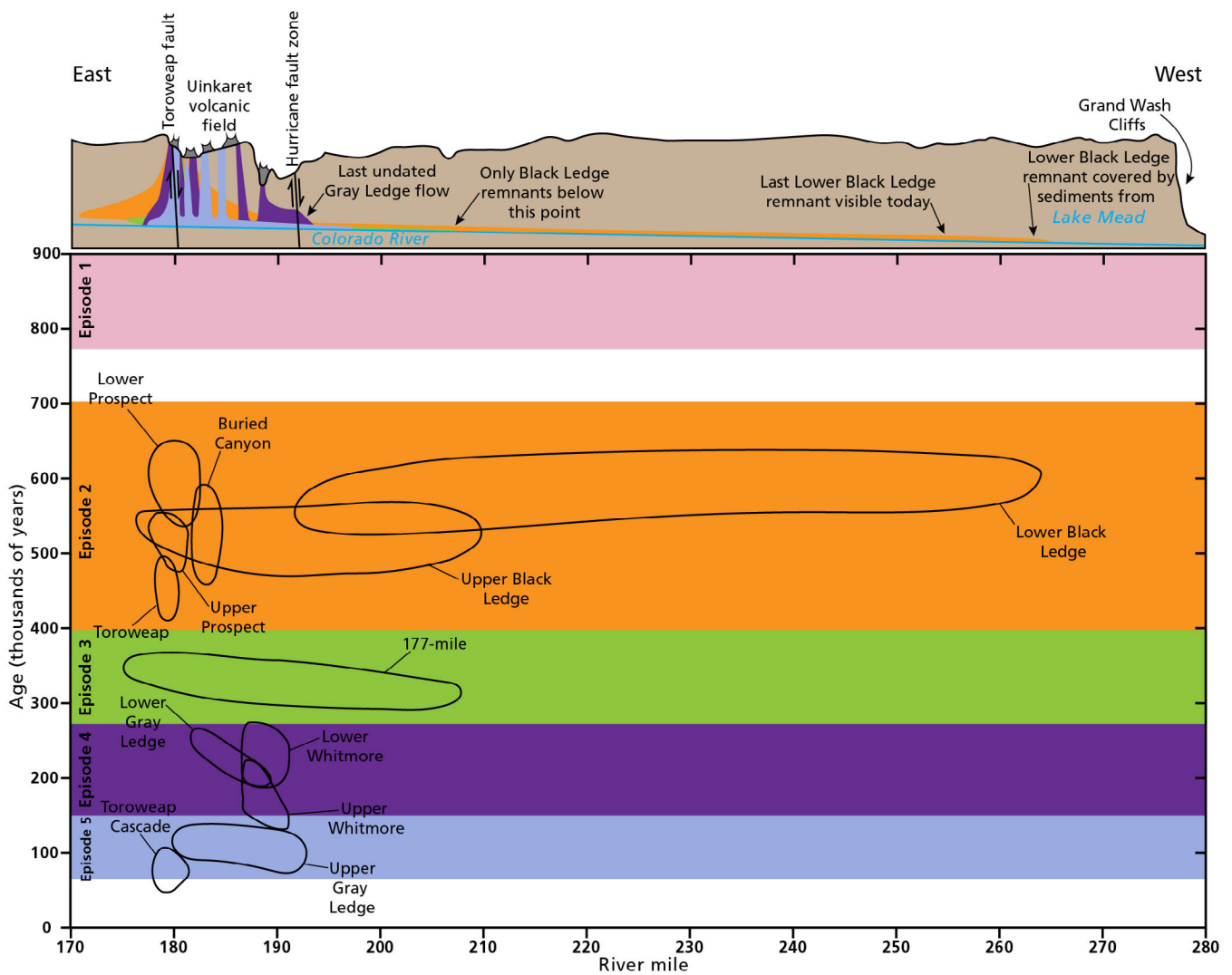


Figure 33. Location and age of lava dams in Grand Canyon.

(A) The source and extent of lava flows in the canyon from the five episodes, color coded to (B), is shown in this simplified longitudinal profile of the river. (B) Graph showing the ages, in thousands of years, of all dated remnants and where they are located, by river mile from Lees Ferry, throughout the canyon. Graphic by Trista Thornberry-Ehrlich (Colorado State University), modified from Crow et al. (2015, figure 7).

Table 9. Lava dams in western Grand Canyon National Park.

From Crow et al. (2015). Age dates are radiometric ages in thousands of years (ka). See Crow et al. (2015) for comparisons to previous lava dam nomenclature.

Volcanic Episode	Lava dam nomenclature	River Mile from Lees Ferry	Age (~ka)	Structure	Maximum thickness in m (ft)	Original length in km (mi)	Other Notable Features
Episode 1	188.7-mile flow	188.7L	829	Single flow	Unknown	Unknown	Oldest Cenozoic basalt in the canyon: 1 km (0.6 mi) downstream from Whitmore Wash.

Table 9, continued. Lava dams in western Grand Canyon National Park.

Volcanic Episode	Lava dam nomenclature	River Mile from Lees Ferry	Age (~ka)	Structure	Maximum thickness in m (ft)	Original length in km (mi)	Other Notable Features
Episode 2	Whitmore Rapid flow	188.1R	630	Single flow	>30 (>100)	Unknown	Black Ledge flow is inset into Whitmore Raptic flow.
	High Remnant flows	176.9L	617	Multiple flows	>330 (>1,100)	Unknown	Three massive flows emplaced quickly.
	Lower Black Ledge flows	195.4L, 246R, 203.4R, 194.2R, 223.1R, 253.5R, 207.6L, 208R	575	Single flow	~45 (~150)	>135 (>81)	Traveled 120–135+ km (72–81 mi) from the Lava Falls area.
	Lower Prospect flows	179.6L, 179.1L	572	Multiple flows	Unknown	Unknown	Found only in Prospect Canyon.
	Buried Canyon flows	182.9–183R	524	Multiple flows	~200 (~660)	Unknown	Only complete cross section of a lava dam in Grand Canyon.
	Upper Prospect flows	179.6L, 179.3L, 179.4L	535	Multiple flows	<<640 (<<2,100)	Unknown	Found only in Prospect Canyon.
	Upper Black Ledge flow	207.6L, 189L, 208.3R, 190.7L, 178	525	Single flow	~70 (~230)	>76 (>46)	Sourced by Vulcans Anvil, which is a volcanic plug.
	183.4-mile flow	183.4R	492	Single flow	>192 (>630)	Unknown	Possible slumped remnant.
	Toroweap flows	179.1–179, 179.5R	448	Multiple flows	~395 (~1,300)	Unknown	Complex set of 5 flow units. Displaced by Toroweap fault.
	Ponderosa	181.6R	424	Single flow	>120 (>390)	Unknown	Set apart from other flows by age data.
Episode 3	177-mile flow	177.3L, 204.6L, 194.8, 192L, 183.9R	322	Multiple flows	~60 (~200)	>44 (>26)	Flowed a short distance upstream.
Episode 4	Lower Whitmore flows	189.6L, 188.3R, 189.1L, 187.5L, 188L, 187.7R	243	Multiple flows	>190 (>620)	>5 (>3)	Unusually thin flows filled Whitmore Wash.
	Lower Gray Ledge flow	187.5L, 186.7R, 182.8R	209	Single flow	>110 (>360)	>16 (>10)	Likely related to Lava Falls remnant.
	180.8-mile flow	180.8R	200	Multiple flows	>70 (>230)	Unknown	Flat-lying basalt flows quenched rapidly by Colorado River.
	Upper Whitmore flows	190R, 188.1L, 187.5L, 187.7R, 187.6R	186	Multiple flows	190–260 (620–850)	>5 (>3)	Unusually thin flows filled Whitmore Wash.
Episode 5	Upper Gray Ledge flow	190.9L, 188.1R, 187.9L, 189.1L, 181.2R, 184.6L, 179.2	102	Single flow	>140 (>460)	>21 (>13)	Only distinguished from Lower Gray Ledge flow by age data.

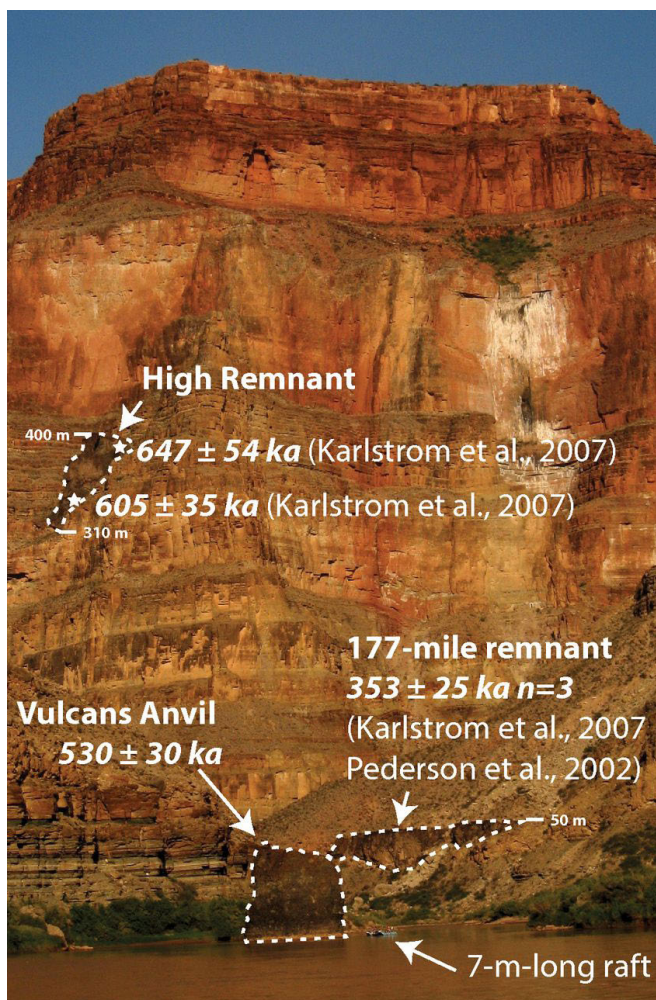


Figure 34. Annotated photograph of Vulcan's Anvil, the 177-mile remnant, and the High Remnant. The High Remnant flows are about 400 m (1,300 ft) above the modern river level and 2 km (1.2 mi) upstream from large flow remnants in the Lava Falls area. Vulcans Anvil is a 530,000-year-old volcanic plug. The 177-mile remnant is the only episode 3 flow identified in the canyon. Note the 7-m (23 ft) raft for scale. Photograph and annotation from Crow et al. (2015, figure 8).

Gravels do not overlie the High Remnant and Toroweap flows, but the sheer thickness of these dams suggest significant blockages to the Colorado River even if water leaked through the dams (table 9). Crow et al. (2015) suggested that considering the pre-Glen Canyon Dam average annual flood discharge of the Colorado River (2,440 m³/s; 86,000 cfs) and the average annual sediment load of 140 million tons (Smith et al. 1960), the Colorado River would have been constricted and a lake would have formed even if a lava dam leaked, especially dams with long upstream and downstream run-outs, such as High Remnant and Lower Black Ledge, respectively.

The stable, distal portions of some lava dams are overlain by mainstream Colorado River gravels, also suggesting that the dams blocked the flow of the river, and once the lake filled, the river overflowed the dam and re-established its stream flow. Benches, channels, and potholes are cut into the 27-m (89-ft)-thick Lower Black Ledge remnant. These features are overlain by clasts that originated outside of the Grand Canyon (Crow et al. 2008, 2015). Foreign clasts on the Lower Black Ledge and Buried Canyon flows indicate that the Colorado River established itself on top of the dams following the lava flow events.

The best estimates on how long it took for the lakes behind the dams to fill with sediment rely on modern estimates associated with Lake Mead and Lake Powell (Crow et al. 2015). Sediment, primarily sand and silt, have been filling these human-constructed reservoirs since their completion in 1935 and 1963, respectively. Prior to the construction of Lake Powell, sediment accumulated in Lake Mead at an annual rate of ~109,000,000 m³/year (3,850,000,000 ft³/year) (Ferrari 2008). At this rate, Lake Mead would have completely filled with 40 km³ (10 mi³) of sediment in ~400 years. Lake Powell should fill with 33 km³ (8 mi³) of sediment in ~300 years. Assuming pre-dam sediment accumulation rates and considering modern topography, 400-, 200-, and 100-m (1,000-, 700-, 300-ft)-high lava dams would completely fill with sediment (ignoring compaction) in 248, 33, and 6 years (Crow et al. 2015). More sediment surely entered the canyon during glacial periods, so these times are probably the maximum amount of time it took for a lake to fill.

Prior to dam construction, ~15 km³ (3.6 mi³) of water passed through the Grand Canyon each year. At this rate, 400-, 200-, and 100-m (1,000-, 700-, 300-ft)-high lava dams would overflow in 1.8 years, 13 weeks, and 15 days, respectively, supporting previous interpretations that the dams filled with water geologically instantaneously (Hamblin 1994, 2003; Crow et al. 2015).

Lava-Water Interactions and Cooling Rates

Textures indicative of lava-water interactions include pillows, peperite, and hyaloclastite. Peperite is a sedimentary rock containing igneous fragments that forms when magma encounters sediments, and hyaloclastite is a breccia containing abundant black volcanic glass that materializes when magma enters bodies of water. These features are found in the upstream extent of 177-mile, Toroweap, 180.8-mile, and Lower and Upper Whitmore flows, indicating that this part of the flow was quenched quickly by river water (Crow et al. 2015). In contrast, the distal parts of flows



Figure 35. Annotated photograph of the Buried Canyon flow sequence. See Crow et al. (2015) for discussion of individual flow units. Stars indicate locations of age-dated samples. Note the textural complexity of the flows, as well as the interbeds. Heights are in meters above the modern river level. Photograph and annotations from Crow et al. (2015, figure 11).



Figure 36. Annotated photograph showing the stratigraphic relationships between the Whitmore and Upper Black Ledge lava flows. Stars indicate age data sample locations. (A) Volcanic cinders underlie the Lower Whitmore flow. View from the river towards the northwest. (B) Outburst flood deposits partially cover the Upper Whitmore flow. View from the north rim toward the southeast. Photographs were taken at RM 187.6. Photograph and annotations from Crow et al. (2015, figure 12).

lack these features, adding credence to the hypothesis that the Colorado River was temporarily blocked during the early stages of dam formation and that much of the lava flowed downstream on a mostly dry river bed, as suggested by Hamblin (1994).

Furthermore, many of the intracanyon flows contain well-formed vertical columns (colonnades) overlain by a thicker zone of irregularly oriented columns referred to as the entablature (fig. 37). The colonnades formed from the magma cooling slowly (upwards) by conduction, while the entablature formed from Colorado River water penetrating the flow from the top, cooling the upper part of the flow convectively (downwards) (Swanson 1967; Saemundsson 1970; Bjornsson et al. 1982; Long and Wood 1986; Degraff et al. 1989; Walker 1993; Lyle 2000). Comparisons of the lava dam textures in the Grand Canyon with those observed at Kilauea Lake in Hawai'i Volcanoes National Park, as well as estimates of past and present annual precipitation rates, support entablature formation because of cooling by the Colorado River rather than rainfall (Hardee 1980; Marchetti et al. 2011; Crow et al. 2015).

Assuming historical discharge rates, the Colorado River overtopped an average lava dam of 200 m (660 ft) in about a year. Solidification of the various lava flows, therefore, would have occurred within a few months to as many as three years depending on the height of the dam (Crow et al. 2015).

Lava Dam Stability, Failure, and Outburst Flood Deposits

Eventually the dams failed. Prior to Crow et al. (2015), models of dam failure predicted that: (1) lava dams lasted tens of thousands of years before failing systematically beginning from the distal part of the flow (Hamblin 1994, 2003), or (2) dams failed catastrophically within years after they formed and before being overtopped by the Colorado River (Fenton et al. 2004, 2006).

New age dates and geochemistry data from Crow et al. (2015), however, demonstrated that flood deposits associated with the lava dams were not only related to outburst-flood events but also to more gradual dam failure (Crow et al. 2015). According to Crow et al. (2015), a multi-staged failure process destroyed the lava dams in the Grand Canyon (fig. 38). The upstream parts of some dams failed quickly, perhaps catastrophically, while down-stream distal parts of the dams lasted long enough to impound short-lived lakes that lasted tens to hundreds of years to perhaps millennia, backing up water throughout much of the Grand Canyon (Crow et al. 2015).

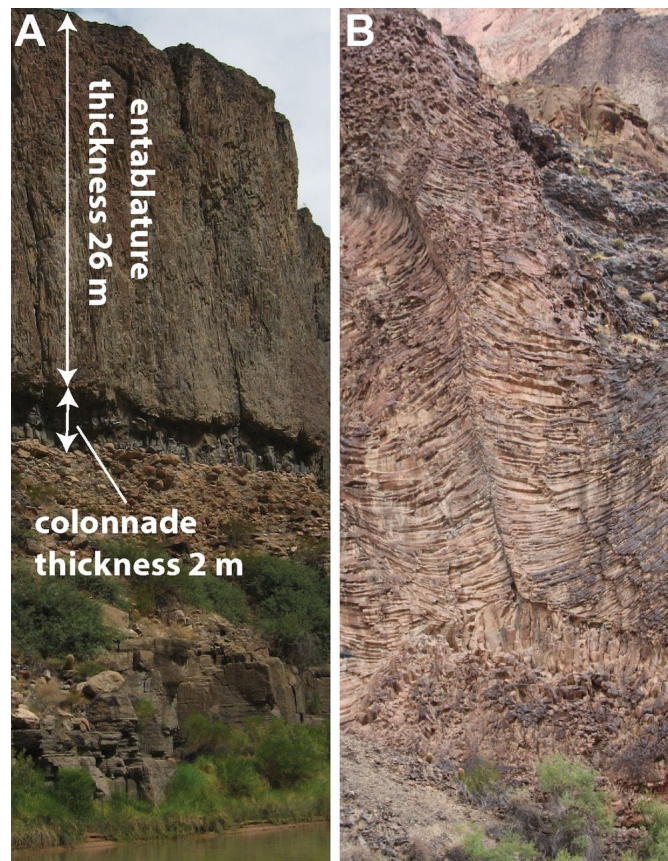


Figure 37. Photographs of cooling structures within a lava dam.

(A) Columns and entablature of a remnant at RM 184R. The columns are orthogonal to a master fracture due to convective flow of water in the fracture. (B) Typical of most remnants, like this one at RM 194R, the entablature is thicker than the colonnade. Photograph and annotations from Crow et al. (2015, figure 20).

Field observations, stratigraphic correlations, volcanic features, geochemistry, age dates, and comparisons to lava dams on Iceland's Skaftá River and on the Boise, Snake, and McKenzie rivers suggested to Crow et al. (2015) a model for lava dam failure that included:

- Dams quickly blocked the Colorado River,
- Far-traveled flows poured down a mostly dry river bed once the river was dammed,
- Flows were quickly overtopped by the river, resulting in the two-tiered cooling structures,
- Lava-water interactions and/or piping, leakage, or seeping river water through brecciated basalt weakened the upstream parts of most dams, causing these parts to fail quickly, in some cases catastrophically,

- Distal ends of the dams lasted longer because they flowed down a dry river bed, thus avoiding brecciation by rapid quenching,
- The remaining portion of a lava dam was removed more slowly as the river's bed-load abraded and eroded the surface and Colorado River water plucked and toppled weakened basalt columns.

The lack of verifiable lake deposits in the canyon suggests that the dams may have failed before they filled with sediment. This is especially true for dams whose remnants are overlain by basaltic gravels derived from the original dam. However, dam remnants that are overlain by far-traveled gravels, such as Black Ledge and Buried Canyon dams, lasted long enough for the lake behind the dam to fill with sediment and the Colorado River to transport sediment over the dam (Crow et al. 2015). Field evidence and age dates suggest that the lava dams existed for an average of less than 20,000 years, although some may have lasted for millennia, and were mostly removed before the emplacement of the next dam (Crow et al. 2015).

Lava Falls

Basaltic lava flowing from the southern tip of the Uinkaret plateau just south of Mt. Emma and across the Esplanade formed the Toroweap Cascades, visible from Vulcan's Throne. The lava cascaded over the rim and plunged 900 m (3,000 ft) into the Inner Gorge (fig. 12; Hamblin 2003; Fenton et al. 2004). The cascades are composed of relatively thin flows, rarely more than 9 m (30 ft) thick (Hamblin 2003). Smaller lava falls occur in the Inner Gorge east of Whitmore Wash.

The Esplanade Cascades, also visible from Vulcan's Throne represent the most recent volcanic activity in the area. Basaltic lava flowed out onto the relatively flat Esplanade surface and spilled over the rim of the Inner Gorge at several places (Hamblin 2003).

Volcanic Cones and Igneous Intrusions

The voluminous lava cascades may give the impression that they provided the lava for the lava dams, but evidence from numerous cones and dikes within the Inner Gorge suggest that the dams primarily formed from lava extruded from within the Inner Gorge (Hamplin 1994, 2003; Crow et al. 2015). Most of the cones are associated with the Toroweap fault (Hamblin 2003; see poster sheet 1). Vulcan's Throne (fig. 12) is the most impressive cone, but a large cone also is found on the canyon rim at the mouth of Prospect Canyon. Remnants of five cones occur in the canyon along the Toroweap fault zone. Several remnants of cinder cones, including Bill's Cone, which is about the same size as Vulcan's Throne, cling to the wall of the Inner Gorge near the Esplanade Cascades (Hamblin 1994).

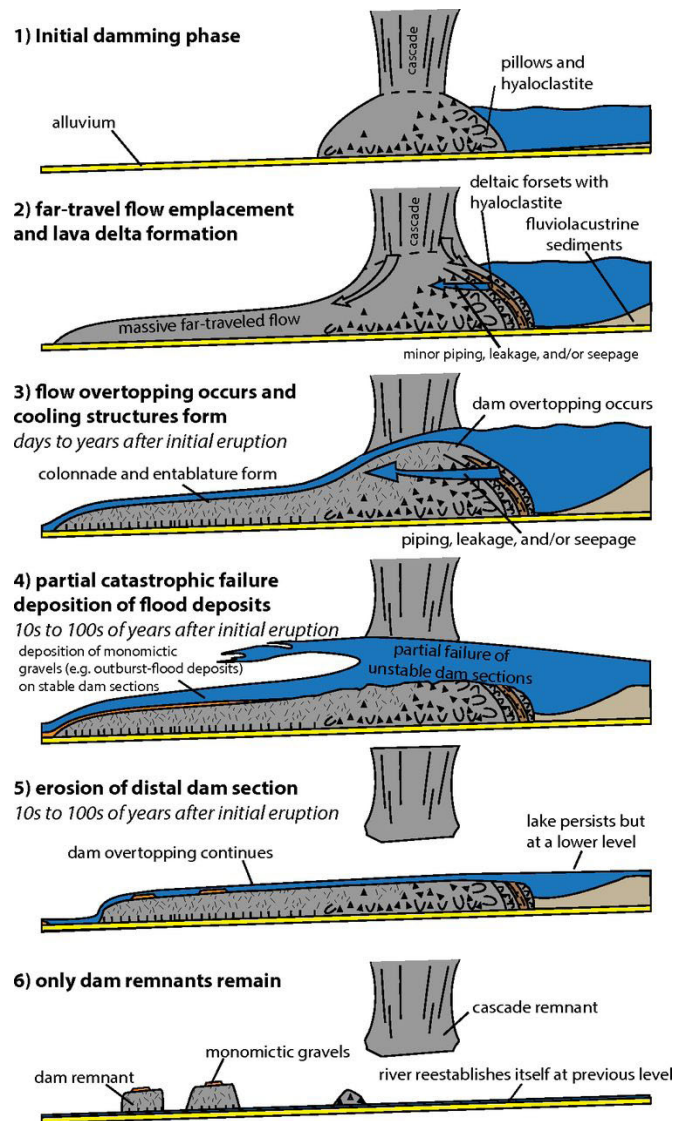


Figure 38. Conceptual model of lava dam failure. In this model, monomictic gravels resulting from outburst floods overlie the lava flow, but some dams, such as the Black Ledge and Buried Canyon dams, are overlain by far-traveled gravels, indicating they failed only after their lakes filled with sediment, allowing the Colorado River carrying far-traveled gravels to overtop them. Diagram from Crow et al. (2015, figure 22).

A volcanic neck of basalt (**Qp**) known as Vulcan's Forge juts from the Colorado River at RM 178 (fig. 39). A volcanic neck develops when lava hardens within a vent of an active volcano and then is exposed by erosion. An exceptional volcanic neck (**Qp**) about the size of Vulcan's Forge can be found near RM 180.2 (Hamblin 2003). The canyon wall cuts across the neck, exposing a vertical cross section of nearly 210 m (700 ft).

Cenozoic intrusions include narrow, 1–2 m- (3–5 ft-) wide dikes and sills. Although most dikes are thin, a prominent dike 10–12 m- (30–40 ft-) thick projects vertically from the surrounding topography near the mouth of Prospect Valley (Hamblin 2003). GRI GIS units containing Cenozoic dikes are listed in table 7. Although dikes are igneous intrusions, table 7 lists these dikes in the extrusive, volcanic column because of the original source map indicated the lithology was basalt. The intrusive equivalent of basalt is gabbro.

Rock fragments and blobs (volcanic bombs) of magma ejected from violent volcanic eruptions freeze into volcanic clasts known as pyroclasts. Pyroclasts in Grand Canyon National Park vary greatly in size. The Pleistocene Yumtheska volcanic vent, for example, ejected football-size volcanic bombs along with basalt fragments, cinders, and ribbons of basalt (**Qpyr**). Cinder-size particles erupted from the Tuckup Canyon Basalt (**Qtp**) and the Basalt of Hancock Knolls (**Qhp**) (table 7).

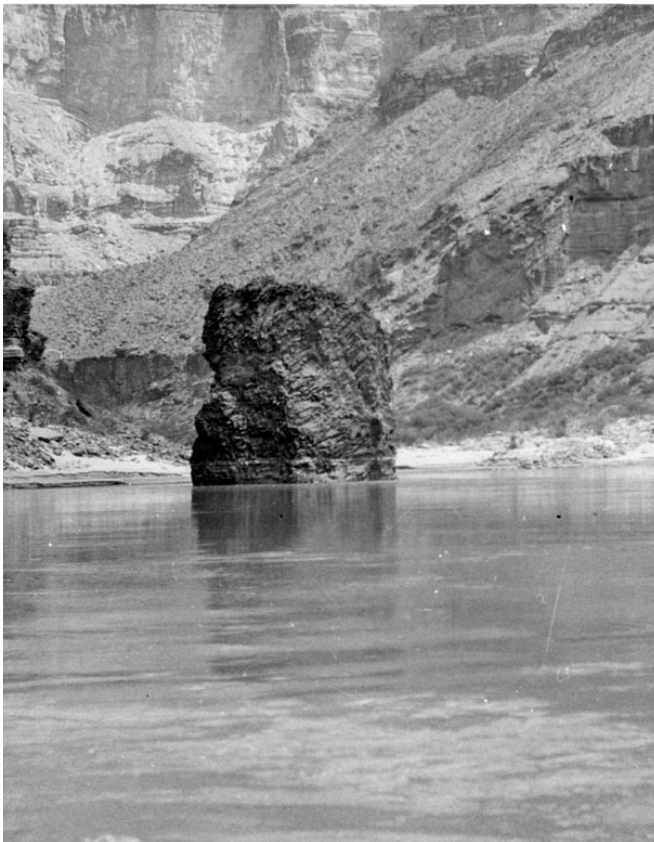


Figure 39. Historic photograph of Vulcan’s Forge at RM 178.

Vulcan’s Forge is a volcanic neck of basalt (Qp) that represents a conduit for extruded magma. Photograph by John Riffey, circa 1947, available at https://www.flickr.com/photos/grand_canyon_nps/7309385340/in/photostream/.

Granite Gorge Metamorphic Rock and Features

John Wesley Powell (1875, p. 213) observed:

We find these lower rocks to be composed chiefly of metamorphosed sandstones and shales, which have been folded so many times, squeezed, and heated, that their original structure, as sandstones and shales, is greatly obscured, or entirely destroyed, so that they are called metamorphic crystalline schists.

Under intense heat and pressure, sedimentary and igneous rocks undergo chemical and physical processes and, without melting, can be altered—metamorphosed—into metamorphic rocks (table 10). Metamorphic rocks can be separated into two broad categories: (1) regional metamorphic rocks and (2) contact metamorphic rocks. Regional metamorphism is associated with large-scale tectonic events, such as mountain building episodes, and reflect moderate to great pressures and temperatures occurring several miles below the surface. Distinguishing characteristics of regional metamorphic rocks include the parallel alignment (“foliation”) of platy minerals, widespread (regional) metamorphic zones, and specific mineral assemblages. Foliation, for example, gives schist its shiny texture and gneiss its characteristic alternating layers of light and dark minerals (fig. 40). Regional metamorphism produced most of the Precambrian metamorphic rocks in Grand Canyon National Park (table 1).

The metamorphic rocks of the Granite Gorge Metamorphic Suite (table 1) provide an excellent record of the growth of the North American continent from approximately 1.8 billion years ago to 1.6 billion years ago (see the “Geologic History” section). Piecing together this ancient history is not easy, however. Complex deformation and metamorphism generated shear zones and tectonically-derived masses of rock (tectonic blocks) that make reconstructing the thickness, stratigraphy, or displacement of the original rocks an extraordinary challenge (table 11). In general, the schist and gneiss of the 1.75 billion–1.74 billion-year-old Rama Schist (**Xr**) suggest a felsic to intermediate volcanic origin. Pillow structures and the lithological composition of the 1.75 billion-year-old Brahma Schist (**Xbr**) are indicative of island arc basalts, which erupted on the Mojave microplate as it collided with the southern margin of the pre-North American continent (fig. 15; Karlstrom et al. 2012a). Sandstones and mudstones deposited on the flanks of eroding island arcs forming on the Yavapai microplate, south of the Mojave microplate (fig. 41), were metamorphosed to form the “metasedimentary” Vishnu Schist (**Xv**; fig. 40) (Karlstrom et al. 2003, 2012).

Table 10. General classification of regional metamorphic rocks.

Metamorphic Rock	Parent Rock	Park Example (map symbol)
Slate	Shale (metamorphosed at lower temperature and pressure)	Not mapped in the park
Schist	Shale (metamorphosed at intermediate temperature and pressure)	Schist (Xs) Vishnu Schist (Xv) Rama Schist (Xr) Brahma Schist (Xbr) Orthoamphibole Schist (Xo)
Gneiss	Shale (metamorphosed at high temperature and pressure)	Vishnu Schist (Xv) Rama Schist (Xr) Brahma Schist (Xbr)
Quartzite	Sandstone	Shinumo Quartzite (Ys)
Marble	Limestone	Not mapped in the park
Metavolcanic	Volcanic	Mafic metavolcanic rocks (Xm)

Metamorphic minerals, such as garnet, sillimanite, staurolite, cordierite, kyanite, and andalusite, can be used to estimate pressures and temperatures at which chemical reactions occurred and therefore, the crustal conditions during metamorphism (Hyndman 1972; Karlstrom et al. 2003). For example, at RM 78 near the Sockdolager Rapid, the mineral assemblages containing sillimanite and potassium feldspar indicate temperatures of 750°C (1,400°F) at the time of metamorphism. At Clear Creek, staurolite–garnet assemblages indicate lower temperatures of 500–600°C (900–1,100°F) and andalusite crystals indicate temperatures <550°C (1,000°F) (Karlstrom et al. 2012a).

In the Upper Granite Gorge, metamorphic minerals indicate a relatively uniform pressure regime equivalent to depths of about 20 km (12 mi). The uniformity in the Upper Granite Gorge metamorphic minerals may indicate that metamorphism occurred after continent-continent suturing had taken place, erasing any evidence of metamorphism that occurred during the deformation event. The uniform pressure may also mean that faulting did not affect the rocks in the Upper Granite Gorge as much as the faults that juxtaposed deeper rocks with shallower rock units in the Lower Granite Gorge (Karlstrom et al. 2003).

In contrast to Upper Granite Gorge, metamorphic minerals in the Lower Granite Gorge cover depths ranging from 15 km (9 mi) to 20 km (12 mi), and they are juxtaposed against units that were never deeper than about 10 km (6 mi). Pressures of Spencer Canyon block (west of Gneiss Canyon shear zone), for example, correspond to 15–20 km (9–12 mi) depths. These rocks were thrust east over Travertine block rocks that were never deeper than 10 km (6 mi).

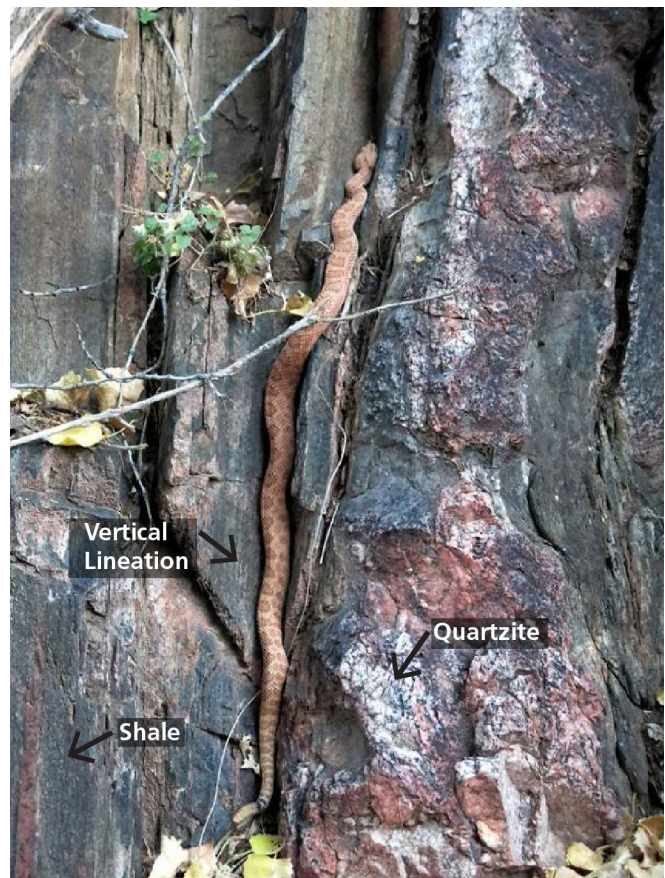


Figure 40. Photograph of metasedimentary rocks of the Vishnu Schist in Grand Canyon National Park. The original sandstone and shale have been metamorphosed to gneiss, forming light (quartzite) and dark (metamorphosed shale) bands. A faint vertical lineation that parallels the rattlesnake is also visible. NPS photograph courtesy of Bruce Heise.

Table 11. Tectonic blocks and shear zones in Granite Gorge.

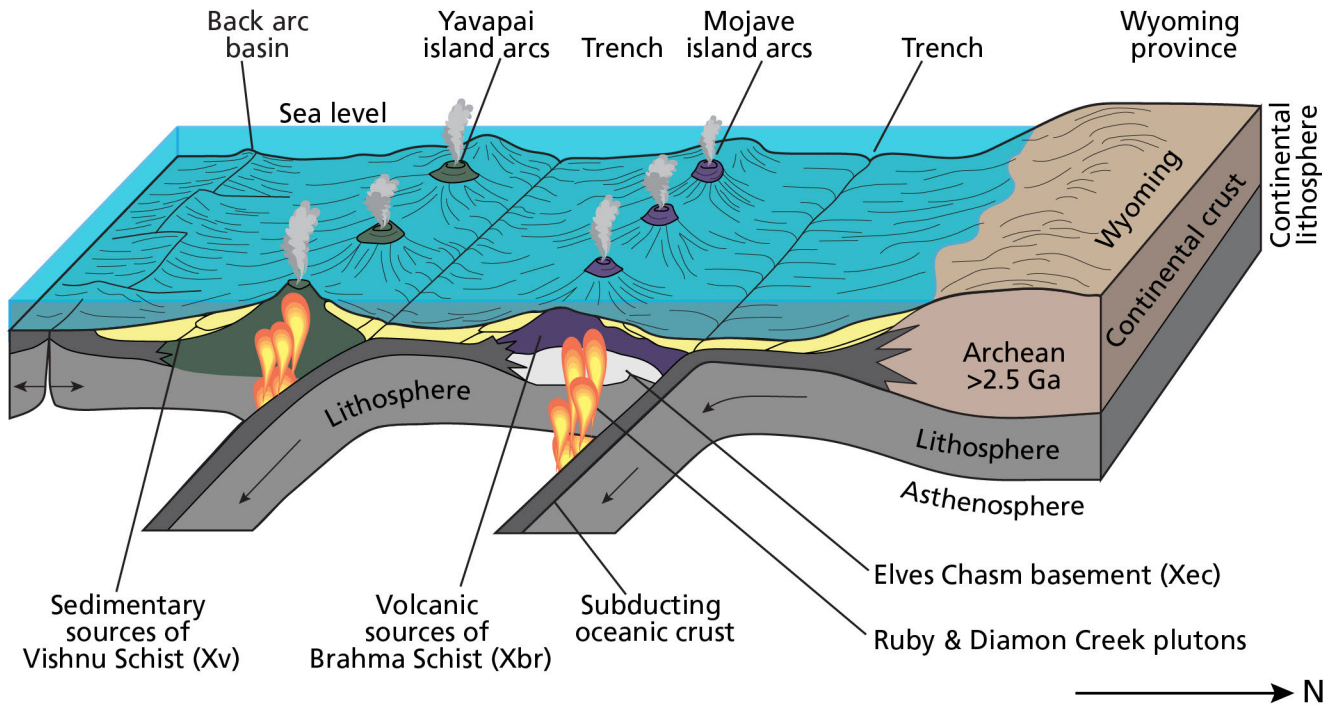
Adapted from Karlstrom et al. (2003, Table 2–2). Their table provides more detailed descriptions of individual blocks and shear zones.

Name		River Mile/Location	Metamorphic Rocks (map symbol)
Upper Granite Gorge	Mineral Canyon block	Mile 77–81	Rama-Brahma-Vishnu schists (Xr, Xbr, Xv)
	Vushnu shear zone	Mile 81	Narrow fault zone
	Clear Creek block	Mile 81–88	Vishnu Schist (Xv)
	Bright Angel shear zone	Mile 88	2-km (1.2-mi)- wide fault zone
	Trinity block	Mile 88–96	Folded Brahma and Vishnu schists (Xbr, Xv)
	96-mile shear zone	Mile 96	300-m (980-ft)- wide fault zone
	Boucher block	Mile 96–98	Vishnu Schist (Xv)
	Crystal shear zone	Mile 98	1-km (0.6 mi)- wide fault zone
	Ruby block	Mile 98–108	Vishnu Schist (Xv)
	Bass shear zone	Mile 107.8–108.2	0.5-km (0.3-mi)- wide fault zone
	Walthenberg-Shinumo block	Mile 108–112 and in Shinumo Creek	Brahma and Rama schists overlain by Vishnu Schist (Xr, Xbr, Xv)
	Contact zone of Elves Pluton with Granite Gorge Metamorphic Suite	Walthenberg, 113-mi, Blacktail Canyons; Middle Granite Gorge	Gneisses mark a 0.5-km (0.3-mi)- wide concordant contact
	Elves Chasm block	Mile 113–127	Gneisses at pluton margins
Middle	Middle Granite Gorge block	Mile 127–139	Metasedimentary schists intruded by granite dikes
	Granite Park block	Mile 209	Metamorphic rock amphibolite with pegmatites
Lower Granite Gorge	Diamond Creek block	East of Hurricane fault, in Diamond Creek	Intermediate volcanic schists interlayered with amphibolite
	Travertine block	Mile 212–234	Vishnu Schist overlain by pillow basalts, then volcanic rocks
	Gneiss Canyon shear zone	Mile 234–242.2	Northwest-side up and dextral oblique slip
	Spencer Canyon block	Mile 242.2–247	Metasedimentary and metavolcanic gneisses
	Surprise-Quartermaster block	Mile 247–261	Metasedimentary rocks in Surprise and Quartermaster plutons

Typically, uniform metamorphic pressures coincide with uniform temperature gradients, but temperature gradients are surprisingly varied in the Upper Granite Gorge. Mineral assemblages indicate that temperatures

ranged from a low of 500°C (930°F) in Boucher, Diamond Creek, and Travertine canyons to nearly 700°C (1,300°F) at RM 78 and near Horn Creek and Spencer Canyon. The temperature changes of >200°C

A. about 1.75 Ga



B. about 1.65 Ga

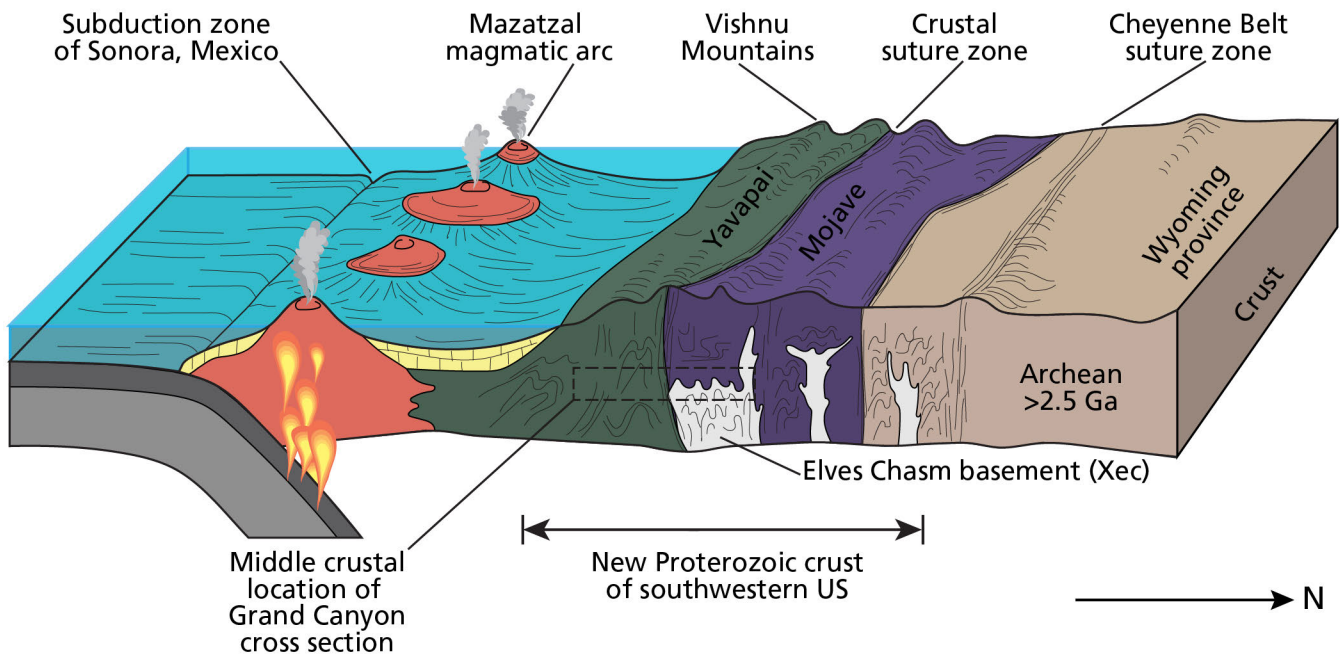


Figure 41. Plate tectonic model for the addition of crust to the southern margin of Laurentia. Diagram illustrates the island arc system during the early history of the Grand Canyon region (A) and during the collision and suturing of the provinces to Laurentia (B), which resulted in the Vishnu Mountains. Modified from Karstrom et al. (2012, figure 6).

(>390°F) occur abruptly across shear zones (e.g., 96-mile shear zone) or within 5–10 km (3–6 mi) of dike swarms and granitic complexes. Karlstrom et al. (2003) suggested that the abrupt changes in temperature resulted from additions of heat from molten material traveling through the dike complexes. This process differs from contact metamorphism (described below). Contact metamorphism releases heat through static cooling over a limited areal extent, but the process described by Karlstrom et al. (2003) suggests a more dynamic process involving heat transfer.

The hardness of the regional metamorphic rocks in the inner canyon is responsible for the steep, craggy landscape and narrow canyon gorge. The Colorado River cannot cut through these rocks as easily as it can through the younger sedimentary rocks. Metamorphic rocks are also not layered like sedimentary rock strata, so erosional stair steps reflecting hard versus soft sedimentary layers do not develop.

Contact metamorphism, the second major type of metamorphism, occurs when molten material intrudes cooler sedimentary or igneous rocks, which are subsequently altered due to the magma's heat. It is primarily distinguished by a narrow metamorphic zone limited by and clearly related to the intruded rock. Contact metamorphic rocks tend to be finer-grained than regional metamorphic rocks.

In Grand Canyon National Park, contact metamorphism occurred when the unnamed diabase sills and dikes unit (Yi) intruded into the Bass Limestone and Hakatai Shale. Heat from the intrusion resulted in the formation of chrysotile asbestos in the Bass Limestone immediately above the sill. At the contact with the Hakatai Shale, contact metamorphism altered the shale at the contact to a fine-grained metamorphic rock known as a "hornfels." Increased temperatures also formed large andalusite and cordierite crystals (porphyroblasts) in the groundmass. These minerals have been subsequently replaced by muscovite and green chlorite, respectively.

Paleontological Resources

Grand Canyon National Park's foundation document recognizes the park's exceptionally diverse fossil record as a fundamental resource (NPS 2010). Fossils listed in table 12 and table 13 range from the Precambrian to Quaternary. Fossils in the Paleozoic are especially significant in recognizing the transition of one depositional environment to another. Quaternary fossils on the Colorado Plateau provide a record of climate change since the late Pleistocene.

Paleontological resources (fossils) record any evidence of life preserved in a geologic context (Santucci et

al. 2009). All fossils are nonrenewable and can be categorized as either body fossils or trace fossils. Body fossils include any remains of the actual organism such as bones, teeth, shells, or leaves. Trace fossils document evidence of biological activity; examples include burrows, trails, tracks, resting sites, or coprolites (fossil dung). Fossils preserved in NPS units may be found in rock strata or unconsolidated deposits, museum collections, and cultural contexts such as building stones or archeological resources. As of September 2019, 272 parks, including Grand Canyon National Park, had documented paleontological resources in at least one of these contexts. As described briefly below, Grand Canyon National Park has examples of fossils found in all contexts.

Fossils continue to be discovered in the park. For example, in 2018, Hodnett and Elliott (2018) identified 31 taxa from a chondrichthyan assemblage in the Late Mississippian Surprise Canyon Formation (Ms) that four new euselachian taxa, two protacrodontids, and two anachronistids, which are best known from the Late Devonian and which have ties to modern sharks (table 12). The park's paleontological resources inventory and monitoring program and issues associated with fossils are summarized in the following Geologic Resource Management Issues section. While this document was in final formatting, the results of a multi-disciplinary paleontological resources inventory effort in late 2019 was completed. See Santucci and Tweet (2020) for the resulting inventory report.

The sedimentary rock layers in Grand Canyon National Park yield abundant fossils (table 12). Almost every formation has significant fossils, especially of marine invertebrates. Some other notable fossil resources include: Proterozoic microfossils; Pennsylvanian and Permian vertebrate tracks; Permian land plants; and Quaternary cave fossils. At least 162 and perhaps as many as 175 fossil taxa have been named from fossils found in and described from the park. This report provides only a cursory summary of the myriad paleontological resources in the park, but extensive discussions of the fossils, with applicable references, may be found in Santucci et al. (2001), Kenworthy et al. (2004), and Tweet et al. (2009). The NPS Fossils and Paleontology website, <https://www.nps.gov/subjects/fossils/index.htm>, provides more information about servicerwide paleontological resources.

Thousands of studies have documented the geology and paleontology of Grand Canyon National Park and contributed critical data to determine, among other things, the relative ages of rock units, the evolution of various taxa, and the depositional environments in which these ancient organisms lived or were entombed (Tweet et al. 2009). For example, the fossils and strata of

Table 12. Precambrian, Paleozoic, and Mesozoic fossils found in Grand Canyon National Park.

Fossils listed in the park were reviewed by Vincent Santucci, NPS (written communication 30 August 2018), Justin Tweet, NPS (written communication 22 August 2018 and 29 April 2019), and J.P. Hodnett, NPS (written communication, 19 April 2019). The “Tonto Group undivided” is either Muav Limestone or Bright Angel Shale with the stratigraphy either being uncertain or the report predating the division of the Tonto Group.

Era	Formation/Member (map symbol)	Fossils
MESOZOIC	Chinle Formation Shinarump Member (TRms)	Petrified logs, but very few Mesozoic fossils have been found in the park (Justin Tweet, NPS GRD, paleontologist, written communication, 20 August 2018).
	Moenkopi Formation undivided (TRm)	None to date.
PALEOZOIC	Kaibab Formation, undivided (Pk)	Fish assemblage as of 2019: <i>Chondrichthyes</i> , <i>Coolyella peculiaris</i> , <i>Cooperella striatula</i> , <i>Deltodus mercurii</i> , - cf. <i>Heslerodus divergens</i> , <i>Megactenopetalus kaibabanus</i> , <i>Mooreyella typicalis</i> , <i>Psephodus</i> sp., indeterminate jalododont, indeterminate euselachian spine, and other unidentified sharks; Osteichthyes- platysomid indeterminate tooth plates, indeterminate large actinopterygian (bony) fish. Invertebrate fossils are listed under the members.
	Kaibab Formation Harrisburg Member (Pkh)	Bryozoans, brachiopods, bivalves, nautiloids, gastropods, scaphopods, trilobites, crinoids, fish teeth/plates.
	Kaibab Formation Fossil Mountain Member (Pkf)	<i>Peniculauris bassi</i> (productid brachiopods), strophomenid brachiopods, <i>Actinocoelia maeandrina</i> (siliceous sponges), conulariids, horn corals, bryozoans, bivalves (<i>Schizodus</i> most common), gastropods, scaphopods, trilobites, crinoids, echinoids, Chondrichthyan fishes: <i>Coolyella peculiaris</i> , <i>Cooperella striatula</i> , <i>Deltodus mercurii</i> , cf. <i>Heslerodus divergens</i> , <i>Megactenopetalus kaibabanus</i> , <i>Mooreyella typicalis</i> , and invertebrate burrows (fucoids).
	Toroweap Formation Woods Ranch Member (Ptw)	Bivalves.
	Toroweap Formation Brady Canyon Member (Ptb)	Bryozoans, brachiopods bivalves, nautiloids, gastropods, scaphopods, ostracodes, crinoids, echinoids, and stromatolites.
	Toroweap Formation Seligman Member (Ptb)	Poorly preserved mollusks at Fossil Mountain (McKee 1938).
	Coconino Sandstone (Pc)	Tetrapod tracks: cf. <i>Varaopus</i> isp., <i>Erpetopus</i> isp., cf. <i>Tambachichnium</i> isp., <i>Ichniotherium sphaerodactylum</i> , and cf. <i>Amphisauropus</i> isp. (Tweet, NPS GRD, paleontologist, written communication, 29 April 2019). Invertebrate traces: possible worms, millipedes, spiders, scorpions (<i>Paleohelcura</i>). Tetrapod tracks of <i>Ichniotherium</i> sp. and <i>Limnopus</i> sp.
	Hermit Formation (Ph)	Tetrapod tracks of ichnospecies: <i>Batrachichnus delicatulus</i> (amphibian); <i>Hyloidichnus bifurcatus</i> and <i>Parabaropus coloradensis</i> (seymouriamorphs, early amniote relatives); <i>Gilmoreichnus hermitanus</i> (pelycosaur, an early “mammal-like reptile”). Plants: 49 taxa; mostly seed ferns (esp. <i>Supaia</i>) and conifers; ginkgoes. Ichnofossils: impression of crustacean or eurypterid similar to <i>Hastimima</i> ; worm burrows; <i>Rivularites</i> (called “old-elephant skin,” it is some kind of microbially mediated sediment texture). Insects: meganeurid (dragonfly relative) <i>Tupus</i> (<i>T. gilmorei</i> and <i>T. permianus</i>); partial odonate (true dragonfly); possible blattoid wing (early cockroach relative). Obscure fossils: resting and possible feeding marks, root bioturbation, and skeletal grains in sand.
	Esplanade Sandstone (Pe)	<i>Rivularites</i> , foraminifera, plant fragments (including the conifer, <i>Walchia</i>), fragments of corals/bryozoans/brachiopods or bivalves/pelmatozoans, unspecified marine fossils, horseshoe-like tracks, and invertebrate burrows.

Table 12, continued. Precambrian, Paleozoic, and Mesozoic fossils found in Grand Canyon National Park.

Era	Formation/Member (map symbol)	Fossils
PALEOZOIC	Wescogame Formation (PNMs)	Land plants, bryozoan fragments, shelly fragments, pelmatozoan fragments, foraminifera, "algae," unspecified marine fossils, the chondrichthyan fish <i>Deltodus</i> sp., invertebrate burrows, invertebrate trails, and amphibian tracks.
	Manakacha Formation (PNMs)	Stromatolites, <i>Rivularites</i> , foraminifera, calcispheres, stems, ferns, bryozoan fragments, ostracode fragments, echinoderm fragments, shelly fragments, "algae," <i>Girvanella</i> fragmentstetrapod tracks, and worm burrows.
	Watahomigi Formation (PNMs)	Marine fauna: brachiopods, foraminifera, corals, bryozoans, bivalves, conulariids, gastropods, trilobites, crinoids, echinoids, the chondrichthyan fish <i>Deltodus</i> sp., <i>Rivularites</i> , stromatolites, "algae," and invertebrate burrows. Early plants: <i>Calamites</i> , <i>Cordaites</i> , <i>Neuropteris</i> , <i>Taeniopteris</i> , and <i>Walchia</i> (conifer).
	Surprise Canyon Formation (Ms)	<i>Calamites</i> , <i>Lepidodendron</i> , <i>Lepidostrobophyllum</i> , other plant fossils, tabulate corals, bryozoans (potentially), brachiopods, bivalves, gastropods, trilobites, echinoderm debris, conodonts, 31 taxa of chondrichthyan fishes (including 4 new euselachian taxa, 2 protacrodontids, and 2 anachronistids, with ties to modern sharks), and other indeterminate actinopterygian (bony) fishes, oncolites, invertebrate trace fossils, and foraminifera.
	Redwall Limestone (Mr)	Calcispheres, foraminifera, corals, bryozoans, brachiopods, nautiloids, gastropods, trilobites, blastoids, crinoids, the chondrichthyan fish <i>Helodus</i> sp., "algae," and invertebrate trace fossils.
	Temple Butte Formation (Dtb)	Fossils are rare. <i>Polygnathus asymmetricus</i> Zone (Middle Devonian) and early Late Devonian conodonts, indeterminate brachiopods, gastropods, rugose corals, placoderm (early jawed fish) <i>Bothriolepis coloradensis</i> and lobe-fin fish <i>Holoptychius</i> , massive stromatoporoids (potentially), cylindrical trace fossils.
	Tonto Group undivided*	Trilobites (most abundant fossils): common genera include <i>Olenellus</i> , <i>Antagmus</i> , <i>Zacanthoides</i> , <i>Albertella</i> , <i>Kootenia</i> , <i>Glossopleura</i> , and <i>Bolaspis</i> . Brachiopods: genera include <i>Lingulella</i> , <i>Paterina</i> , and <i>Nisusia</i> . Also, hyoliths, bradoriids, and invertebrate trace fossils.
	Muav Limestone (Cm)	Trilobites, archaeocyathid sponges (potentially), brachiopods, hyoliths, spicules of enigmatic <i>Chancelloria</i> (six-rayed sclerites), rare structures of <i>Girvanella</i> (cyanobacteria), gastropod-like helcionelloids and <i>Scenella</i> , invertebrate trace fossils, stromatolites and algal balls, pellets.
	Bright Angel Shale (Cba)	Trilobites, brachiopods, bradoriids (bivalve arthropods), <i>Hyolithes</i> , eocrinoids, enigmatic invertebrates (<i>Chancelloria</i> , <i>Margaretia</i> , <i>Tontoia</i>), filament mats, microbial wrinkle structures, invertebrate trace fossils, palynomorphs (spores, cuticle fragments, possible egg cases, leiospheres).
	Tapeats Sandstone (Ct)	Primarily invertebrate trace fossils, with uncommon brachiopods and possibly trilobites.
	Sixtymile Formation (Zs)	Fossils have not been found in the park, yet.

Table 12, continued. Precambrian, Paleozoic, and Mesozoic fossils found in Grand Canyon National Park.

Era	Formation/Member (map symbol)	Fossils
NEOPRO- TEROZOIC	Kwagunt Formation Walcott Member (Zkw)	<i>Chuar</i> circularis (disc-like, carbonaceous fossil; algae?) and other acritarchs (organic microfossils that cannot be classified as anything else), stromatolites, unicells, <i>Melanocyrtium</i> and other testate amoebae (vase-shaped microfossils that are the earliest evidence for marine heterotrophic eukaryotes).
	Kwagunt Formation Awatubi Member (Zka)	<i>Boxonia</i> (stromatolite), <i>Chuar</i> circularis, other acritarchs, <i>Sphaerocongregus variabilis</i> (bacteria), filamentous bacteria, possible eukaryotic algal filaments, vase-shaped microfossils.
	Galeros Formation Duppa Member (Zgd)	Acritarchs (microfossils).
	Galeros Formation Carbon Canyon Member (Zgcc)	<i>Baicalia</i> (stromatolite), <i>Chuar</i> circularis, acritarchs, unicells and filaments.
	Galeros Formation Jupiter Member (Zgj)	<i>Inzeria</i> (stromatolite); <i>Stratifera</i> (stromatolite); microfossils including acritarchs such as <i>Chuar</i> circularis.
	Galeros Formation Tanner Member (Zgt)	<i>Chuar</i> circularis, other acritarchs.
	Nankoweap Formation (YZn)	Putative “jellyfish impression” <i>Brooksella canyonensis</i> possibly a trace fossil but more likely an inorganic feature such as a gas or fluid escape feature (sand volcano).
MESOPR- OTEROZOIC	Dox Formation Comanche Point Member (Ydc)	Stromatolites.
	Shinumo Quartzite (Ys)	Controversial burrow structures and possible algal traces.
	Hakatai Shale (Yh)	Possible pseudofossils (inorganic objects, markings, or impressions that might be mistaken for fossils).
	Bass/Hakatai transition zone	Stromatolites in beds of Bass Formation lithology.
	Bass Formation (Yb)	Stromatolites and microfossils, also pseudofossils variously described as algae, jellyfish-, sponge-, or worm-like objects or sedimentary structures.

Table 13. Cenozoic fossils found in caves in Grand Canyon National Park.

Cave names, fossils, and radiocarbon age dates in years before present (BP) are from Santucci et al. (2001), Kenworthy et al. (2004), and Tweet et al. (2009). Reviewed by Vincent Santucci, NPS (written communication 30 August 2018), Justin Tweet, NPS (written communication 22 August 2018 and 29 April 2019), and J.P. Hodnett, NPS (written communication, 19 April 2019).

Formation (map symbol)	Cave	Fossils (radiocarbon age dates)
Redwall Limestone (Mr)	Bridge Cave	Limited research. <i>Gymnogyps californianus</i> (condor) (11,140 BP).
	Chuar Cave	Limited research. <i>Oreamnos harringtoni</i> (Harrington’s extinct mountain goat) and an amalgamated dung layer (29,380 BP).
	Coconino Cavern	Limited research. <i>Nothrotheriops</i> remains.
	Crescendo Cave	<i>Lepus</i> sp., <i>Corvus</i> sp., and <i>Gymnogyps californianus</i> . Packrat (<i>Neotoma</i> spp.) midden. Dung from <i>Oreamnos harringtoni</i> ? (10,950 BP). Contains over 11 rock cairns.
	Crystal Forest Cave and Cave of the Domes	Packrat middens (20,630–510 BP) show the transition from a late Pleistocene mixed conifer forest and arid juniper scrubland with <i>Juniperus osteosperma</i> , <i>Atriplex confertifolia</i> (shadescale), and <i>Artemisia tridentate</i> (sagebrush) to today’s pinyon-juniper woodland and desert scrub dominated by <i>Coleogyne ramossissima</i> and <i>Ephedra viridis</i> (green ephedra).

Table 13, continued. Cenozoic fossils found in caves in Grand Canyon National Park.

Formation (map symbol)	Cave	Fossils (radiocarbon age dates)
Redwall Limestone (Mr)	Disappearing Cave	Small, stratified section of sediments, plant remains, and <i>Oreamnos harringtoni</i> dung pellets (27,360 BP).
	Five Windows Cave	Extensive faunal remains, packrat midden, and a mat of <i>Oreamnos</i> or <i>Ovis</i> dung. Avian taxa: bones of several <i>Gymnogyps californianus</i> , <i>Zenaida macroura</i> , <i>Falco sparverius</i> , <i>Catoptrophorus semipalmatus</i> (willet), <i>Anas</i> sp. (duck), and an unidentified passerine. Lizard skull; squirrel femur.
	Hummingbird Cave	Hundreds of bones from small animals, such as birds and rodents, along with rodent feces (probably <i>Peromyscus</i>). No packrat activity. Avian taxa: <i>Anas crecca</i> (green-winged teal), <i>Aythya affinis</i> (lesser scaup) <i>Circus cyaneus</i> (northern harrier), 2 species of <i>Falco</i> , <i>Larus</i> sp. (gull), an unidentified passeriform, mummified <i>Corvus corax</i> (raven), and a headless <i>Sphyrapicus varius</i> (yellow-bellied sapsucker) skeleton.
	Left Eye Cave	<i>Ovis canadensis</i> (bighorn sheep) or <i>Oreamnos harringtoni</i> dung. Packrat midden.
	Luka Cave	<i>Gymnogyps californianus</i> skeletal remains. Late Pleistocene mixed conifer forest dominated by <i>Pinus flexilis</i> (no longer present within the park) between elevations of 1600 m (5,200 ft) and 1800 m (5,900 ft). Packrat middens (14,050 and 15,840 BP). Split-twigg figures.
	Midden Cave	Limited research. <i>Gymnogyps californianus</i> (22,180 BP).
	Rebound Cave	Packrat middens. Dung from <i>Ovis canadensis</i> or <i>Oreamnos harringtoni</i> (16,640 BP). Partial artiodactyl humerus.
	Right Eye Cave	<i>Ovis canadensis</i> or <i>Oreamnos harringtoni</i> bone fragments.
	Sandblast Cave	Three caverns merge to form a small complex of caves. May represent a nest or roost for raptors: thousands of bones of fish, lizards, snakes, birds, and rodents scattered on floor. <i>Gymnogyps californianus</i> : 64 bones; at least 5 individuals (13,110–9,580 BP). Packrat midden fossils; fragments of large mammal limbs from <i>Equus</i> , <i>Bison</i> , <i>Camelops</i> , and <i>Mammuthus</i> ; <i>Oreamnos harringtoni</i> skeletal remains and dung pellets (>33,110 BP); avian remains from <i>Podilymbus podiceps</i> (pied-billed grebe), <i>Aechmophorus occidentalis</i> (western grebe), <i>Cathartes aura</i> (turkey vulture), 3 species of <i>Anas</i> (ducks), <i>Aythya</i> (duck), <i>Buteo</i> (hawk), 3 species of <i>Falco</i> (falcons), <i>Fulica americana</i> (American coot), cf. <i>Porzana carolina</i> (sora), <i>Zenaida macroura</i> (mourning dove), <i>Aeronautes saxatalis</i> (white-throated swift), and <i>Corvus</i> sp. (crow or raven). Driftwood (beyond 40,000-year limit of radiocarbon dating).
	Shrine Cave	Packrat middens (Late Pleistocene): bone, skull, horn sheaths, teeth, and dung from either <i>Oreamnos harringtoni</i> or <i>Orvis Canadensis</i> . Contains 33 rock cairns and 2 split-twigg figures (3,500–3,900 BP), which have dung pellets (<i>Orvis canadensis</i> ?) wrapped inside them.
	Skull Cave	Age from anhydrite deposit: ~16,000 BP. Floor is littered with bones of small animals and <i>Neotoma</i> (packrat) and <i>Peromyscus</i> (deer mice) feces. Mammalian taxa: <i>Pipistrellus heperus</i> (western pipistrelle), <i>Sylvilagus</i> (cottontail rabbit), <i>Lepus</i> sp. (hare and jackrabbit), <i>Neotoma</i> , <i>Peromyscus</i> , <i>Spilogale putorius</i> (eastern spotted skunk), <i>Oreamnos harringtoni</i> , <i>Ovis canadensis</i> , and unidentified large mammal bones. Avian taxa: <i>Gymnogyps californianus</i> , <i>Chen caerulescens</i> (snow goose), 4 species of <i>Anas</i> (duck), <i>Aythya</i> sp.(duck), cf. <i>Colinus virginianus</i> (bobwhite quail), <i>Phalaropus lobatus</i> (red-necked phalarope), <i>Colaptes auratus</i> (northern flicker), cf. <i>Junco</i> sp. (junco), and <i>Agelaius phoeniceus</i> (red-winged blackbird). <i>G. californianus</i> skeletal remains dated to ~12,210 BP.
	Skylight Cave	Avian taxa: <i>Podilymbus podiceps</i> , cf. <i>Podiceps nigricollis</i> (eared grebe), <i>Gymnogyps californianus</i> , two species of <i>Anas</i> (duck), <i>Falco spaverius</i> (American kestrel), <i>Recurvirostra americana</i> (American avocet), Picidae specimen; and an unidentified Passeriformid. <i>Gymnogyps californianus</i> tissue (~11,345 BP).
Stanton's Cave	Yielded 23 mammal species; 70 bird species. Artiodactyl (ungulate), perhaps <i>Ovis canadensis</i> (<11,000 BP; early Holocene). <i>Gymnogyps californianus</i> (~14,260 BP). <i>Oreamnos harringtoni</i> dung pellets and skeletal remains (17,300–10,870 BP). Foot elements of <i>Miracinonyx trumani</i> (American "cheetah"). Split-twigg figures. A Paleozoic vertebrate trackway was discovered in what was believed to be either a paleochannel in the Surprise Canyon Formation (Ms) or Supai Group sediments.	

Table 13, continued. Cenozoic fossils found in caves in Grand Canyon National Park.

Formation (map symbol)	Cave	Fossils (radiocarbon age dates)
Redwall Limestone (Mr)	Stevens Cave	Cave sediments date to 700,000 BP. <i>Canis dirus</i> (dire wolf) or <i>C. lupus</i> (gray wolf). <i>Gymnogyps californianus</i> skull (12,540 BP). <i>Oreamnos harringtoni</i> skeletal remains and dung pellets.
	Three Springs Cave	Limited research. <i>Gymnogyps californianus</i> .
	Tooth Cave	Limited research. <i>Gymnogyps californianus</i> .
	Tse'an Bida Cave (Bida Cave)	<i>Oreamnos harringtoni</i> skeletal remains, pellets (24,190–11,850 BP), and a skull (~12,930 BP). Pollen from <i>O. harringtoni</i> and <i>Ovis canadensis</i> dung. Late Pleistocene pollen dating back to 24,000 BP. Glacial pollen included abundant <i>Artemisia</i> (sagebrush) and <i>Picea</i> (spruce) suggesting cool, dry conditions. Interglacial pollen included abundant <i>Pinus</i> . Packrat middens with numerous animal taxa and plant material including remains of <i>Neotoma</i> (pack rat; 13,780–6,800 BP), <i>Peromyscus</i> (deer mice; 8,470 BP), <i>Thomomys</i> sp. (pocket gopher), <i>Sceloporus</i> sp. scale (spiny lizard), cf. <i>Sonorella</i> (land snail) shell fragment, <i>Microtus</i> (vole), and <i>Coleonyx variegatus</i> (banded gecko). Split-twig figures.
	Tse'an Kaetan Cave (Kaetan Cave)	<i>Oreamnos harringtoni</i> skeletal remains and dung pellets (30,000–14,220 BP). Single calcaneum of <i>Miracinonyx trumani</i> . Pollen from Late Pleistocene flora: <i>Pinus</i> , <i>Artemisia</i> , <i>Juniperus</i> . Plant macrofossils (30,600, 24,000, 17,500, and 14,000 BP). <i>Gymnogyps californianus</i> ulna (~16,290 BP). Split-twig figures.
	White Cave	Limited research. <i>Oreamnos</i> or <i>Ovis</i> dung. Split-twig figures.
	unidentified cave	Limited research. Mummified canid, mats of late Pleistocene <i>Oreamnos harringtoni</i> dung, and masses of late Pleistocene to Holocene packrat middens.
	Unnamed high-elevation caves	Abundant Pleistocene packrat middens dominated by needles of <i>Picea pungens</i> (blue spruce) and <i>Juniperus communis</i> (common juniper) and mixed coniferous forest species.
Muav Limestone (Cm)	Rampart Cave	Two extensive layers of <i>Nothrotheriops shastensis</i> (Shasta ground sloth) dung (40,000–24,000 and 13,000–11,000 BP) contained 72 genera of plant. Over 200 <i>Nothrotheriops shasterensis</i> bones and skeletal remains of <i>Oreamnos harringtoni</i> (with dung pellets ~18,430 BP), <i>Gymnogyps californianus</i> , <i>Erethizon dorsatum</i> (porcupine), and <i>Marmota flaviventris</i> (marmot). Uncemented packrat midden with plant material (24,000–14,000 BP). Cemented packrat middens contained 60 plant types including <i>Fraxinus anomala</i> twigs (18,890 BP) and <i>Agave utahensis</i> (9,520 BP); small mammal and reptile remains included 1 tortoise species, 3 lizard species, 3 snake species, the vampire bat <i>Desmodus stocki</i> , 4 <i>Neotoma</i> species, and 1 <i>Peromyscus</i> sp. (deer mouse). Two individuals of <i>Miracinonyx trumani</i> (American “cheetah”) and large feline dung. Soft tissues included 8 goat horn sheaths (10,140–28,700 BP), hair, sinews, tracheal remains, a goat forefoot with muscle, cartilage, and skin. Bat guano near the rear of the cave (>35,500 BP).
	Vulture Cave	A large room formed from 3 major conduits merging. From 15 packrat middens: 45 plant taxa, with twigs and seeds of <i>Juniperus</i> sp. (33,600 BP) being the most abundant; bones and teeth from 37 vertebrate taxa included 1 tortoise, 8 species of lizard, 10 snake species, 3 bird species, 1 shrew species, 9 rodent species, 4 artiodactyl species, and 1 carnivore species. <i>Lampropeltis pyromelana</i> (Arizona mountain kingsnake) was the first Pleistocene find of the snake in Grand Canyon. <i>Trimorphodon biscutatus</i> (lyre snake) was the first one found in Grand Canyon; <i>Microtus</i> (vole) are the only known remains of those taxa in Grand Canyon; <i>Notiosorex</i> (shrew) was the first late Pleistocene occurrence in Grand Canyon; <i>Camelops</i> tooth was the largest mammal from Vulture Cave. From a <i>Bassariscus astutus</i> (ringtail refuse deposit ~1,930 BP): 540 elements representing 22 taxa included 7 lizard species, 6 snake species, 3 bird species, and 6 mammalian species (most common vertebrate was <i>Neotoma</i>). Arthropods, mostly members of the Diplopoda, were also found. <i>Oreamnos harringtoni</i> and <i>Gymnogyps californianus</i> skeletal remains. Unidentified insects.
	Muav Caves (3 small caves)	No formal excavations. <i>Oreamnos harringtoni</i> skeletal remains; <i>Nothrotheriops shastensis</i> dung (11,140 and 11,290 BP); <i>N. shastensis</i> dung boluses (11,810–10,650 BP).

the Grand Canyon Supergroup contain an exceptional record of the middle and late Proterozoic in North America. The bacterium *Sphaerocongregus variabilis* from the Awatubi Member of the Kwagunt Formation (**Zka**), Chuar Group, correlates with worldwide glaciations (Dehler et al. 2012, 2017). Although enigmatic and subject to controversy, a sedimentary feature found in the Nankoweap Formation (table 12) may represent the earliest record of complex life on earth if it turns out to be a trace fossil impression of a stranded jellyfish or a worm burrow (Ford and Dehler 2003).

The marine invertebrate fossils common throughout the Paleozoic section document the many transgressions and regressions that affected the western margin of North America (fig. 28). Fossil plants and a dragonfly wing in the Hermit Formation (**Ph**) (fig. 23) and vertebrate trackways in the Supai Group and Coconino Sandstone (**Pc**) (fig. 16) document the transition from marine to non-marine environments in Pennsylvanian and Permian Periods (Upper Paleozoic strata).

Until 2013, the most significant tetrapod track in the eolian Coconino Sandstone was *Chelichnus*. In 2013, the first record of *Ichniotherium* was discovered in a fallen boulder of Coconino Sandstone adjacent to the Dripping Springs Trail along the southern rim of the canyon (fig. 16; Francischini et al. 2018). Not only was this the first *Ichniotherium* trackway to be discovered in Grand Canyon National Park but it was also the geologically youngest record of the ichnogenus. According to Francischini et al. (2018, p. 52), “the presence of *Ichniotherium* in the Coconino Sandstone is the first evidence of the occupation of a desert environment by diadectomorphs, which makes this record an important clue for understanding the evolution of the adaptations of non-amniotes to living in arid environments.”

In 2019, the tetrapod tracks in Grand Canyon National Park were revised and assigned to cf. *Varaopus* isp., *Erpetopus* isp., cf. *Tambachichnium* isp., *Ichniotherium sphaerodactylum*, and cf. *Amphisauropus* isp (table 12; Justin Tweet, NPS GRD, paleontologist, written communication, 29 April 2019; Marchetti et al. 2019). The *Ichniotherium* tracks in the Coconino Sandstone are now considered to be the oldest evidence of occupation of deserts by non-amniote tetrapods (Francischini et al. 2019). The significance of the relatively abundant *Ichniotherium* tracks in the desert environment of the Coconino Sandstone suggests that species diversity may not be as limited as previously thought. Francischini et al. (2019) provide a more detailed discussion of the Coconino Sandstone ichnofauna.

In addition to scientific research, fossils in Grand Canyon National Park are used for education

and interpretation. Fossil invertebrate sites in the Kaibab Formation (**Pk**), for example, are used for interpretive purposes near Grand Canyon Village and on the Hermit, South Kaibab, and Bright Angel Point trails (Tweet et al. 2009). Vertebrate track sites in the Coconino Sandstone (**Pc**) offer interpretive opportunities on the Hermit and South Kaibab trails (fig. 16). They are also part of the park’s Trail of Time, an interpretive walking trail that focuses on Grand Canyon’s vistas and rocks.

The oldest fossils preserved in Grand Canyon National Park are stromatolites, layers of limy sediment trapped and bound by mats of cyanobacteria (blue-green algae). Stromatolites are abundant in the billion-year-old Bass Formation (**Yb**), and along with a few other single-celled organisms, they are the most common record of life on Earth from about 3.6 billion to 0.55 billion years ago (fig. 26). Modern-day stromatolites provide important information regarding paleoenvironments associated with ancient stromatolites. Abundant stromatolites, for example, currently populate the shallow, marine environment in Shark Bay, Australia.

Caves and Paleontological Resources

Numerous cave deposits and packrat middens in Grand Canyon National Park have yielded a sizeable fossil record containing significant information about past ecology and climate dating to the late Pleistocene (table 13; Kenworthy et al. 2004; Tweet et al. 2009). Packrat (*Neotoma* spp.) middens are accumulations of plant material and food waste cemented by urine (Tweet et al. 2012). In addition to packrat middens, dung (fig. 42), pollen, skeletal remains, and soft tissue, such as hair, muscle, ligaments, and horn sheaths of the extinct Harrington’s mountain goat *Oreamnos harringtoni*, have been exceptionally preserved because of the arid climate of the Grand Canyon (fig. 43). Because many of the caves are very difficult to access, vandalism is rare.



Figure 42. Photograph of 20,000-year-old giant ground sloth dung in a cave in Grand Canyon National Park.
NPS photograph by Robyn Henderik (Zappitello et al. 2017, p. 13).



Figure 43. Photograph of a Harrington's Mountain Goat cranium with horns and sheaths and teeth discovered in the caves in Grand Canyon National Park.

Fossil remains indicate that Harrington's Mountain Goats occupied the Grand Canyon for 18,000 years before becoming extinct by 11,160 radiocarbon years before present. NPS photograph available at https://www.flickr.com/photos/grand_canyon_nps/5111927440.

The Muav Limestone (**Cm**) contains most of the fossil-bearing caves in the western section of the park, while the Redwall Limestone (**Mr**) holds most caves in the eastern part of the park (Kenworthy et al. 2004; Lucas and Morgan 2005). Spamer (1984, 1992), Santucci et al. (2001), Kenworthy et al. (2004), and Tweet et al. (2009) provide summaries and taxonomic lists of cave fossils from over three dozen caves in Grand Canyon National Park.

Rampart Cave (table 13) in the Muav Limestone, one of the first caves to be studied in the park, may be the best-known fossil cave in the park and is a good example of the variety of paleontological resources found in Grand

Canyon caves. NPS employee Willis Evans first entered Rampart Cave in 1936 and discovered exceptional deposits of *Nothrotheriops shastensis* (Shasta ground sloth) dung representing at least two distinct time periods during the Pleistocene epoch: (1) from over 40,000 years ago to about 24,000 years ago, and (2) from about 13,000 years ago to the beginning of the Holocene epoch 11,000 years ago (Santucci et al. 2001; Tweet et al.

2009; Hunt et al. 2012). The cave contains rich organic layers, uncommon in the arid southwest.

The 72 plant genera found within the dung showed that the sloths were bulk feeders with a diet of desert globemallow, Nevada Mormon tea, saltbush, catclaw acacia, cacti, reeds, and yucca that varied with the seasons (Hansen 1978; Phillips 1984). In 1976, a fire in Rampart Cave destroyed an estimated 70% of the deposit. Before the fire, the cave contained the thickest and least disturbed deposit of stratified *Nothrotheriops shastensis* dung from any known locality (Carpenter and Mead 1999; Santucci et al. 2001; Tweet et al. 2009).

When the sloths went extinct, the plants that made up their diet were doing well, suggesting that food scarcity was not a cause of extinction (Hansen 1978). Discovery of 11,810–10,650-year-old dung boluses of *N. shastensis* in three Muav caves upstream from Rampart Cave correspond to the end of the Pleistocene, the arrival of Clovis hunters into North America, and the extinction of *Oreamnos harringtoni* and 31 other large mammal genera (Santucci et al. 2001).

The layer between the two dung deposits in Rampart Cave occurred during the glacial maximum and includes an uncemented packrat midden with perfectly preserved plant material dating from 24,000 to 14,000 years before present, mountain goat dung and bones, and marmot bones. The midden may be the largest Pleistocene packrat deposit ever found. Thirty additional packrat middens were found within and around Rampart Cave and provided significant data for Pleistocene paleoecological reconstruction (Santucci et al. 2001). Rampart Cave has also yielded archeological material (Spamer 1984).

Fossils in Cultural Resource Contexts

Several caves in Grand Canyon National Park contained split-twig figures, some with goat dung pellets wrapped inside them, and cairns left by prehistoric visitors (table 13; Kenworthy and Santucci 2006; Tweet et al. 2009). The oldest split-twig figure dates to at least 4,390 years ago (Tweet et al. 2009). Some cave shrines include split-twig figures along with *Oreamnos harringtoni* horn sheaths.

In the park's collections, 36 catalog numbers containing 4,297 items represent definite or potential evidence of fossils and nonfossils found in cultural resource contexts (Tweet et al. 2009). Nonfossils include such items as obsidian used for projectile points. The collection includes both unworked and worked items.

Historic structures at Grand Canyon National Park also contain fossils (Tweet et al. 2009). Several buildings on the South Rim, such as in the Headquarters (former

Visitor Center) courtyard and the benches on the Bright Angel Lodge patio, contain slabs of track-bearing Coconino Sandstone (Pc). The Yavapai Observation Station, Canyon View Visitor Center, the paved trails in the Village area, and the Mary Colter-McKee fireplace at the Bright Angel Lodge incorporated local fossil-bearing rock into their construction.

Caves, Karst, and Springs

Karst landscapes develop through the dissolution of soluble rock, most commonly carbonates such as limestone or dolomite (Toomey 2009). Caves, sinkholes, disappearing streams, springs, and internal drainage are characteristic features of karst landscapes. As of September 2017, cave or karst resources have been documented in at least 159 parks, including Grand Canyon National Park (fig. 44). Karst hydrology of Grand Canyon, especially the Redwall-Muav aquifer, the primary water-bearing unit in the park, have been studied in detail by Huntoon (1970, 1974, 1981, 1995, 1996, 2000a, 2000b), and more recently by researchers working with hydrologist and cave specialist Ben Tobin (Gandee et al. 2015; Henderek et al. 2015; Hoffman et al. 2015; Springer et al. 2015; Valle et al. 2015; Jones et al. 2016a, 2017a; Jones et al. 2016b, 2017b; Zappitello et al. 2016, 2017; Dohm et al. 2017; Tobin et al. 2018). These contemporary studies have significantly contributed to understanding of the cave/karst resources in the region. The NPS Cave and Karst website, <https://www.nps.gov/subjects/caves/index.htm> provides additional information.



Figure 44. Photograph of an entrance to a cave in the Redwall Limestone, Grand Canyon National Park. Scientists for scale. NPS photograph by Dale Pate.

Grand Canyon Caves

The total number of caves varies from an estimated 1,000 to 2,500 (Land et al. 2013; NPS 2015a). Rather than estimating how many caves might be in the park, Pate (2016) recommended focusing on the cave resources in the known caves in the park and in the Greater Grand Canyon Landscape Assessment Area. As of 2015, over 335 known caves in the park contained extinct Late Pleistocene fauna and archeological material, and at least 474 caves were known from the assessment area (Henderek et al. 2015; Pate 2016).

Exploration and documentation of the park's caves is just beginning. As of 2016, about 100 caves had been surveyed with a total of over 140 km (85 mi) of passage (Ben Tobin, NPS Grand Canyon National Park, hydrologist, written communication, 30 August 2018). Grand Canyon ranks fifth in the number of surveyed caves of any NPS unit, behind four parks that were established specifically for their cave resources: Mammoth Cave National Park, Carlsbad Caverns National Park, Jewel Cave National Monument, and Wind Cave National Park (Stortz et al. 2018).

The park's caves contain mineral deposits, paleontological resources, significant archeological remains, and important biological systems, including bat habitat, as well as a connection to the regional hydrological systems. The Redwall Limestone (**Mr**) contains most of the caves in Grand Canyon National Park (fig. 44). Thousands of caves in the Redwall Limestone have been documented throughout the Colorado Plateau and Basin and Range province. For example, caves riddle the Redwall Limestone in the Peach Springs Canyon–Diamond Creek area.

The caves in the Grand Canyon region evolved from as many as four extensive dissolution events that involved, in chronological order (Huntoon 1990; Wenrich and Sutphin 1994; Hill and Polyak 2010):

- A widespread karst landscape of sinkholes on the emerging Redwall surface during the Late Mississippian (Huntoon 1990).
- Erosion and strong groundwater gradients, especially in western Grand Canyon, during the Late Cretaceous–Early Paleogene Laramide Orogeny.
- Post-Laramide uplift that initiated dissolution along Miocene and younger extensional faults and fractures.
- Colorado River incision of the Grand Canyon.

Grand Canyon Karst

Based on GIS analysis of the USGS cave density map by Weary and Doctor (2014), Stortz et al. (2018) estimated that 70%–90% of the area within Grand Canyon

National Park is considered karst (fig. 45). Within the National Park System, only Everglades National Park has karst area more than Grand Canyon National Park (Weary and Doctor 2014; Jones et al. 2017a). The park contains over 4,000 km² (1,500 mi²) of karst features, including a surficial karst system, major cave development, and a deeper karst system in the Redwall and Muav limestones (Bills et al. 2016; Jones et al. 2017a; Tobin et al. 2018).

Karst systems are difficult to quantify because of their heterogeneity and anisotropic dynamic nature, but the depth of the park's main karst strata adds to the complexity (Jones et al. 2017a). Karst in the Redwall and Muav formations is buried over 1,000 m (3,000 ft) below the surface (Beus 2003b).

Surface Karst System

Sinkholes in the Kaibab and Toroweap formations connect the near-surface karst system to the C aquifer, a water-table aquifer with depths to water of a few tens of meters to 500 m (a few hundred feet to more than 1,500 ft) (fig. 46; Huntoon 1974, 2000b; Bills et al. 2016). Using 1 m (3.3 ft) LIDAR resolution data, statistical analysis, and field measurements, Jones et al. (2017a) documented 7,457 sinkholes spread over the 1,450 m² (15,600 ft²) Kaibab Plateau. The Hazard Point Features layer in the GRI GIS data includes 709 sinkholes and collapse structures. Of these, 333 are in the park. Of those 333, 112 are identified as sinkholes and 221 are collapse structures/features.

Volumes of these sinkholes ranged from 0.40 m³ (14 ft³) to over 1,400,000 m³ (49,400,000 ft³), with most of the sinkholes on the smaller end of the spectrum (Jones et al. 2017a). Larger conduit systems capable of channeling, storing, and discharging greater amounts of water characterize steeper, more erosive sinkholes. Shallow, wide sinkholes have a lower drainage capacity. The frequency and depth distributions of the Kaibab Plateau sinkholes resembles the sinkhole plain of south-central Kentucky (Jones et al. 2017a).

Density data from Jones et al. (2017a) support Huntoon's hypothesis (1974, 2000b) that major conduit systems are associated with faults and fractures. In 2015, Valle et al. subdivided the sinkholes on the Kaibab Plateau into four types based on LiDAR data: patterned ground, cleft (linear), escarpment, and large sinkholes (Valle et al. 2015). Cleft sinkhole groups appeared to be the primary sinkhole type associated with fractures and open joints. Further research will help define the relationships between size, density, structural characteristics, and overall geomorphology of the karst conduit system on the Kaibab Plateau and how these characteristics influence groundwater distribution patterns (Jones et al. 2017a).

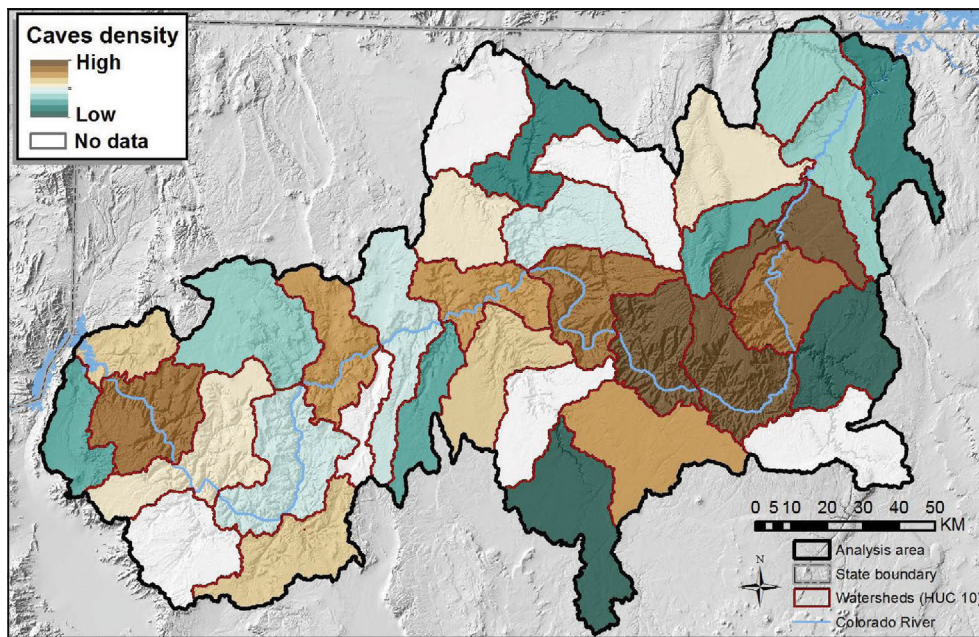


Figure 45. Map showing the cave density in the greater Grand Canyon landscape assessment area. Diagram from Stortz et al. (2018, fig. 56).

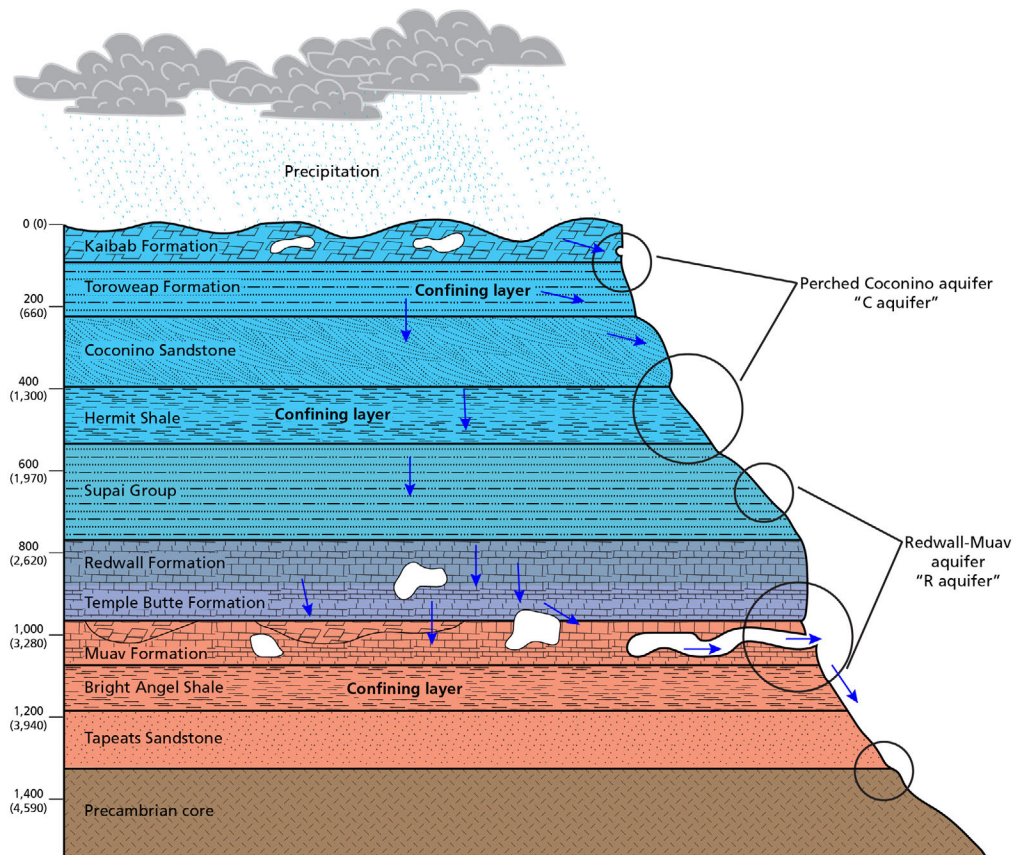


Figure 46. Hydro-stratigraphic schematic profile of the aquifer system in Grand Canyon National Park. Faults (blue lines) serve as vertical conduits for groundwater. Large circles represent the dominant location of springs. Smaller circles represent additional locations of springs. The three confining layers represent relatively thick zones of impermeable rock. Graphic by Trista Thornberry-Ehrlich (Colorado State University), modified from Jones et al. (2017a) and Tobin et al. (2018).

Deep Karst System

Various impermeable confining layers lie between the C aquifer and the R aquifer in the deeper karst system (fig. 46). The R aquifer in the Redwall-Muav formations ranges from at least 900 m (3,000 ft) to more than 1,000 m (3,200 ft) below land surface, and groundwater flow properties in the aquifer are exceptionally complicated (Huntoon 2000b; Flynn et al. 2007; Bills et al. 2016; Jones et al. 2017a; Tobin et al. 2018). Buried beneath a thick sequence of Paleozoic strata (fig. 46), the aquifer is only exposed in deeply incised canyons to the east, west, and south of the plateau. Faults and fractures connect the C and R aquifers and provide conduits for groundwater (Huntoon 2000b; Jones et al. 2017a; Tobin et al. 2018). Groundwater flow may be flashy or variable depending on the precipitation and the season (Huntoon 2000b; Jones et al. 2017a). Although geophysical data to map these conduits are limited, the morphology of the sinkholes above the conduits can indicate conduit size and the ability to channel, store, and discharge incoming water (Panno et al. 2013; Jones et al. 2017a).

Faults, joints, and bedding planes in the strata between the C and R aquifers significantly alter the groundwater flow dynamics above and within the R aquifer.

Understanding these flow dynamics is important, especially on the Kaibab Plateau, because Roaring Springs, the sole water source for the park, emerges from the plateau's R aquifer. Jones et al. (2017a) studied the interconnection between the two karst aquifers on the Kaibab Plateau by analyzing data from a dye tracer study and hydrograph analysis of discharge from the deep aquifer. Theoretical flow paths from Huntoon (1974) suggested that injected dye would discharge to Roaring Springs or to adjacent springs in Bright Angel Creek. To test this hypothesis, Jones et al. (2017a) injected dye into two sinkholes associated with the same fault. On the same day in April, uranine dye was injected into the northernmost of the sinkholes, while eosin dye was injected into the southernmost of the two sinkholes.

Eosin was not detected near Bright Angel Creek. Rather, the dye discharged at springs to the west and to the east at Vaseys Paradise Spring (fig. 47). Eosin was detected within one month after injection and stayed in the system for an additional two months. Uranine was detected in tributaries to Bright Angel Creek downstream from Roaring Springs three months following injection and stayed in the system for an additional two months (fig. 47). After 15 months of monitoring, two other injected dyes were not detected at any of the dye receptors (Jones et al. 2017a). The study nullified a previous assumption that recharge was universally distributed (Zappitello et al. 2016).

Although eosin was not detected in Bright Angel Creek, flow patterns suggested that flow directions along faults coincided with those described by Huntoon (1974; Jones et al. 2017a). Unexpected conduit flow paths are common in complicated karst systems, and fault-related structures on the Kaibab Plateau could act as major conduits. However, the heterogeneity of the various layers of limestone, sandstone, and shale complicates this interpretation. Shale typically deforms plastically along faults and usually blocks groundwater flow. Results from the dye tracer study suggest that faulted shale either does not act as a barrier to groundwater or that flow is predominantly along parallel and sub-parallel fractures related to the faults. Caves in the region generally follow major fractures that are sub-parallel to larger regional faults, and because deformation restricts groundwater flow along the faults, more water likely follows these fractures than the faults themselves (Huntoon 1974; Jones et al. 2017a). In addition, cave passage patterns show strong fracture control.

The timing and locations of the detected dyes indicate that the vertical connection between C and R aquifers probably occurs along fractures. However, the downward movement of groundwater along these vertical conduits and horizontal flow within the two aquifers is extremely complex (Jones et al. 2017a). For example, Springer et al. (2015) found that snowmelt entering sinkholes on the surface of the Kaibab Plateau took only a few days before discharging at springs 1,000 m (3,000 ft) deep and thousands of meters lateral flow. Dye trace studies by Jones et al. (2017a), however, showed much different results. Jones et al. (2017a) suggested two possible explanations to the late arrival of uranine in Bright Angel Creek compared to the arrival of Eosin at the receptors: (1) each sinkhole had different horizontal and vertical flow paths, or (2) the water moving the dyes through the system differed in type, source, and timing. Although both dyes were injected on the same day, heterogeneity in snowmelt may have delayed the movement of uranine through the system or eosin may have been injected closer to a major conduit.

Monsoon events may also have influenced the movement of the dyes through the system. Relatively slow and homogeneous infiltration associated with snowmelt may produce quite different flow patterns compared to intense, highly heterogeneous monsoon precipitation. The later detection times associated with the uranine dye receptors may reflect that the dye was only partially transported vertically during snowmelt and then mobilized more rapidly during the monsoonal season. Conversely, eosin, detected within the first month of injection, may indicate more immediate transport through the system with only snowmelt (Jones et al. 2017a).

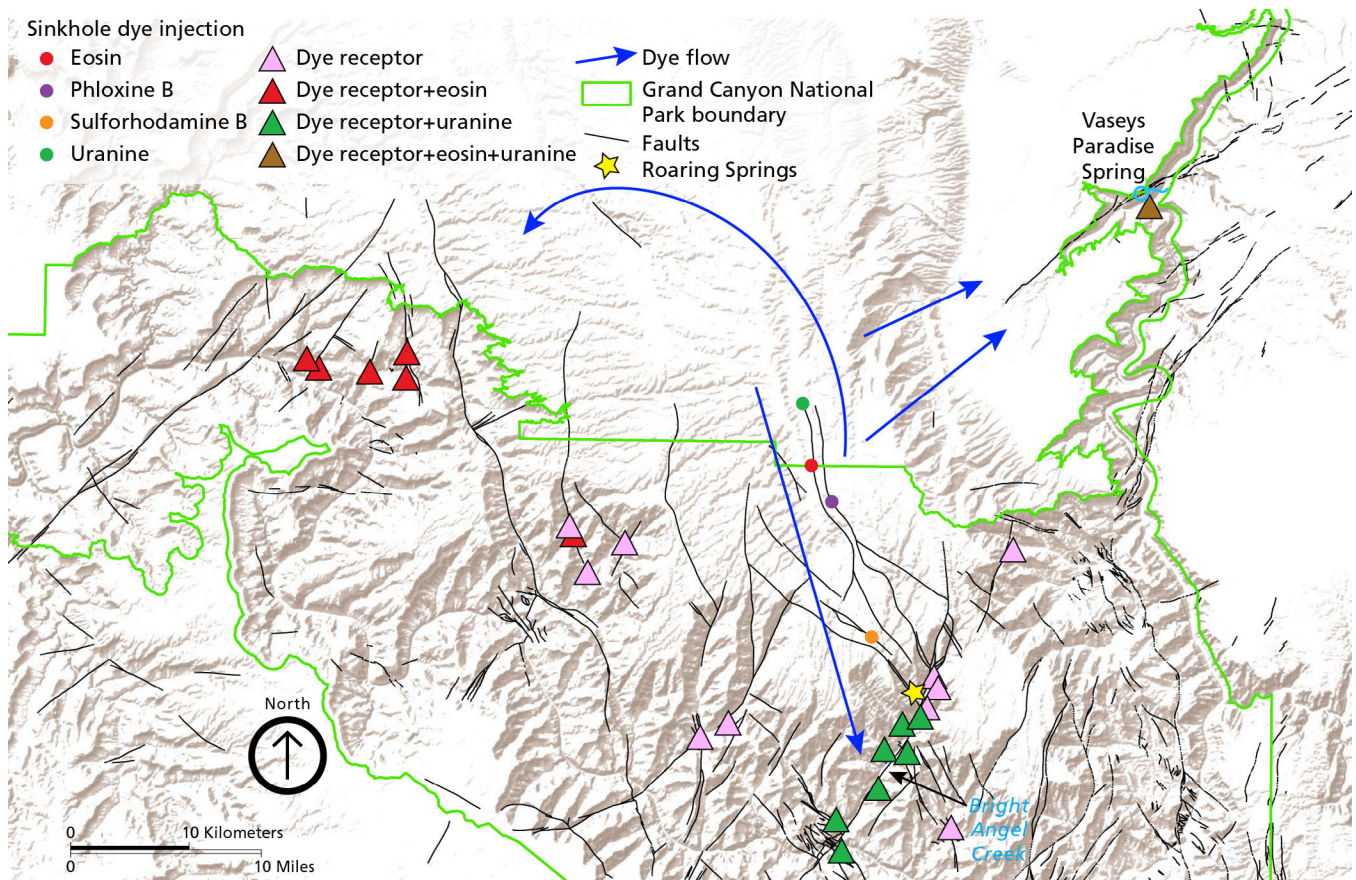


Figure 47. Locations of four dye injection sites, flow paths, and the 29 receptor sites on the Kaibab Plateau. The yellow star marks the location of Roaring Springs. Injection of phloxene B and sulforhodamine B occurred during April 2015; eosin and uranine were injected during February 2016. Eosin (red triangles) and uranine (green triangles) were detected between February and July 2016. Both were detected at Vaseys Paradise Spring. The potential generalized flow paths of the eosin and uranine dyes along faults are superimposed on the map. Phloxene B and sulforhodamine B had not been detected by July 2016. Map by Trista Thornberry-Ehrlich (Colorado State University), modified from Jones et al. (2017a, figure 11).

Roaring Springs Discharge and the Deep Karst Aquifer

To further understand the complexities of the deep karst aquifer, Jones et al. (2017a) analyzed spring discharge at Roaring Springs, chosen because it is the sole water source for the park. Spring discharge hydrographs allow for the determination of aquifer water storage and discharge distributions over time because discharge can be directly measured at the spring.

Discharge analysis demonstrated a connection between the R aquifer and surface recharge and characterized the vertical flow patterns through over 1,000 m (3,000 ft) of lithostratigraphic units, as well as horizontal flow patterns in the perched C aquifer (Jones et al. 2017a). According to Jones et al., the hydrograph data for the deep karstic R aquifer “indicate a complex, unknown

history of transit time, flow paths and residence times” (Jones et al. 2017a, p. 16).

Jones et al. (2017a) found that the base flow, the relatively constant flow in the system, emerges from groundwater stored in the intergranular matrix of the rock units and that this base flow indicates a significantly lower permeability than in most karst systems worldwide. This is understandable because the low-permeability Coconino Sandstone is often the primary water-bearing unit in the C aquifer, and the water it slowly releases from storage becomes an important contributor to the base flow of the R aquifer. The well-indurated limestones of the R aquifer have negligible matrix permeability, but dissolution along fractures and bedding planes can contribute to base flow.

Qualitative assessment of storm responses concluded that snowmelt events recharge the R aquifer's base flow by soaking into the rock's intergranular matrix, as well as through faults and fractures. Precipitation from summer monsoon events, on the other hand, rapidly infiltrates through conduit/fracture flow paths and bypasses the rock matrix. Groundwater discharge from the caves varies greatly from season to season and may cause water levels to suddenly rise to dangerous levels. For example, groundwater flow in Falls Cave at Vasey's Paradise increased only 12 hours after rainstorms occurred 16 km (10 mi) away on the Kaibab Plateau (Huntoon 1970; Hill and Polyak 2009).

These differences in hydrograph responses to snowmelt and monsoonal events may account for the variations in dye flow paths, arrival times, and locations (Jones et al. 2017a). The heterogeneity of rainfall, the shape of the flow path, and the distance from the recharge source to the spring may account for travel time variations.

Grand Canyon Springs

Grand Canyon National Park contains approximately 750 known springs (Tobin et al. 2018). The springs in Grand Canyon result from the complex relationship between caves and karst in the canyon. Smaller springs emerge from the near-surface C aquifer (fig. 46). The C aquifer consists of three main geologic formations: the Kaibab Formation, the Toroweap Formation, and the Coconino Sandstone (Huntoon 1974; Flynn and Bills 2002; Tobin et al. 2018). The larger springs, including Roaring Springs, emerge from the R aquifer, which is composed of Redwall and Muav limestones.

Between the two aquifers lie a series of confining layers, or aquitards, with variable porosities and permeabilities. The Hermit Shale underlies the C aquifer and acts as an aquitard, as do the interbedded sandstones and shales of the Supai Group (fig. 46; Jones et al. 2017a; Tobin et al. 2018). While small, ephemeral springs may be found within the Supai Group, the unit, in general, is an aquitard. The Bright Angel Shale beneath the R aquifer acts as a regional aquitard allowing only minimal water to flow from springs in the underlying Tapeats Sandstone or Precambrian basement rocks (Billingsley 2000b).

Incision by the Colorado River has bisected these aquifers into separate flow systems on the north and south sides of the river. North of the river, the C and R aquifers are connected via faults and fractures on the Kaibab Plateau. Direct recharge of the C aquifer on the Kaibab Plateau occurs from infiltration of surface water through sinkholes. Groundwater flowing from the C aquifer to the R aquifer feeds many large springs on the Kaibab Plateau. Some of the springs emerging from

the Kaibab Plateau aquifer system include the Roaring, Deer, Thunder, Tapeats, Cheyana, and Vasey's springs (Huntoon 2000b; Hill and Polyak 2010).

The largest springs are primarily located below the Kaibab Plateau. Two major exceptions include Havasu Springs and Blue Springs. Below the South Rim, Havasu Springs discharges into the Grand Canyon from the Coconino Plateau, an area twice the size of the state of Delaware. The Coconino Plateau also provides groundwater to 20 smaller springs, such as Cottonwood Springs (Crossey et al. 2009). Blue Springs, the largest magnitude spring in Arizona and the largest spring adjacent to Grand Canyon National Park, is in the Little Colorado River area (Flynn and Bills 2002; Tobin et al. 2018).

While most of the water emerging from the springs is epirogenic, originating from the surface, some researchers have found evidence for hypogenic flow, sourced from deeper geologic units below the R aquifer. Regional volcanism or hydrocarbon sources have been proposed as origins for the ascending hypogenic fluids (Crossey et al. 2006, 2009; Klimchouk 2007). This warmer, hydrogen-sulfide and helium-rich groundwater may have been the primary cause of limestone dissolution and subsequent cave formation in the upper part of the R aquifer (Huntoon 2000; Ford and Williams 2007; Hill and Polyak 2010). As the Colorado River incised the canyon, the caves and conduits drained, and the regional water table lowered (Hill et al. 2008; Polyak et al. 2008).

Speleothems in Grand Canyon Caves

Speleothems (cave formations) mark the progressive lowering of the water table that accompanied the incision of the Grand Canyon (fig. 48). As the water table lowered, the Grand Canyon caves evolved through a series of events that included:

1. Formation of calcite spar crystals. In the deeper saturated zone, CO₂ slowly decreased, allowing calcite to slowly precipitate and form large calcite spar crystals. A cave in eastern Grand Canyon contains individual crystals as much as 56 cm (22 in) long (Hill and Polyak 2010).
2. Formation of calcite mammillaries. Calcite mammillaries then formed at, or just below, the water table. Dating mammillaries can locate the position of the water table over time and help determine the rate of incision and headward erosion of the Grand Canyon. Grand Canyon mammillaries are associated with two other speleothems, cave rafts and folia, that also form at a water surface (Hill and Forti 1997; Hill and Polyak 2010). Thin, planar cave rafts float on the surface of cave pools or the

water table. Folia, believed to form under hypogene conditions, resemble interlocking wavy ribs that project downward and outward from cave ceilings and overhanging walls (Audra et al. 2009).

3. Gypsum replaced limestone. Gypsum ($\text{CaSO}_4 \cdot 2\text{H}_2\text{O}$) rinds replaced the limestone wall rock at the water table and often overlie mammillary coatings. Some of the gypsum rinds are 6 cm (2 in) thick. Sulfur isotopes support two deep sources for the gypsum. Sulfur isotopes from cave gypsum in eastern Grand Canyon match sulfur isotope values from hydrocarbons in the the Precambrian Chuar Group, while in western Grand Canyon, gypsum isotope values correspond to a volcanic/magmatic source (Hill et al. 2001; Hill and Polyak 2010). Grand Canyon-style gypsum is also found in Carlsbad Caverns and Lechuguilla Cave in the Guadalupe Mountains of New Mexico (Hill 1990). In contrast, gypsum, such as the gypsum found in Kentucky's Mammoth Cave, may form when gypsum in overlying units dissolves and is transported downward by meteoric groundwater to precipitate on cave walls and ceilings (Hill and Forti 1997; Hill and Polyak 2010).
4. Formation of subaerial speleothems. Once the water table lowered below cave level, stalactites, stalagmites, flowstone, and other subaerial speleothems formed in the confined caves. Most of the speleothems probably developed during wetter conditions during the Pleistocene ice ages. Currently, active calcite and gypsum speleothem growth occurs in numerous caves (Ben Tobin, NPS Grand Canyon National Park, hydrologist, written communication, 30 August 2018).

Miocene-age Basin and Range extension may have triggered the growth of caves in the Grand Canyon. During the early Miocene, tectonic extension opened fractures in the Bright Angel Shale and Supai Group strata, creating conduits for both meteoric groundwater flow and hypogenic fluids. Meteoric groundwater and heated groundwater from greater depths could have enhanced the circulation of groundwater in the Redwall Limestone (Huntoon 2000a).

In the late Miocene, calcite solubility may have increased as hypogenic fluids ascended along the massive joints forming parallel to the Basin and Range faults. When calcite solubility increased, large calcite crystals began to grow (Dublyansky 2000; Hill and Polyak 2010).

As incision continued, springs emerged from the Redwall-Muav aquifer, but these springs, which discharge under confining pressure (artesian flow), were not responsible for dissolving the limestone and

developing the confined caves in the Grand Canyon. Flow rates at these springs can be quite high, such as the 410 liters/second (108 gal/s) measured at Fence Springs (Huntoon 1981). Under turbulent conditions such as these, asymmetrical hollows (scallops) typically form along cave walls, but they are not found in the Grand Canyon confined caves. Rather, calcite spar crystals, mammillary speleothems, and gypsum rinds represent slow-moving, relatively stagnant aquifer conditions, characteristic of hypogene karst (Hill and Polyak 2010).



Figure 48. Photograph of speleothems of gypsum. NPS photograph by Dave Bunnell (Zappitello et al. 2017, p. 15).

Unusual Minerals

Elements combine to form minerals, which are the building blocks of rocks. The internal structure of each mineral species is unique, and this chemical blueprint not only determines the crystal's form but also its physical and optical properties, such as hardness, density, transparency, color, luster, and behavior under a microscope. Mineral aggregates that are responsible for the rocks in the Grand Canyon are neither unique to Grand Canyon National Park nor are they uncommon. However, the park does contain some unusual minerals that are not universally distributed on the Colorado Plateau (table 14).

Table 14 includes minerals that may have a specific economic purpose (see also "Breccia Pipes and Ore Deposits"). Barite, for example, is a barium sulfate, and when mixed with water, forms a mud that lubricates drill bits when drilling for hydrocarbons. Barite is also used in the manufacture of paper and rubber. Malachite (green) and azurite (blue) are copper carbonates. Galena (**PbS**) and sphalerite (**ZnS**) produce lead and zinc ore, respectively. Metamorphism of the

Table 14. Rock type, unit, location, and physical properties of unusual minerals found in the park.

Minerals are listed, with references, in www.mindat.org, and the list of cave minerals is from mindat.org and Wenrich and Stuphin (1994). *Streak refers to the color left by the residue of a mineral scratched across a tile of white unglazed porcelain known as a “streak plate” and is included in the table only when it is a distinctive physical property.

Rock Type	Unit	Location	Mineral	Visible Physical Properties
Igneous	Pegmatite	Hermit Creek	Schorl (Tourmaline)	Submetallic luster. Black (known as black tourmaline). Striated crystals.
Metamorphic	Vishnu Schist (Xv)	Mile 83 (dikes)	Talc and Tremolite	Talc: greasy, waxy, pearly luster. Multicolored (white to brown). Very soft (scratch with fingernail). Distinct greasy feeling. Tremolite: vitreous, silky luster. Usually white or yellow. Splintery, fibrous crystals.
	Precambrian	Travertine Canyon	Anthophyllite and Cordierite	Anthophyllite: vitreous, pearly luster. White, gray, green. Fibrous to blocky crystals. Cordierite: vitreous luster. Pleochroic (violet-blue to yellowish). Prismatic to stubby crystals; transparent to opaque.
	Schist/gneiss	Lone Tree Canyon	Garnet Group and Staurolite	Both are hard minerals with a vitreous, dull luster. Garnet Group: all colors except for bluish shades. Well formed, distinct, dodecahedral & trapazohedral crystals. Staurolite: brown and gray. Distinct shape where two rectangle crystals intersect to form a perfect cross.
	Archean rocks	Inner Gorge	Almandine Garnet and Silimanite	Almandine Garnet: vitreous luster. Red, black. The most common garnet. Silimanite: vitreous, silky. Gray, brown, white. Mostly fibrous crystals; radiating crystal sprays in matrix.
	Bass Formation (Yb)	Various locations	Asbestos	Silky luster. Multi-colored. Fibrous; slightly harder than talc.
Sedimentary	Coconino Sandstone (Pc)	Maricopa Point area	Torbernite	Vitreous, waxy, pearly luster. Varieties of green. Soft as asbestos; cube-shaped crystals.
	Redwall Limestone (Mr)	Horseshoe Mesa	Grandviewite	Vitreous luster. Turquoise-blue. Rosasite-like sprays of acicular crystals; soft; type locality is Grandview Mine.
	Redwall Limestone (Mr)	Kaibab Trail	Barite	Vitreous, pearly luster. Multi-colored, may show banding. Heavy; crystals often twinned; commonly fluorescent.
	Redwall Limestone (Mr)	Various locations	Malachite, Azurite, Galena, Sphalerite, Pyrite	Malachite: vitreous, silky, dull luster. Green. Opaque; Rare large individual crystals. Azurite: Vitreous, dull luster. Blue to very dark blue. Usually small crystals in aggregates. Galena: metallic luster. Steel-gray. Commonly cubic; heavy but not hard. Sphalerite: metallic, resinous luster. Multi-colored (black to orange). Common tetrahedral crystals; usually twinned; also botryoidal. Pyrite: metallic. Yellow, like brass. Cubic crystals; lighter than gold and has sharper edges; distinct black streak.*
	Redwall Limestone (Mr)	Various Park Caves	Barite, Hydro-magnesite, Ankerite, Hematite, Selenite Gypsum, Powellite, Carnotite, Conicalcite, Talmessite, Hörnesite	Barite: see above description. Hydro-magnesite: Vitreous, silky, pearly, earthy luster. Colorless, white. Known as moonmilk; most common cave carbonate after calcite and aragonite. Ankerite: pearly luster. Brown, gray, tan. Iron-bearing dolomite; rhombohedral crystals. Hematite: metallic to dull luster. Black, gray, brown, red. Many forms: massive, mammillary, boytriodal, others; distinct reddish streak. Selenite Gypsum: vitreous luster. Colorless. Forms drusy crystals. Powellite: adamantine luster. Multi-colored. Small dipyrmidal or pseudo-octahedral crystals. Carnotite: vitreous, resinous, waxy, silky, dull, earthy. Yellow. Soft; rare diamond-shaped, rhombohedral, flattened, or lath-like crystals; yellow streak. Conicalcite: vitreous, greasy, earth luster. Green. Fibrous aggregates to, botryoidal masses; light-green streak. Talmessite: vitreous luster. Colorless, white, pale green, pink. Prismatic crystals or radiating fibrous aggregates; contains arsenic. Hörnesite: vitreous, silky, pearly luster. Colorless to white. Soft prismatic and flattened crystals.

Bass Formation (**Yb**) and Vishnu Schist (**Xv**) produced asbestos (tremolite) and talc. Gypsum, a sulfate used in the manufacture of wallboard and plaster and a variety of ornamental purposes, is found in the Harrisburg Member of the Kaibab Formation (**Pkh**) and commercially mined outside the park boundary (Billingsley and Workman 2000).

Uranium is an integral element in the chemical structure of the mineral torbernite in the Coconino Sandstone (**Pc**) and carnotite in the Redwall Limestone (**Mr**) (table 14). Naturally occurring uranium is also responsible for some of the radionuclides found in the Little Colorado River, Paria River, Havasu, Kanab, and Lava Chuar creeks, and Pumpkin Springs. High concentrations of arsenic, chromium, lead, zinc, copper, cadmium, nickel, and beryllium have also been found in minerals in the Paria River, Lava Chuar Creek, and Pumpkin Springs (National Park Service 2016a).

The cave mineral assemblages in Grand Canyon National Park indicate the presence of sulfur-rich fluids and support a hypogene groundwater system (see “Cave and Karst Features”). They are also associated with breccia pipes and ore bodies found in the Grand Canyon. Redwall Limestone caves contain a variety of minerals (table 14). Calcite and aragonite compose the speleothems, which are now mostly dry and desiccated in western Grand Canyon. Although the speleothems are dusty and brittle, they still form spectacular features in the caves (fig. 48). Some of the stalactites are as much as 2 m (7 ft) long (Wenrich and Stuphin 1994).

Selenite, transparent crystals of gypsum, covers the walls and collapsed blocks of limestone. The selenite crystals take the relatively rare shape of a ram’s horn and thus, are known as “ramshorn” selenite (Wenrich and Stuphin 1994). About 350 m (1,150 ft) into Corkscrew Cave, which was named for the 12 cm (5 in)-long corkscrew-shaped stalactite about 30 m (100 ft) from the entrance, ramshorn selenite and bright white encrustations of calcite and aragonite cover the walls of a pit and dome.

Green bands and yellow patches in the calcite and aragonite result from several minerals that had not been identified in caves until 1994 (Wenrich and Stuphin 1994). Radioactive carnotite and powellite provide the yellow color, and the green color results from the arsenate minerals conichalcite and talmessite. In short-wave ultraviolet light, powellite fluoresces yellow and talmessite fluoresces a brilliant green. In the United States, talmessite has only been found in breccia pipes from Corkscrew Cave in the Peach Spring Canyon area south of Diamond Creek on the Hualapai Indian Reservation and the Gold Hill Mine in western Utah (fig. 49; Wenrich and Stuphin 1994; Onac et al.

2007; Mindat.org 2016a). Hörnesite, another mineral containing arsenic, forms white crystals in association with aragonite.

Abandoned mines contain some of the more unusual minerals in the park (table 15). The Grandview Mine is the type locality for the uncommon, turquoise-blue mineral, grandviewite, a copper aluminum silicate (fig. 50). Grandviewite has splays of delicate, fibrous crystals associated with cyanotrichite, a hydrous copper aluminum sulfate mineral. Minerals in the mines often occur together. For example, in the Grandview Mine, the copper sulfate mineral gypsum is associated with the copper carbonate minerals azurite, malachite, and smithsonite (fig. 51; table 15).



Figure 49. Photograph of talmessite from the Gold Hill Mine, western Utah.

Photograph by Rob Lavinsky, iRocks.com – CC-BY-SA-3.0, <https://commons.wikimedia.org/w/index.php?curid=10122675>.



Figure 50. Photograph of grandviewite from Grandview Mine, Grand Canyon National Park.

NPS photograph by Michael Quinn, available at https://www.flickr.com/photos/grand_canyon_nps/6214787896/in/album-72157627701076787/.

Table 15. Documented minerals and associated commodities from abandoned mines in the Grand Canyon National Park area.

Information from the NPS AML database and Billingsley (1974). Additional history of individual mines is available in Billingsley (1974).

Mine	Location	Commodity	Minerals
Grandview Mine	Grandview Trail	Copper	Sulfates: grandviewite, cyanotrichite, brochantite, chalcoalumite, langite, barite, deulline, chalcantite, antlerite, gypsum. Carbonates: aurichalcite, azurite, malachite, smithsonite. Arsenates: phillipsbornite, metazeunerite, zeunerite, scorodite, olivenite, adumite. Minor: hemimorphite, kaolinite, illite, pyrite.
Orphan Mine	South Rim	Copper	Over 60 different minerals including uranium, antimony, arsenic, gold, iron, lead, silver, copper, magnesium, manganese, molybdenum, nickel, cobalt, mercury, selenium, vanadium, zinc.
Grand Gulch	Esplanade bench of the Grand Wash Cliffs	Copper	Azurite, brochantite, chalcocite, chrysocolla, cotunnite, cuprodescloizite, malachite, limonite.
Ridenour Mine	West of Prospect Valley, South Rim	Copper	Major: malachite, azurite, chalcocite. Minor: chrysocolla, bornite, chalcopyrite, carnotite (uranium-vanadium), volborthite (copper-vanadium).
Copper Mountain Lode	Imperial Point, Nannoweap Creek	Copper	Malachite, azurite, chrysocolla, chalcocite, limonite, hematite.
McCormick Mine	Beamer Trail, Palisades Creek	Copper	Traces of copper mineralization in the form of malachite.
Bass Copper Mine	Copper Canyon	Copper	Bornite, chalcocite, chalcopyrite, galena.
Anita Copper (Emerald) Mine	Near Anita, Arizona	Copper	Chalcopyrite and carbonates of copper (not profitable).
Boucher Mine	Boucher Trail	Copper	Copper and graphite (not profitable).
Kaibab Plateau	Kaibab Plateau	Copper	Major: malachite and azurite. Minor: cuprite, copper glance, chalcopyrite, silver, gold.
Hacks Mine	Hacks Canyon	Copper, Uranium	Torbenite (uranium-copper mineral).
Pinto Mine	Tuckup Trail	Copper	Unspecified
Copper Grant	Mile 65.2	Copper	Unspecified
Bridal Veil Mines	Havasu Canyon	Lead-zinc	Vanadium, galena, sphalerite, limonite, siderite, smithsonite, various lead oxides, calcite, barite, gypsum, pyrite, cerussite, anglesite, smithsonite, calamine.
Hance Asbestos Mine	Asbestos Canyon	Asbestos	Asbestos fibers as much as 10 cm (4 in) long, chlorite, serpentine, talc.
Bass Asbestos Mine	Hakatai Canyon	Asbestos	Asbestos in serpentine.
Bat Guano Mine	Western Grand Canyon	Guano	Mined for fertilizer from the late 1940s to middle 1950s.



Figure 51. Photograph of minerals from the Grandview Mine. These samples contain azurite (dark blue), gypsum (colorless, rhombohedral crystals), malachite (green), and smithsonite (yellow). NPS photograph by Michael Quinn, available at https://www.flickr.com/photos/grand_canyon_nps/6214786042/in/gallery-lasvegasgrandcanyontours-72157632077629800/.

Breccia Pipes and Ore Deposits

The Grandview Mine, Orphan Mine, and many other historic mines in the Grand Canyon are associated with breccia pipes, which are vertical, pipe-shaped columns filled with broken rock, or breccia. These collapse structures are as great as 900 m (3,000 ft) high and 90 m (300 ft) in diameter. The breccia pipes developed in the Redwall Limestone when overlying Pennsylvanian, Permian, and Triassic sandstones, shales, and limestones collapsed into Mississippian caves and sinkholes (fig. 52; Wenrich et al. 1986; Wenrich et al. 1989; Wenrich and Stuphin 1994; 1994; Huntoon 1996). Over 1,300 known or suspected breccia pipes are scattered throughout the Grand Canyon region (Spencer and

Wenrich 2011). The GRI GIS data includes 233 breccia pipes, 126 of which are mapped within Grand Canyon National Park.

Breccia pipes crop out in the canyons, form circular features on the ceilings of some Redwall caves, and have developed bowl-shaped depressions on the surface of the Harrisburg Member of the Kaibab Formation (**Pkh**) and Woods Ranch Member of the Toroweap Formation (**Ptw**) on the surrounding plateaus (Wenrich and Huntoon 1989; Huntoon et al. 1996; Billingsley 2000b; Billingsley and Workman 2000; Billingsley and Wellmeyer 2004). The vertical pipes extend upward from the Redwall Limestone (**Mr**) to as high as the Triassic Chinle Formation (**TRc**).

Breccia pipes, which served as conduits for groundwater, were targeted by miners in what is now Grand Canyon National Park and throughout the Colorado Plateau. Oxidizing meteoric waters rich in copper and uranium mixed with reducing hypogenic groundwater originating from hydrocarbon or volcanic/magmatic sources containing arsenic, cobalt, nickel, molybdenum, zinc, and lead to generate ore deposits in the breccia zones (Wenrich and Stuphin 1994; Huntoon 1996; Crossey et al. 2006; Spencer and Wenrich 2011; Hill and Polyak 2010).

Breccia pipes have been mined on the Colorado Plateau since the late 1800s. The Grandview Mine and Orphan Mine retain evidence of these early mining days in Grand Canyon National Park. In 1892–1893, miners built the 6 km (4 mile) Grandview Trail to haul ore from the Grandview Mine (also called the Last Chance Mine), a mineralized breccia zone on Horseshoe Mesa (Anthony et al. 1995). The breccia pipe is exposed on the crest of the west–northwest-trending Grandview Phantom Monocline (Huntoon et al. 1996). Transportation costs were too high for the mine to be profitable, and it officially closed in 1907 (Mindat.org 2016b). The Grandview Mine became part of Grand Canyon National Park when William Randolph Hearst sold the property to the NPS in 1940 (Mindat.org 2016b).

Located near West Rim Drive, between Maricopa and Powell Points, the Orphan Mine opened in 1893 (Anthony et al. 1995). Its breccia pipe extends vertically for a minimum of 506 m (1,660 ft) from the middle of the Redwall Limestone (**Mr**) to the Coconino Sandstone (**Pc**) and varies in diameter from about 60 m (200 ft) to over 150 m (500 ft) (Kofford 1969; Chenoweth 1986). A zone of faulted and fractured sedimentary rock (known as the “annular ring”) surrounds the pipe. Within the annular ring, sandstone units of the Esplanade Sandstone (**Pe**) contained most of the ore produced from the mine (Chenoweth 1986).

Unconformities

An “unconformity” is a contact between rock layers of different ages. It represents a gap in the completeness of the stratigraphic record resulting from either non-deposition or erosion of previously deposited material. Unconformities are classified as nonconformities, angular unconformities, or disconformities (fig. 53). Grand Canyon National Park contains excellent examples of all three types of unconformities, including the “Great Unconformity” and the many unconformities in the Grand Canyon Supergroup. The unconformities in the park are world famous and have been studied and visited by geologists for well over 100 years.

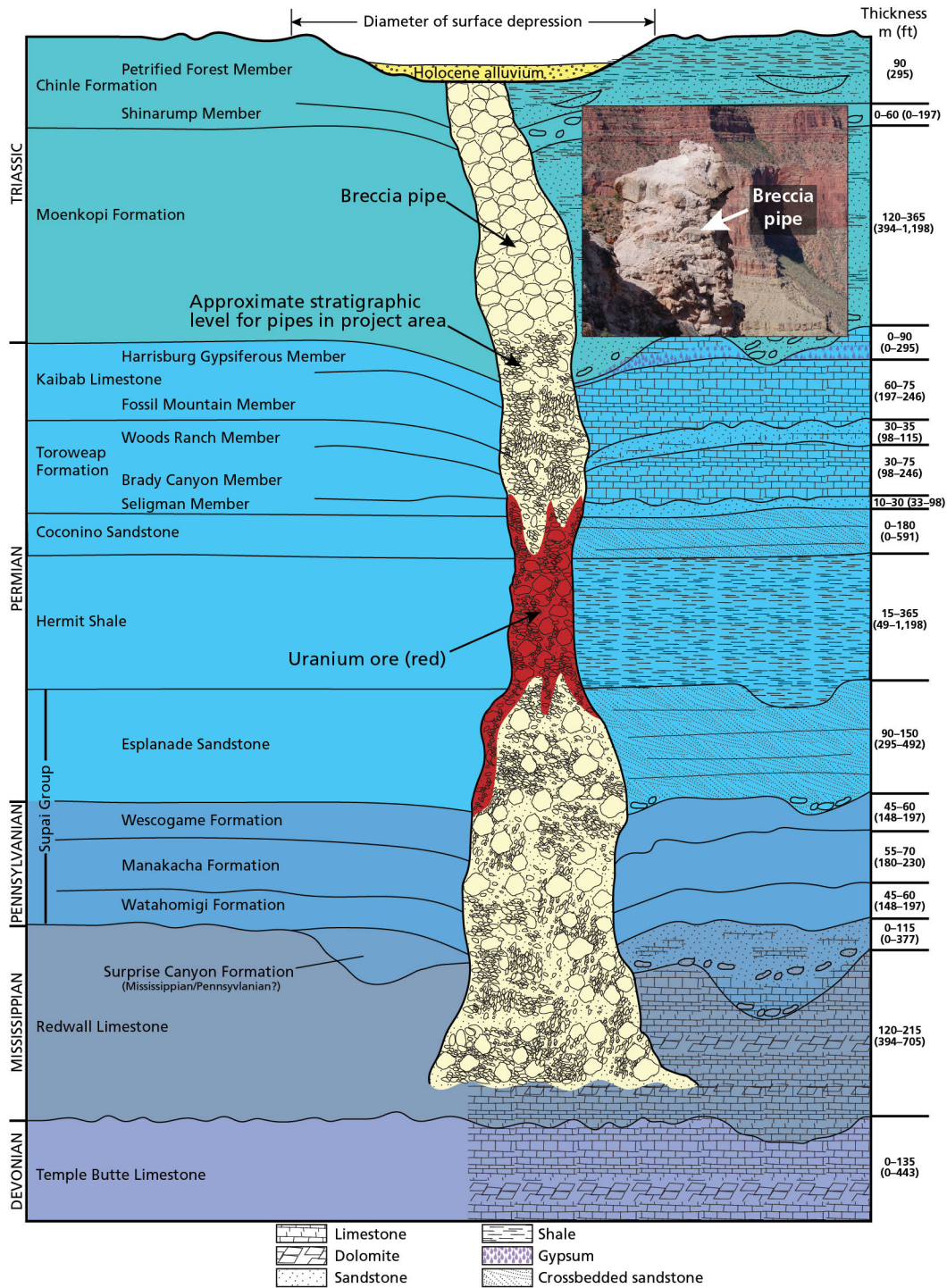


Figure 52. Breccia pipes in Grand Canyon National Park. Schematic cross-section of a breccia pipe. Dissolution of the Redwall Limestone causes overlying strata to collapse into the sinkhole or cavern. Minerals, primarily uraninite, copper minerals, and vanadium-bearing minerals, precipitate out of groundwater that percolates through the breccia. Cross section by Trista Thornberry-Ehrlich (Colorado State University), modified from Van Gosen and Wenrich (1989, figure 3). Inset photograph of an eroded remnant of a breccia pipe on the South Kaibab Trail. Commonly associated with sinkholes, breccia pipes concentrate minerals, such as uranium. Photograph by Brian F. Gootee, available at <http://azgeology.azgs.az.gov/azgs/image-of-the-day/images/gooteebreccia-pipe>.

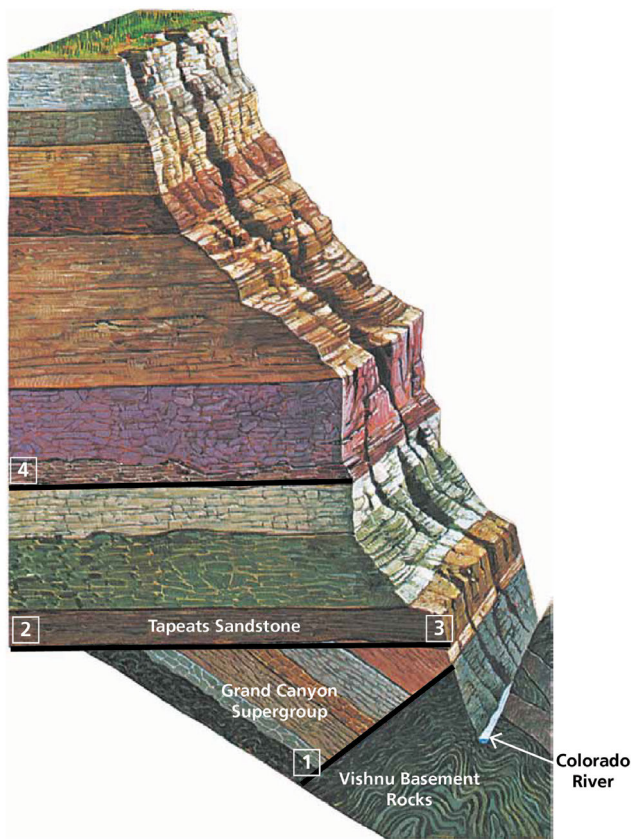


Figure 53. Illustration showing the three types of unconformities.

A nonconformity exists between the Vishnu Basement Rocks and the Grand Canyon Supergroup (Line 1); an angular unconformity separates the Grand Canyon Supergroup from the Tapeats Sandstone (Line 2); and a disconformity forms the contact between the Cambrian Muav Limestone and Devonian Temple Butte Formation (TB) (Line 4). Line 3 represents Powell's Great Unconformity that separates Paleozoic rocks from underlying Vishnu basement rocks. In other parts of the canyon, the Great Unconformity also separates Paleozoic rocks and the Vishnu Schist from the Grand Canyon Supergroup. Subsequent mapping has placed the Great Unconformity underneath the Tapeats Sandstone, and the unconformity between the Bass Formation and underlying crystalline rocks is the Greatest Angular Unconformity (George Billingsley, USGS, retired, geologist, written communication, 20 August 2018). Modified from Karlstrom and Timmons (2012, figure 1B), who modified Powell's original drawing (Powell 1875).

A nonconformity occurs where stratified sedimentary rock overlies metamorphic or igneous rocks. Nonconformities record a dynamic, albeit missing, history of tectonic compression and erosion.

An angular unconformity occurs where younger rocks (often sedimentary) overlie an eroded surface of tilted or otherwise deformed rocks. In the canyon, for example, relatively horizontal Cambrian Tapeats Sandstone (**Ct**) and Bright Angel Shale (**Cba**) strata overlie the tilted Precambrian Grand Canyon Supergroup (fig. 54). Angular unconformities represent the following sequence of events: 1) horizontal deposition of sedimentary strata, 2) deformation and tilting of the sequence by orogenic (mountain-building) events, 3) planation (made level by erosion) of the tilted layers, and 4) deposition of overlying, relatively flat-lying sedimentary units.

A disconformity records a period of erosion or nondeposition between two relatively parallel sedimentary rock layers. Unlike a nonconformity or angular unconformity, a disconformity does not involve tilting or deformation during the erosional episode. Disconformities may be difficult to recognize, especially if the adjacent rock units are similar. Their identification typically hinges on distinct changes in fossil assemblages across the contact or an abrupt change in lithology.

The strata in the Grand Canyon contain many disconformities. One of the more significant disconformities occurs in eastern Grand Canyon at the contact between the Redwall Limestone (**Mr**) and the underlying Cambrian Tonto Group (table 1). The contact represents as much as 150 million years of missing strata. A disconformity also formed where sediments that became the Surprise Canyon Formation (**Ms**) were deposited within sinkholes and depressions that formed on the karst landscape of the Redwall Limestone.

The Great Unconformity

Exploring the Grand Canyon in 1869, John Wesley Powell documented the Great Unconformity, which includes nonconformities, angular unconformities, and contacts that are both angular and nonconformities (Powell 1875; Karlstrom and Timmons 2012). The Great Unconformity represents an extraordinary amount of time. For example, the contact between the relatively flat-lying layers of Cambrian Tapeats Sandstone (**Ct**) and the underlying Paleoproterozoic metamorphic Vishnu Schist (**Xv**) represents as much as 1.2 billion years (approximately 25% of Earth's history) (fig. 53).

Cambrian strata overlying tilted strata of the Grand Canyon Supergroup form angular unconformities spanning much less time than the nonconformities, but still resulting in a significant hiatus (fig. 53). Where the Tapeats Sandstone (**Ct**) overlies the Chuar Group, for example, the angular unconformity spans approximately 0.5 billion years.

The Great Unconformity not only represents vast amounts of time but it also documents remarkable episodes of metamorphism, mountain-building, tectonic compression, deformation, uplift, erosion, and deposition (Karlstrom et al. 2003; Karlstrom and Timmons 2012). Prior to deposition of the Grand Canyon Supergroup, sediments that now form the Granite Gorge Metamorphic Suite were metamorphosed at depths up to 25 km (15 mi). During a mountain-building episode (orogeny), tectonic compression exhumed these basement rocks and rotated them to near vertical. The basement rocks were beveled by erosion prior to deposition of the Mesoproterozoic Bass Formation (Yb). The deposition of the sedimentary Unkar Group on tilted igneous and metamorphic rocks formed an angular unconformity, as well as a nonconformity (fig. 53). The presence of Supergroup sedimentary beds above the basement rocks indicates that the 25 km (15 mi) of exhumation, the growth of the Vishnu Mountains, and subsequent

erosion that beveled the mountains occurred within about half a billion years (Karlstrom and Timmons 2012; Karlstrom et al. 2012a; Timmons et al. 2012).

Currently, the sedimentary layers of the Grand Canyon Supergroup tilt at ~20°, but they were originally deposited horizontally. These horizontal strata were subjected to another episode of tectonic compression, uplift, deformation, and erosion prior to deposition of the Cambrian Tapeats Sandstone (Ct) (Karlstrom et al. 2003; Karlstrom and Timmons 2012). The contact between the Tapeats Sandstone and the Grand Canyon Supergroup forms an angular unconformity, but where the Tapeats Sandstone is in contact with the Vishnu basement rocks, the Great Unconformity becomes both a nonconformity and an angular unconformity (Karlstrom and Timmons 2012). These unconformities can be seen from the panoramic Lipan Point viewpoint, along the East Rim's Desert View Drive (fig. 55).



Figure 54. Annotated photograph showing an angular unconformity. The angular unconformity (black line) is between the Precambrian Grand Canyon Supergroup and the Cambrian Tonto Group. Dipping Shinumo Quartzite (Ys), unnamed diabase sills and dikes (Yi), Hakatai Shale (Yh), and Bass Formation (Yb) strata underlie relatively flat-lying Tapeats Sandstone (Ct) and Bright Angel Shale (Cba). View is to the northwest towards Shinumo Creek and Powell Plateau. Photograph and annotation by G. H. Billingsley (2000b, figure 3).

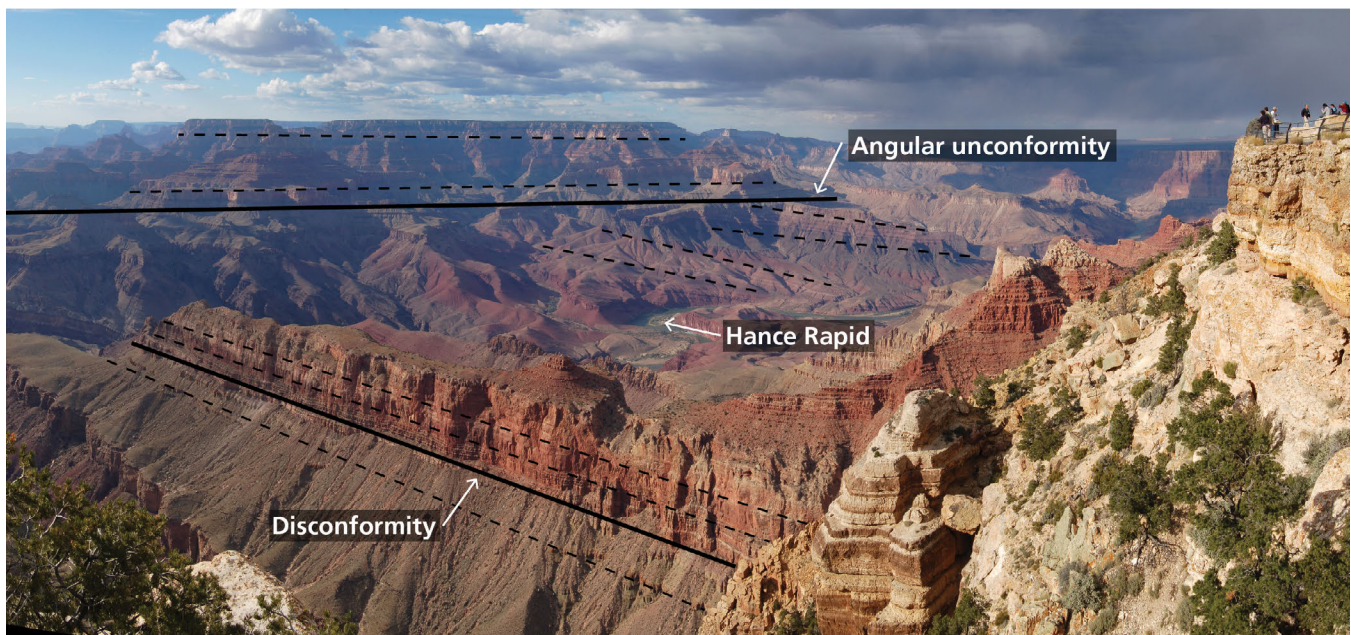


Figure 55. Annotated photograph of the view from Lipan Point, Desert View Drive, East Rim, Grand Canyon National Park.

Features visible from this viewpoint include Grand Canyon Supergroup strata, unconformities (solid dark lines), and Hance Rapid. Dashed lines mark some of the bedding surfaces in the strata. NPS Photograph by Michael Quinn, available at https://www.flickr.com/photos/grand_canyon_nps/5446829074/in/album-72157624074679317/.

Grand Canyon Supergroup Unconformities

Once erosion had exposed the Paleoproterozoic basement rocks at the surface, shallow basins formed on the continent, and these basins filled with sediment that became the Grand Canyon Supergroup (table 1). The Grand Canyon Supergroup consists primarily of layered sedimentary rock interrupted by basaltic flows, such as the Cardenas Basalt (Yc). Powell measured 3,000 m (10,000 ft) of tilted Grand Canyon Supergroup below the horizontal Tapeats Sandstone (Powell 1875).

The Grand Canyon Supergroup can be subdivided into two sequences of strata: 1) the 1,200 million–1,000 million-year-old Unkar Group and 2) the 782 million–742 million-year-old Chuar Group (table 1). Distinct sedimentary rock layers define each sequence of strata, and disconformities or low-angle angular unconformities separate the sequences from one another. Analyses of the sedimentary layers, pressure/temperature analysis, and the thermochronology of various minerals, especially micas and feldspars, suggest that the Grand Canyon Supergroup unconformities may be summarized as follows (Timmons et al. 2005; Karlstrom and Timmons 2012; Karlstrom et al. 2012a; Dehler et al. 2017; Karlstrom et al. 2018):

- Pre-Unkar Group nonconformity. Rapid erosion of the newly formed Vishnu Mountains decompressed

the basement rocks from 25 km (15 mi) to ~10 km (6 mi) between 1.7 billion and 1.66 billion years ago. A final exhumation of the basement rocks occurred between 1.3 billion and 1.2 billion years ago.

- Pre-Shinumo disconformity. The duration of this unconformity is not well defined. The age of the Bass Formation (Yb) ranges from 1.25 billion to 1.15 billion years ago, while deposition of the overlying Dox Formation (Yd) occurred between 1.15 billion and 1.10 billion years. Thus, the hiatus represented by the unconformity may be minimal or it may represent as much as 50 million years.
- Pre-Nankoweap angular unconformity/nonconformity. The Cardenas Basalt (Yc) at the top of the Unkar Group is approximately 1.1 billion years old, and the beds of the Unkar Group tilt at <math><10^\circ</math>. The roughly 782-million-year-old Nankoweap Formation (YZn) overlies the Cardenas Basalt, suggesting a gap in the rock record of as much as 300 million years occurs between the rock units.
- Intra-Nankoweap unconformity. Eroded pebbles of Cardenas Basalt found within the Nankoweap Formation indicate that uplift, perhaps from fault movement, exposed the basalt to erosion. The intra-Nankoweap unconformity formed by this erosional episode is poorly understood and may have only affected local areas.

- Pre-Sixtymile disconformity. At Nankoweap Butte, steep-walled channels eroded into the Kwagunt Formation and filled with sedimentary breccia underlie the siltstone, sandstone, and black shale of the Sixtymile Formation (Zs). An ash bed at the top of the Kwagunt Formation constrains the top of the Chuar Group to approximately 742 million years ago. Deposition of the Sixtymile Formation began about 527 million years ago, suggesting this unconformity may span approximately 215 million years.
- Pre-Tapeats angular unconformity. The angular unconformity between Grand Canyon Supergroup units and the Cambrian Tapeats Sandstone (Ct) may be considered a Grand Canyon Supergroup unconformity as well as part of the Great Unconformity. Tectonic compression and mountain-building processes tilted the Grand Canyon Supergroup about 20° (and the pre-Supergroup rocks an additional 20°), and erosion truncated the strata prior to deposition of the Tapeats Sandstone. The Tapeats Sandstone is time transgressive, which means it is not everywhere the same age. In western Grand Canyon, the unit is Early Cambrian (540 million years old), but in eastern Grand Canyon, deposition occurred 525 million years ago during Middle Cambrian time. Thus, where the Tapeats Sandstone rests on the Chuar Group, the angular unconformity may represent a gap in the rock record of as much as 175 million years.

Folds and Faults

Folds and faults in Grand Canyon National Park offer clues to the deformational history of the region (see the “Geologic History” section), and both types of features are included in the GRI GIS data. Folds form curves or bends in originally flat structures, such as rock strata, bedding planes, or foliation. The two primary types of folds include “A-shaped” (convex) anticlines and “U-shaped” (concave) synclines. As bedrock is compressed, anticlines and synclines typically form adjacent to each other. A monocline, which is a type of anticline, forms a one-limbed, step-like fold in otherwise relatively horizontal or gently dipping strata (fig. 8). Monoclines are common on the Colorado Plateau. Folds frequently “plunge,” meaning the fold axis tilts. In the GRI GIS data, the more significant anticlines, synclines, and monoclines are named.

A fault is a fracture along which rocks have moved. The three primary fault types, named for the relative motion of rocks on either side of the fault plane, include normal, reverse, and strike-slip (fig. 7). Reverse faults indicate horizontal shortening resulting from compression oriented perpendicular to the fault plane. Normal faults result from extension or stretching of

the crust perpendicular to the fault plane. Oblique or horizontal movement along fault planes produces strike-slip faults or a combination of all three.

The faults in the Grand Canyon have been reactivated throughout geologic time so that faults that may have been reverse faults are now normal faults. Normal faults that formed grabens (basins resulting from faulting) in the Precambrian were reactivated to form horsts (upthrown blocks) during the Paleozoic (fig. 56). Most faults throughout the canyon currently show normal fault displacement (see the GRI GIS data). Measured total displacement on the faults is quite varied, ranging from 0.5 m (1.6 ft) to as much as 850 m (2,790 ft) (table 16).

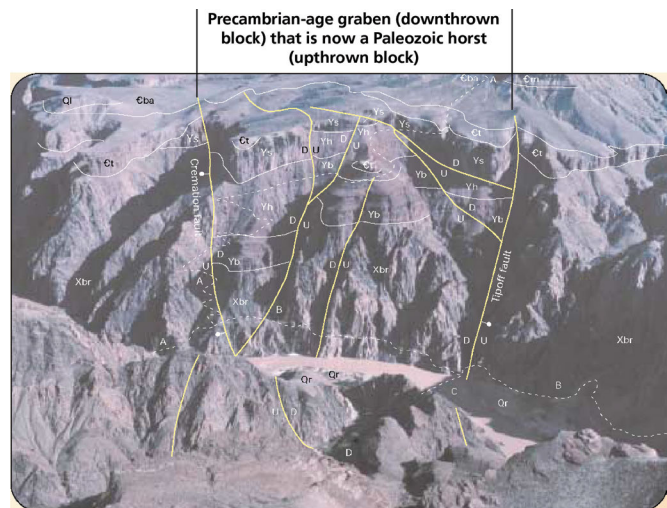


Figure 56. Annotated photograph of Precambrian and Paleozoic faults.

View is to the southeast to the mouth of Bright Angel Creek where “D” is the Bright Angel Campground, “A” (dashed line) is the lower part of south Kaibab Trail, “B” (dashed line) is the Bright Angel Trail, and “C” is the lower bridge crossing the Colorado River. “U” (upthrown) and “D” (downthrown) represents Proterozoic offsets; bar and ball represent Paleozoic offsets, with the ball on the downthrown side of the fault. The Paleozoic horst (upthrown block) between the Cremation and Tipoff faults was a graben (downthrown block) in the Proterozoic, as shown. Qr: Colorado River gravel deposits. Ql: landslide deposits. Cm: Muav Limestone. Cba: Bright Angel Shale. Ct: Tapeats Sandstone. Ys: Shinumo Quartzite. Yh: Hakatai Shale. Yb: Bass Formation. Xbr: Brahma Schist. Photograph and annotation by G. H. Billingsley (2000b, figure 4).

Table 16. Fault offsets on major normal faults in Precambrian and Paleozoic units, Grand Canyon.

Major faults are listed from east to west, in general. See the GRI GIS data for other, less areally extensive fault offsets. Offset amounts are from Billingsley (2000b) and Billingsley and Wellmeyer (2003) and are reported in the GRI GIS data. Faults in the Lake Mead area displace Paleozoic and younger units.

Fault		General Orientation	Movement and Estimated offset in meters (ft)
Faults that displace Precambrian rocks (River Mile 83–136)	Ottoman Fault	NW–SE	Down–to–northeast: 182 (597), 45.5 (149)
	Near Phantom Ranch	NW–SE	Down–to–northeast: 24.5 (80.4)
	Phantom Fault	NW–SE	Down–to–southwest: 7.5 (25)
	Near Crystal and Dragon creeks	N–S	Down–to–east: 152.5 (500.4)
	Muav Fault north of Dox Castle	NNW–SSE	Down–to–west: 30 (100)
	Burro Canyon fault zone	NW–SE, bend to NE, NW–SE	Down–to–southwest: 76 (250). Down–to–northwest: (15 (49). Down–to–northeast: 122 (400)
	West of Serpentine Rapids	N–S	Down–to–west: 61 (200)
	West of Bass Rapids	W–E	Down–to–north: 152.5 (500.4)
	Fault zone north of Shinumo Rapids	NW–SE	Down–to–southwest: 61 (200), 122 (400)
	Fault zone north of Shinumo Rapids	NW–SE	Down–to–northeast: 45.5 (149), 60 (200), 76 (250), 81 (270), 122 (400)
	Bedrock Rapids area	WNW–ESE	Down–to–northeast: 15 (49)
	Deubendorff Rapids area	WNW–ESE	Down–to–southwest: 45.5 (149), 10 (30)
	East of RM 133	WNW–ESE	Down–to–south: 15.2 (49.9)
Faults that displace Paleozoic strata (River Mile 81.5–172)	Obi Fault	NW–SE	Down–to–southwest: 6 (20)
	Deva Fault	NW–SE	Down–to–southwest: 4.5 (15)
	McKee Fault	NE–SW	Down–to–northwest: 3 (10), 15 (49)
	Uncle Jim Fault south of Upper Tater Canyon	N–S	Down–to–east: 18.5 (60.7), 39.5 (130)
	Uncle Jim Fault in Upper Tater Canyon	N–S	Down–to–west: 61 (200)
	Bright Angel Fault	NE–SW	Down–to–southeast: 61 (200), 82 (270)
	Phantom Fault	NW–SE	Down–to–southwest: 244 (801)
	Roaring Springs Fault	NW–SE	Down–to–northeast: 18.5 (60.7), 39.5 (130)
	Basin Fault	NW–SE	Down–to–southwest: 7.5 (25)
	Hermit Fault	NNE–SSW	Down–to–northwest: 2.5 (8.2), 9 (30)
	Milk Fault	N–S	Down–to–west: 12 (39)
	Crystal Fault	N–S	Down–to–west: 15 (49)
	Big Springs Fault	N–S	Down–to–west: 24.5 (80.4), 13.5 (44.3)
	Piute Fault	NW–SE	Down–to–southwest: 3 (10)
	Bass Fault	NE–SW	Down–to–southeast: 20 (66)
	Noble Fault	N–S	Down–to–west: 24.5 (80.4)
	Muav Fault	N–S	Down–to–west: 167.5 (549.6), 222 (728)
	Tapeats Fault	N–S	Down–to–east: 12 (39)
	Butchart Fault	N–S	Down–to–west: 9 (30)
	Fishtail Fault	NE–SW	Down–to–northwest: 1 (3)
	Havasus Springs Fault	W–E	Down–to–north: 0.5 (2)
Sinyala Fault	NE–SW	Down–to–northwest: 1 (3), 1.5 (4.9)	
Supai Monocline en echelon faults	NW–SE	Down–to–southwest: 45.5 (149), 24.5 (80.4), 15 (49)	
Mohawk Stairway Fault	NNE–SSW	Down–to–southeast: 10.5 (34.5), 24.5 (80.4)	

Table 16, continued. Fault offsets on major normal faults in Precambrian and Paleozoic units, Grand Canyon.

Fault		General Orientation	Movement and Estimated offset in meters (ft)
Faults that displace Paleozoic strata (River Mile 183–205)	Laguna Graben boundary faults	N–S	Down–to–west: 18 (59) and Down–to–east: 73 (240)
	Toroweap Fault	N–S	Down–to–west: 54 (180), 159 (522), 175 (574), 198 (650)
	Lava Fault	NE–SW	Down–to–northwest: 122 (400)
	Hurricane Fault	N–S	Down–to–west: 275 (902), 400 (1,300), 550 (1,800), 850 (2,790 ft)
	Parashant Graben boundary faults	NW–SE	Down–to–southwest: 10 (30), 37 (120), 48 (160) Down–to–northeast: 37 (120)
	Frog Fault south of Colorado River	NNE–SSW	Down–to–northwest: 33 (110), 115 (377), 122 (400)
	Frog Fault north of Colorado River	NW–SE	Down–to–southwest: 73 (240), 183 (600)
Lake Mead Recreation Area	Andrus Graben boundary faults	NW–SE	Down–to–southwest: 45 (150)
	Grassy Fault	NW–SE	Down–to–northeast: 73 (240)
	Andrus Fault north of graben	NW–SE	Down–to–northeast: 24 (79), 40 (130)
	Dellenbaugh Fault	NE–SW	Down–to–northwest: 85 (280), 122 (400)
	Main Street Fault	N–S	Down–to–west: 12 (39), 50 (164)
	Fault at 205 mile rapids	NE–SW	Down–to–northwest: 10 (30)

Precambrian Folds and Faults

The Paleoproterozoic igneous and metamorphic rocks exposed in the Inner Gorge of Grand Canyon National Park have been complexly deformed by folds and fractured by faults, providing an exceptional window through which to study the evolution of the southwestern margin of Laurentia, the pre-North American craton (see the “Geologic History” section). These rocks formed at 20–25 km (12–15 mi) depths, deep in the roots of an old mountain belt (Karlstrom et al. 2012a). The rocks became folded and faulted as microplate collisions accreted land to what would become the southern margin of North America.

Deformation features in the Zoroaster Pluton Complex and Granite Gorge Metamorphic Suite, such as folds, igneous intrusions, foliation (schistosity), and faults, document metamorphic and tectonic processes associated with a Paleoproterozoic orogeny (Karlstrom et al. 2012a). The sequence of deformation also helps geologists determine the relative timing of these events. For example, the Vishnu Schist (**Xv**) contains layers that were folded, refolded, and then thrust over themselves. Because granitic dikes cross-cut the folds, folding must have occurred prior to the emplacement of the intrusions.

Folds and faults also occur in Unkar Group strata, and their orientation indicates northwest–southeast

compression during the Mesoproterozoic (Timmons et al. 2012). Red, Vishnu, Bright Angel, and Bass canyons preserve northeast-trending reverse faults draped with monoclinical folds.

Reactivation of the Paleoproterozoic fault pattern approximately 1.2 billion–1.0 billion years ago created northwest-trending normal faults in the Unkar Group, such as the Palisades fault (table 16; Karlstrom and Timmons 2012). The Palisades fault zone extends northwest from Palisades Creek, crosses the Colorado River upstream from Lava Canyon Rapids, and continues into Lava Canyon and Chuar Valley. Northwest-trending normal faults resulted from plate collisions farther south (where Texas is today).

Faults and folds in the Unkar Group and north–south-trending normal faults and folds in the overlying Chuar Group document the Mesoproterozoic collision of Laurentia with other large landmasses to form the supercontinent Rodinia and the subsequent rifting of Rodinia in the Neoproterozoic. The Butte Fault, a north–south-trending normal fault that crosses the Colorado River near Tanner graben and RM 68, and the associated Chuar syncline that formed adjacent to the fault provide a rare glimpse into the early rifting of the supercontinent (Dehler et al. 2012). The Precambrian Butte Fault, which now forms the main fault of the Laramide-age East Kaibab monocline, was reactivated in the Cambrian and during the Laramide Orogeny, a

mountain-building episode beginning approximately 70 million years ago in the Late Cretaceous Period and continuing until about 40 million years ago in the Eocene Epoch.

In some areas, huge blocks of rocks slid relatively horizontally past each other, creating shear zones, areas of intense deformation. Shear zones represent zones of weakness and ductile flow. The grinding and ductile deformation in shear zones creates a metamorphic fabric known as mylonite, characterized by fine-grained textures and a strong foliation indicative of the direction of shearing. A major shear zone near Crystal Rapids (RM 98) marks the location of suturing between the Mojave and Yavapai microplates (fig. 41; Karlstrom et al. 2012a). The shear zone extends from the mylonitic dikes, whose original igneous rocks have undergone ductile deformation, at RM 77 westward to Lower Granite Gorge.

Alternating domains of northwest-trending and northeast-trending foliations in the Paleoproterozoic basement fabric set the stage for the dominant northwest- and northeast-trending faults that offset strata throughout the Mesoproterozoic, Neoproterozoic, and Phanerozoic.

Mesozoic Folds and Faults

Except for a geologically brief period in the Devonian, the Grand Canyon region was either submerged or relatively close to sea level throughout the Paleozoic and most of the Mesozoic (see the “Geologic History” section). Approximately 60 million–70 million years ago, during the Cretaceous Period, the angle of the Farallon plate’s subducting slab along the western margin of North America began to flatten. The subducting slab carried fluids to great depths, and these fluids, which included magma, escaped upward along conduit systems, such as shear zones and faults. Changes in buoyancy uplifted the relatively rigid Colorado Plateau microplate (Karlstrom and Timmons 2012).

Flat slab subduction is responsible for the Laramide Orogeny. West–east compressive forces were felt far inland, impacting the Colorado Plateau and giving rise to the Rocky Mountains. The Colorado Plateau is generally described as relatively stable and undeformed, especially compared to the neighboring Rocky Mountains, but a map of the faults on the plateau suggests it is more like a shattered glass bowl.

North–south-trending Proterozoic extensional normal faults were reactivated as Laramide reverse faults. For example, normal, west-side-down movement on the Butte Fault occurred during deposition of the Chuar Group, but during the Laramide Orogeny when the

Butte Fault was reactivated, compression caused west-side-up slip on the fault plane (Karlstrom and Timmons 2012). In western Grand Canyon, the larger west-dipping reverse faults include, from west to east, the Quartermaster, Meriwhitica, Lone Mountain-Dellenbaugh, Hurricane, and Toroweap faults.

Reverse faulting was also responsible for most of the monoclines seen today on the Colorado Plateau, such as the East Kaibab, Supai, Monument, Black Point, and Echo Cliffs monoclines (see GRI GIS data; Tindall and Davis 1999; Karlstrom and Timmons 2012). The upward movement of the basement blocks forced the overlying sedimentary rocks to bend over the reverse fault plane, forming the steep limb of the monocline. The steep limb separated the relatively flat-lying beds of the upthrown block from the flat-lying beds of the downthrown block (fig. 9; Karlstrom and Timmons 2012). In general, Laramide compression pushed western blocks up and over eastern blocks so that the steeper limbs of the monoclines dip east.

Cenozoic Folds and Faults

When compression from the Laramide Orogeny ended in the Eocene, the Farallon plate delaminated and an increase in volcanism warmed and weakened the lithosphere (Karlstrom and Timmons 2012). The tectonic regime changed from compression to extension. Approximately 17 million years ago in the early Miocene Epoch, north–south-trending normal faults dropped down western blocks of rock relative to eastern blocks, creating the current Basin and Range province (fig. 3). Grand Canyon National Park lies in the transition zone between the Basin and Range province and the Colorado Plateau.

The Grand Wash normal fault, which forms the Grand Wash Cliffs, forms the boundary between the Colorado Plateau and Basin and Range provinces. At the mouth of the Grand Canyon, an estimated 3,000 m (10,000 ft) of slip on the Grand Wash juxtaposed Paleozoic Era strata on the east side of fault against Cenozoic Era strata on the west side of the fault (Lucchitta 1979; Billingsley 2000b; Billingsley and Workman 2000; Billingsley 2003; Huntoon 2003; Billingsley and Wellmeyer 2004; Karlstrom and Timmons 2012). Drowning and rotation of the western block created the Grand Wash trough, which filled with sediments.

The large west-side down displacements that formed faults like the Grand Wash Fault had mostly waned by ~10 million years ago, but then, a wave of extension migrated eastward into the Colorado Plateau (Jackson 1990). Following the deposition of the 3.6 million-year-old Bundyville basalt, down-to-the-west offset on the Hurricane Fault about 3.5 million years ago separated

the lower Shivwits Plateau from the higher Uinkaret Plateau and formed the Hurricane Cliffs (fig. 57). Offset on the fault ranges from 275 (902 ft) to 850 m (2,790 ft) (table 16; Billingsley and Workman 2000). Reverse drag flexures associated with movement along the fault have caused the strata on the downthrown side of the fault to dip as much as 20° toward the fault plane in some locations (Billingsley and Workman 2000).

The Toroweap Fault initially moved from 2 million to 3 million years ago as a result of Basin and Range extension (Karlstrom et al. 2007). Total offset on the Toroweap Fault varies. For example, near Heaton Knolls, total offset is about 60 m (200 ft); offset near Graham Ranch ranges from 67 m (220 ft) to 74 m (240 ft) (GRI GIS data). Like the Grand Wash Fault and Hurricane Fault, strata on the west side of the Toroweap Fault moved down relative to strata on the east side of the fault. The Toroweap and Hurricane faults continue to be active.

Many of the normal faults that resulted from Neogene extension moved along the same fault planes that accommodated reverse faults during the Laramide Orogeny. Because most of the Paleogene and Neogene deposits have been removed from the Colorado Plateau, determining the ancestry, timing, and amount of slip on

the faults remains difficult (Huntoon 2003; Karlstrom and Timmons 2012).

Normal faults in the Grand Canyon have influenced the incision rate of the Colorado River (Fenton et al. 2001a; Pederson et al. 2002a, 2002b; Karlstrom and Timmons 2012). From Lees Ferry to Toroweap fault (eastern Grand Canyon), the Colorado River incises into bedrock at a rate of 175–250 m/million years (574–820 ft/million years). West of the Hurricane fault, incision rates range 50–80 m/million years (160–260 ft/million years). The incision rate discrepancy results from the mantle-driven epeirogenic uplift (upheavals or depressions of land exhibiting long wavelengths and broad undulations) of the eastern Grand Canyon and Colorado Plateau in the last 6 million years (Karlstrom et al. 2008, Karlstrom and Timmons 2012; Karlstrom et al. 2012b). Relative to the western Grand Canyon block across the Toroweap and Hurricane fault systems, the eastern Grand Canyon block is rising at a rate of >100 m/million years (330 ft/million years). The dynamic interaction among canyon carving, active normal faulting, and regional uplift contributes to the rugged topography and steep river gradients in the Grand Canyon (Karlstrom et al. 2012b).

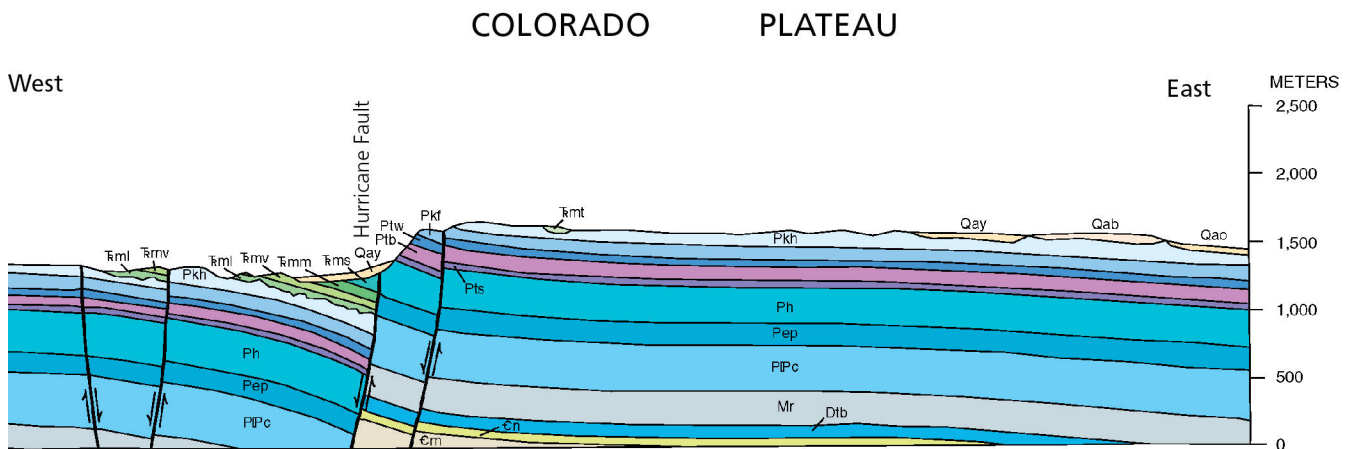


Figure 57. Segment of a west–east geologic cross-section showing normal faulting on the Hurricane Fault. Normal faulting in this part of the canyon resulted from west–east extension that pulled apart the crust, generating the Basin and Range Province to the west. The folding on the down-thrown side of the fault may be reverse drag flexures resulting from fault movement. Unconformities, although not labeled, also are present on the cross-section. For example, major unconformities exist at the contact of the Triassic Moenkopi Formation (Trm) and the Harrison Member of the Lower Permian Kaibab Formation (Pkh) and at the contact between the Devonian Temple Butte Formation (Dtb) and the Upper Cambrian Nopah Formation (Cn), which is not mapped in the park. Not all the Quaternary units are shown. Horizontal scale: 1:100,000. Vertical exaggeration: x4. Modified from Billingsley and Workman (2000) and available in the GRI GIS data.

Features in Side Canyons

Side canyons, best explored from the river, offer an opportunity to examine the details of many of the geological features exposed in the park. The location and morphology of side canyons have been significantly influenced by structural features such as folds and faults, as well as rock hardness (Huntoon et al. 1996; Potochnik and Reynolds 2003). Based on the general morphology of the side canyons, Potochnik and Reynolds (2003) subdivided the Grand Canyon into four major segments (table 17). From Lees Ferry, these four segments include: (1) Marble Canyon, (2) Chuar, (3) Kaibab Plateau, and (4) Esplanade (fig. 58).

The Marble Canyon segment contains short, narrow, relatively unbranched gorges with streams flowing parallel to the strata's regional northeast dip. Side canyons in the other three segments are controlled by the regional trend of faults and folds.

In the Chuar segment, the East Kaibab monocline strongly influenced canyon formation. Faults tend to fracture and brecciate rock units, making them easier to erode than non-deformed strata. Fold- and fault-controlled side canyons, like Bright Angel Canyon, tend to be linear and long. By comparison, side canyons along the South Rim tend to be short and steep with unbranched tributaries flowing against regional dip. The Little Colorado River, flowing from the east, is the only large tributary entering the Colorado River from the South Rim.

Long, fault-controlled North Rim tributaries display a well-developed dendritic pattern in the Kaibab segment. The Kaibab segment also illustrates the influence different rock types have on side canyon morphology. Vertical, v-shaped canyons develop in hard, erosion-resistant rocks, such as the Vishnu Schist (**Xv**) or the Redwall Limestone (**Mr**). Broad, bowl-shaped canyons with rounded, receding walls form in the relatively soft, easily eroded rocks like the sandstone in the Dox Formation (**Yd**) and the siltstones in the Chuar Group (Potochnik and Reynolds 2003).

North-trending normal faults also control the morphology of the uncommonly long and linear side canyons in the Esplanade segment, named for the broad topographic bench formed on the Esplanade Formation (**Pe**). Regional folds also control the location of some major tributaries, such as Havasu Creek, which flows through a low sag that formed in folded strata.

Elevation change and base level (the lowest point to which a stream can flow) also influence side canyon morphology. Higher regions, such as the Kaibab Plateau, receive more precipitation, which provides

more erosive power to streams. Climate affects precipitation rates and thus, incision rates and erosion. In the past, side canyons may have developed faster in the warmer, more humid, Eocene Epoch compared to the colder, drier Oligocene Epoch (Potochnik and Reynolds 2003). Global climate change models predict a drier Southwest, which will impact future side canyon incision rates.

The base level for all the tributaries is the Colorado River. As the Colorado River incises into bedrock, tributaries adjust to this base level change. Erosion increases at the mouth of the tributary and continues upstream. The extreme gradient change of the Little Colorado River illustrates this process. For most of its length across northeastern Arizona, the Little Colorado River meanders in a broad, open valley developed in Mesozoic strata. Within the last 48 km (30 mi), however, the gradient of the Little Colorado River increases by about 500% as it cuts a gorge through the entire 884-m (2,900-ft) section of Paleozoic rock on its way to the Colorado River. About 4 million years ago, the Little Colorado River flowed into Lake Bidahochi, which was centered in the present Little Colorado River Valley. When the lake drained, the Little Colorado River integrated into the Colorado River system. Erosion increased at the mouth of the Little Colorado River and cut an impressive canyon as it adjusted to its new base level. The Little Colorado River will probably continue to adjust its gradient for thousands of years to come (Potochnik and Reynolds 2003).

Desert Varnish

The thin, red-to-black coating known as desert varnish is found throughout arid regions, such as the Colorado Plateau. In Grand Canyon National Park, this surface stain often coats the Coconino Sandstone (**Pc**) (fig. 15). The color of the varnish depends on the amount of iron relative to manganese. Varnish high in manganese appears black while an abundance of iron colors the varnish red to orange. Varnishes intermediate in composition are usually a shade of brown.

In addition to iron and manganese, microorganisms play a role in developing desert varnish. Microorganisms oxidize the manganese, which cements clays and other particles to rock surfaces. Most rock surfaces in desert environments contain these microorganisms, which may be able to use both organic and inorganic nutrition sources. Sources of manganese and iron originate from outside the exposed rock, probably from atmospheric dust and surface runoff.

Because desert varnish takes thousands of years to form, it more commonly occurs on erosion-resistant strata rather than on easily eroded surfaces. The coating

Table 17. Side canyons and morphological divisions in Grand Canyon National Park.

Summarized from Potochnik and Reynolds (2003).

Morphological Divisions		Side Canyon Examples
Marble Canyon Segment	Includes all canyons cut into the Marble Platform below Lees Ferry to Little Nankoweap Creek (RM 52).	North Canyon (RM 20): narrow cleft cut into Supai Group. Steep canyon. Curved fractures in Esplanade Sandstone (Pe). Nautiloid Canyon (RM 36): narrow cleft in Redwall Limestone (Mr). Cross sections of cone-shaped chambered Nautiloids, as much as 55 cm (20 in) long. Buck Farm Canyon (RM 41): contains 15 m (50 ft) of Devonian Temple Butte Limestone (Dtb), which is missing along the river.
Chuar Segment	Little Nankoweap Creek to Upper Granite Gorge.	Carbon Canyon (RM 65): honey-combed weathering and colorful iron oxide staining (Liesegang banding) in Tapeats Sandstone (Ct). Strata folded by the Butte Fault, which parallels the East Kaibab monocline.
Kaibab Segment	Includes all canyons controlled by the Kaibab upwarp between Red Canyon (RM 77) and Kanab Creek (RM 143). Mostly within the narrow, steep-walled Upper Granite Gorge.	Monument Creek (RM 95): Proterozoic metamorphic and igneous rocks. The Great Unconformity. Boulders from debris flows formed Granite Falls rapid. Blacktail Canyon (RM 117): narrow, tube-like notch with excellent exposures of the Great Unconformity. Tapeats Creek (RM 134): Unkar Group. Fossil algal mats in Bass Limestone (Yb); ripple marks and mudcracks in Hakatai Shale (Yh). Igneous sill in Yb . Thunder Springs emerges from a Muav Limestone (Cm) cavern.
Esplanade Segment	Includes the entire western Grand Canyon downstream from Kanab Creek.	Havasu Creek (RM 157): large tributary second only to the Little Colorado River in size. Known for spectacular waterfalls and travertine deposits. Whitmore Wash (RM 188): below Lava Falls rapids, this canyon preserves remnants of basalt flows that filled Grand Canyon to a depth of 427 m (1,400 ft).

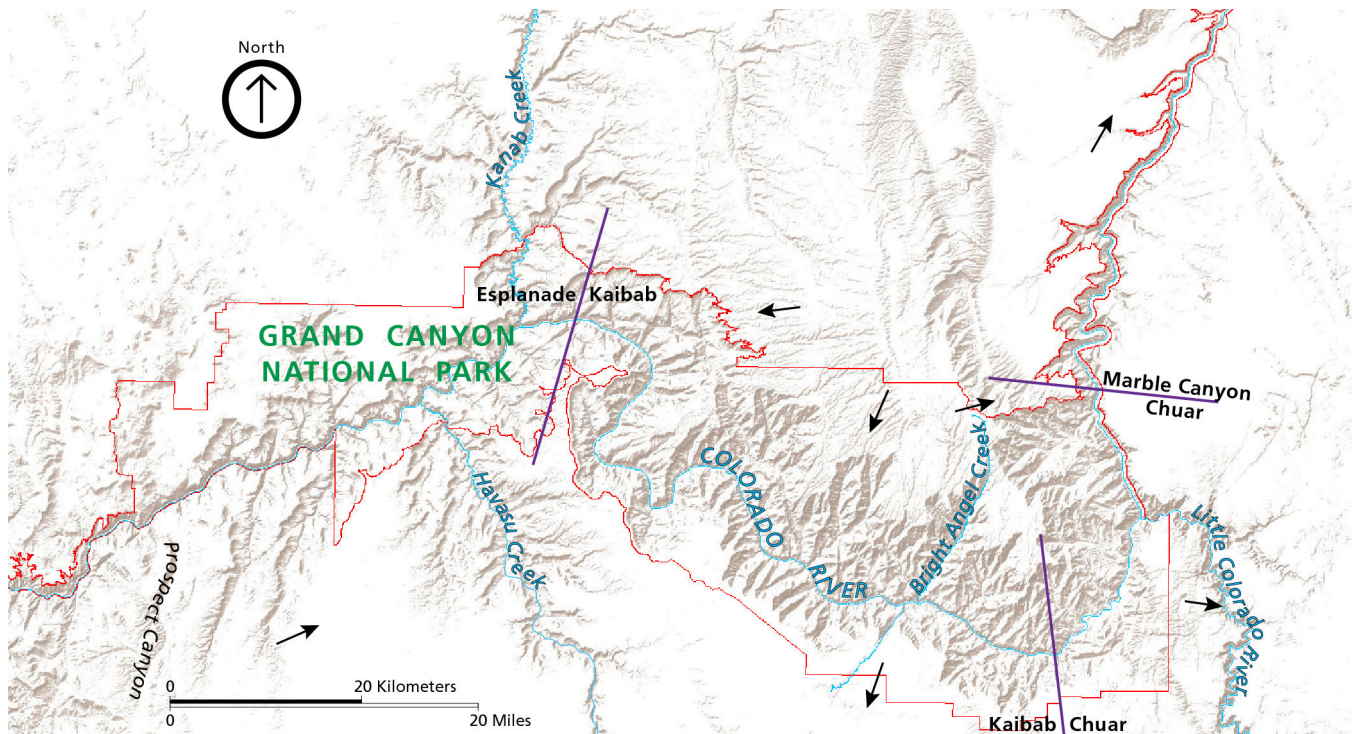


Figure 58. Simplified drainage network map of eastern Grand Canyon. Map shows the four segments of side canyons discussed in the text. Segments include: M, Marble Canyon; C, Chuar; K, Kaibab; and E, Esplanade. Tributaries are labeled as: BA, Bright Angel Creek; HC, Havasu Creek; KC, Kanab Creek; LC, Little Colorado River, and PC, Prospect Canyon. Modified from Potochnik and Reynolds (2003, figure 21.4).

deteriorates under acidic conditions, such as acid rain, and may be chemically eroded by lichens.

In addition to Grand Canyon National Park, many NPS units in the western United States, such as Arches National Park, Canyonlands National Park, Capitol Reef National Park, Dinosaur National Monument, Hovenweep National Monument, and Natural Bridges National Monument, contain desert varnish. For more information about desert varnish and photographs of desert varnish in National Park units, visit <https://www.nps.gov/articles/desertvarnish.htm#>.

Geomorphic Features and Unconsolidated Deposits

A variety of geomorphic features grace the river banks and cliffs in Grand Canyon National Park. These features capture the dynamic processes that, over millions of years, shaped today's landscape. These features and processes allow the visitor to witness the energetic and vibrant forces of nature.

Pools and Rapids

As the Colorado River flows from Lees Ferry to Diamond Creek, about 350 km (220 mi), the water surface drops in elevation from 944 m (3,116 ft) to 405 m (1,336 ft). Throughout this elevation drop, the river does not maintain a constant gradient, but consists instead of a series of relatively flat, tranquil pools and steep, turbulent rapids (fig. 19). The river bed also does not have a uniform gradient. Pools tend to be flat bottomed. The general geomorphology consists of a series of pools and rapids and the transition zone between the two known as the runout. The characteristics of the water surface and channel bottom are the result of thousands of years of interactions between the hydraulic action of the river and the tectonic uplift of the Colorado Plateau (Kieffer 2003).

Rapids in the Grand Canyon occur almost exclusively where large boulders have been deposited by floods and debris flows emerging from tributary canyons (fig. 59). Water in the deeper, tranquil pools upstream of the debris fans typically flows at less than 0.3 meters per second (m/s) (1 ft/s). By comparison, water velocities at the end of a rapid are an order of magnitude greater. Velocities at Hermit Rapids, for example, have been measured at 10 m/s (33 ft/s) (Kieffer 1988, 2003).

Water jets downstream from the toe of a rapid, and an eddy forms between the jet of water and the channel boundary. Sand in these low velocity eddies gets deposited along the banks to form beaches downstream from the rapids (fig. 60). These beaches provide a substrate for riparian vegetation, as well as popular sites for rafters. Since the construction of the Glen Canyon

Dam and the decrease in sediment load, these beaches often suffer significant erosion (Kieffer 2003; Burke et al. 2003; see the "Geologic Resource Management Issues" section).

Cobble bars (or rock gardens) accumulate downstream from the rapids and eddies (Kieffer 2003). The bars consist of boulders and cobbles (**Qs**, **Qf**, **Qgy**), transported out of the constricted channels by floods and distributed downstream once the velocity sufficiently decelerated. With regulated flow, fewer floods have the capacity to transport the larger boulders that had been moved by floods prior to Glen Canyon Dam.

Debris Flows and Fans

Debris flows, a generic name for a fluid containing at least 80% sediment, are relatively common throughout Grand Canyon National Park, and they have significantly contributed to the growth of debris fans in both the pre-dam and post-dam eras (see the "Flash Floods and Debris Flows" section in "Geologic Resource Management Issues"; Webb et al. 2003). Debris flows initiate from factors such as intense summer thunderstorms, an arid climate, narrow side canyons, and sparse vegetation.

Sediment in a typical debris flow consists of 50–90% gravel to cobble size particles, 10–25% sand, and 1–5% clay (Melis et al. 1994; Webb et al. 2003). Less than 20% of the sediment includes boulders, but they are the most visible remnant of a debris flow. Debris flows in steep tributary canyons deliver large boulders to the main channel, many of which are too large to be moved downstream by the regulated flow of the Colorado River (fig. 59; fig. 29).

Of the 525 tributaries along the Colorado River corridor, 444 have debris fans (fig. 61; Webb et al. 2003). Prior to Glen Canyon Dam, large floods periodically reworked debris fan deposits. Since the dam construction, only 25% of debris-fan volume is reworked. Regulated flows from the dam do not transport particles larger than sand any significant distance downstream (Webb et al. 2000, 2003).

At least five, pre-dam Holocene and Pleistocene alluvial fan deposits have been mapped within the park (**Qa1**, **Qa**, **Qa2**, **Qay**, **Qa3**). The deposits include cobbles and boulders and are partly cemented by calcite, gypsum, and clay. Dune sand and sand sheet (**Qd**, **Qes**) deposits partially cover the debris fans.

Debris fans constrict the Colorado River both laterally and vertically (Kieffer 2003). Once the Glen Canyon Dam was completed, debris fans began to build farther



Figure 59. Photograph shot in October 2012 of a dory maneuvering in Hance Rapid. Rapids occur where large boulders, as seen here, have been deposited by floods. Debris washed down Red Canyon over the years during flash flood events formed Hance Rapid. A flash flood in September 2012 added additional rock and debris, changing the shape of Hance Rapid. NPS photograph by Kristen M. Caldon, available at https://www.flickr.com/photos/grand_canyon_nps/8242334970/in/album-72157626635172217/.



Figure 60. Photograph of Phantom Ranch boat beach. Sand is deposited along the shoreline downstream from the rapids at RM 88.1. Phantom Ranch is located 0.8 km (0.5 mi) up Bright Angel Creek. NPS photograph by Michael Quinn, available at https://www.flickr.com/photos/grand_canyon_nps/6705376193/in/album-72157626635172217/.



Figure 61. Photograph of the alluvial fan at the mouth of Clear Creek, RM 87. Sediment from debris flows has formed a fan-shaped deposit where the steeper gradient of the canyon enters the Colorado River. The rafts are docked at Cremation boat camp, upriver from the Phantom Ranch boat beach (fig. 59). NPS photograph by Michael Quinn, available at https://www.flickr.com/photos/grand_canyon_nps/6313935718/in/album-72157626635172217/.

into the river, narrowing the canyon. As a debris fan grows into the river, a bulge develops in the streambed, vertically constricting the channel. Controlled flooding, referred to as High Flow Experiments (HFEs), have been conducted to restore some of the pre-dam conditions (see the “Restoring Colorado River Sediment Load” section in the “Geologic Resource Management Issues”).

River Terraces

River terraces, sand dunes, and debris fans reflect pre-dam and post-dam conditions. Prior to Glen Canyon Dam, Rocky Mountain snowmelt in late spring and summer flooded the Grand Canyon. However, the dam now traps all the upstream sediment and regulates seasonal flooding. Since completion of Glen Canyon Dam, small ephemeral streams have eroded through high-level, pre-dam terraces and exposed archeological remains, mostly affiliated with the 1,000–1,150 CE Pueblo II Anasazi (Burke et al. 2003). These areas also attract thousands of rafters each year.

River terraces formed in wide reaches of the Colorado River corridor and are rare in the narrow stretches of the upper and lower Granite Gorges (Burke et al. 2003). Pre-dam terraces are higher above the river than post-dam alluvial deposits. The oldest terrace deposits mapped in the park (**QTg4, QTg5**) record Miocene, Pliocene, and Pleistocene deposition of alluvial clay, silt, sand, gravel, and cobbles within Moenkopi Wash, the Little Colorado River, Tappan Wash, and Cataract Canyon (Billingsley et al. 2006b; Billingsley et al. 2007; Billingsley et al. 2012). Channel incision has isolated these older terraces 45–60 m (150–200 ft) above the modern drainage in the Little Colorado River, 9–14 m (30–45 ft) above Moenkopi Wash, and 37 m (120 ft) above the tributary in Cataract Canyon. Composition of the gravel includes fossil fragments derived from Cretaceous rocks, rounded Precambrian quartzite, Paleozoic limestone and chert, and volcanic clasts eroded from the San Francisco Volcanic Field.

Although not mapped as distinct terraces in the GRI GIS data, two Pleistocene terraces form the margins of the Colorado River near Lees Ferry, Nankoweap Rapids, Furnace Flats, and Granite Park (Burke et al. 2003). The terrace gravels fill ancient, concave channels, and the contact between the gravel and bedrock slopes towards the modern river. Both deposits are weakly to moderately consolidated and as thick as 30 m (100 ft). In addition to pebble-size gravel, the deposits contain rounded boulders of Paleozoic limestone and sandstone (Burke et al. 2003).

Holocene and/or Pleistocene (**Qgy**) terrace-gravel deposits, mapped on the Kanab and Uinkaret plateaus and in Grand Wash Trough, occur 1.2–9 m (4–30 ft) above local streambeds and are as thick as 30 m (100 ft) in Grand Wash Trough (Billingsley and Wellmeyer 2004; Billingsley et al. 2008). Modern arroyo erosion has cut deeply into the terraces. For example, incision in the upper reaches of Kanab Creek is as much as 18 m (60 ft).

Four pre-dam Holocene terrace deposits are mapped in Grand Canyon National Park. Old terrace-gravel deposits (**Qg3**) form terraces 24–30 m (80–100 ft) above the Colorado and Paria Rivers and in Kaibito and Navajo Creeks. Deposits of poorly sorted clay, silt, sand, gravel, cobbles, and boulders are as much as 24 m (80 ft) thick. Intermediate terrace-gravel deposits (**Qg2**) and young terrace-gravel deposits (**Qg1**) contain a similar mixture of unconsolidated sediments. Intermediate terraces form benches about 4.5–9 m (15–30 ft) above modern streambeds and about 2–7.5 m (6–25 ft) above the younger terraces (**Qg1**). Meandering channels have severely eroded the banks of some of these terraces. Young terrace-gravel deposits (**Qg1**) contain boulders that originated as far away as Colorado, Utah, and New Mexico. The terraces are 1–3.5 m (3–12 ft) above stream channel (**Qs**) or floodplain (**Qf**) deposits along the Colorado and Paria Rivers and Navajo and Kaibito Creeks (Billingsley et al. 2012; Billingsley and Priest 2013). General terrace-gravel deposits (**Qtg**) similar to young terrace-gravel deposits form benches about 1–100 m (3–300 ft) above the modern post-dam Colorado River.

Burke et al. (2013) distinguish the following five Holocene terrace deposits that pre-date the Glen Canyon Dam:

- Striped alluvium (2500–1300 BC to 300 CE)
- Alluvium of Pueblo II age (700 CE–1200 CE)
- Upper mesquite terrace (1400 CE–1880 CE)
- Lower mesquite terrace (1884 CE to early 1920s CE)
- Pre-dam alluvium (early 1920s to 1957–1958 CE)

These terraces are not differentiated in the GRI GIS data, but their descriptions may be found in Burke et al. (2003).

The operation of Glen Canyon Dam controls the distribution of all post-dam alluvial deposits. These deposits have been classified as channel-margin deposits, reattachment bars, and separation bars, and they have accumulated in areas of low current velocity. (fig. 62; Schmidt and Graf 1990; Burke et al. 2003). Reattachment bars develop downstream from a large channel constriction, usually a debris fan. The fan causes flow to separate from the main current and move upstream, rejoining the main current at the head of the recirculation zone, or eddy. In general, the post-dam alluvial deposits record depositional activity following the 1983 flood, an unplanned flood release that had a peak discharge of 2,700 m³/s (96,000 ft³/s) and sustained flows above 1,400 m³/s (50,000 ft³/s) (Burke et al. 2003; see the “Geologic Resource Management Issues” section).

Sand Dunes and Sand Sheet Deposits

Sand deposits accumulate near debris fans, and like terraces, they are popular camp sites. Undivided, moderately well-sorted eolian sand deposits (**Qd**), which include sand dunes and sand sheets, actively shift and cover older unconsolidated and bedrock units. Along the Colorado River corridor, eolian deposits occur downwind of sand flats formed on gravel bars (Burke et al. 2003). The dunes along the river primarily result from wind-blown sand that forms hummocks or mounds adjacent to plants, which partially anchor the sand.

Eolian sand on the plateaus form a variety of dune shapes and sand sheets that mantle bedrock slopes. In the Echo and Vermilion Cliffs, the sand grains derived from Paleozoic and Mesozoic sedimentary rocks. Proterozoic, Paleozoic, and Mesozoic rocks provided the sand for the deposits in the Coconino and Marble Plateau areas.

Sand primarily eroded from ancient, preserved sand dunes in the Navajo Sandstone (**Jn**) has been sculpted into dunes north and south of Moenkopi Wash, along the Echo Cliffs, and within drainages on the Moenkopi and Kaibito Plateaus (Billingsley et al. 2012). Navajo Sandstone is also the primary source for the sand deposits in the Paria and Kaibito Plateau areas (Billingsley and Priest 2013). On Moccasin Mountains and Paria Plateau above the Vermilion Cliffs, sand from the Navajo Sandstone accumulates in dunes along local stream drainages and on gentle slopes of alluvial fan deposits. Grass and small high-desert shrubs partially stabilize sand deposits south of State Highway 389 and

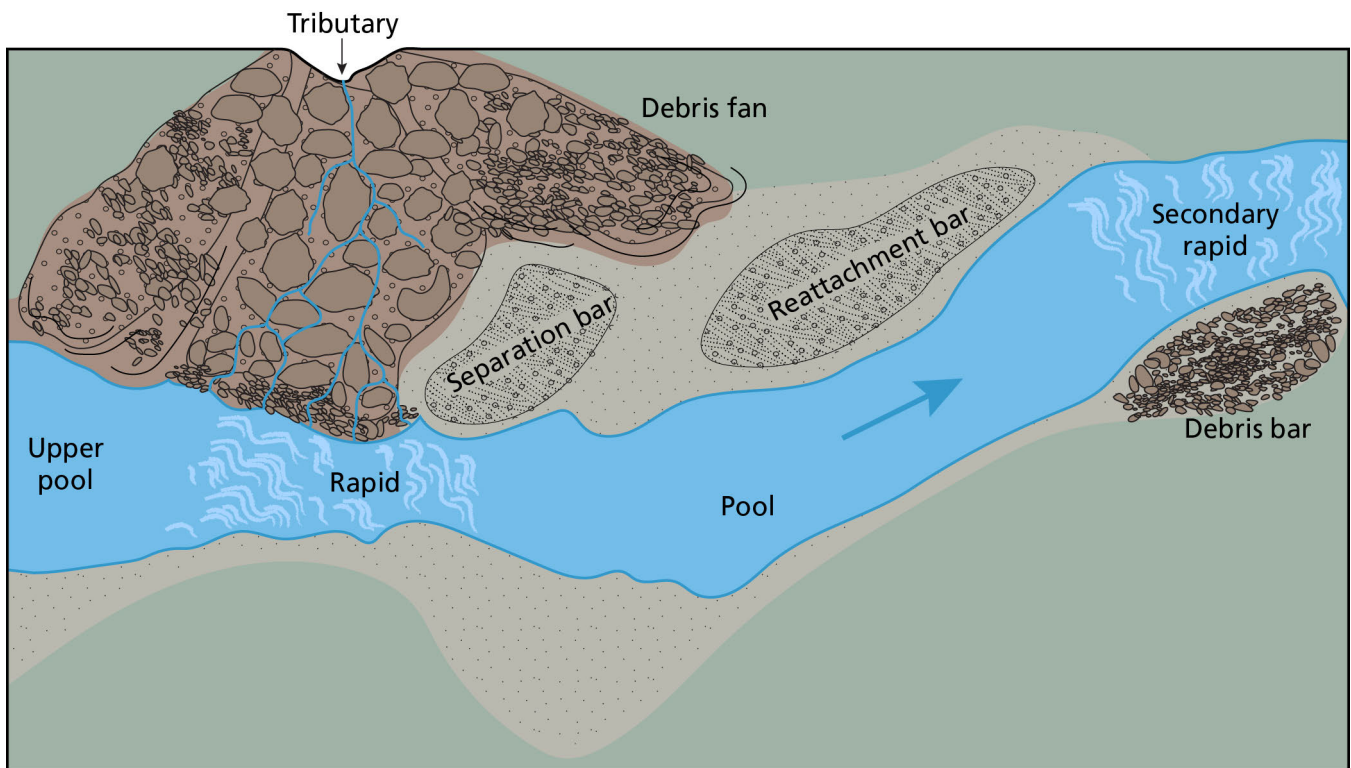


Figure 62. Schematic diagram of the pool-debris fan-rapid-eddy complex on the Colorado River in Grand Canyon.

Debris fans constrict the channel, resulting in rapids. Downstream from the constriction, the river velocity decreases and sediment is deposited along the margins of the river, forming reattachment and separation bars. Graphic by Trista Thornberry-Ehrlich (Colorado State University) redrafted from Webb and Griffiths (2014, figure 1), <http://pubs.usgs.gov/fs/FS-019-01/>.

in House Rock Valley (Billingsley et al. 2008). Triassic and Jurassic sedimentary strata provide sand sheets that mantle slopes in the Little Colorado River area.

Quartz and chert grains from the Harrisburg Member of the Kaibab Formation accumulate in lumpy, undefined geometric sand dunes or sand sheets in the Coconino Plateau and Gray Mountain area. Sand accumulates on floodplain (**Qf**) and young terrace-gravel (**Qgy**) deposits along Sandstone Wash, Rodgers Draw, and Farm Dam Draw in the west-central part of the park. Minor accumulations occur along Coconino Wash and Red Horse Wash in the northeast part of the park. Forest growth in the Kaibab National Forest south of Grand Canyon covers most of these deposits (Billingsley et al. 2007).

Slope Movement Deposits

Debris flows, landslides, and other hillslope processes determine the shape and width of the canyon above the high-water mark (Hereford and Huntoon 1990; George Billingsley, verbal communication, 26 June 2001). Rockfalls and other slope movements are common, although they are not often recorded. Seventeen

rockfalls ranging in size from numerous small rocks to an estimated 32 metric tons (35 US tons) of rock were recorded in the Grand Canyon from 1968–1973 (Hereford and Huntoon 1990; George Billingsley, verbal communication, 26 June 2001).

In the Grand Canyon, Holocene and Pleistocene slope movement (e.g. landslide) deposits (**Ql**) form large unconsolidated to partly consolidated masses of primarily Paleozoic rock debris (fig. 63). The deposits include detached blocks of strata that have rotated backward and slid downslope, local talus debris (**Qtr**), rock glacier, and rock-fall debris. In the Vermilion Cliffs area, landslide masses are as large as 3 km (2 mi) in length, 0.8 km (0.5 mi) wide, and have slid downslope 153–213 m (500–700 ft) (Billingsley et al. 2008). Most landslides include car- and house-size boulders. The thickness of landslide deposits in the map area ranges from 3 to 183 m (10 to 600 ft).

Earthquakes associated with major faults in the area, such as the Hurricane and Meriwhitica faults, may trigger some of the larger landslides in Grand Canyon (Billingsley et al. 2006a, 2007, 2008). Many small



Figure 63. Photograph of a rockslide as seen from Hopi Point. On August 23, 2012, visitors witnessed canyon building in action as a plume of red dust rose from the Supai layer below Cheops Temple. The plume enlarged and changed to white as the rockfall hit the Redwall Limestone. NPS photograph by Jacob Fillion, available at https://www.flickr.com/photos/grand_canyon_nps/7851921418/in/album-72157630889521118/.

landslide masses with variable thickness between 3 to 60 m (10 to 200 ft) commonly occur below cliffs of Kaibab Formation (**Pk**), Coconino Sandstone (**Pc**), Redwall Limestone (**Mr**), and Tapeats Sandstone (**Ct**). In the Grand Wash Trough and Vermillion Cliffs areas, landslides may become unstable during wet conditions, especially in areas where the deposits overlie claystone and siltstone of the Kayenta Formation (**Jk**) or Petrified Forest Member of the Chinle Formation (**TRcp**). In Kanab Creek and some other tributary canyons, detached blocks of Permian strata have either fallen or slid down soft gypsiferous slopes of the Woods Ranch Member of the Toroweap Formation (**Ptw**) (Billingsley et al. 2008). Eolian dune sand and sand sheet (**Qd**) deposits often partly cover landslide deposits.

Hazards and risks associated with slope movements in Grand Canyon National Park are described in the “Geologic Resource Management Issues” section.

Travertine Deposits

Gray and tan travertine (**Qt**), limestone fashioned by the chemical precipitation of calcium carbonate from

springwater discharge (fig. 20), occurs as massive encrustations on steep slopes or cliffs or as “travertine dams” in tributary streams. Faults that offset basement rocks and form Laramide monoclines mark the locations of many travertine deposits and travertine-depositing springs. Exceptional amounts of Quaternary-aged travertine can be found where fault zones intersect the Muav Limestone on the south and east sides of eastern Grand Canyon and both sides of western Grand Canyon (Szabo 1990; Crossey et al. 2006).

Travertine deposits vary considerably in thickness. At Slide Spring in Slide Canyon, an eastern tributary to Snake Gulch in upper Kanab Canyon, travertine deposits range from 2 to 18 m (6 to 60 ft) thick, but thick travertine dams as much as 60 m (200 ft) thick occur in Meriwitica, Spencer, Travertine, and Quartermaster canyons (Billingsley et al. 2006a, 2008). Thick deposits also occur in Havasu Canyon below Supai and at Royal Arch Creek east of Supai (Billingsley 2000b). Along the east side of the Colorado River and the north side of Little Colorado River, travertine deposits develop primarily near the base of the Cambrian Muav

Limestone (**Cm**). Locally, small dams of travertine intercept the flow of the Little Colorado River and Havasu Creek. Outside of the park in the Moenkopi Wash area, minor deposits precipitate from seeps along the contact between the Kayenta Formation (**Jk**) and the Navajo Sandstone transition zone (Billingsley et al. 2012).

Precipitation of travertine involves three processes. First, groundwater must acquire abundant CO_2 . Then, the CO_2 -rich groundwater dissolves carbonate minerals from limestone, enriching the groundwater with calcium and magnesium. At Earth's surface, CO_2 -degassing occurs and calcium-carbonate precipitates (Crossey et al. 2006). In the Grand Canyon region, CO_2 -degassing plays a much more significant role than evaporation in the formation of travertine (O'Brien 2002).

The key question to travertine precipitation in Grand Canyon National Park rests with the origin of the CO_2 . Researchers in the past have proposed a surficial source of CO_2 resulting from a mixing of atmospheric and soil gas from microbial activity (Giegengack et al. 1979; Szabo 1990). However, geochemical data from Crossey et al. (2006) has shown that near-surface processes alone cannot account for the abundant dissolved CO_2 in the travertine-depositing water. Rather, the CO_2 may have originated from crustal metamorphism, hydrocarbons, or mantle degassing (Crossey et al. 2006). The groundwater also contained abundant mantle-derived helium. Similar to the CO_2 and helium associated with Mammoth Springs, California, the Permian Basin of Texas and New Mexico, and Saratoga Springs, New York, the CO_2 and helium responsible for the travertine in Grand Canyon National Park may have been released by mantle partial melting and transported upward during earthquakes (Sorey et al. 1998; Ballentine et al. 2001; Siegel et al. 2004; Crossey et al. 2006).

CO_2 concentrations, groundwater temperature, salinity, sulfur content, strontium isotopes, and mantle-derived helium in groundwater support a magmatic, deeply derived groundwater source leading to the eventual precipitation of travertine in Grand Canyon National Park. Under confined conditions, the slow-moving, high temperature groundwater dissolves the surrounding limestone and becomes enriched in carbon dioxide and dissolved calcium. When the water discharges, such as at Blue and Havasu Springs, carbon dioxide is lost to the atmosphere and travertine precipitates (Hill and Polyak 2010).

Several travertine deposits represent springs that were probably active during the Pleistocene Epoch but are currently dry. The deposits are porous, stained light-red,

often banded, and may incorporate angular clasts and boulders of talus and rounded Colorado River gravel.

Waterfalls

Many of the caves in Grand Canyon play a significant role in the park's hydrology. For example, waterfalls and springs emerge from caves in such locations as Vaseys Paradise, Cheyava Falls, and Roaring, Thunder, and Tapeats springs. The waterfall emerging from Deer Spring is popular with park visitors (fig. 64).

The most spectacular waterfalls in the Grand Canyon area are located within the Havasupai Indian Reservation. Havasupai Creek cascades over bedrock forming such exceptional waterfalls as New Navajo Falls, Fifty Foot Falls, Havasu Falls, Mooney Falls, and the remote Beaver Falls.



Figure 64. Photograph of the waterfall emerging from Deer Spring.

Note the lush vegetation growing in the immediate vicinity of the waterfall. Park visitors for scale.

NPS photograph by Erin Whittaker, available at https://www.flickr.com/photos/grand_canyon_nps/6081022003/in/album-72157626635172217/.

Geologic Type Sections

A type section is an area where a sequence of strata was originally described. The type section serves as an objective standard with which to compare spatially separated strata. Preferably, a type section is designated in an area where the unit shows maximum thickness and both the top and bottom of the unit are exposed. The USGS “GEOLEX” website provides location information and nomenclatural summaries for geologic map units across the country and is a source of additional information: <http://ngmdb.usgs.gov/Geolex/search>.

Type sections are typically selected for layers of sedimentary rocks which share similar characteristics, such as rock type (e.g., sandstone, shale, siltstone), color, or distinctive features. Such a rock unit is called a “formation.” Geologists usually name formations to reflect a geographic feature such as a river, mountain, or city where the layers are best seen (e.g., Temple Butte Formation). Formations can be lumped together into “groups” (e.g., Chuar Group) or “supergroups” (groups of groups; e.g., Grand Canyon Supergroup) or

subdivided into “members” (e.g., Walcott Member of Kwagunt Formation).

Each formation and/or member in the entire stratigraphic column has only one official type section. Type sections allow geologists to correlate geologic units across vast reaches of both space and time. In addition, type sections continue to yield valuable scientific information long after their official designation. Grand Canyon National Park contains more geologic type sections than perhaps any other National Park Service unit (table 18; NPS 2010). Excellent exposures and intense geological interest in the Grand Canyon dating back to John Wesley Powell’s expedition has resulted in 23 type sections of formations and 11 type sections of members exposed in the park. Some units, such as the Rama and Vishnu schists, do not have designated, official type sections, but they have been described only from the Grand Canyon (Karlstrom et al. 2003). By protecting so many type sections, Grand Canyon National Park protects an exceptional geologic heritage that will be available to many future geologists and generations to come.

Table 18. Designated type sections in Grand Canyon National Park.

Formation (map symbol)	Type Location	Reference
Moenkopi Formation (TRm)	Moenkopi Wash	Wilmarth, M. G. (1957)
Kaibab Formation (Pk)	Kaibab Plateau (not an official designation)	Darton, N. H. (1910)
Kaibab Formation, Fossil Mountain Member (Pkf)	Bass Trail on Fossil Mountain	McKee, E. D. (1938)
Toroweap Formation (Pt)	East wall of Toroweap Valley	McKee, E. D. (1938)
Hermit Formation (Ph)	Hermit basin	Noble, L. F. (1922)
Esplanade Sandstone (Pe)	Not designated. Described from Grand Canyon	White, D. (1929a)
Wescogame Formation (PNMs)	Wescogame Point, Havasu Canyon	McKee, E. D. (1975)
Manakacha Formation (PNMs)	Manakacha Point, Havasu Canyon	McKee, E. D. (1975)
Watahomigi Formation (PNMs)	Watahomigi Point, Havasu Canyon	McKee, E. D. (1975)
Surprise Canyon Formation (Ms)	Tributary canyon of Colorado River, 18 km (11 mi) west of Surprise Canyon	Billingsley, G. H., and S. S. Beus (1985)
Redwall Limestone (Mr)	Redwall Canyon	Gilbert, G. K. (1875b)
Temple Butte Formation (Dtb)	Temple Butte	Walcott, C. D. (1889)
Muav Limestone (Cm)	Muav Canyon	Noble, L. F. (1914)
Bright Angel shale (Cba)	Bright Angel Canyon	Noble, L. F. (1914)
Tapeats Sandstone (Ct)	Tapeats Creek	Noble, L. F. (1914)
Sixtymile Formation (Zs)	Top of Nankoweap Butte and on north side of Sixty Mile Canyon and Awatubi Canyon	Ford, T. D., and W. J. Breed (1973)
Kwagunt Formation Walcott Member (Zkw)	Head of Walcott Glen and upper part of Nankoweap Butte	Ford, T. D., and W. J. Breed (1973)

Table 18, continued. Designated type sections in Grand Canyon National Park.

Formation (map symbol)	Type Location	Reference
Kwagunt Formation Awatubi Member (Zka)	Awatubi Canyon	Ford, T. D., and W. J. Breed (1973)
Kwagunt Formation Carbon Butte Member (Zkcb)	Shelf of red sandstone surrounding Carbon Butte	Ford, T. D., and W. J. Breed (1973)
Galeros Formation Duppa Member (Zgd)	Duppa Butte, Kwagunt Canyon	Ford, T. D., and W. J. Breed (1973)
Galeros Formation Carbon Canyon Member (Zgcc)	West fork of Carbon Canyon and mid-Chuar Canyon	Ford, T. D., and W. J. Breed (1973)
Galeros Formation Jupiter Member (Zgj)	Jupiter Temple, Chuar Canyon	Ford, T. D., and W. J. Breed (1973)
Galeros Formation Tanner Member (Zgt)	Overlooking Tanner Rapids in cliffs of Basalt Canyon	Ford, T. D., and W. J. Breed (1973)
Nankoweap Formation (YZn)	Basalt Canyon, south of Little Colorado River	Van Gundy, C. E. (1951)
Cardenas Basalt (Yc)	Cardenas Butte and Cardenas Creek	Keyes, C. (1938) and Ford, T. D., W. J. Breed, and J. W. Mitchell (1972)
Dox Formation (Yd)	Dox Castle	Noble, L. F. (1914)
Dox Formation Ochoa Point Member (Ydo)	Ochoa Point, west of Basalt Canyon	Stevenson, G. M., and S. S. Beus (1982)
Dox Formation Comanche Point Member (Ydc)	Tributary creek to Tanner Canyon, 1.6 km (1 mi) west of Comanche Point	Stevenson, G. M., and S. S. Beus (1982)
Dox Formation Solomon Temple Member (Yds)	2.4 km (1.5 mi) northeast of Solomon Temple	Stevenson, G. M., and S. S. Beus (1982)
Dox Formation Escalante Creek Member (Yde)	Escalante Creek	Stevenson, G. M., and S. S. Beus (1982)
Shinumo Quartzite (Ys)	Canyon of Shinumo Creek	Noble, L. F. (1914)
Hakatai Shale (Yh)	Hakatai Canyon	Noble, L. F. (1914)
Bass Formation (Yb)	Bass Canyon	Noble, L. F. (1914)
Brahma Schist (Xbr)	Inner Gorge of Grand Canyon	Maxson, J. H. (1961)

Geologic Resource Management Issues

Some geologic features, processes, or human activities may require management for human safety, protection of infrastructure, and preservation of natural and cultural resources. The NPS Geologic Resources Division provides technical and policy assistance for these issues.

During the 2001 scoping meeting (NPS 2001) and 2015 conference call, participants (see Appendix A) identified the following geologic resource management issues:

- Climate Change and Water Supply
- Flash Floods and Debris Flows
- Restoring and Monitoring Colorado River Sediment Load
- Slope Movement Hazards
- Cave and Karst Inventory, Monitoring, and Protection
- Trans-Canyon Pipeline Replacement
- Paleontological Resource Inventory, Monitoring, and Protection
- Earthquakes
- Abandoned Mineral Lands
- Uranium Mining
- Hydrocarbon Exploration
- Lake Mead Delta

Issues identified during the scoping meeting and conference calls were also documented in the 2010 foundation document, which lists current conditions, trends, issues and concerns, stakeholder interest, relevant laws and regulations, available information, planning and information needs for fundamental geologic resources (NPS 2010). According to the foundation document, the following issues are relevant to the park's geologic resources (listed in the order they appear in the document):

- Alteration of natural river processes by Glen Canyon Dam.
- Negative impacts on park resources, including groundwater, from mineral mining activities, especially uranium, associated with breccia pipes near the park boundary, notably on the Coconino and Kanab Plateaus.
- Regional water availability and the alteration of existing geologic processes, such as slope movement and debris flows, resulting from climate change.
- Lack of a baseline inventory database documenting cave resource extent, scope, and significance. Because only about 10% of the park's caves have

been inventoried and mapped, cave resources are “at risk.”

- Lack of paleontological resources inventory and monitoring data.
- Unpermitted visitation to cave formation, and a lack of inventory, monitoring, and mitigation protocol.
- Potential adverse effects resulting from geologic hazards such as earthquakes, rockfalls, debris flows, and renewed volcanism in the Uinkaret Volcanic Field.
- Human-health hazards resulting from radionuclides present in water discharged from some springs.
- Human risks, including poor air quality, collapse, and other hazards, associated with a variety of Abandoned Mineral Lands.

Some water resource issues listed in the foundation document, such as the influence of Glen Canyon Dam and inventory and monitoring of park springs, are intimately connected to geologic resource issues (NPS 2010). However, water resource issues involving surface and groundwater quantity and quality are not addressed in this report. The NPS Water Resources Division may be contacted for detailed information relevant to the water resource issues summarized in the foundation document (<https://www.nps.gov/orgs/1439/index.htm>).

Resource managers may find Geological Monitoring (Young and Norby 2009; <http://go.nps.gov/geomonitoring>) useful for addressing geologic resource management issues. The manual provides guidance for monitoring vital signs—measurable parameters of the overall condition of natural resources. Each chapter covers a different geologic resource and includes detailed recommendations for resource managers, suggested methods of monitoring, and case studies.

Geologic Resource Management Assistance

Contact the Geologic Resources Division (<http://go.nps.gov/geology>) for assistance with resource inventories, assessments, and monitoring; impact mitigation, restoration, and adaptation; hazards risk management; law, policy, and guidance; resource management planning; data and information management; and outreach and youth programs (Geoscientists-in-the-Parks and Mosaics in Science). Park staff can formally request assistance via <https://irma.nps.gov/Star/>.

The Geoscientists-in-the-Park (GIP) and Mosaics in Science (MIS) programs are internship programs to place scientists (typically undergraduate students) in parks to complete geoscience-related projects that may address resource management issues. At least 39 GIPs have worked on a variety of projects at Grand Canyon National Park between 2000 and 2016. Projects have included

- Geology education and interpretation,
- Geologic hazards research,
- Paleontology inventory and monitoring,
- Cave/karst research,
- Hydrology inventory and monitoring, and
- Energy and minerals inventory and monitoring.

Products created by the program participants are available by contacting the Geologic Resources Division.

Climate Change and Water Supply

Global climate change may be the single most comprehensive issue facing resource managers at Grand Canyon National Park. Changing climate will most likely have a cascading effect where one alteration will trigger a series of impacts. On the Colorado Plateau, elevation strongly controls temperature, precipitation and evapotranspiration (Spence 2001). In general, precipitation increases, and potential evaporation decreases as elevation increases. The arid-humid climate boundary occurs at approximately 2,730 m (8,957 ft) (Spence 2001). Grand Canyon National Park lies entirely on the arid side of this climate boundary. For reference, the average elevation along the North Rim is 2,400 m (8,000 ft). Point Imperial, the highest point, measures 2,700 m (8,800 ft) above sea level. The South Rim is approximately 300 m (1,000 ft) lower than the North Rim, and the elevation at the boundary of Lake Mead is 360 m (1,200 ft). At Phantom Ranch, the Colorado River measures 720 m (2,400 ft) above sea level.

Primary climate change concerns derive from projected decreases in, and timing of, precipitation and increases in temperature. Echoing what many climate scientists have said for years, the park's foundation document (NPS 2010) states that climate change may further impact regional water availability and alter existing geologic processes, such as hill slope processes and debris flow initiation.

Precipitation is projected to decrease in the southwestern United States, and higher temperatures caused by continued greenhouse gas emissions are predicted to sharply increase the risk of dry periods

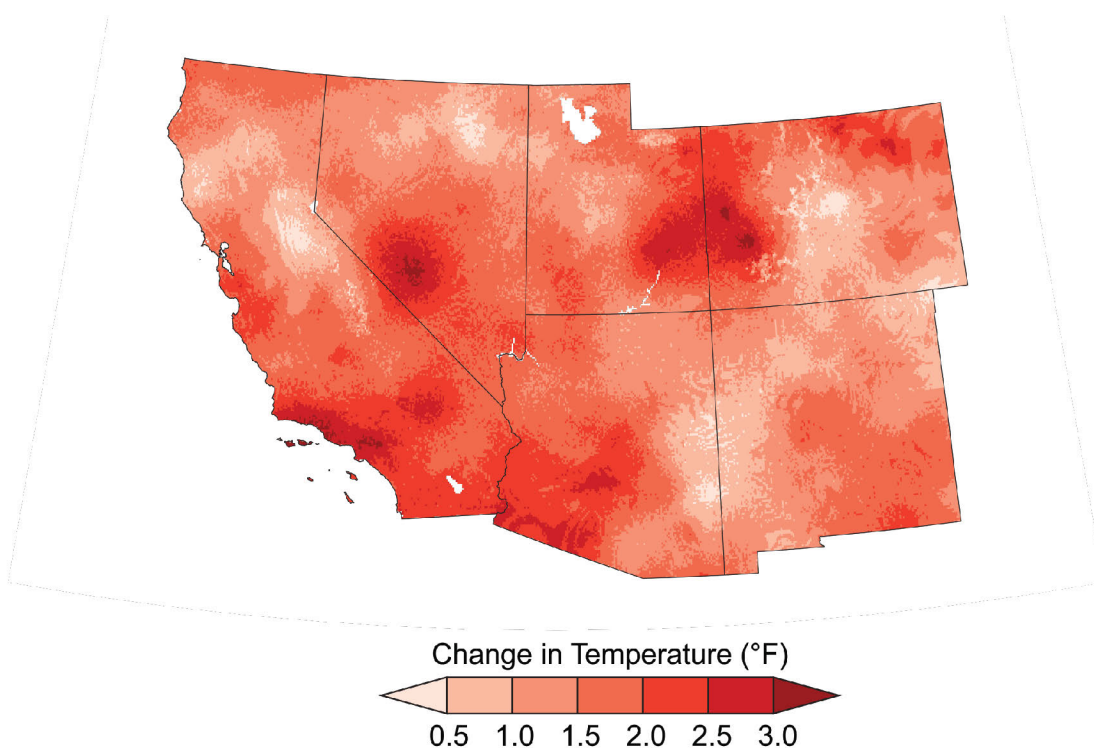
lasting 10 years or more (known as megadroughts). These megadroughts are expected to become more frequent, intense, and longer lasting than historical droughts in the Colorado River Basin (Karl et al. 2009; Intergovernmental Panel on Climate Change 2014; Melillo et al. 2014; Cook et al. 2015; Gonzalez et al. 2018). Megadroughts cause increased competition among agricultural, municipal, industrial, and ecological uses for scarce water resources, which are already overallocated (Bates et al. 2008; Karl et al. 2009; Intergovernmental Panel on Climate Change 2014; Melillo et al. 2014; Gonzalez et al. 2018).

Increasing temperatures in this arid environment have significantly altered the water cycle in the Southwest (fig. 65; Gonzalez et al. 2018). Over the past century, the duration and extent of snow cover, mountain snow equivalent, and annual precipitation has decreased in the southwestern US. In California, for example, above-freezing temperatures through the winter of 2014–2015 led to the lowest snowpack on record (Gonzalez et al. 2018). Winter and spring precipitation is predicted to decrease even further by 2100, although a trend towards a slight increase in winter precipitation on the Colorado Plateau has occurred over the last 30–40 years (Spence 2001; Bates et al. 2008; Melillo et al. 2014). Peak stream flow occurs earlier in the year because more precipitation is falling as rain rather than snow (Knowles et al. 2006; Loehman 2009; Gonzalez et al. 2018). Changes such as these exacerbate hydrological drought.

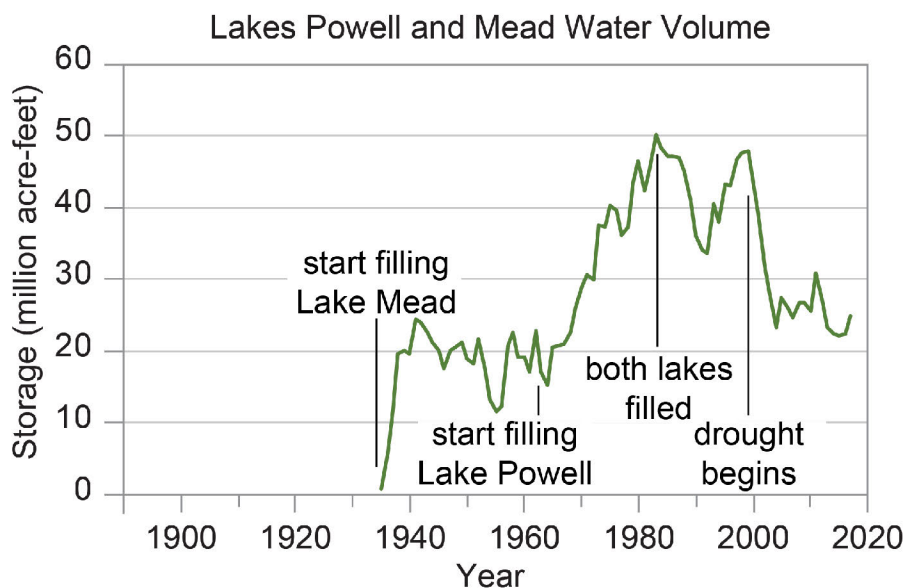
In addition, dust and soot transported by winds from lowland regions will accumulate on the surface of snowpack, increasing the amount of the sun's energy absorbed by the snow and resulting in an earlier snowmelt and evaporation. Already lower than 20th century average rates, streamflow in the Colorado River basin is projected to decline because of decreased snowpack and subsequent reduced spring runoff and soil moisture (Bates et al. 2008; Intergovernmental Panel on Climate Change 2014; Melillo et al. 2014; Gonzalez et al. 2018).

A decrease in precipitation may also lead to fewer flash floods, and thus, a decrease in sediment deposited in the debris fan at the mouth of the Paria River and subsequent sediment load. Decreases in sediment load at the mouth of the Paria River would limit the rejuvenation of sand bars and thus, decrease camping areas and the preservation of archeological sites along the river.

Projected decreases in precipitation or the seasonal timing of precipitation events also may decrease groundwater availability. The Redwall-Muav aquifer, the



(A) Average temperature differences between 1986-2016 and 1901-1960.



(B) Decrease in water volume in Lake Powell and Lake Mead.

Figure 65. Effects of global climate change on the southwestern United States. Hot, dry conditions will impact the water resources in Grand Canyon National Park. (A) Map showing the difference between 1986–2016 average temperature and 1901–1960 average temperature. The greatest temperature increases occurred in southern California and western Colorado. (B) This graph shows the fluctuation in water volumes in Lake Powell and Lake Mead. Drought, increased temperature and evaporation in the Upper Colorado River Basin, which resulted in decreased stream flow, and increased Lower Basin water consumption beginning in the 1990s led to reduced reservoir volumes. Data from Gonzalez et al. (2018, figures 25.1 and 25.3) <https://nca2018.globalchange.gov/chapter/southwest>.

sole water source for the park, is recharged primarily by snowmelt, and to a lesser extent by extreme summer monsoon events (Jones et al. 2016b). A decrease in groundwater availability will threaten spring flow, which will decrease potable water availability and subsequent deliverability via the Trans-Canyon Pipeline (TCP) to the over 5 million park visitors each year, as well as altering riparian habitat along the Colorado River corridor (Hoffman et al. 2015).

Increases in aridity, a shift from snow to rain events, increased development, and potential groundwater contamination make understanding the Redwall-Muav aquifer essential for the protection of the park's water supply and the canyon's ecological resources (Hoffman et al. 2015). Hydrograph analyses of the first-ever dye trace studies in the park, conducted in 2013 and 2014, indicated that aquifer storage decreases with increased aridity and that the retention time for groundwater in the aquifer is relatively short (Hoffman et al. 2015). Results from these studies suggested that the Redwall-Muav aquifer and associated downstream ecosystem may be vulnerable if climate change significantly reduces groundwater flow.

Even with no or minor changes in precipitation, increased temperatures may decrease the amount of water available to flow through the canyon (Spence 2001). In the Upper Colorado River Basin, increased temperatures have increased plant water use and evaporation, which has reduced lake inflows and lake volumes (fig. 65; Gonzalez et al. 2018). Severe droughts and associated evaporation since 2000 CE have significantly decreased the water level of Lake Powell and Lake Mead. During the drought years of 2000–2005, the lake level of Lake Powell dropped roughly 30 m (100 ft) as 13 million acre-feet of water were lost. Climate change predictions suggest that Lake Powell will rarely achieve full capacity, and Glen Canyon Dam's usefulness for generating power will decrease (Christensen et al. 2004; Bates et al. 2008). Demand for freshwater may lower Lake Powell lake levels even farther, which will alter the amount of water delivered through Grand Canyon National Park via the operation of Glen Canyon Dam.

Since 2000, the water level in Lake Mead has fallen 40 m (130 ft), and the lake has lost 60% of its volume because of the ongoing Colorado River Basin drought and continued water withdrawals by cities and agriculture (Gonzalez et al. 2018). Recent droughts and climate change predictions have allowed the 1990s proposal to drain Lake Powell to fill Lake Mead to gain traction (Patterson 2017). If Lake Powell was drained, the shoreline and channel morphology of the Colorado

River downstream from the Glen Canyon Dam would undergo significant adjustments.

Because of the decreased water volume in Lake Powell and Lake Mead and the increased risk of water shortages across much of the Southwest, local water utilities, the governments of seven U.S. states, and the federal governments of the United States and Mexico have voluntarily developed and implemented solutions to minimize the possibility of water shortages for cities, farms, and ecosystems (Gonzalez et al. 2018). For example, California implemented a water conservation plan in 2014 that reduced water use 25% from 2014 to 2017.

Changes in both precipitation amount and distribution, as well as changes in the number of temperature fluctuations across the freeze/thaw gradient can alter the stability of slopes. Frost wedging is one potential cause of slope instability and triggers rockfall and other slope movements (see "Slope Movement Hazards and Risk").

Large proposed commercial, residential, and tourist attraction development projects outside the park on both rims of the canyon would further strain limited groundwater resources (NPS n.d.). Large projects proposed on the Navajo Nation and near Tusayan were not approved based, at least in part, on the availability of water resources. See Cart (2014), Roberts (2015), Sottile and Dahlgren (2015), Landry (2015), and Howard (2016) for examples of media coverage of the developments.

The NPS has begun to address climate change in the parks with several websites. The NPS Climate Change website (<https://www.nps.gov/subjects/climatechange/index.htm>) provides general background information on how climate change is affecting national parks and how the NPS is responding. Adapting to climate change in national parks includes the following five goals:

- Incorporate climate change consideration and responses in all levels of the NPS planning framework.
- Implement adaptation strategies that promote ecosystem resilience and enhance restoration, conservation, and preservation of park natural resources.
- Develop, prioritize, and implement management strategies to preserve climate-sensitive cultural resources.
- Include climate-related vulnerability assessments in project approval and funding decisions.
- Enhance the sustainable maintenance, design, and construction of park infrastructure.

Grand Canyon National Park is a “Climate Friendly Park” (see <https://www.nps.gov/subjects/climatechange/cfpprogram.htm>). The Climate Friendly Parks (CFP) Program provides tools and resources to address climate change and to reach the goals of the CFP, which include:

- Measure park-based greenhouse gas (GHG) emissions,
- Educate staff, partners, stakeholders, and the public about climate change and demonstrate ways individuals and groups can act to address the issue, and
- Assist parks in developing strategies and specific actions to address sustainability challenges, reduce GHG emissions, and anticipate the impacts of climate change on park resources.

The CFP is one of many initiatives supporting the NPS Green Parks Plan (<https://www.nps.gov/subjects/sustainability/green-parks.htm>), a long-term strategic plan for sustainable management of NPS operations. Progress on meeting the goals of the Green Parks Plan may be found on the Monitoring and Tracking page (<https://www.nps.gov/subjects/sustainability/monitor.htm>). As of February 2018, annual performance briefs were available for 2013, 2014, and 2015.

Flash Floods and Debris Flows

Flash floods and debris flows are common in northern Arizona and present safety issues for hikers in narrow slot canyons. In August 1997, for example, twelve hikers in Lower Antelope Canyon, a narrow twisting canyon that enters Lake Powell National Recreation Area from Page, Arizona, were caught in a flash flood that filled the canyon with water 15 m (50 ft) deep. That same year, two hikers in Grand Canyon died from a flash flood in Phantom Creek. In 2001, a flash flood in Havasu Canyon swept away a family of three.

Flash floods also wash out trails and disrupt infrastructure (fig. 66). A flash flood in 2004 damaged the Indian Gardens mule corral on the Bright Angel Trail (fig. 67). In 2005, the Grandview Trail was closed for months because a long section of the trail had been washed out. A 2008 flood in Havasu Canyon reshaped a series of short waterfalls known as Navajo Falls. The flood redirected the Havasu Creek channel, which abandoned Navajo Falls but created two new waterfalls, New Navajo Falls and Rock Falls. Debris flows and flash floods have also ruptured the TCP (see “Trans-Canyon Pipeline Replacement”).

Although a safety hazard, debris flows contribute needed sediment to the riparian habitat and aquatic ecosystem of the Colorado River (see “Debris Flows

and Fans” in the “Geologic Features and Processes” section). Monitoring coarse sediment input from debris flows is critical for managing components of the Colorado River ecosystem (Webb and Griffiths 2014). As described in “Debris Flows and Fans,” debris flows build debris fans where tributaries join the Colorado River, and these debris fans constrict the river and form rapids (fig. 68).

The debris fans and debris bars that develop below rapids provide a stable substrate for aquatic organisms. Pools and eddies trap fine sediment in sand bars. The fan-eddy complex also attracts the endangered humpback chub (*Gila cypha*). Monitoring coarse sediment input and its long-term redistribution allows effective management of these resources. Monitoring methods relevant to the Grand Canyon, which include surveys of debris fan topography, measuring particle size distribution, aerial mapping photography (fig. 68), LiDAR, and remote sensing techniques are explained in Melis (1997), Melis et al. (1994, 1997), Webb and Griffiths (2014), and Webb et al. (1999a, 1999b, 2000).



Figure 66. Photograph of Grand Canyon’s trail crew rebuilding a wall.

The wall is along the North Kaibab Trail in 2012 just above the Box in Bright Angel Canyon. The wall protects the trail and TCP from seasonal flooding on Bright Angel Creek. The trail crew rebuilt 30 m (100 ft) of wall in fourteen days. Rock material came from local sources, while helicopters transported the mortar, mixers, and other supplies to the site. NPS photograph by Kristen M. Caldon, available at https://www.flickr.com/photos/grand_canyon_nps/7309570218/in/album-72157629986699376/.



2004



2013

Figure 67. Photographs of Indian Gardens mule corral following the 2004 flash flood on Bright Angel Trail. The flash flood occurred on July 14, 2004, damaging the corral and leaving behind mud and boulders. NPS photograph by Chris Brothers (Kelkar 2013b).

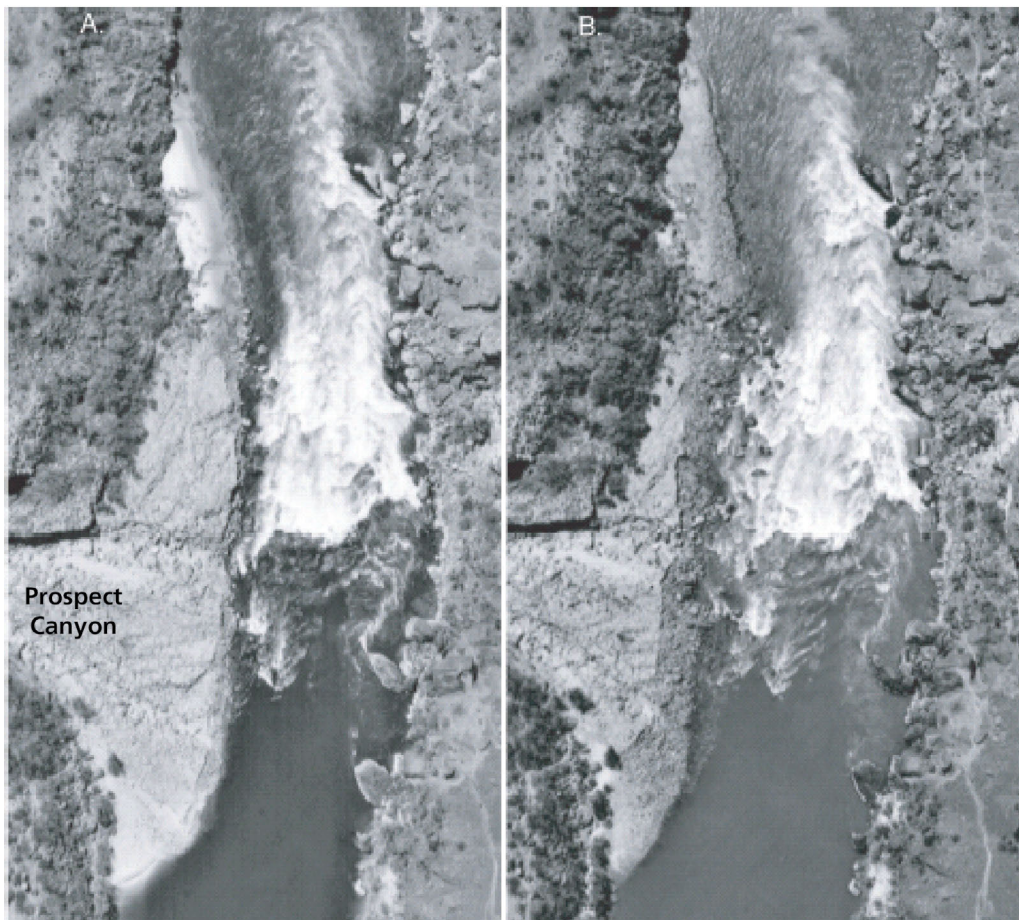


Figure 68. Aerial photograph of the 1995 debris fan at Lava Falls Rapid. A) Lava Falls Rapid was constricted by the 1995 debris flow from Prospect Canyon (to the left in the photographs). B) The 1996 controlled flood removed sediment from the edge of the fan, increasing the width of the rapid by an average of 5 m (16 ft). USGS photograph from Webb and Griffiths (2014, figure 2), available at <http://pubs.usgs.gov/fs/FS-019-01/>.

Peak discharges for most debris flows in Grand Canyon range from 100 m³/s to 300 m³/s (350–11,000 ft³/s) with peak velocities ranging from 2 m/s to 10 m/s (6.5–33 ft/s). However, many larger debris flows have occurred in Grand Canyon during the last century, and they have dramatically impacted the rapids and channel morphology at the mouth of the drainages (Griffiths et al. 1996; Webb et al. 2003).

The largest historic event occurred in 1939 when a debris flow from Prospect Canyon deposited boulders that completely changed Lava Falls Rapid, the most formidable stretch of rapids in Grand Canyon and according to Webb et al. (1999b, p. 1) “one of the most famous rapids in the world.” Discharge from this debris flow measured 1,000 m³/s (35,000 ft³/s) (Webb et al. 1999b, 2003).

In December 1966, a debris flow with a discharge of 280 m³/s (10,000 ft³/s) transformed Crystal Rapid from a gentle rapid to challenging whitewater. The 1966 rainstorm also produced a debris flow/flash flood in Bright Angel Creek that destroyed part of the TCP and impacted Phantom Ranch and Bright Angel Campground (Allyson Mathis, NPS Grand Canyon National Park, park ranger, personal communication, 2005; see “Trans-Canyon Pipeline Replacement”).

No one witnessed the 1939 or 1966 debris flows, but eyewitness accounts of debris flows in 1889 and 1984 speak to the awesome power behind these types of flash floods. In 1889, Robert Brewster Stanton’s expedition party started hiking up South Canyon when a thunderstorm hit. Before long they saw, “the whole sides of the canyon seemed to be moving down upon us. . . and as the larger rocks plunged ahead of the streams, they crashed against other rocks, breaking into pieces; and the fragments flew in to the air in every direction, hundreds of feet above our heads. . .” (Stanton, qtd. in Webb et al. 2003, p. 373).

Unbeknownst to two rafting company guides who were driving trucks up the Diamond Creek road on July 20, 1984, a thunderstorm had just inundated the creek’s headwaters. When they saw the 2-m-(6-ft-)high debris flow front bearing down on them, they scrambled to safety and watched as the floodwaters picked up their trucks, flipped them over, and swept them out of sight in a dark slurry of mud, broken branches, and boulders (Ghiglieri 1992; Webb et al. 2003). These few examples speak not only to the power of debris flows but also to the unpredictability of flash floods.

Initiation of Grand Canyon debris flows requires intense rainfall on steep slopes resulting in slope failure in either unconsolidated or consolidated sediment (see “Slope Movement Hazards”). Most of the debris flows

in Grand Canyon result from intense, often protracted, thunderstorms that occur primarily from July through September. However, varying climate conditions throughout the year may trigger debris flows. The 1996 Crystal Creek flood, for example, resulted from rain falling on a preexisting snowpack (Webb et al. 2003). Global climate change models predict a decrease in precipitation in the Southwest, but also a shift towards earlier spring rain-on-snow events, which may increase debris flow frequency in Grand Canyon (Knowles et al. 2006; Loehman 2009; see the “Climate Change and Water Supply” subsection).

Certain rock types are more commonly found in debris flows than others. Shales, such as those found in the Hermit Formation (**Ph**), form unstable slopes, prone to failure. On the other hand, the massive, cliff-forming sandstones and limestones in the park, such as the Redwall Limestone (**Mr**), are very stable, although small debris flow channels appear to develop and become entrenched within the top of the formation (Rosenberg 2013). Units with alternating layers of sandstone, limestone, and shale, such as the Supai Group (**Pe**, **Pep**, **PNMs**) tend to be unstable and susceptible to failure. Rainfall may erode shale units that underlie cliffs, thus undercutting stable units, compromising support, and leading to cliff collapse. The Hermit Formation, Bright Angel Shale (**Cba**), and many units in the Grand Canyon Supergroup, especially the Dox Formation (**Ydo**), contain significant amounts of clay that contribute to slope failure. Debris at the base of these slopes becomes entrained by subsequent flash floods.

Typically, non-swelling terrestrial clays containing illite and kaolinite tend to fail more readily than marine shales containing swelling clays, such as smectites (Webb et al. 2003). In non-swelling clays, rainwater percolates through cracks to failure surfaces, whereas in swelling clays, cracks close after becoming wet, preventing deep percolation of rainwater. The lacustrine shales in the Chinle Formation (**TRc**) are the only terrestrial shales not typically found in debris flows. The Chinle shales contain abundant volcanic ash, which alters the single-layer, non-swelling clays to smectite (Webb et al. 2003).

About 13% of the historic debris flows in Grand Canyon contain bedrock clasts transported from higher elevations due to slope failure (see “Slope Movement Hazards”). These bedrock failures have a greater potential energy to mobilize falling debris into slurries and are responsible for many of the larger flows (Webb et al. 2003). Most debris flows originate from failure of loose, unconsolidated sediment at the base of the Redwall Limestone cliffs (Webb et al. 2003). Runoff from thunderstorms erodes gullies into the loose

sediment until a slurry forms and the slope fails. Debris flows initiated in these unconsolidated sediments are generally small and travel only short distances. Massive slope failure may occur in unconsolidated sediment, however, because of the “firehose effect,” which involves water pouring over a cliff and cascading onto the exposed sediment.

The frequency and distribution of debris flows is not random in Grand Canyon. More debris flows occur in eastern than in western Grand Canyon. The average recurring interval in 60% of the individual tributaries is 10–50 years, although some tributaries did not have a debris flow in the 20th century (Webb et al. 1997, 2003). Debris flows also occur more often in drainages that trend south–southwest, such as Bright Angel Creek, which is significant because most of the summer storms originate from a southerly direction (Griffiths et al. 1996; Webb et al. 2003).

Grand Canyon National Park’s website (<https://www.nps.gov/grca/planyourvisit/weather-dangers.htm>) lists safety tips for visitors hiking in Grand Canyon, especially during the summer months from July to mid-September when the monsoon season sweeps across Arizona and severe thunderstorms can develop rapidly. Thunderstorms as far away as 40 km (25 mi) may generate devastating flash floods in the narrow slot canyons of the park.

Flash flood warning signs have been posted in stream beds, narrow canyons, and washes subject to flooding. Rock type, clay mineralogy, and side canyon orientation data gleaned from the enclosed GRI GIS data may further identify potential areas prone to flash flooding and debris flows. Repeat photography, which has been used to estimate debris flow occurrence throughout Grand Canyon, may be used to inventory and monitor high profile canyons subject to repeat flooding (Webb et al. 2003). These data, along with real-time weather forecasting, may help minimize visitor risks associated with debris flows and other types of slope movements (see “Slope Movement Hazards and Risk”).

Restoring and Monitoring Colorado River Sediment Load

Glen Canyon Dam dramatically altered the sediment budget and discharge rate of the Colorado River and proved President Theodore Roosevelt’s insight about man’s inability to improve the Grand Canyon correct. Seasonal flow of an unregulated Colorado River varied considerably with higher flows and floods occurring during late spring and early summer, especially during El Niño years (Price 1999; Burke et al. 2003). Average annual flood discharges through Grand Canyon were 2,190 m³/s (77,500 ft³/s), but larger floods were

common, like the one in 1884 that discharged at a rate of 8,500 m³/s (300,000 ft³/s) (Kieffer 2003).

Lake Powell reached maximum capacity in 1980. Excluding the inordinate discharges due to severe flooding in 1983 when the floodgates of Glen Canyon Dam were opened for the first time since 1963, the regulated discharge from 1980 to 2016 recorded at the Phantom Ranch gage station ranged from 310 m³/s (10,900 ft³/s) to 558 m³/s (19,700 ft³/s) (USGS 2016a).

Prior to the dam, sediment load in the river past Phantom Ranch exceeded 270 metric tons (300 US tons) per day. This sediment replenished sandbars in Glen, Marble, and Grand canyons. Since the completion of Glen Canyon Dam, sediment load averages about one-sixth that amount, or 45 metric tons (50 US tons) per day. Most of the sediment now comes from two large tributaries, the Paria River and the Little Colorado River, located 27 km (17 mi) and 130 km (79 mi) downstream from the dam, respectively (Kieffer 2003). The dam traps upstream suspended- and bed-load sediment that once flowed into Grand Canyon and releases clear, relatively sediment-free discharges (Topping et al. 2000). In 2000, sandbar area averaged 25% less than pre-dam years (Wright et al. 2005).

Flash floods and debris flows from side canyons deposit cobbles and boulders in the Colorado River. When the dam was built, the Colorado River lost the capacity to transport these particles downstream. Debris fan deposits narrowed sections of the canyon while the sediment-starved main channel eroded sand from sandbars and transported finer-grained sediment out of the system (Webb et al. 2000, 2003).

Decreased sediment resulted in smaller camping beaches, which reduced the area available for riparian vegetation, and led to degradation of archeology sites along the river. Before the dam, wind-transported sand covered and potentially preserved some of the culturally significant archeological sites in Grand Canyon (Draut and Rubin 2006, 2008; Draut et al. 2009, 2010). The windblown sand also slowed gully erosion, which has the effect of both exposing and destroying archeological sites (Hereford et al. 1993; Petersen et al. 2002; Schott et al. 2014).

The dam also regulated Colorado River water temperature. Prior to the dam, water temperature fluctuated from 29° C (84° F) in summer to freezing in winter, fluctuations that agreed with the endangered humpback chub. Post-dam river temperatures average 8°–10° C (46°–50° F) year-round, which allows introduced cold water trout to thrive, but stresses the native fish (Cook 2013).

The post-dam influence of Glen Canyon Dam on the Colorado River began to change in 1992. The 1992 Grand Canyon Protection Act mandated that Glen Canyon Dam be operated in a manner that protects, mitigates adverse impacts to, and improves the values for which Grand Canyon National Park and Glen Canyon National Recreation were established. The Act allowed for controlled flooding (the High Flow Experiments) of the Grand Canyon as part of the Glen Canyon Dam management strategy (US Geological Survey 1996).

High Flow Experiments (HFEs) were conducted in 1996, 2004, 2008, 2012, 2014, and 2016 to restore some of the pre-dam conditions, especially with regards to available sand for beach development, riparian habitat, dune field restoration, and debris fan morphology (Collier et al. 1997; Draut and Rubin 2006; Grams 2013; NPS 2014; Mueller et al. 2018). Findings from all HFE releases are available on the USGS's Grand Canyon Monitoring and Research Center (GCMRC) website <http://www.gcmrc.gov/>. The GCMRC website provides data on the HFEs, photos taken during the releases, and relevant articles documenting the results of each release.

Overall, the HFEs have demonstrated that controlled floods are effective in increasing sandbar volumes, and although the sand is eroded through time on vegetated sandbars, the HFEs will likely continue to contribute needed sand to a majority of the river corridor (Mueller

et al. 2018). For example, the initial March 1996 HFE, which lasted one week at a maximum discharge of 1,270 m³/s (44,800 ft³/s), included a 3–34% volume decrease in debris fan area, transportation of cobbles and boulders to the distal margins of the fans, an increase of 4–30 m (13–98 ft) in the width of the reworked zone, and a slight decrease in river constrictions (fig. 68; Webb et al. 1999a; Webb and Griffiths 2014). The flood created 84 new campsites, destroyed three, and increased the size of 50 established campsites (Kearsley et al. 1999). However, erosion removed most of the new sand from the established campsites within months.

The November 2004, 60-hour HFE, which discharged at 1,200 m³/s (41,000 ft³/s) (enough water to fill the Empire State Building in 20 minutes), demonstrated the importance of “sand triggering,” that is, timing the controlled flood when large amounts of sand have accumulated downstream because of flooding on the Paria tributary (Draut and Rubin 2006; Cook 2013). The 2008 HFE recognized that sandbars quickly erode unless the dam discharge is <255 m³/s, which is much less than the 910 m³/s (32,000 ft³/s) needed to generate electricity (fig. 69; Hazel et al. 2010; Cook 2013; Glen Canyon Dam Adaptive Management Program 2013). The 2008 HFE also illustrated that grain size of the sand supply must be considered (Topping et al. 2010). Larger grain size results in lower rates of sandbar deposition, and although finer sand accumulates more rapidly on sandbars, it is also more quickly eroded.



Figure 69. Photograph of a sandbar on the Colorado River deposited by the 2008 controlled flood. The river flows left to right. Discharge was held at 1,180 m³/s (41,500 ft³/s) for 60 hours. The HFE increased sandbar area all the way to Lake Mead. This sandbar is located approximately 100 km (64 mi) downstream from Lees Ferry, Arizona. People for scale. USGS photograph by Matt Kaplinski, available at <https://www.usgs.gov/media/images/sandbar-colorado-river-grand-canyon>.

Since 2012, the sand triggering concept has been used in four HFEs that have been timed to follow large inputs of sand from a major tributary (Mueller et al. 2018; <http://www.gcmrc.gov/>). To support the timing and duration of the HFEs, the GCMRC monitors the amount of sand supplied by the Paria River and other tributaries (Grams 2013). Following a HFE, the GCMRC tracks the downstream movement of sand and documents changes to the Colorado River corridor, such as the growth and erosion of sandbars, backwater habitats, and upslope accumulations of eolian sand.

To monitor these changes, researchers have used a variety of techniques. Grams (2013), for example, compared a flux-based method and a topographic method. The flux-based method measured changes (flux) in total sand transport between stations spaced 50–100 km (30–60 mi) apart and provided a continuous record of changes in storage (deposition or erosion) between stations. It did not, however, provide information about individual deposits between stations. The topographic method measured changes to individual sand deposits by using a multibeam echosounder to map the underwater portion of the sandbar. While the flux-based method monitored short-term changes in sand storage, the topographic method, which proved to be time consuming and costly, monitored long-term trends. Mueller et al. (2018) grouped long-term monitoring sites established in 1990 according to geomorphic setting and then used a principal component analysis (PCA) to correlate differences in sandbar behavior. They found that

less-vegetated sandbars sites in narrow reaches were dynamic with sand storage changing primarily in eddies rather than the main channel. On the other hand, sandbars in wider reaches tended to be stabilized by vegetation and sand accumulated on the vegetated sandbar surfaces during floods.

Continued HFEs offer an excellent opportunity for GCMRC scientists and cooperators, which should include the park resource managers or GIP personnel, to measure such interrelated factors as sand supply, vegetation, and riparian habitat along the Colorado River. Measuring the sand budget may provide resource managers the needed data on the size, distribution, and behavior of individual sand-storage locations to allow for a cost-effective and spatially representative monitoring program (Grams 2013).

Slope Movement Hazards

Slope movements are natural elements of landscape change (see “Geomorphic Features and Unconsolidated Deposits”) that may adversely impact park resources, infrastructure, or visitor safety (fig. 70). While injuries have happened, very few visitors have been killed by naturally occurring falling rocks (Ghiglieri and Myers, 2001). Visitors falling off the canyon rim or along trails present a much more serious hazard. Nevertheless, cliffs that are undercut by erosion have the potential to collapse and to generate landslides, which might impact trails and visitor safety. Areas with visible cracks, loose material, or overhangs are especially hazardous (fig. 71).



Figure 70. Photograph of the rockslide that closed Tanner Trail in October 2004. Members of the Grand Canyon National Park trail crew for scale. Dashed yellow line represents the location of the trail prior to the slide. NPS photograph by Chris Brothers in Kelkar (2013a).



Figure 71. Photograph of potential rockfall hazards in the Box, North Kaibab Trail. Hikers walk under overhangs of fractured basement Vishnu Schist (Xv) as they enter the narrow canyon known as “the Box.” The Great Unconformity (black line) marks the contact between the Vishnu Schist and the overlying Tapeats Sandstone (Ct). A previous rockslide can be seen in the upper right. NPS photograph by Michael Quinn, available at https://www.flickr.com/photos/grand_canyon_nps/6924531077/in/album-72157626760891634/.

Documenting Slope Movements in the Park

In 2013, park staff and GIP and MIS interns began to qualitatively and quantitatively document slope movements in the park and created a geohazards database (fig. 72; Rosenberg 2013, Kelkar 2013a, 2013b). As of 2013, the database contained 83 mapped sites, 45 documented sites, and 47 potential sites (Rosenberg 2013).

The GRI GIS data includes talus and rockfall deposits (**Qtr**) and landslide (**Ql**) deposits large enough to appear on geologic maps. Note that, in order to not obscure details of the bedrock map, many talus and rockfall deposits were not included by the source mappers for the central and western portions of the park. Talus and/or rockfall deposits are noted in the source descriptions of other units, as well. Terrace gravel deposits (**Qtgr**) mixed with landslide debris may represent deltaic deposits that formed when the Surprise Valley landslide near Tapeats Creek temporarily dammed the Colorado River (Billingsley and Hampton 2000; GRI-GIS data). Landslide deposits intertongue with older

alluvial terrace deposits (**Qgo**), and in Little Colorado River Gorge and Cataract Canyon, young terrace gravel deposits (**Qgy**) mix with landslide deposits. Intermediate terrace gravels (**Qg2**) mix with landslide deposits throughout the map area. Landslide debris mixes with alluvial fan deposits (**Qay**, **Qa3**, **Qao**) below Vermillion Cliffs and Echo Cliffs and with Colorado River gravel and silt deposits (**Qr**).

Slope movements commonly occur in areas where a blocky, cliff-forming unit, such as a sandstone or limestone, overlies a softer, slope-forming unit, such as shale. The softer unit erodes more easily, creating undercut areas that may subsequently collapse. According to Kelkar (2013a, 2013b), particularly unstable lithologic contacts include those between the (1) Coconino Sandstone (**Pc**) and Hermit Formation (**Ph**) and (2) Redwall (**Mr**) or Muav Limestone (**Cm**) and the Bright Angel Shale (**Cba**). Areas where trails, the TCP, or other infrastructure cross those contacts are at increased risk of damage from slope movements.

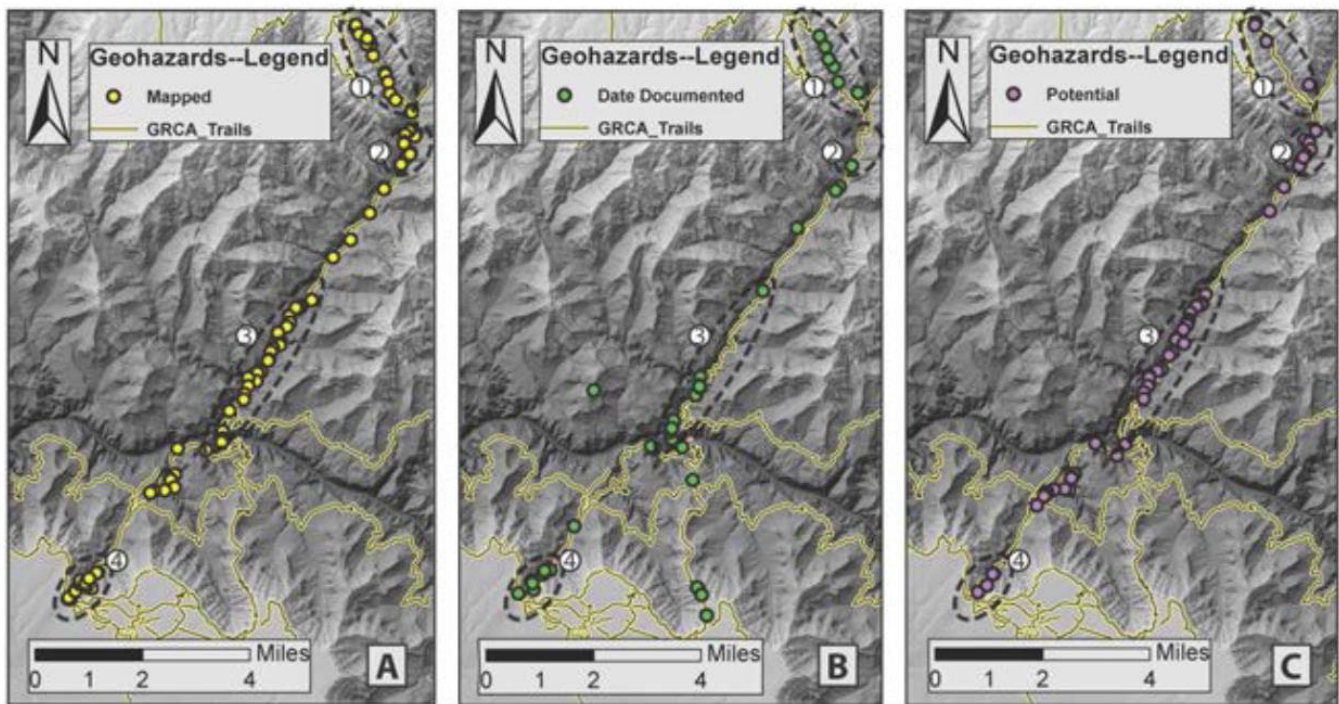


Figure 72. Rockfall data collected along the North Kaibab Trail within Grand Canyon National Park. The data reside in the Grand Canyon National Park 2013 Geohazards Database. (A) Localities mapped using the Grand Canyon National Park field form to collect pertinent geologic data. (B) Prior documented rockfall hazards that have dates associated with their localities. (C) Localities identified as potential hazards using the Grand Canyon National Park field form. Dashed lines indicate areas, numbered 1–4, of high event density. Recurrence intervals for rockfalls vary. For example, hazards within the Tapeats Sandstone (**Ct**), zone 2, may represent a much longer time scale than rockfalls documented within zone 3, the area known as the Box. The highest density of mapped, documented, and potential rockfall hazards occurs in zone 3. From Rosenberg (2013, figure 2).

According to Rosenberg (2013), ~61% of mapped mass movement deposits are rockfalls occurring predominantly within the Kaibab Formation (**Pk**), Coconino Sandstone (**Pc**), Tapeats Sandstone (**Ct**), and “Vishnu type” basement rocks (**X** units). Slides commonly occur in softer lithologic units, such as the Hermit Formation (**Ph**), Bright Angel Shale (**Cba**), Dox Formation (**Yd** units), and Hakatai Shale (**Yh**). Rockfalls and slides also occur within the varied rock types mapped in the Supai Group (**Pe**, **Pep**, **PNMs**, **MPNu**).

Rosenberg’s study focused on the corridor trail system, which includes the Bright Angel Trail, North Kaibab Trail, South Kaibab Trail, and follows the route of the TCP (Rosenberg 2013). Most park visitors use these trails. One preliminary result of the study suggested that the highest density of potential, mapped, and documented mass movements were within Vishnu Schist (**Xv**) along the North Kaibab Trail near Phantom Ranch, in an area known as “the Box” (fig. 71; Rosenberg 2013). This roughly 6 km (4 mi) stretch of trail contained approximately 33% of all mapped slope movement deposits (fig. 72). Rockfall, probably associated with the closely spaced joints within the Vishnu Schist, was the dominant type of slope movement.

The data collected by Rosenberg confirmed the qualitative assessment of the rockfall potential in the Box by many backcountry rangers (Rosenberg 2013). Rosenberg’s study incorporates the views of backcountry staff that small rockfall events occur often and that these small events cause many of the injuries and incidents involving rockfall, especially in the Box (fig. 73).

Precipitation from thunderstorms may increase slope movement hazards. In 2012, a passing thunderstorm caused a rockfall in the Box about 14 km (9 mi) below the North Rim. A hiker was injured, and part of the River Trail was damaged. Kelkar (2013a, 2013b) also noted potential correlation between precipitation events and slope movements (fig. 74). These relationships require further research.

Human-caused rockfalls also occur in the park. In 2011, hikers on a switchback dislodged loose rocks, injuring two hikers on the trail below them.

Mitigating Hazards and Reducing Risk

With regards to visitor safety, alerting visitors to the hazards associated with rockfall near the base of cliffs is a first step toward reducing risk. The park website, brochures, signage, and/or verbal communication from park staff could present such information.

If funding permits, resource managers could consider obtaining quantitative information to assess the frequency and magnitude of rockfall (and other slope movements) in high visitation areas. The Unstable Slope Management Program is one venue to provide quantitative information (see https://westerntransportationinstitute.org/research_projects/development-of-unstable-slope-management-program-for-federal-land-management-agencies-phase-2/ or contact NPS Geologic Resources Division). Developing a photomonitoring program is another possibility. The Geoscientist-in-the-Parks program is an option to support such projects. The NPS Geologic Resources Division Photogrammetry website (http://go.nps.gov/grd_photogrammetry) provides examples of how photographic techniques support structural analysis of rockfall areas.

A geologic hazard evaluation was recently completed for Glen Canyon National Recreation Area by the Utah Geological Survey (Knudsen et al. 2016, also see GRI report by Graham 2016). A similar effort along selected trail corridors, Trans-Canyon Pipeline construction sites, or other areas of interest would provide more detailed assessment and recommendations for park managers.



Figure 73. Photograph of a small rockfall that caused a serious injury in 2012. The rockfall occurred along the North Kaibab Trail. NPS photograph by Bil Vandergraf in Rosenberg (2013, figure 3).

Documented Events by Season



Figure 74. Chart illustrating the potential seasonal influence on mass movement events in the park. The monsoon season occurs from mid July to early September. The chart suggests that seasonal precipitation may be associated with mass movements in the canyon. Graphic from Kelkar (2013b).

Additional Sources of Information

The following references provide additional background information, suggested vital signs, and resources for assessing and documenting slope movements:

- In the *Geological Monitoring* chapter about slope movements, Wieczorek and Snyder (2009) described five vital signs for understanding and monitoring slope movements: (1) types of landslide, (2) landslide causes and triggers, (3) geologic materials in landslides, (4) measurement of landslide movement, and (5) assessment of landslide hazards and risks.
- US Geologic Survey publication *The landslide handbook—A guide to understanding landslides* (Highland and Bobrowsky 2008)
- US Geological Survey landslides website (<http://landslides.usgs.gov/>)
- NPS Geologic Resources Division Geohazards website (<https://www.nps.gov/subjects/geohazards/index.htm>)

Cave and Karst Inventory, Monitoring, and Protection

Cave Resources

Considered to be fundamental resources in Grand Canyon National Park, cave resources are nonrenewable (NPS 2010). The Federal Cave Resources Protection Act of 1988 requires the identification of

“significant caves” in NPS areas, the regulation or restriction of use as needed to protect cave resources, and inclusion of significant caves in land management planning. The act also imposes penalties for harming a cave or cave resources and exempts park managers from releasing specific location information for significant caves in response to a FOIA request (see Appendix B).

Inventoring the caves in Grand Canyon National Park and developing a monitoring program presents a monumental task. The cave paleontological inventory conducted in Redwall Limestone and Muav Limestone caves and hydrogeologic studies of the more accessible caves, especially those accessible from the Colorado River, included many documented caves (table 13) (Huntoon 2000; Crossey et al. 2006; Hill and Polyak 2010). While Redwall Limestone caves often occur around trail and river access routes, many caves in the Redwall and other formations are extremely difficult to access in the canyon. Even the caves in the paleontological study were not easy to access, and some required rappelling 100–200 m (330–670 ft) down vertical cliffs (Kenworthy et al. 2004). Challenging access is a limiting factor to a cave monitoring program, but it also enhances cave preservation.

Addressing human impacts to the caves, preserving archeological artifacts and fossils found in the caves, and understanding cave hydrology are priorities for park management (NPS 2015a). Except for Cave of the Domes on Horseshoe Mesa, the caves in Grand Canyon National Park are closed to visitors without permits. However, vandalism remains one of the major problems facing cave management staff. Unauthorized entry to Rampart Cave in 1976 led to a fire that destroyed much of the sloth dung and organic layers in the cave (Santucci et al. 2001). A bat gate, emplaced to protect the endangered Townsend’s big-eared bat, currently bars entrance to Stanton’s cave (table 13; National Parks Blog 2011).

Knowing the quality of the Bigfork High School (BHS) Cave Club’s GIS-based monitoring work in Glacier National Park, Steve Rice, Grand Canyon National Park’s Hydrologist and Cave Resource Management Specialist, invited the club to Grand Canyon National Park in 2011 and 2012 to monitor several backcountry caves in the park (Bodenhamer 2012). The monitoring program included documenting and photographing cave features, analyzing visitor impacts, measuring cave temperature and humidity, and relocating and repeating historic photo views, as well as establishing new photo points (fig. 75). All the monitoring data was transcribed into a GIS database.



Figure 75. Photograph of delicate speleothems. A Bigfork High School Cave Club member documents delicate speleothems in a Grand Canyon National Park cave. NPS photograph available at <https://home.nps.gov/grca/learn/news/bigfork-high-school-cave-club-completes-inventory-and-impact-mapping-of-caves-in-grand-canyon-national-park.htm>.

In 2016, GIP Robyn Henderek significantly contributed to the park's paleontological inventory by collecting spatial and abundance data of artiodactyl (hooved mammals) and other fossils in the park's remote cave systems (fig. 76). By analyzing the association between archeological Split Twig Figurines from the middle to late Archaic culture and fossils of the extinct Harrington's mountain goat, Henderek also was able to correlate the exact ages of the figurines to a climate model from the Late Holocene. In addition, she created 3D models of these paleontological and archaeological resources.

Photogrammetry, used primarily to generate 3D maps of surface geologic resources, is being used in the park to document and monitor cave paleontological and archeological sites (Henderek et al. 2015). The technique is especially adapted for national park in-cave use where artifacts and significant remains of extinct fauna are preferred to be left in-situ.



Figure 76. Photograph of fossils in a cave. GIP Robyn Henderek examining the jawbone of an extinct Pleistocene mountain goat in Grand Canyon National Park. NPS photograph available at <https://www.nps.gov/media/photo/gallery.htm?id=6EF7D56B-1CD1-4697-9811-A3458BA39FE0>.

Karst Landscape: Sinkholes, Remote Springs, and Groundwater Recharge

ArcGIS, LiDAR analysis, hydrograph analysis, and dye trace studies have been used to characterize the morphology, distribution, and function of sinkholes on the Kaibab Plateau so that the role sinkholes play in recharging groundwater could be better understood (see the “Geologic Features and Processes” Section). Further characterization of the geologic structural framework and its relationship with the Redwall-Muav aquifer is needed to characterize the connection between surface fractures, cave passage orientation, and groundwater flow paths.

Monitoring all the remote springs in Grand Canyon National Park and defining the character of groundwater flow and recharge of the karst aquifer that discharges through Roaring Springs are daunting tasks in terms of access, time, and required resources. The easiest wilderness spring to access, for example, requires hiking 7 km (4 mi) from the nearest road and then 1,000 m (3,300 ft) down to the base of a canyon (Tobin et al. 2015).

Threats to the water quality and quantity at Roaring Springs include impacts from climate change (see Climate Change and Water Supply), increased development, and potential contamination from land use practices (Hoffman et al. 2015). Water samples continue to be collected at Roaring Springs, Bright Angel Creek, Emmett Springs, Angel Springs, and Phantom Creek (Brown et al. 2008). Monsoon and winter precipitation samples also have been collected from North Rim monitoring locations. Geochemical data from these samples may provide enough information to develop a groundwater flow model of the hydrogeological system connecting the Kaibab Plateau to North Rim springs (Brown et al. 2008; Brown 2010). These data may also help to determine how much water is available for people, wildlife, riparian habitats, and fire protection.

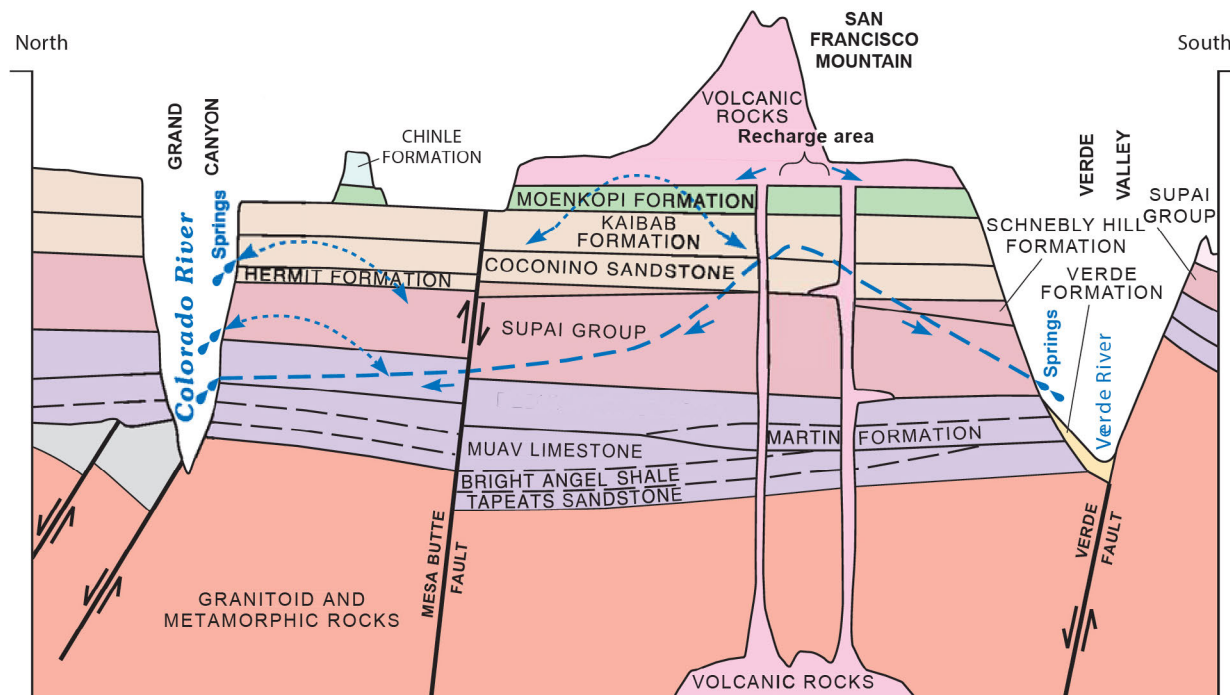
In 2015, Tobin et al. evaluated two methods that might be used to characterize and monitor the springs in the park: (1) a geomorphic method and (2) a hydrochemical method. The geomorphic method groups springs according to their morphological features, focusing on similar aquatic habitats. The hydrochemical method groups springs according to their major ion data, water quality, and discharge. Preliminary research suggests that each method may be used to provide long-term monitoring utilizing a reduced number of sites, but each method requires a monitoring program with specific characterization goals because the groupings within each method are distinctly different (Tobin et al. 2015).

Also in 2015, Gandee et al. focused on the vulnerability of groundwater responsible for recharging the Redwall-Muav aquifer (Gandee et al. 2015). Researchers used the COP and EPIK methods to assess and map the variability of groundwater vulnerability on the Kaibab Plateau. The COP method used the concentration of flow (C), overlying lithological layers (O), and precipitation regime (P) to quantify groundwater vulnerability. Factors involved with the EPIK method included epikarst (E), protective cover (P), infiltration conditions (I), and karst development (K). This first of a kind study for the park used GIS to create a groundwater vulnerability map. Results from both methods suggested that vulnerability in the Kaibab catchment basin is low to moderate (Gandee et al. 2015).

The springs and seeps in the park provide water for wildlife and visitors, are locations of exceptional natural beauty, and may hold cultural significance for American Indians. Because they are critical to aquifer systems and riparian habitats, Grand Canyon National Park has partnered with the US Geological Survey and Grand Canyon Wildlands Council to conduct research on the influence of increased development, groundwater withdrawal, and climate change on these water resources (NPS 2015a).

In 2002, because of concerns of a growing population and the impact on water resources south of Grand Canyon, the NPS partnered with the USGS, the Arizona Department of Water Resources, Coconino County, the city of Flagstaff, the city of Williams, the Navajo Nation, the Hopi Tribe, the Havasupai Tribe, and the Grand Canyon Trust to develop a hydrogeologic framework, hydrogeologic conceptual model, and water budget to provide a better understanding of the occurrence and movement of ground water on the Coconino Plateau (Bills et al. 2016).

Although hydrogeologic data exists for the larger metropolitan areas on the Coconino Plateau, such as Flagstaff and Sedona, hydrogeologic data regarding water resources and groundwater sustainability remains sparse for most of the plateau. (Bills and Flynn 2002; Flynn and Bills 2002; Bills et al. 2016). On the Coconino Plateau, the C aquifer is primarily in the eastern and southern parts of the plateau and consists of hydraulically connected water-bearing zones in the Kaibab Formation, Coconino Sandstone, Schnebly Hill Formation, and sandstone layers of the Upper and Middle Supai Formations in the Flagstaff area (fig. 77; Bills et al. 2000). The R aquifer occurs throughout the Coconino Plateau (fig. 77). In the northeast and eastern sections of the Coconino Plateau, the C and R aquifers are connected by faults and fractures (Flynn et al. 2007).



Bills and Flynn, 2002

EXPLANATION

- SURFICIAL DEPOSITS; VERDE FORMATION
- YOUNGER BASALTIC ROCKS
- VOLCANIC ROCKS
- CHINLE FORMATION
- MOENKOPI FORMATION
- SEDIMENTARY ROCKS—Kaibab Formation, Toroweap Formation, and Coconino Sandstone on the Colorado Plateau
- SEDIMENTARY ROCKS—Schnebly Hill Formation, Hermit Formation, Supai Group, and Naco Group
- SEDIMENTARY ROCKS—Redwall Limestone, Muav Limestone, Temple Butte (Martin) Formation, and Tonto Group
- PRECAMBRIAN SEDIMENTARY ROCKS
- GRANITOID AND METAMORPHIC ROCKS
- REGIONAL WATER TABLE
- PERCHED WATER-BEARING ZONE
- DIRECTION OF GROUND-WATER FLOW
- FAULT—Arrows indicate direction of movement

Figure 77. Generalized hydrogeologic cross-section of the Coconino Plateau. The C aquifer occurs in the eastern and southern parts of the plateau while the R aquifer occurs throughout the region. Arrows indicate the direction of groundwater flow. Diagram from Bills and Flynn (2002, figure 3) available at <https://pubs.usgs.gov/of/2002/0265/>.

Although Havasu Springs was included as a sample site in the Coconino Plateau study by Bills et al. (2016), most of the data was collected from groundwater wells drilled beyond the boundaries of the park (Bills and Flynn 2002; Flynn and Bills 2002; Bills et al. 2016). These data are presented in Bills et al. (2016). To fully understand the dynamics of flow paths throughout the karst systems within Grand Canyon National Park will require significant additional work at springs and sinkholes that are not easily accessible. Research that includes these less accessible sites, such as the study by Jones et al. (2017a), will enable resource managers to better quantify potential impacts from climatic variability and human disturbances on a spring-scale and a regional scale, as well as provide options to mitigate these concerns. As Tobin et al. (2018) point out, “An improved understanding of springs of Grand Canyon will help the National Park Service better manage these precious desert ecosystems into the second century of the park” (Tobin et al. 2018, p. 13).

Cave and Karst Management

In 2011, recommendations for a cave and karst management plan that would help develop a formal cave and karst program included (Pate 2011):

- a plan to develop a cave and karst database of information;
- an estimate of needed expertise;
- a plan for recreational caving;
- a long-term plan to conserve and protect park caves and karst areas;
- a cave exploration plan;
- a cave and karst education plan for park staff and visitors;
- a plan to house and track scientific studies and research on park caves and karst areas;
- a plan for volunteers to systematically explore and document park caves and karst systems;
- a cave safety plan and guidance, including standard and approved routes;
- a park Search and Rescue team coordination plan;
- a plan for a permit system to control entry into all caves;
- a law enforcement plan to address resource theft, illegal entry, and other protection issues;
- a guide to the laws, regulations, policies, guidelines, Director’s Orders and other related legal mandates for caves and karst areas; and

- a plan to compile standard documents for a C&K Program, such as survey and inventory standards, data collection and storage standards, cave permits, trip report forms, nondisclosure form, a cave classification system, and cave discovery forms.

In their evaluation of cave and karst programs, Land et al. (2013) singled out Grand Canyon National Park as one of the parks that needs to delineate groundwater drainage basins because potential contaminants drain from inside the park. They also recognized the park as having water quantity issues but no monitoring program to monitor groundwater and recharge volume or to gather information on water use and aquifer response (Land et al. 2013).

According to Land et al. (2013), the park believes that the carrying capacity of its caves is being exceeded although the carrying capacity still needs to be determined. Grand Canyon National Park offers recreational caving but has neither a general nor a cave-specific safety and rescue plan (Land et al. 2013). The following considerations were recommended in 2011 about developing a recreational cave plan (Pate 2011):

- The ease or difficulty of access to and passage through the caves provide a wide range of experiences.
- A permit system would greatly help to regulate and track a recreational cave program.
- The significance of and access to the various cave resources should be a primary factor when permitting caves.
- Selected spelunker caves should have their initial conditions documented and they should be monitored over time to register any negative impacts.
- The park should develop a list of the educational values that participants in this program will receive.
- The park should determine if Cave of the Domes should continue to be available as a recreational cave without a permit.
- Because of the tremendous threat posed by White-Nose Syndrome, caves with significant bat use should not be opened for recreational caving.

Recommendations in 2011 also included adding a minimum of two full-time employees dedicated to the Cave and Karst Program. These employees would work closely with various staff from other agencies and groups in a variety of disciplines (e.g., archeology, biology, hydrology, paleontology, and others) to coordinate and advance program objectives (Pate 2011). According to the Grand Canyon cave website (<https://www.nps.gov/grca/learn/nature/cave.htm>) a

cave monitoring program has been established in the park (NPS 2017). Contact the park for more specific information.

In the *Geological Monitoring* chapter about caves and associated landscapes, Toomey (2009) described methods for inventorying and monitoring cave-related vital signs, many of which may be difficult to apply at Grand Canyon National Park because of cave accessibility. These vital signs include: (1) cave meteorology, such as microclimate and air composition; (2) airborne sedimentation, including dust and lint; (3) direct visitor impacts, such as breakage of cave formations, trail use in caves, graffiti, and artificial cave lighting; (4) permanent or seasonal ice; (5) cave drip and pool water, including drip locations, rate, volume, and water chemistry, pool microbiology, and temperature; (6) cave microbiology; (7) stability issues associated with breakdown, rockfall, and partings; (8) mineral growth of speleothems, such as stalagmites and stalactites; (9) surface expressions and processes that link the surface and the cave environment, including springs, sinkholes, and cracks; (10) regional groundwater levels and quantity; and (11) fluvial processes, including underground streams and rivers.

Trans-Canyon Pipeline Replacement

Water from Roaring Springs is delivered through the Trans-Canyon Pipeline (TCP) that was installed between 1965 and 1970 and has now surpassed its expected length of service by more than 20 years (NPS 2016c). The TCP traverses 21 km (13 mi) of canyon floor and then 1.6 km (1.0 mi) of sheer cliff on the South Rim and 11 km (7 mi) to the North Rim. The pipeline regularly ruptures, in some cases because of debris flows, flash floods, slope movements, or other geologic processes (fig. 78). These ruptures require repair from a few to a few dozen times per year. A long-term solution to replace the pipeline is needed, but the estimated replacement cost (~\$100–150 million) far exceeds the park’s total yearly budget of approximately \$21 million (less than \$2 million is budgeted for construction, repair, and rehabilitation) (NPS 2016c).

The massive scale of the replacement project creates many potential impacts to geologic features or processes, including disturbance of paleontological resources and cultural resources, creating unstable slopes or triggering slope movements. In addition, slope movements, debris flows, flash floods, and earthquakes will continue to threaten the integrity of the current and replacement pipeline. Those features, processes, and issues are discussed in their respective sections of this report.

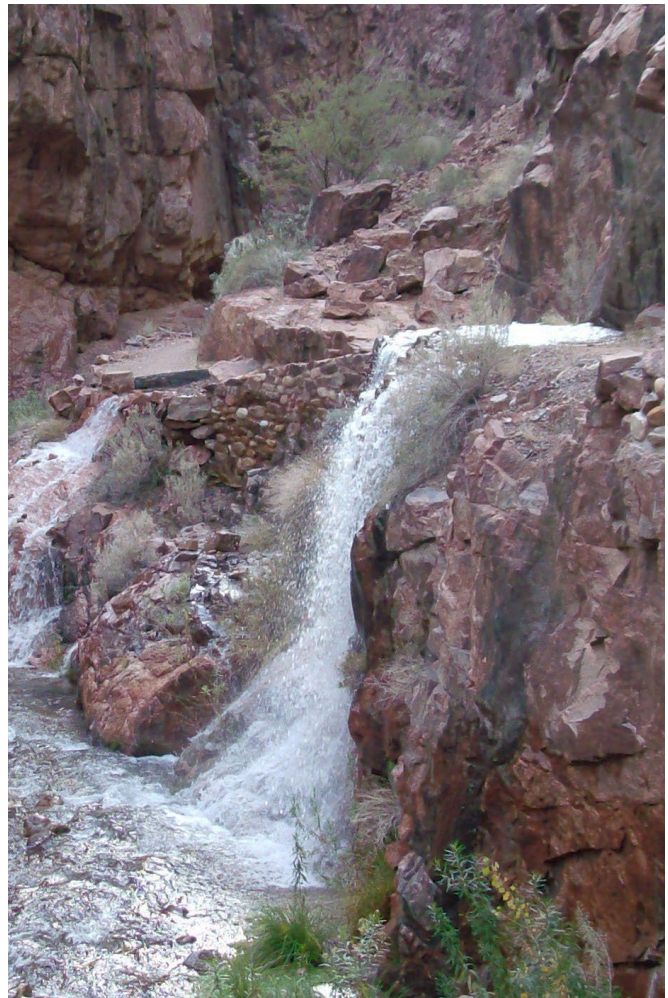


Figure 78. Photograph of water gushing from a break in the Trans-Canyon Pipeline. The Trans-Canyon Pipeline (TCP) transports water from Roaring Springs, located about 1,100 m (3,500 ft) below the North Rim, to the South and North rims. In this photograph, the TCP is buried beneath the North Kaibab Trail and water is flowing into Bright Angel Creek. Exposed sections of the pipeline are also susceptible to breaks. NPS photograph available at <https://flic.kr/p/iRvgVn>.

Paleontological Resource Inventory, Monitoring, and Protection

All paleontological resources are nonrenewable and subject to science-informed inventory, monitoring, protection, and interpretation as outlined by the 2009 Paleontological Resources Preservation Act (see Appendix B). Participants at a 2001 workshop at Grand Canyon National Park expressed interest in a paleontological resource inventory for the park that would document in situ fossil occurrences (NPS 2001). Park staff have approved a GRD-coordinated Grand

Canyon National Park Centennial Paleontological Survey for 2019, and a multi-disciplinary team was recruited for this inventory with a PaleoBlitz taking place at the park in September 2019. See Santucci and Tweet (2020) for the resulting inventory report; completed while this document was in final formatting.

The Southern Colorado Plateau Network's (SCPN) paleontological inventory and monitoring report cites significant references that document the fossil record in Grand Canyon (Tweet et al. 2009). The report also summarizes the fossils existing in the park collections and those housed in various museum repositories.

The SCPN report included the following recommendations for an inventory and monitoring program at Grand Canyon National Park (Tweet et al. 2009):

- Document and assess the condition of significant fossil localities, but leave fossils and associated surrounding rock in place unless they may be potentially degraded by artificially accelerated natural processes or direct human impacts,
- Monitor significant sites at least once a year, and monitor areas with high visitor use regularly,
- Encourage park staff to observe exposed sedimentary rock and associated eroded deposits while conducting their usual duties,
- Photodocument and monitor in situ fossil occurrences,
- Relocate and map (using GPS) historic sites, such as those found in Gilmore (1926, 1927, 1928), McKee (1938), and White (1929a, 1929b),
- Continue staff training in natural resource protection and paleontological resource monitoring to cope with fossil theft and vandalism,
- Document fossils found in a cultural context with the input of an archeologist,
- Participate with archeologists in excavations or infrastructure developments to document and protect fossil resources,
- Contact the NPS Geologic Resources Division for paleontological resource management assistance.

In Grand Canyon National Park, fossil loss due to erosion and theft present significant resource management issues (fig. 79). Where the TCP crosses fossiliferous rock units, any disturbances related to construction or repair work should avoid damage to paleontological resources.

In the *Geological Monitoring* chapter about paleontological resources, Santucci et al. (2009) described five methods and vital signs for monitoring in situ paleontological resources: (1) erosion (geologic

factors), (2) erosion (climatic factors), (3) catastrophic geohazards, (4) hydrology/bathymetry, and (5) human access/public use. Resource managers may find the monitoring methods and vital signs helpful in developing an inventory and monitoring program.

Earthquakes

Earthquakes are ground vibrations—shaking—that occur when rocks suddenly move along a fault, releasing accumulated energy (Braile 2009). Earthquake intensity ranges from imperceptible by humans to destruction of developed areas and alteration of the landscape. Earthquakes can directly damage park infrastructure or trigger other hazards such as slope movements that may impact park resources, infrastructure, or visitor safety. Real-time and historical data for earthquakes and seismic hazards are available on the USGS Earthquake Hazards Program, <https://earthquake.usgs.gov/hazards/hazmaps/>.

Until 1979, earthquakes were measured using the Richter magnitude scale which is based on a logarithmic scale from 1 to 10. Seismologists now measure earthquake magnitude using the moment magnitude (energy released) scale, which is more precise than the Richter scale but retains the same continuum of magnitude values. The Modified Mercalli Intensity Scale is a measure of the effect of an earthquake on Earth's surface. It consists of a series of key responses such as sleeping people awakening, furniture moving, chimneys damaged, and finally, severe destruction.

The Grand Canyon region is seismically active. Most earthquakes are small magnitude and do not produce damage to surface features. From March 28, 2016, to May 10, 2016, a swarm of 57 small magnitude (1.0–3.8) earthquakes was recorded in northwestern Arizona by the Nevada Seismological Laboratory (NSL) (Allison 2016). The initial magnitude 2.1 event was centered in the Grand Wash cliffs area within Grand Canyon–Parashant National Monument, approximately 33 km (20 mi) north of the western border of Grand Canyon National Park.

These small magnitude earthquakes may be more common than previously thought. The Arizona Geological Survey's broadband seismic network includes only eight seismometers, which do not record small magnitude earthquakes in northwestern Arizona (Conway 2016). Between 1973 and March 2012, the USGS recorded only two, relatively small seismic events in northwestern Arizona (USGS 2016b). However, combining the earthquake detection stations of both the NSL and the Arizona Geological Survey has extended coverage into northwestern Arizona, which allowed recognition of the earthquake swarm.

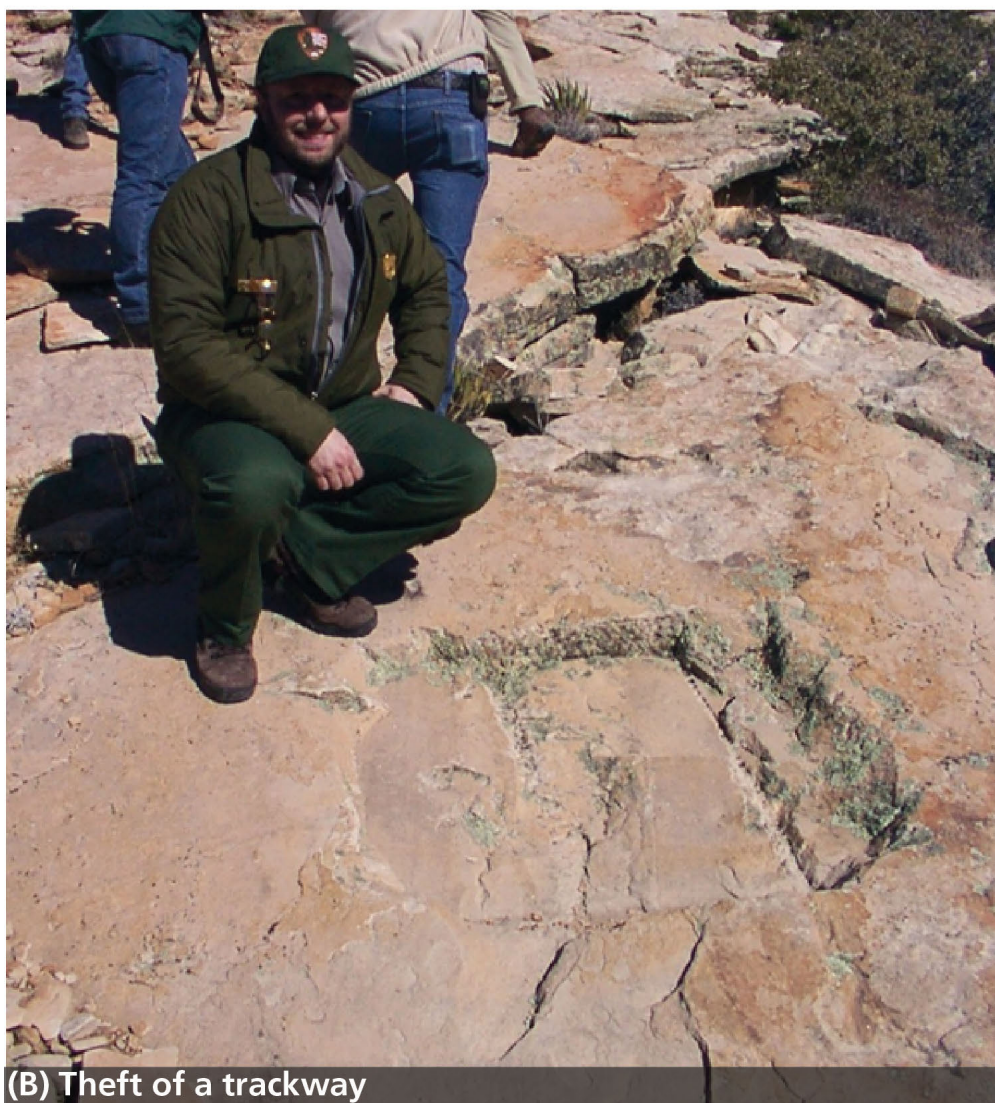


Figure 79. Photographs of vandalism of paleontological resources in Grand Canyon National Park. (A) The attempt to remove a fossil brachiopod by using a nail. (B) Evidence of a stolen trackway in the Coconino Sandstone. NPS paleontologist Vincent Santucci for scale. Photographs courtesy of Vince Santucci.

The earthquakes occur on west-dipping normal faults associated with the boundary between the Colorado Plateau and the Basin and Range province. This is a region of active crustal extension, as well as the southern end of the Intermountain Seismic Belt (ISB). The ISB marks the eastern boundary of the Great Basin region and extends from Montana through Utah, terminating in northwestern Arizona (Allison 2016).

Although rare, large earthquakes have occurred in Arizona. Approximately 3,000 years ago, a displacement of 2.2 m (7 ft) along the Toroweap fault caused an estimated magnitude 7 earthquake (Jackson 1990; Fenton et al. 2001a). In September 1993, a magnitude 5.6 earthquake occurred southeast of St. George, Utah. Between 1900 and 1993, at least 44 earthquakes, five of which were magnitude 5.0 or greater, shook the Grand Canyon region (Brumbaugh 2003). The probability of a moderate earthquake (magnitude 5.0 or greater) occurring the next 50 years is between 0.15 and 0.40 (15% and 40% “chance”).

Ancient Earthquakes

The Precambrian faults mentioned in the “Geologic Features and Processes” section and which are part of the GRI GIS data have been reactivated throughout Phanerozoic time, but the most recent reactivation is due to crustal extension that began in the Miocene Epoch and opened the Basin and Range province (Marshak et al. 2000; Timmons et al. 2003; Huntoon 2003). The most active faults in northwestern Arizona over the last 5 million years have been the north-trending Hurricane and Toroweap faults (Jackson 1990; Fenton et al. 2001a). Offset across the Hurricane fault in the Grand Canyon ranges from more than 800 m (2,600 ft) at Three Springs Canyon to 400 m (1,300 ft) at the Colorado River (Fenton et al. 2001a; Huntoon 2003). Total vertical displacement along the length of the Toroweap fault is 150–265 m (492–869 ft) with 180 m (590 ft) of displacement in the Grand Canyon region (Fenton et al. 2001a).

Estimates of Quaternary displacement rates along the Hurricane Fault range from 70 m (230 ft) per million years to 170 m (558 ft) per million years (Fenton et al. 2001a). Along the Toroweap fault, displacement rates vary 70 m (230 ft) to 180 m (590 ft) per million years (Fenton et al. 2001a; Pederson et al. 2002a). The Toroweap and Hurricane Faults have moved within the last 30,000 to 400,000 years. However, the Toroweap Fault has not ruptured 3,000-year-old Quaternary alluvial fans, and the Hurricane Fault has not displaced 8,000-year-old Quaternary alluvial fans, suggesting movement on the faults has not occurred within the last few thousands of years (Fenton et al. 2001a).

Earthquakes resulting from a reactivation of northwest-trending faults, such as the Grandview–Phantom fault, suggest that crustal extension occurs in a northeast–southwest direction, perpendicular to the Grandview–Phantom trend. If this is the case, crustal extension is predicted to cause the tectonic boundary of the Colorado Plateau to migrate towards the interior of the plateau, leaving the Grand Canyon region seismically quiet (Brumbaugh 2003).

Additional Resources

In the *Geological Monitoring* chapter about earthquakes and seismic activity, Braile (2009) described the following methods and vital signs for understanding earthquakes and monitoring seismic activity: (1) monitoring earthquakes, (2) analysis and statistics of earthquake activity, (3) analysis of historical and prehistoric earthquake activity, (4) earthquake risk estimation, (5) geodetic monitoring and ground deformation, and (6) geomorphic and geologic indications of active tectonics. Braile (2009), the NPS Geologic Resources Division Seismic Monitoring website (<https://www.nps.gov/subjects/geology/geological-monitoring.htm>), the USGS Earthquakes Hazards website (<http://earthquake.usgs.gov/>), the Arizona Geological Survey’s Center for Natural Hazards (<https://azgs.arizona.edu/center-natural-hazards>), the Arizona Earthquake Information Center (<http://www.cefn.nau.edu/Orgs/aeic/index.html>), and the Arizona Geological Survey’s hazard viewer (<https://uagis.maps.arcgis.com/apps/webappviewer/index.html?id=98729f76e4644f1093d1c2cd6dabb584>) provide more information.

Abandoned Mineral Lands

Abandoned mineral lands (AML) are lands, waters, and surrounding watersheds that contain facilities, structures, improvements, and disturbances associated with past mineral exploration, extraction, processing, and transportation, including oil and gas features and operations, for which the NPS acts under various authorities to mitigate, reclaim, or restore in order to reduce hazards and impacts to resources. The NPS AML website, <https://www.nps.gov/subjects/abandonedmineralands/index.htm> provides further information.

Although no mining currently occurs in the park, the park includes AML sites that are a testament to this legacy. According to the servicewide AML database (accessed 24 August 2015) and Burghardt et al. (2014), Grand Canyon National Park contains 75 documented AML features at 38 sites (table 19). Eight AML features have been mitigated and 16 require mitigation. Twelve of the sites require mitigation. Of those that require

Table 19. Abandoned mines in Grand Canyon National Park.

Information from NPS spreadsheet. Additional history of individual mines is available in Billingsley (1974).

Mine	Type	Hazard? (feature)	Geology and Impact Notes
Alternate Dam Site	Underground Mine	No (tunnel)	No details in database.
Bass Asbestos Mine	Underground Mine	No (unknown)	No details in database.
Bass Copper Mine	Underground Mine	No (adit)	No details in database.
Bat Guano Mine	Underground Mine	No (other)	No details in database.
Bonnie Tunnel	Underground Mine	Unknown (unknown)	Sedimentation to the Havasu River.
Boucher Mine	Underground Mine	No (waste rock) Unknown (unknown)	Vishnu Schist (Xv). Sedimentation to Boucher Creek.
Cameron Claims	Underground Mine	Unknown (unknown)	No details in database.
Cameron North 1	Underground Mine	No (waste rock) Yes (adits)	Completed in Bright Angel Shale (Cba). Sedimentation to intermittent streams.
Cameron North 2	Underground Mine	No (waste rock) No (prospect)	Complete in Bright Angel Shale (Cba). Sedimentation downgradient of site is primary impact.
Cameron North 3	Underground Mine	No (waste rock) Yes (adit)	Adit enters Bright Angel Shale (Cba). Sedimentation to intermittent channel.
Cameron North 4	Underground Mine	No (waste rock) No (prospect)	No details in database. Sedimentation to intermittent channel.
Cameron South 1	Underground Mine	No (waste rock) Yes (adit)	Adit enters Bright Angel Shale (Cba). Waste rock has washed into intermittent channel.
Cameron South 2	Underground Mine	Yes (adit) No (waste rock)	Adit enters Bright Angel Shale (Cba). Sedimentation to intermittent channel.
Cameron South 3	Other	No (waste rock) No (building)	Bright Angel Shale (Cba). Sedimentation downgradient of site is primary impact.
Cameron South 4	Other	No (building)	Bright Angel Shale (Cba). Sedimentation to intermittent streams and perennial (Garden Creek) channels is primary impact.
GRCA BA12	Surface Mine	Unknown (surface mine)	No details in database.
GRCA BA4	Surface Mine	Unknown (surface mine)	No details in database.
GRCA BA6	Surface Mine	Unknown (surface mine)	Sand and gravel. No details on impacts in database.
GRCA NK2	Surface Mine	Unknown (surface mine)	No details in database.
GRCA NK5	Surface Mine	Unknown (surface mine)	No details in database.
GRCA NK8	Surface Mine	Unknown (surface mine)	No details in database.
GRCA SK2	Surface Mine	Unknown (surface mine)	No details in database.
GRCA SK4	Surface Mine	Unknown (surface mine)	Sand and gravel. No details on impacts in database.
Hance Asbestos Mine	Underground mine	Unknown (adit)	No details in database.
Havasu	Underground mine	No (waste rock)	Adit/workings in Muav Limestone (Cm). Massive Redwall Limestone (Mr) overlies adit. Sedimentation to the Havasu River.
Havasu Adit	Underground Mine	Unknown (adit)	No details in database.

Table 19, continued. Abandoned mines in Grand Canyon National Park.

Mine	Type	Hazard? (feature)	Geology and Impact Notes
Havasu Lower	Underground Mine	Yes (waste rock) Yes (adits) No (prospect)	Adit/workings in Muav Limestone (Cm). Massive Redwall Limestone (Mr) overlies adit. Sedimentation to the Havasu River.
Last Chance (Grandview) Copper Mine	Underground Mine	Unknown (shaft) Unknown (structure) Unknown (adit) No/yes (adits) Unknown (waste rock)	No details in database.
Little Chicken Mine	Underground Mine	Unknown (unknown)	No details in database.
Magician Mine 1	Underground Mine	No (waste rock) Yes (adit)	Vishnu Schist (Xv) and breccia pipes in adit. No details on impacts in database.
Magician Mine 2	Underground Mine	No (prospect) No (equipment) Yes (structure) Yes (adit)	Vishnu Schist (Xv). No details on impacts in database.
Magician Mine 3	Underground Mine	No (waste rock) No (prospect) Yes (adit)	Nearly vertical pegmatite dike. Erosion because of sparse vegetation.
Marble Canyon Dam Site	Underground Mine	Unknown (other)	No details in database.
McCormick Mine	Underground Mine	Unknown	No details in database.
Morning Star Mine	Underground Mine	Unknown (unknown)	No details in database.
Orphan Mine	Underground Mine	Unknown (structure) Unknown (glory hole) Unknown (shaft) Unknown (waste rock) Unknown (adit)	No details in database.
Pinto Mine	Underground Mine	Unknown (unknown)	No details in database.
Snyder Mine	Underground Mine	Unknown (unknown)	No details in database.

mitigation, 4 sites and 7 features are classified as high priority, 7 sites and 8 features as medium, and 1 site and 1 feature as low priority. (Burghardt et al. 2014). In 2014, the estimated cost of mitigating the features and sites was \$343,814 (Burghardt et al. 2014).

AML features pose a variety of resource management issues such as visitor and staff safety and environmental quality of air, water, and soil. According to the database, health and safety hazards documented at AML sites and features in the park include high levels of radon, radioactive soils, occurrence of asbestos, unstable debris, unstable slopes/overhanging boulders, hazardous openings or structures, and subsidence.

Sedimentation to adjacent streams or rivers is a documented natural resource impact for at least 11 AML sites in Grand Canyon National Park.

AML features can also provide habitat for bats and other animals, some of which may be protected under the Endangered Species Act or state species listings.

According to the AML database, at least 11 AML features host bats; 34 additional features are listed as “unknown” for presence of bats.

Resource management of AML features requires an accurate inventory and reporting. All AML features should be recorded in the servicewide AML Database (the NPS Geologic Resources Division may be able to help). An accurate inventory identifies human safety hazards and contamination issues, and facilitates closure, reclamation, and restoration of AML features.

When appropriate for resource management and visitor safety, AML features can also present opportunities for interpretation as cultural resources. For example, the Grandview (Last Chance) Mine is on the National Register of Historic Places and the Orphan Mine may be eligible for listing. At least 15 of the park’s 38 AML sites have some cultural significance.

In 2009, the Grandview Mine adits were gated to protect bat species, including Townsend’s Big-eared

Bat (*Corynorhinus townsendii*), support on-going bat research, preserve historic mine resources, and promote visitor safety (fig. 80; Mindat.org 2016b). A detailed description of the operations required to close the adits may be found at <http://minegates.com/grandviewlastchancemine1.htm>. Funds from the American Recovery and Reinvestment Act of 2009 (ARRA) were used to install bat-accessible gates at four additional mine sites and to secure a total of eight mine features (NPS 2015b).

A major concern documented at the Orphan Mine was the presence of gamma radiation well beyond the fenced perimeter and in the two adits below the rim (Hom 1986; Burghardt 1995). During a site visit in 1995, John Burghardt, geologist with the Resource Evaluation Branch of the NPS Geologic Resources Division, Linden Snyder of the US Bureau of Mines, and Heather Davies, Hazardous Materials Coordinator for the former Western Regional Office, measured gamma radiation at the above ground site and found background values of 30–40 microrems/hr within 15–30 m (50–100 ft) east and south of the fenced enclosure. However, elevated values, like those recorded by Hom (1986), were found west of the fence. The highest radiation value of 1,250 microrems/hr was measured 30 m (100 ft) from the West Rim Trail (Burghardt 1995). For context, the Nuclear Regulatory Commission’s evacuation level is 2,000 microrems/hr and the US Environmental Protection Agency’s Radiation Protection Guideline (RPG) for radiation exposure of the public is 10,000 microrems/year (Burghardt 1995).

In 1995, a specific cleanup standard for the above ground site was dependent on the park’s decision of how the surface facilities were to be used. Burghardt (1995) suggested that cleanup to background levels would be difficult and prohibitively expensive. Since 1995, a taller fence has been installed and the headframe has been removed (Bennett 2010; John Burghardt, personal communication to Jason Kenworthy, 20 January 2017). An Environmental Assessment (EA) has been prepared for closures of Abandoned Mine Lands at Grand Canyon National Park, including Orphan Mine (Bennett 2010; NPS 2015b). The NPS Abandoned Mine Lands website: <https://www.nps.gov/grca/learn/news/abandoned-mine-lands-safety-projects-begin-in-grand-canyon-national-park.htm> provides additional information about access to the EA. Burghardt (1996) provides a guide to effective management of radioactive hazards at AML sites on the Colorado Plateau.

Uranium Mining

Beginning in the 1950s with the discovery of ores with high concentrations of uranium oxide (e.g., Orphan Mine), uranium miners have had a great interest in



Figure 80. Photograph of the installation of Grandview Mine bat gates in 2009. NPS photograph available at <https://www.nps.gov/grca/learn/news/abandoned-mine-lands-safety-projects-begin-in-grand-canyon-national-park.htm>.

the Grand Canyon area (within and outside the park) (Wenrich and Stuphin 1994). In 1990, the USGS estimated that breccia pipe deposits in northern Arizona contain 1.3 million tons (2.6 billion pounds) of undiscovered uranium (U_3O_8), an estimate about three times the total uranium reserves in the rest of the United States, as estimated by the US Energy Information Administration in 2003 (Finch et al. 1990; Otton and Van Gosen 2010; Bills et al. 2011).

In 2009, the USGS began a short-term study of uranium resources in northern Arizona to determine how much uranium was unavailable for exploration, development, or mining because of previous withdrawals of Federal land and by proposed withdrawals (fig. 81). About 35% of the estimated uranium resources were excluded from mining prior to 2009. These areas included Grand Canyon National Park, two national monuments, a game preserve on forest lands and Tribal lands (fig. 81; Otton and Van Gosen 2010; Bills et al. 2011). In 2012, then Secretary of the Interior Ken Salazar signed a Record of Decision (ROD) to withdraw over 1 million acres in the North, South, and East Segregation Areas for twenty years, subject to valid existing rights (US

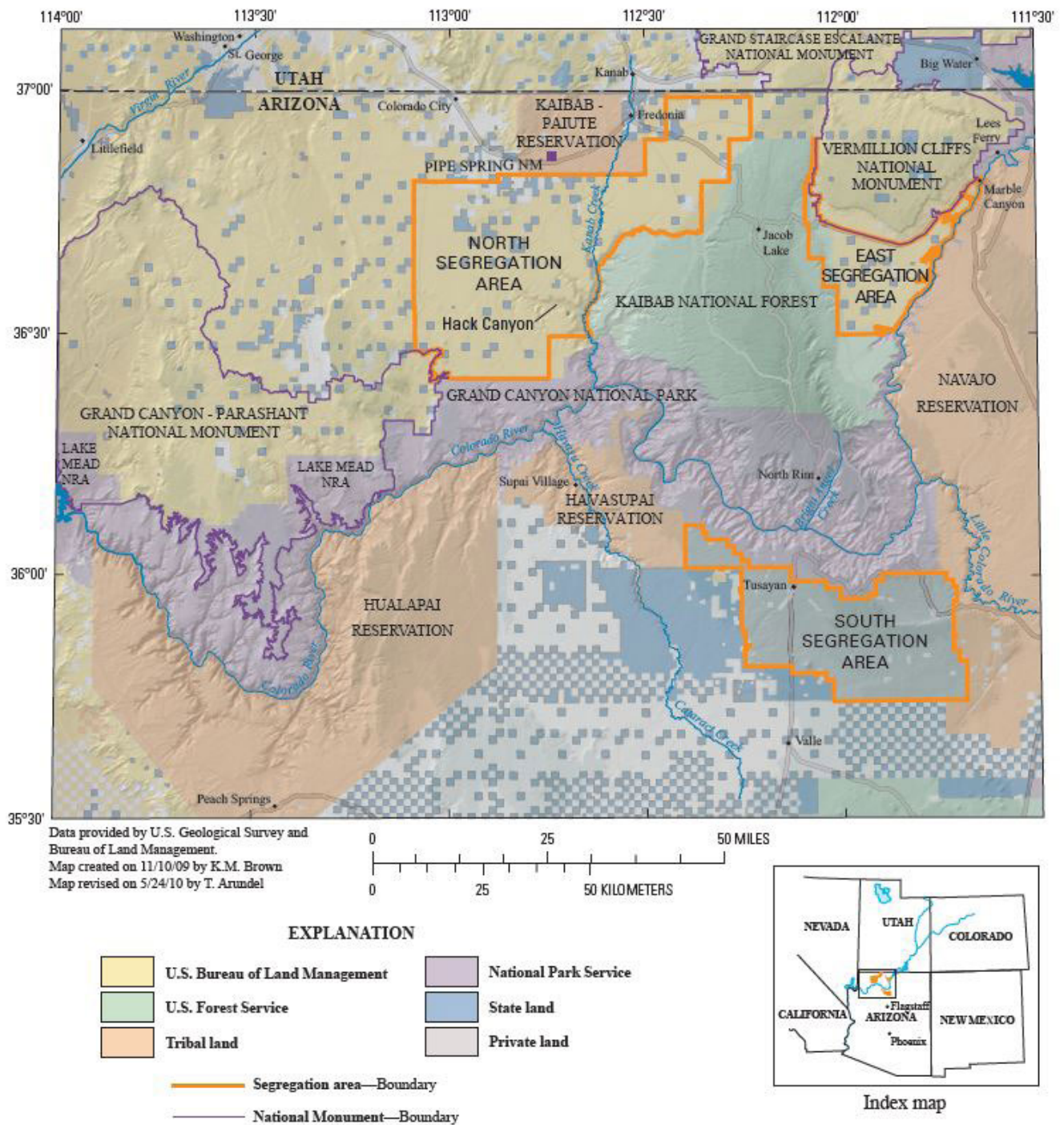


Figure 81. Map showing land ownership in northwestern Arizona and the three Segregation Areas withdrawn from mining in 2012. The North and South Segregation Areas contain most of the mining claims (see Otton and Van Goshen 2010, figure 2). USGS map from Bills et al. (2011, figure 2).

Department of the Interior 2012; Beisner et al. 2016). These areas contain another 12% of the total uranium reserves. A significant reason for the ROD was the lack of scientific data and uncertainty of potential impacts of uranium mining activities on water resources in the area.

The 2009 study analyzed uranium availability, historical effects of uranium mining, water chemistry in wells, streams, and springs, and biological pathways of exposure for uranium and associated radioactive contaminants. Examples of some, but not all, uranium concentrations found in springs, streams, waste piles, and wells in the Grand Canyon region are listed in table 20. Details of this study, as well as recommendations for future research, are available from the USGS (2011), Bills et al. (2010), Hinck et al. (2010), Otton and Van Gosen (2010), and Otton et al. (2010). Updates on uranium resources and environmental investigations in northern Arizona and other regions of the country are available on the USGS Energy Resources Program website, <https://energy.usgs.gov/OtherEnergy/Uranium.aspx#3900255-research>.

In 2018, the Supreme Court refused to hear an appeal by mining industry groups, effectively putting to rest the legal challenges to the mining ban (Reimondo 2019). However, two recent executive orders from the current administration have again raised the issue of the mining ban. Executive Order 13783 requires an immediate review of existing regulations that may burden the development or use of domestically produced energy resources and to suspend, revise, or rescind any regulations that unduly burden the development of these resources. In response to this executive order, the Agriculture Department included the Grand Canyon mining ban on a list of recommended actions for review and revision by 2020 (Reimondo 2019).

In December 2017, Executive Order 13817 directed then Interior Secretary Ryan Zinke to develop a new list of critical minerals. The USGS had released an updated list of critical minerals the day before the executive order was announced, and this list did not include uranium. However, the new list, which was finalized in May 2018, included uranium. Under the executive order, the Commerce Department is required to prepare a report that presents recommendations to streamline permitting and review processes related to discovering and producing critical minerals, including uranium in the Grand Canyon (Reimondo 2019).

The National Park Service has specific regulations involving mining activities within the borders of a park (see Appendix B). The National Park Service works with adjacent land managers and other permitting entities

to help ensure that National Park System resources and values are not adversely impacted by external mineral exploration and development. Potential impacts include groundwater and surface water contamination, erosion and siltation, introduction of exotic plant species, reduction of wildlife habitat, impairment of viewsheds and night skies, excessive noise, and diminished air quality. Visitor safety and overall degradation of the visitor experience are concerns. The NPS Energy and Minerals website, <https://www.nps.gov/subjects/energyminerals/index.htm>, provides additional information.

Impacts from Uranium Mining

Uranium mining may degrade water resources and lead to permanent contamination. Such concerns about uranium mining in areas adjacent to Grand Canyon National Park led to the 20-year moratorium on new mines beginning in 2012. The uranium industry and state of Arizona challenged the moratorium with a lawsuit. A pair of federal court cases may decide the fate of the moratorium as well as existing mining operations. However, the Arizona Department of Environmental Quality has allowed one of these mines, the Canyon Uranium Mine, which is located south of the park, to re-open and stockpile uranium ore (Clark 2016; Howard 2016). Prior to any active mining, however, USGS scientists collected and analyzed 84 environmental samples to establish baseline data (table 20). These data will help assess whether contaminants escape from the mine site (USGS 2016c).

One primary concern about uranium mining is its potential contamination of drinking water for approximately 25 million downstream users. The EPA maximum contaminant level (MCL) for drinking water is 30 parts per billion (ppb), or 0.03 parts per million (ppm). The 2009 study of soils, waste rock, and sediments associated with several reclaimed or inactive breccia-pipe uranium mines in the Kanab Creek area north of the park (see poster sheet 2) found uranium to be a primary trace element of concern (Otton et al. 2010). Uranium concentrations in the soil at the Kanab North Mine were more than 10 times background concentration (table 20). Lower concentrations reported for the reclaimed Hermit Mine may be because the mine was active for less than one year. Geologic processes also influenced the data. Flash floods, for example, eroded ore and waste-rock piles at the Hack 1 Mine during mining and after the mine had been reclaimed (Otton et al. 2010).

The 2009 study summarized historical uranium concentration data from 1,014 samples from 428 sites including 88 springs, 63 stream locations, 74 wells, a mine shaft, and 2 mine sumps (the lowest point in

Table 20. Examples of uranium concentrations in the Grand Canyon area.

ppb = parts per billion. Concentrations not presented as ranges are average values. References include Otton et al. (2010), Bills et al. (2010), Beisner et al. (2016), and USGS (2016c). The EPA drinking water MCL for uranium is 30 ppb (0.03 ppm).

Area	Site	Sample	Uranium (ppb)
Kanab Creek/Kanab Plateau	Surrounding area (background)	Soil	2,400
	Jumpup Canyon (background)	Stream sediments	1,700
	Upper Jumpup Spring	Spring	3.8–3.9
	Pigeon Mine	Soil (disturbed area)	4,400
	Pigeon Mine	Soil (undisturbed area)	6,300
	Pigeon Mine	Mine sump	170
	Pigeon Spring	Pre-Pigeon Mine	44
	Pigeon Spring	Post-Pigeon Mine	73–92
	Table Rock Spring	Pre-Pigeon Mine	5.2
	Table Rock Spring	Post-Pigeon Mine	6.6
	Wildband Spring	Pre-Pigeon Mine	14
	Wildband Spring	Post-Pigeon Mine	8.7
	Rock Spring	Pre-Pigeon Mine	15
	Rock Spring	Post-Pigeon Mine	14–16
	Slide Spring	Pre-Pigeon Mine	1.5
	Slide Spring	Post-Pigeon Mine	2.7–2.8
	Willow Spring	Pre-Pigeon Mine	10
	Willow Spring	Post-Pigeon Mine	14–18
	Kanab North Mine	Soil	27,800
	Kanab South drill site	Soil	1,300–2,700
	Kanab South drill site	Stream sediments	1,500–3,600
	Hermit Mine	Soil (disturbed area)	3,100
	Hermit Mine	Soil and stream sediments (undisturbed area)	1,600
	Hermit Mine	Monitoring well	<7 (25 samples)
	Hermit Mine	Monitoring well	24.0 (1 sample)
	Hermit Mine	Mine shaft	20–42
	Hermit Mine	Mine sump	3,310–36,600
	Hack 1 Mine	Stream sediments	2,400–10,200
	Hack 2 & 3 Mines	Stream sediments	5,000
	Hack 2 & 3 Mines	Waste-rock fragment	7,760,000
	Canyon Uranium Mine	Soil and stream samples inside mine perimeter	3,300–9,900
	Canyon Uranium Mine	Soil and stream samples outside mine perimeter	1,400–6,200
	Canyon Uranium Mine	Well	4.1–309
USGS sample GCAD505R	Well	32	
USGS sample GCAD511R	Well	33	
USGS sample GCAD501R	Well	86	

Table 20, continued. Examples of uranium concentrations in the Grand Canyon area.

Area	Site	Sample	Uranium (ppb)
Horn Creek	Horn Spring and Horn Creek	Spring and stream	18.9–67.8
	Horn Up	Spring	312–400
	Horn West	Spring	135–202
	Horn Down	Stream	362
Pipe Spring National Monument	USGS sample GCAE517R	Spring	250
Hualapai Reservation	USGS sample 23168	Spring	57
	USGS sample 23169	Spring	51
Colorado River sites	Bright Angel Canyon	Stream samples	≤5
	Near Hualapai Reservation	Stream samples	≤10
Pinenut Mine	Monitoring well	Well	<13

a mine shaft into which water drains) in the Grand Canyon region (Bills et al. 2010). As Bills et al. (2010) noted, however, limited temporal data exists for the sites sampled. Data from 95% of the spring samples contained concentrations of uranium below 30 ppb, with the notable exceptions of Horn Creek and Horn Spring below the Orphan Mine (table 20) (Bills et al. 2010; Schaar 2011; USGS 2011). In total, 15 of the 288 spring sites contained samples with uranium concentrations greater than or equal to 30 ppb (Bills et al. 2010). Colorado River stream samples from near Bright Angel Canyon and the Hualapai Reservation registered 10 ppb or less dissolved uranium (Bills et al. 2010). The highest concentrations of uranium in stream samples were from the Horn Down stream site, which is presumably fed by groundwater discharge from Horn Creek, Horn Up, and Horn West springs (table 20). Well, sump, and the Hermit Mine shaft samples also recorded elevated uranium concentrations (table 20).

Rainfall and carbonate-rich solutions may leach uranium from soils, un-weathered ore, wind-transported fine-grained material, weathered ore and waste rock, pond sludge, and surficial salts (Gallegos and Otton 2012). While concentrations were high for specific sites, such as the Kanab North Mine, experiments using synthetic rainwater to simulate leaching indicated contributions of trace elements from percolating water to be less than 0.001 ppm (<1 ppb), although the efficiency of natural attenuation processes requires further study (Otton et al. 2010).

Since 2012, the USGS has been conducting scientific investigations to better understand the potential contamination from uranium mining. By 2015, USGS scientists had analyzed samples from 36 springs in the North Rim area (USGS 2015). Of these, Pigeon Spring, located approximately 1.6 km (1.0 mi) from the former Pigeon Uranium Mine, had the highest dissolved uranium concentration (table 20; Beisner et al.

2016). However, uranium concentrations were elevated prior to mining, and results from the study suggest that the uranium concentrations at Pigeon Spring are related to an upgradient uranium source rather than from the Pigeon Mine (Beisner et al. 2016). These results emphasize the complex nature of groundwater flow paths and the interaction of mining and water resources.

The Colorado River naturally carries about 60 metric tons (66 tons) of dissolved uranium through the canyon each year (Spencer and Wenrich 2011; Bills 2012). This amount equates to about 4 micrograms per liter, which is equivalent to 4 ppb by mass. In one proposed worst-case scenario by Spencer and Wenrich (2011), if a truck carrying 30 metric tons (33 tons) of 1% uranium ore were to overturn in a flash flood in Kanab Creek and spill into the Colorado River to become part of the annual dissolved uranium content, the uranium in river water would increase from 4.00 ppb to 4.02 ppb. With an EPA maximum contaminant level for uranium in drinking water of 30 ppb, the increase would not only be trivial but also the additional amount would not be detected above the natural variation of uranium in the river water.

With renewed interest in nuclear energy, the price of uranium has increased, which will continue to drive the interest in the uranium resources near the Grand Canyon, as well as research into the effects of mining on natural resources and human health.

The NPS Geologic Resources Division is available to provide the park with policy and technical assistance regarding minerals and energy issues. Recommendations include remaining aware of public and private mineral ownership and speculation, exploration, or drilling activity on lands in the park's vicinity. Regulations and permit procedures vary among states.

Hydrocarbon Exploration

With increased temperature from burial and over time, micro-organisms in the Awatubi Member (**Zka**) and Walcott Member (**Zkw**) of the Kwagunt Formation (**Zk**) transformed into hydrocarbons (Wiley et al. 1998, 2002). The kerogen type for the Awatubi Member is not definitive, but kerogen types in the Walcott Member indicate that the unit is a potential gas source and possibly an oil source as well. In the Awatubi Member, hydrocarbons migrated into the unit, as well as being generated in situ. In contrast, 95% of the hydrocarbons in the organic-rich Walcott Member were generated in situ. Hydrocarbons in these units may migrate into overlying sandstone reservoirs in the Sixtymile Formation (**Zs**) or Tapeats Sandstone (**Ct**) (Wiley et al. 1998).

In 1906, the first oil well was drilled near the Grand Canyon (Billingsley 1974). Since then, many more unsuccessful exploratory wells have been drilled on the Uinkaret Plateau, north of Grand Canyon National Park (Rauzi 2012). Maximum depths of most of these wells reached upper Paleozoic units, primarily Pennsylvanian and Devonian formations. Very few wells penetrated the Tapeats Sandstone or Sixtymile Formation. However, samples collected from Sixtymile, Carbon, and Nankoweap canyons indicate that the Walcott (**Zkw**) and Awatubi (**Zka**) Members of the Kwagunt Formation, Chuar Group (table 1), contain hydrocarbons (Wiley et al. 1998, 2002). Rauzi (2012) lists all wells drilled for hydrocarbons in northwestern

Arizona through 2011. Well information for each well on Rauzi's list includes well location, permit, operator, lease number, date drilled, elevation of the well, well status (e.g., dry hole), and the formation encountered at the bottom of the well. The Arizona Geological Survey (<http://www.azgs.az.gov/>, accessed 28 May 2016) provides additional information on hydrocarbon exploration in Arizona. As with external Uranium mining, any external oil and gas development could bring a variety of negative consequences to the park's natural resources. Currently, renewed hydrocarbon exploration near the borders of Grand Canyon National Park is unlikely.

Lake Mead Delta

Participants at the 2015 conference call raised concerns about the delta that has been expanding where the Colorado River empties into Lake Mead (fig. 82). Lake levels have dropped since 2000 as drought has gripped the southwest, and maximum sediment thickness currently exceeds 80 m (262 ft) where the Colorado River enters Lake Mead (NPS 2016b). Global climate change predictions suggest drought will increase in the future. The growth of a delta at the interface of the Colorado River with Lake Mead is a geomorphic process to be expected whenever a dam is constructed. Delta growth may adjust the riparian environment in the immediate area, and perhaps influence archaeological sites, but the severity of this issue remains to be seen.



Figure 82. NASA photograph of the delta being formed where the Colorado River enters Lake Mead. In 2016, maximum thickness of sediments entering Lake Mead exceeded 80 m (262 ft). Image acquired 30 March 2013, available at <https://earthobservatory.nasa.gov/NaturalHazards/view.php?id=80948>.

Geologic History

This chapter describes the geologic events that formed the present landscape.

The rocks of the Grand Canyon record almost 2 billion of the 4.6 billion years of Earth's existence (table 1). This record includes the tectonic collisions, the advance (transgression) and retreat (regression) of shallow seas, aggressive volcanic activity, ice ages, and the incision of the Colorado River into the uplifted Colorado Plateau. Episodes of plate collisions and crustal extension accompanied all these events. However, the record is far from complete. Major regional unconformities represent extensive gaps in the stratigraphic record in the Grand Canyon.

Visitors may experience the expanse of geologic history in the park by walking the Trail of Time, a 4.56 km (2.83 mile) long geologic timeline (http://www.trailoftime.org/what_is_it.html). Rock samples and exhibits along the trail explain the formation of the Grand Canyon.

Paleoproterozoic Era (2.5 billion–1.6 billion years ago): Magma, Metamorphism, and Deformation

In the Grand Canyon region, the Elves Chasm pluton, the oldest rock known in the southwestern United States, was emplaced about 1.84 billion years ago and signals the beginning of an orogeny (mountain-building event) that lasted until about 1.65 billion years ago (fig. 83). In Grand Canyon, the orogeny includes the Zoroaster Plutonic Complex and the Granite Gorge Metamorphic Suite (table 1). Volcanic islands (volcanic arcs) formed above subduction zones, and continued collision sutured the arcs onto the Archaean rocks of the supercontinent Rodinia. The Paleoproterozoic Grand Canyon region resembled today's Indonesian region where subduction of the Pacific Oceanic plate is slowly welding the volcanic island arcs, arc basins, and older continental fragments to the Asian continent. Intense compression 1.69 billion–1.60 billion years ago resulted in complex deformation events, metamorphism, and subsequent cooling at depths of 10 km (6 mi) (Karlstrom et al. 2003).

Sediments eroded from the volcanic islands were buried to depths of 20–25 km (12–15 mi), squeezed and folded and deformed, and then metamorphosed to form the Vishnu, Rama, and Brahma schists and gneiss of the Granite Gorge Metamorphic Suite (table 1). Sequences of graded bedding in the Vishnu Schist suggest deposition by submarine turbidites (underwater slope movement deposits in which coarse sediments initially settle out of the water column followed by finer-grained sediment), possibly on the flanks of eroding volcanic islands (Babcock 1990; Karlstrom et al. 2003). Mats

of algae in thin layers of carbonate rock are the only evidence of life in the Proterozoic Vishnu Sea (Babcock, 1990).

Pillow structures in the Brahma Schist, such as those found in Clear Creek, Horn Creek, 92-mile Canyon, Crystal Creek, Slate Creek, Shinumo Creek, near Blacktail Canyon, and "Pillow Basalt Canyon" (mile 229.5) characterize submarine mafic lava flows (Karlstrom et al. 2003). Exposures of the contact between the Elves Chasm pluton and Granite Gorge Metamorphic Suite occur in several areas, notably at Walthenberg, 113-mile, and Blacktail canyons and several places in the Middle Granite Gorge.

The intrusive rocks of the Zoroaster Plutonic Complex record a long and complex evolution of the crust. Subdivided into four groups of plutons, they represent: 1) older basement (Elves Chasm pluton), 2) arc plutons, 3) syncollisional granites, and 4) post-orogenic granites that were emplaced 1.7 billion–1.4 billion years ago (Karlstrom et al. 2003).

From 1.74 billion to 1.71 billion years ago, melting above the subducting plate produced large magma chambers that fed volcanic eruptions within the volcanic island arcs (fig. 41). When the magma cooled, the granodiorite and gabbro-diorite complexes became arc plutons. Their original shape has changed so that some are now large folded sheet-like plutons (Zoroaster, Trinity, and Ruby plutons), while others are massive plutons (Diamond Creek pluton) or smaller stock-like bodies (Pipe Creek, Horn Creek, Boucher, and Crystal plutons). Igneous intrusions of the arc plutons occurred before the period of intense deformation 1.70 billion–1.68 billion years ago (Karlstrom et al. 2003).

The granites and pegmatites of the Zoroaster Plutonic Complex (table 1) represent igneous intrusions occurring simultaneously with island arc/continental collision and peak metamorphism. These granitic rocks have a different composition, intrusive style, and deformational character than the arc plutons. At this time, magma from partial melting of the lower crust rose along cracks and shear zones and solidified to form dike swarms or coalesced as plutons of various sizes (Karlstrom et al. 2003). In the Upper Granite Gorge, these dike swarms include the Cottonwood, Cremation, Sapphire, and Garnet Canyon complexes. In Lower Granite Gorge, the intrusives are more massive and pluton-like and include the Travertine Falls, Separation, and Surprise plutons.

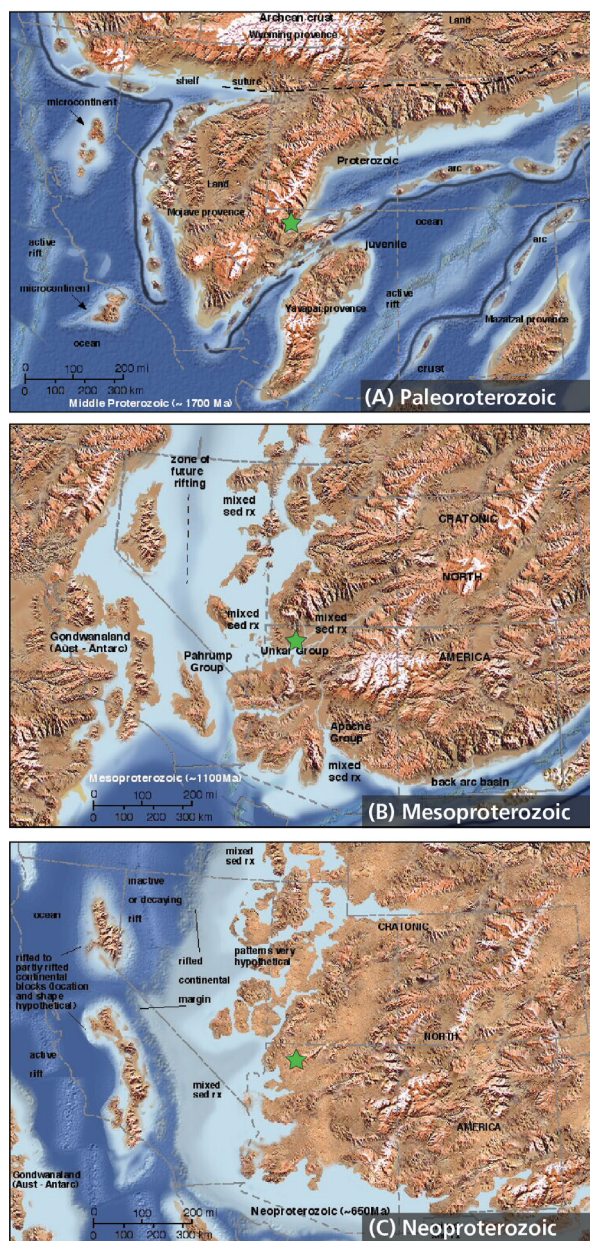


Figure 83. Proterozoic Eon paleogeographic maps of southwestern North America.

(A) In the Paleoproterozoic Era, along the southwestern margin of the supercontinent Rodinia, the Mojave province had accreted to the Wyoming province, and the Yavapai and Mazatzal oceanic magmatic arcs followed as subduction continued. **(B)** Nearshore marine and marginal marine depositional environments dominated the Grand Canyon region during the Mesoproterozoic Era. **(C)** In the Neoproterozoic Era, Rodinia broke apart and western North America became a passive tectonic margin. The green star approximates the location of Grand Canyon National Park. Base paleogeographic maps are from the “Paleogeography of Southwest North America” © 2012 Colorado Plateau Geosystems Inc, used under license.

The folds in the Zoroaster Pluton Complex and the Granite Gorge Metamorphic Suite resulted from northwest–southeast subhorizontal compression and document at least two regional episodes of deformation between 1.8 billion and 1.6 billion years ago (Karlstrom et al. 2012a). At the time, pressures and temperatures had partially melted these rocks so they stretched and folded like taffy or putty. Preexisting bedding and platy minerals, like micas, were compressed, folded, and rotated perpendicular to the compressive stress, forming the characteristic foliation (schistosity) in the metamorphic schists. Layers in the Vishnu Schist (**Xv**) were folded and refolded and thrust over themselves. Axes of some of the folds are nearly vertical. Granitic dikes cross-cut the folds, indicating that folding occurred prior to the emplacement of the igneous intrusions. On a grand scale, the northeast–southwest-oriented Vishnu Mountains resulted in response to this tectonic compression (fig. 41). Grand Canyon National Park preserves one of the few exposures of this evolution of the continental crust that eventually became the southwestern part of the United States (Karlstrom et al. 2012a).

Although primary Paleoproterozoic deformation and metamorphism ended approximately 1.68 billion years ago in the Grand Canyon region, local deformation and plutonism continued until 1.66 billion years ago (e. g., Phantom pluton). Magmatism, deformation, and metamorphism ceased about 1.65 billion years ago at which time a long period (200 million years) of tectonic stability began (Karlstrom et al. 2003). During this time, the 1.4 billion-year-old granite and pegmatite (**Yg**) were emplaced.

Paleoproterozoic gaps in the stratigraphic record represent the famous Great Unconformity, recognized and named by John Wesley Powell (see the “Unconformities” section in the “Geologic Features and Processes” chapter). At locations in the Grand Canyon where Grand Canyon Supergroup rocks are present, the next 500 million years of geologic history are unrecorded (table 1). At locations where rocks of the Grand Canyon Supergroup are missing, the stratigraphic gap is approximately 1.2 billion years!

Mesoproterozoic Era (1.6 billion–1.0 billion years ago): Coastal Environments Dominate North America’s Southern Margin

The 1.35 billion-year-old Quartermaster pluton and related pegmatites represent the final emplacement of plutonic rocks in the Grand Canyon. The granitic rocks record a period of intracratonic magmatism in the southwestern United States (Karlstrom et al. 2003).

About 10 km (6 mi) of rock in the Upper Granite Gorge eroded during the 1.7 billion–1.65 billion-year-old deformation episode. Between 1.35 billion years and 1.25 billion years ago, erosion of an additional 10 km (6 mi) of rock created a broad plain that would eventually receive sediments that lithified into the Grand Canyon Supergroup (Karlstrom et al. 2003).

From about 1.25 billion years to 1.07 billion years ago, the Unkar Group, which includes the oldest formations in the Grand Canyon Supergroup, accumulated in a shallow sea or in environments near sea level (fig. 83; Hendricks and Stevenson 2003; Timmons et al. 2003). Local topographic relief was probably no more than 45 m (150 ft). The sedimentary sequence records a major west-to-east transgression (Hendricks and Stevenson 2003).

Sedimentary features (table 6) in the Bass Formation (**Yb**), the basal formation in the Unkar Group, indicate deposition in relatively low-energy intertidal to supratidal environments (Hendricks and Stevenson 2003). During the maximum incursion of the sea, carbonates and deep-water mudstones accumulated in western Grand Canyon while in the east, stromatolites and shallow-water mudstones predominated. Ripple marks, mudcracks, and deposits of oxidized shales in the upper part of the Bass Formation suggest periods of subaerial exposure as sea level slowly lowered. Eventually, a deltaic system predominated, which marked the beginning of Hakatai Shale (**Yh**) deposition (Hendricks and Stevenson 2003).

Oxidation of iron-bearing minerals produced the purple to red to brilliant orange colors of the Hakatai Shale. Termination of deposition into the mudflat and shallow marine environments of the Hakatai Shale coincides with tectonic activity along a series of northwest-trending, high-angle reverse faults (Sears 1973; Reed 1974; Hendricks and Stevenson 2003). The unconformity between the Hakatai Shale and overlying Shinumo Quartzite (**Ys**) truncates Hakatai cross-beds, recording the erosion of previous channel deposits.

Sedimentary features (table 6) in the massive, cliff-forming sandstones and quartzites of the Shinumo Quartzite indicate continuation of near-shore, shallow, marginal marine environments interspersed with fluvial and deltaic environments (Daneker 1974; Hendricks and Stevenson 2003). A relatively rapid transgression flooded the depositional environments of the Shinumo Quartzite and deposited the marine sandstones and shales of the Escalante Creek Member of the Dox Formation (**Yde**) (Stevenson and Beus 1982). Some of the Escalante Creek sediments may have originated from a western source, opposite to the inferred source

direction for the other units of the Unkar Group (Hendricks and Stevenson 2003).

Greater than 900 m (3,000 ft) thick, the Dox Formation (**Yd**) is the thickest formation in the Unkar Group (Hendricks and Stevenson 2003). Following the initial transgression, the Dox Formation paleoecosystem transitioned gradually into subaqueous delta, floodplain, and tidal flat environments as sea level slowly fell.

Igneous activity about 1.07 billion years ago culminated in the Cardenas Basalt (**Yc**) that caps the Unkar Group. Exposed only in the eastern Grand Canyon, Cardenas Basalt forms a series of basalt and basaltic andesite flows and sandstone interbeds ranging in thickness from 239 m (785 ft) to nearly 300 m (985 ft) (Ford et al. 1972; Hendricks and Stevenson 2003). When the basalt erupted, the region may have been at or very near sea level so that the lava flowed over the unconsolidated sandy and silty tidal flat environment of the Dox Formation (Stevenson and Beus 1982; Hendricks and Stevenson 2003). When the volcanic activity ceased, the sediments and igneous rocks of the Unkar Group were tilted gently toward the northeast, and an unknown amount of lava was eroded prior to deposition of the Neoproterozoic Nankoweap Formation (**YZn**).

Major outcrops of the Unkar Group occur in seven separate locations within Grand Canyon National Park: 1) Big Bend region of eastern Grand Canyon, 2) Clear Creek, 3) Bright Angel Creek, 4) Phantom Creek-Phantom Ranch, 5) Crystal Creek, 6) Shinumo Creek, and 7) Tapeats Creek (GRI GIS data).

Faults and folds in the Unkar Group document the Mesoproterozoic collision of Laurentia with other large landmasses to form the supercontinent Rodinia. An episode of northwest–southeast compression folded and faulted Unkar Group strata. Northeast-trending reverse fault planes are preserved within side canyons such as Red, Vishnu, Bright Angel, and Bass canyons. Monoclines in the Unkar Group, smaller in scale than the younger Colorado Plateau monoclines, folded over the reverse faults. Exposures in Vishnu and Red canyons document monoclines that developed during deposition of the Bass Formation (**Yb**), approximately 1.2 billion years ago (Timmons et al. 2005; Timmons et al. 2012). In Red and Bright Angel canyons, the flat-lying Tapeats Sandstone (**Ct**) truncates one of these small-scale monoclines in the Unkar Group, indicating that the monocline pre-dated the Paleozoic Era (Timmons et al. 2012).

No Proterozoic monoclines deform rocks younger than the Shinumo Quartzite (**Ys**), restricting the compressive episode to early Unkar time. Furthermore, all the

Proterozoic monoclines and reverse faults are northeast trending, suggesting that regional scale tectonic forces from the northwest compressed the Laurentian crust.

Reactivation of the Paleoproterozoic fault pattern approximately 1.2 billion–1.0 billion years ago created northwest-trending normal faults in the Unkar Group, such as the Palisades fault (table 16; Karlstrom and Timmons 2012).

Neoproterozoic Era (1.0 billion–541 million years ago): Extensional Tectonics, Glaciation, and Climate Change

In Basalt Canyon, the Nankoweap Formation overlies exposures of the Cardenas Basalt (**Yc**) that have been tilted ~10°, forming an angular unconformity. The contact records displacement and tilting, probably along Unkar-age faults, prior to the erosion of Cardenas Basalt and deposition of the Nankoweap Formation (Timmons et al. 2012). The extensional faults that tilted the Unkar Group rocks disappear within the Nankoweap Formation (**YZn**), indicating an Unkar age to the faulting.

Visible from the Desert View Tower overlook, exposures of the Nankoweap Formation form cliffs overlooking Basalt, Tanner, and Comanche canyons. The lithology and sedimentary features suggest a quiet shallow water environment for the lower part of the Nankoweap, perhaps a lake or pond, and a moderate to low energy, shallow water, marine or lake environment for the upper Nankoweap (Ford and Dehler 2003).

Unconformities separate the Nankoweap Formation from both the Unkar Group and the overlying Galeros Formation. Within the formation, a low-angle unconformity and evidence of normal faulting suggest active extensional faulting during Nankoweap time (Elston et al. 1993; Timmons et al. 2003).

North–south-trending normal faults and folds in the Chuar Group document the splitting of Rodinia beginning ~800 million years ago in the Neoproterozoic. Rodinia began to break apart during one or more extensional tectonic episodes about 750 million years ago (Timmons et al. 2003; Karlstrom et al. 2018). Rifting continued throughout the Neoproterozoic, generating north–northwest trending normal faults that included Butte Fault, Phantom Fault, Bright Angel Fault, Cremation Fault, Crystal Fault, Muav Fault, Wheeler Fault, and 137 Mile Fault (Timmons et al. 2003; Dehler et al. 2012; GRI GIS data).

The Butte Fault records the longest movement history and largest displacement of any Precambrian fault in the Grand Canyon region (Timmons et al. 2003). The

Butte Fault is the easternmost fault of all the exposed Precambrian faults (GRI GIS data). Movement on the Butte Fault was occurring during deposition of the 2 km (1.2 mi)-thick Chuar Group and continued into the Cambrian where the Sixtymile Formation (**Zs**) was deposited in the fault-bounded Chuar Syncline (Karlstrom et al. 2018). West-side-down Precambrian displacement on the fault was on the order of 3,200 m (10,500 ft) (Timmons et al. 2003).

Sedimentary features such as mud-coated symmetrical ripple marks, mud cracks, small-scale (decimeter) cross-bedding, low-angle cross-bed sets, as well as at least six different types of stromatolites, some associated with the microfossil *Chuararia circularis* and some forming reefs or mounds, suggest the Chuar Group was deposited in a relatively quiet, shallow (tens of meters or less) marine environment subject to tidal and wave processes, occasional large storms, microbial activity and carbonate precipitation, and the accumulation of mud and organic matter (table 6; Timmons et al. 2003; Dehler et al. 2012).

Paleoenvironments in the Galeros Formation primarily represent near-shore to coastal depositional settings. The dolomite, *Chuararia*-bearing black shales, and sedimentary features (table 6) in the basal Tanner Member (**Zgt**) are indicative of a shallow subtidal or intertidal environment that transitions into a deeper water environment or a sediment-starved, organic-rich basin (Reynolds and Elston 1986; Ford and Dehler 2003). The Jupiter (**Zgj**), Carbon Canyon (**Zgcc**), and Duppa (**Zgd**) Members represent fluctuating subtidal, nearshore, coastal, swamp, and alluvial plain conditions (Reynolds and Elston 1986; McKenney et al. 2001; Ford and Dehler 2003).

The sandstone of the Carbon Butte Member of the Kwagunt Formation (**Zkcb**) that forms the cliffs of Carbon Butte documents the only thick sandstone in the Chuar Group (table 1). Rising sea level transformed the nearshore, sandy conditions of the Carbon Butte Member to deeper water, subtidal environments of the Awatubi Member (**Zka**) and carbonate ramp of the Walcott Member (**Zkw**) (Cook 1991; McKenny et al. 2001; Ford and Dehler 2003). Near the top of the Walcott Member, a dolomite unit, known as the “karsted dolomite,” signals a regression of the sea from the area. This 12 m-(40 ft)-thick unit, which is only found in Sixtymile Canyon, contains crystalline dolomite pockmarked with cavities, dissolution features, and brecciated dolomite and sandstone clasts (Ford and Dehler 2003).

The strata in the Chuar Group are stacked in cycles consisting of shale overlain by dolomite or sandstone.

The cycles represent sea level fluctuations. In general, deposition of mud, which lithifies into shale, occurs during transgressive episodes when sea level rises. When sea level falls (regression), dolomite is deposited in the shallower marine environments. The cycles in the Chuar Group resemble the Milankovich cycles that have been applied to younger strata in the geologic record (e.g., Beach and Ginsburg 1978; Goldhammer et al. 1987; Sagaman et al. 1997). Milankovich orbital cycles range from 10,000 to 100,000 years and include variations in the shape of Earth's orbit (eccentricity) and the tilt and wobble of the Earth's axis (obliquity and precession) (Milanković 1941). These orbital parameters influence the amount of radiation the planet receives and subsequently, the amount of ice at the poles, which affects Earth's climate.

The Chuar Group contains over 300 meter-scale cycles that are hypothesized to reflect changes to the planet's orbit. Each cycle represents durations ranging from 40,000 to 100,000 years, suggesting the Chuar Group represents a maximum of approximately 40 million years of geologic time (Dehler et al. 2001; Dehler et al. 2012). This age is consistent with other age estimates from U-Pb analyses, paleomagnetic data, stromatolites and microfossil successions, and carbon-isotope compositions (see references in Dehler et al. 2012).

Fewer cycles occur in the upper Chuar Group, and these cycles are all capped with dolomite. The thicker cycles infer a relatively higher magnitude of sea-level change, which commonly occurs due to melting and freezing of glacial ice. The cycles indicate that global ice existed throughout Chuar time, with an increase in the volume of global ice and a decrease in global temperatures during the Kwagunt Formation of late Chuar time (Dehler et al. 2012). During deposition of the Walcott Member (**Zkw**) of the Kwagunt Formation, the planet's climate transitioned into what's known as the Sturtian Ice Age (approximately 750 million–700 million years ago) (Dehler et al. 2000; Karlstrom et al. 2000; Dehler et al. 2001).

Furthermore, the Chuar Group cycles can be grouped into four depositional sequences represented by a bundling of sandstone-rich cycles, followed by a bundling of dolomite-rich cycles (Dehler et al. 2012). These sequences provide information about the carbon cycle during the Neoproterozoic. In general, sandstone-rich intervals represent deposition during wetter times, with more available sediment, warmer temperatures, less glacial ice, and higher sea levels. Dolomite-rich sequences, on the other hand, indicate lower sea levels, drier conditions, decreased available sediment, cooler global temperatures, and more glacial ice (Dehler et al. 2012). High organic carbon reflects high primary

productivity and high rates of sedimentation (Dehler et al. 2005).

Unlike glacial deposits today, many Neoproterozoic glacial deposits accumulated in equatorial regions near sea level. Chuar Group glacial deposits are also associated with the extreme variability recognized in the carbon-isotope curve. Many hypotheses have been offered to explain these relationships (see a review of these hypotheses in Hoffman and Schrag 2002). The best-known hypothesis is the “snowball Earth” hypothesis which suggests that the Earth's oceans were completely frozen over for periods of at least 10 million years during Chuar time (Harland 1964; Kirschvink 1992; Hoffman et al. 1998; Dehler et al. 2012). No glacial deposits occur in the Chuar Group, but the carbon-isotope and stratigraphic data indicate that ice was on Earth between 782 million and 742 million years ago, although not at low elevations as suggested by the “snowball Earth” hypothesis. These data help confine the timing of a “snowball Earth” (Dehler et al. 2005, 2012, 2017).

The fossil record provides indirect evidence to support low-latitude glaciation during Chuar time. Lower Chuar Group deposits contain a varied community of acritarchs, suggesting that eukaryotes were diversifying (Nagy et al. 2009; Porter 2004). However, the diversity disappears in the Awatubi Member (**Zka**) of the Kwagunt Formation. Rather, blooms of the bacterium *Sphaerocongregus variabilis*, which are typically associated with worldwide “snowball Earth” glacial deposits, replace the acritarch community (Knoll et al. 1981). The bacterial blooms coincide with stratigraphic evidence for global increased ice volume (Dehler et al. 2012).

When combined with other syn-extensional deposits, the Butte Fault and Chuar syncline provide evidence for continent-scale rifting along the western margin of North America (Dehler et al. 2012). As rifting continued, basins may have served as sediment traps. Combined with changing global sea level and local rainfall patterns, enough carbon may have been buried in sediments to cause an abundant decrease in atmospheric carbon dioxide, leading to low latitude glaciation (Dehler et al. 2012).

In summary, the tectonics, stratigraphy, fossils, and carbon-isotope data of the Chuar Group in Grand Canyon offer significant information relating to Earth's history during the Neoproterozoic. The combined data suggest that the Chuar Group was deposited during, or just before, the onset of low-latitude glaciation and during the early rifting of the supercontinent Rodinia (Dehler et al. 2012). Why large-scale (possibly

snowball-Earth-style) glaciations occurred and how these changes influenced biotic evolution are questions still to be answered. The carbon-isotope curve for the Chuar Group in Grand Canyon is like data from other, worldwide Neoproterozoic strata, suggesting the cyclicity in the Chuar Group reflects a global phenomenon (Dehler et al. 2017).

Exposures of the Chuar Group (table 1) are only visible from the river immediately north of Basalt Canyon in eastern Grand Canyon. Outcrops also occur in the upper parts of several side canyons, including Nankoweap, Kwagunt, Carbon, Chuar, and Basalt canyons. The Butte normal fault separates the Chuar Group from the Colorado River to the east and Powell's Great Unconformity separates the Chuar Group from the overlying Cambrian Tapeats Sandstone (Ford and Dehler 2003).

The Mesoproterozoic and Neoproterozoic sedimentary rocks and unconformities record about 700 million years of earth history – a record longer than the entire Phanerozoic. Consequently, the depositional and tectonic history of the Late Precambrian is still poorly understood.

An Atlantic-style rift margin developed in western North America in the Late Proterozoic, and the immense length of this margin suggests that a major continental mass rifted away from the North American continent (fig. 83). Plate reconstructions for the Late Proterozoic remain a topic of debate. One model suggests that Siberia was attached to western North America in the Late Proterozoic prior to rifting and the development of the Western Cordillera (Sears and Price 1978; Timmons et al. 2003). Another hypothesis contends that Australia and Antarctica bordered North America when the supercontinent Rodinia was assembled about 1.0 billion years ago, and North America drifted away from these land masses when Rodinia broke apart between 750 million to 550 million years ago (Dehler et al. 2000; Karlstrom et al. 2000; Schwab 2000; Dehler et al. 2001; Timmons et al. 2003).

In Grand Canyon National Park, the Mesoproterozoic and Neoproterozoic Grand Canyon Supergroup (table 1) consists of a series of gently tilted sedimentary rocks that are separated from the relatively flat-lying Paleozoic sedimentary units by an angular unconformity that is part of the Great Unconformity (Hendricks and Stevenson 2003). As with all angular unconformities, the angular unconformity separating the Grand Canyon Supergroup from the overlying Tapeats Sandstone (**Ct**) represents a period of deformation and erosion.

Paleozoic Era (541 million–252 million years ago): Tectonics, Transgressions, and Assembling Pangea

In the Paleozoic Era, subduction zones bordered the coastal margin of Laurentia, the ancient landmass that would form the geological core of the North American continent. Tectonic collisions between oceanic plates and the continent formed long, linear mountain ranges (fig. 4) along the continental margin, and transgressive episodes that inundated much of the continent accompanied these orogenies. During times of tectonic quiescence, the sea regressed, and open marine environments were replaced with shallow, nearshore, estuarine and lagoonal environments often with restricted circulation.

In addition, complex animal and plant life burst upon the scene in the Paleozoic (fig. 4). The first shelled organisms evolved in the Cambrian Period, and invertebrates dominated the oceans until they were joined by fish and amphibians in the Devonian and later, reptiles. The first land plants appeared in the Silurian and the first evergreen forests in the Devonian. By the end of the Paleozoic, two great landmasses, Laurentia and Gondwana, had sutured together to form the supercontinent, Pangea (also spelled Pangaea).

Cambrian Period

With the breakup of Rodinia, one of the most dramatic marine transgressions in Earth history flooded the basement rocks on many continents with shallow marine sandstones (fig. 84). New evidence from the Grand Canyon region and southwestern North America indicates that this transgression occurred more rapidly than previously thought, covering a 300-km (480-mi)-wide cratonic region during an interval of 505 million to 500 million years ago (Karlstrom et al. 2018). The Sixtymile Formation (**Zs**) and Tonto Group in the Grand Canyon record this extraordinary transgression.

The Sixtymile Formation represents a drastic change in depositional environments from those in the Chuar Group. Rifting of Rodinia produced fault-bounded basins along the southwestern margin of Laurentia. The breccias and sandstones of the Sixtymile Formation that are exposed in Sixtymile and Awatubi Canyons and that cap Nankoweap Butte represent lacustrine, shallow marine, and fluvial environments, and the numerous landslides or subaqueous slumps suggest deposition occurred in a fault-bounded basin that formed with the reactivation of the Butte Fault (Ford and Dehler 2003; Karlstrom et al. 2018). Furthermore, the many angular unconformities and soft-sediment deformation in the Sixtymile Formation reveal repeated faulting and epeirogenic uplift on the craton.

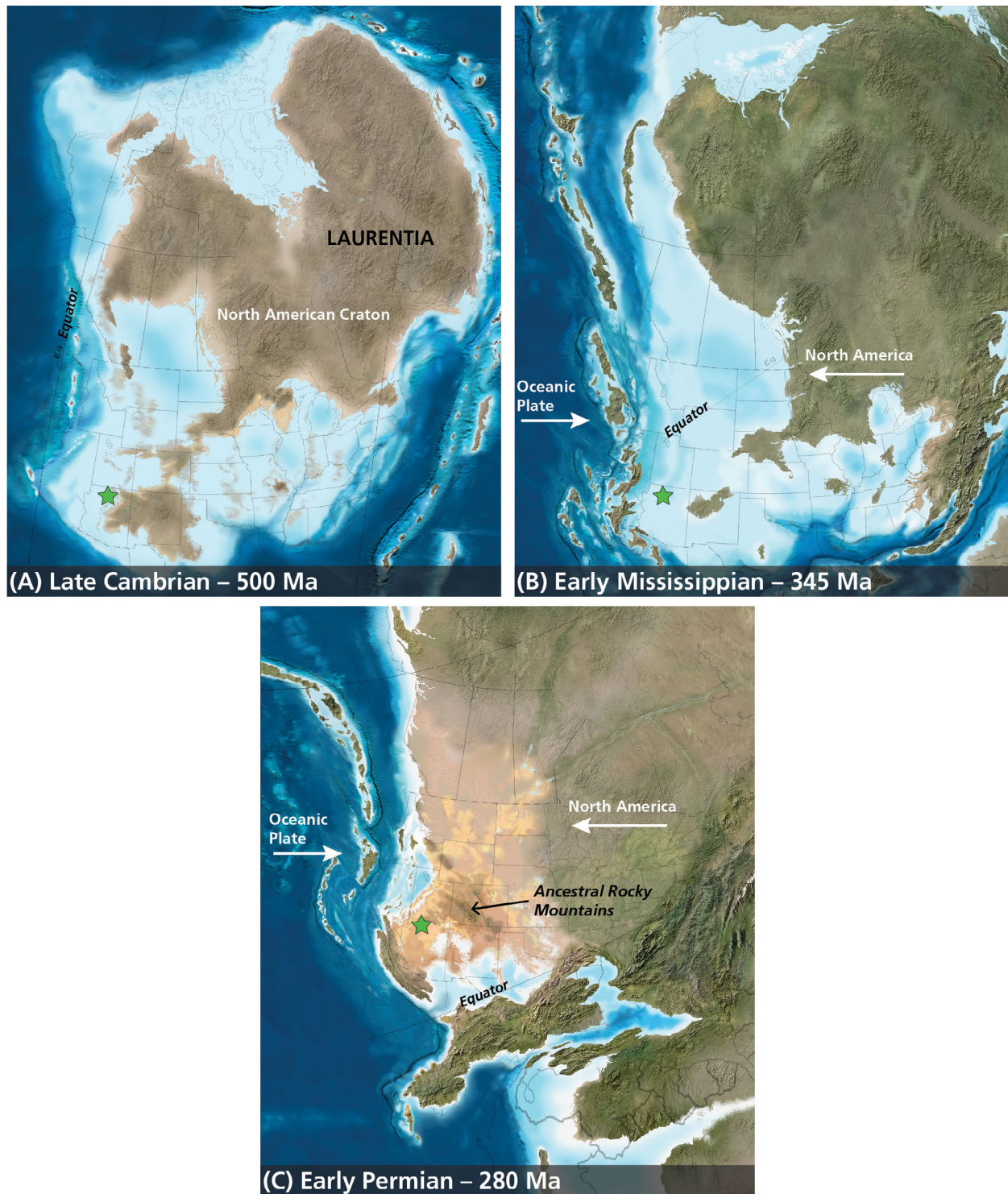


Figure 84. Paleozoic Era paleogeographic maps of North America.

(A) Shallow seas inundated the Grand Canyon region during deposition of the Cambrian Tonto Group. A subduction zone has developed off the east coast of Laurentia. (B) The Antler Orogeny extends along the entire western margin of North America, causing a major transgression and deposition of the Redwall Limestone in the Grand Canyon region. Subduction continues along the eastern and southern margins, as well. (C) In the Early Permian, nearshore, marginal marine, and coastal dunes dominate the depositional environment of the Grand Canyon region. White arrows indicate direction of plate movement. The green star approximates the location of Grand Canyon National Park. Base paleogeographic maps are from the "North American Key Time Slices" © 2013 Colorado Plateau Geosystems Inc, used under license.

Age-dates from detrital zircons and biostratigraphic data from trilobite zones indicate that the Sixtymile Formation and the formations of the Tonto Group were deposited at the same time (Karlstrom et al. 2018). The Tonto Group is exposed on the Tonto Platform and along the banks of the Colorado River in western Grand Canyon.

Stream deposits at the base of the Tapeats Sandstone (**Ct**) are overlain by beach and intertidal mudflats that grade upward into shallow, subtidal sand wave complexes. Large channels up to 4 m (13 ft) deep and 18 m (60 ft) wide at the top of the Tapeats resulted from offshore flow in a subtidal channel complex (Middleton and Elliott 2003).

The Bright Angel Shale (**Cba**) records the continued rise in sea level. This unit was originally interpreted as a continental shelf environment below wave base in which fine-grained sand and clay were deposited (Middleton and Elliott 2003). Trilobites in the unit indicate a predominantly marine depositional environment for the Bright Angel Shale in the park (Karlstrom et al. 2018). In the eastern Grand Canyon, sedimentary features such as wrinkle structures, desiccation cracks, and dune features along with carbon and strontium isotope data, ichnology, and clay mineralogy also indicate a limited fluvial–eolian influence present in the Bright Angel Shale (Baldwin et al. 2000; Gallagher 2003).

The Muav Limestone (**Cm**) documents continued transgression as deeper, subtidal environments developed. In western Grand Canyon, laminated intertidal limestones and supratidal dolomites interbedded with the deeper marine strata suggest that offshore shoals and islands, like those found in today's Caribbean Sea, emerged in the Cambrian sea (Wanless 1975; Middleton and Elliott 2003).

Mechanisms behind the rapid world-wide transgression in the Cambrian are still being studied. The transgression appears to have occurred in pulses and these punctuated episodes may have resulted from thermal subsidence following the final breakup of Rodinia combined with global eustatic changes (Dickenson 2004; Karlstrom et al. 2018). Thermal subsidence would have occurred following the separation of Gondwana from Laurentia, the two supercontinents resulting from Rodinia rifting. Correlative transgressive events occurred, for example, in New York, Jordan, Antarctica, and Australia. Hypotheses associated with this global eustatic sea-level rise include punctuated climate forcing, changes in mantle heat flow, mantle dynamics, true polar

wandering, or crystallization of the inner core (see references in Karlstrom et al. 2018).

Cambrian worldwide transgressions expanded warm, shallow seas onto the continental shelves and cratonic margins. These nutrient-rich waters may have contributed to the extraordinary evolution and relatively rapid distribution of the diverse invertebrate species found in Cambrian strata, including the trilobites, brachiopods, and other invertebrates found in the Tonto Group.

Devonian and Mississippian Periods

Following the Cambrian, subduction ceased, and the western margin of the ancestral North American continent became a passive margin, similar to the modern East Coast of the United States. Ordovician, Silurian, and Lower Devonian strata are missing in Grand Canyon National Park so that the Middle–Upper Devonian Temple Butte Formation (**Dtb**) rests unconformably above the Tonto Group. In eastern Grand Canyon and Marble Canyon, the Temple Butte Formation fills channels cut into the underlying Muav Limestone or into undifferentiated Cambrian dolomite (Beus 2003a; Potochnik and Reynolds 2003). These lens-shaped deposits are less than 30 m (100 ft) thick, but they may reach 120 m (400 ft) wide. In central and western Grand Canyon, the Temple Butte forms a continuous band of dolomite above local channel-fill deposits. The formation gradually thickens to more than 140 m (450 ft) at Iceberg Ridge, 8 km (5 mi) west of the mouth of Grand Canyon (Beus 2003a).

The original limestone of the Temple Butte Formation has been altered by dolomitization, so the depositional environment and processes are not well understood (Beus 2003a). Nevertheless, Temple Butte fossils suggest deposition in shallow, subtidal, open-marine environments in central and western Grand Canyon. Temple Butte strata in Buck Farm Canyon, eastern Grand Canyon, suggest a scenario in which regression occurred following Muav Limestone deposition and streams carved channels into the landscape. Subsequent west-to-east transgression of the sea in the late Middle Devonian filled the channels with Temple Butte limestone. Even greater thicknesses of Temple Butte Formation accumulated in western Grand Canyon. The region re-emerged during the Late Devonian, and the Temple Butte and underlying Muav Limestone were eroded down to a peneplain so that only Temple Butte limestone at the bottom of channels was preserved in eastern Grand Canyon. Renewed transgression in the middle Mississippian deposited the Redwall Limestone (**Mr**) (Potochnik and Reynolds 2003). The pulsed, transgressive–regressive episodes resulted from the

collision of the oceanic plate with the western margin of Laurentia, resulting in the Antler Orogeny (fig. 4).

The Antler Orogeny began in the Arctic in the Early Silurian as the passive margin transitioned to an active subduction zone, but it did not impact the western margin of ancestral North America until the Middle Devonian (Johnson et al. 1991). The tectonic collision between the ancestral North American plate and the Pacific plate caused a rapid sea level rise, resulting in the most extensive transgression of the Paleozoic Era (Johnson 1970; Johnson et al. 1985; Johnson and Sandberg 1989; Johnson et al. 1991).

The Antler Orogeny produced the northeast–southwest trending Roberts Mountains Thrust, a thrust sheet composed of intricately stacked Paleozoic strata exposed from Idaho through central Nevada and into southeastern California (Johnson et al. 1991). A relatively deep trough formed in front of the advancing thrust sheet, and a carbonate platform formed landward of the trough (Poole and Sandberg 1977, 1991).

The Redwall Limestone (**Mr**) in Grand Canyon National Park documents the pulsed episodes of sea level rise and fall during the Antler Orogeny (fig. 84). High-energy currents in the rising sea produced oolitic shoals in nearshore, shallow, subtidal environments (basal Whitmore Wash Member of the Redwall Limestone), and with continued transgression, skeletal grainstones and packstones accumulated under quieter water and open-marine conditions (McKee and Gutschick 1969; Beus 2003b). Abundant chert layers and bryozoan communities indicate shallower conditions as the sea regressed to the west (Thunder Springs Member of the Redwall Limestone). This regression was short-lived, however, as a second marine transgression developed open-marine, offshore conditions across northern Arizona (Mooney Falls Member of the Redwall Limestone). Great Basin National Park in Nevada contains rock units correlative with the Redwall Limestone that document the depositional environments that formed adjacent to the advancing Roberts Mountains Thrust (see the Great Basin National Park GRI by Graham 2014).

Compared with other orogenies, the Antler Orogeny was relatively rapid. In all, active thrusting lasted only about 25 million years, but the Antler Orogeny was the first event in a long-lasting compressional tectonic regime that developed on the western margin of North America. Collisions between the North American and Pacific plates would continue for hundreds of millions of years, and still occur today.

Once the Roberts Mountains Thrust was emplaced and the orogeny shut down in the Middle Mississippian,

relative sea level fell. Increasingly shallow and more restricted conditions developed during a final, slow regression of the sea (Horseshoe Mesa Member of the Redwall Limestone). A karst and cave landscape developed on the emerging Redwall Limestone platform.

As sea level continued to fall, a broadly dendritic stream valley system developed. Channels as much as 122 m (400 ft) deep cut into the underlying limestone. With subsequent sea level rise, these channels filled with the limestone and sandstone deposits that represent the intertidal and estuarine environments. This regressive/transgressive sequence is represented by three major depositional events in the Surprise Canyon Formation (**Ms**): (1) nearshore infilling of river channels incised into the karstic landscape of the lower member as sea level fell, (2) a shallow marine, bioherm, and estuarine middle member as sea level rose, and (3) a deeper open marine environment in the upper member as sea level continued to rise, displacing the estuarine environments to the east (Grover 1987; Billingsley et al. 1999; Billingsley and Wellmeyer 2004; Beus 2003b; Hodnett and Elliott 2018).

The paleovalley system and marine environments resulting from fluctuating sea level are well displayed in the Bat Tower and Fern Glen areas. In the Granite Park area, strata record a more fluvial- and ebb tide-dominated valley where sand supply and deposition were greater than marine limestone deposits.

In western Grand Canyon, the diverse fossil chondrichthyan assemblage (table 12) in the Surprise Canyon Formation documents an open marine environment (Hodnett and Elliott 2018). Limestone beds and marine fossils are almost totally missing from easternmost Grand Canyon and Marble Canyon, however. Rather, the mudstones and local conglomerates of the Surprise Canyon Formation (fig. 20) record mainly fluvial and perhaps brackish water conditions.

East-west compression associated with the Antler Orogeny reactivated Precambrian faults and generated folding and thrust faulting (Billingsley 2000b; Huntoon 2003). For example, the Precambrian Bright Angel Fault was reactivated, resulting in reverse motion and a low angle (10°), west dipping thrust fault. Uplift caused major erosion of the Redwall Limestone, including at least 46 m (150 ft) on the crest of a minor anticline at a site along the Tanner Trail.

Pennsylvanian and Permian Periods

During the Pennsylvanian, more land was accreted to the western margin of the United States by the Sonoma

Orogeny (fig. 4). The orogeny compressed and attached continental shelf and slope rocks to the continental margin and caused episodic marine transgressions onto the continental interior.

The Grand Canyon region was located approximately 10° north of the Equator. The undifferentiated Watahomigi, Manakacha, and Wescogame Formations (**PNMs**) of the Supai Group represent the Pennsylvanian Period in the Grand Canyon. In contrast to the Surprise Canyon Formation, the Watahomigi Formation contains only two chondrichthyan taxa: a xenacanth and the holocephalan *Deltodus* (Hodnett and Elliott 2018). Regional unconformities separate the formations, which, in general, were deposited on a broad coastal plain in an arid environment as sea level fell (Blakey 2003).

Earlier studies of the Supai Group suggested a fluvial, deltaic, beach, shallow-marine, or estuarine origin for the sandstones in the Grand Canyon region, but additional evidence supports an eolian origin for at least some of the sandstones (McKee 1982; Blakey 2003). For example, sandstones in the Manakacha Formation record a strong influx of eolian material from the north that began a trend of eolian deposition that would continue periodically for over 150 million years (Blakey et al. 1988; Blakey 2003). The widespread Wescogame Formation cliff unit is believed to be mostly an eolian deposit and may represent the development of a large erg (desert with sand dunes), or of several ergs, across the region (Blakey 2003).

In general, the Pennsylvanian strata in Grand Canyon National Park document fluctuating sea levels with eolian coastal dunes forming during regressions and being reworked by transgressive, shallow-marine environments, such as those found in the Watahomigi Formation. To the west, a broad, shallow, epicontinental sea encroached into the area and deposited limestones (western facies of the Manakacha and Wescogame Formations and the upper one-third of the Watahomigi Formation). To the east, mud and fine-grained sand accumulated in lagoons, on tidal flats, and in river channels.

Transgressive–regressive cycles continued in the Permian as South America sutured to the Gulf Coast, Africa and Europe collided with the eastern seaboard to form the Appalachian Mountains, and the Pacific plate collided with the ancestral North American continent (fig. 84). Ripple effects of the South America–North America suturing caused uplift of the northwest-trending Ancestral Rocky Mountains in Colorado.

In the Grand Canyon, Permian strata consist of the undivided Esplanade Sandstone and Pakoon Limestone

(**Pep**), the Esplanade Sandstone (**Pe**) (the uppermost formation in the Supai Group), Hermit Formation (**Ph**), Coconino Sandstone (**Pc**), Toroweap Formation (**Pt**), and Kaibab Formation (**Pk**) (table 1). The Esplanade Sandstone, which contains the highest percentage of sandstone of any formation in the Supai Group, forms one of the most distinctive horizons in the Grand Canyon. The formation steadily thickens to the northwest (Blakey 1980; McKee 1982; Blakey 2003).

While coastal-plain and minor eolian environments developed in the lower slope unit of the Esplanade Sandstone in eastern Grand Canyon, the Pakoon Limestone was being deposited in a variety of clear-water, shallow-marine environments that formed as the sea advanced from the west as far east as the central Grand Canyon. Esplanade eolian sand spread southward across the Colorado Plateau region and inundated these earlier deposits (Blakey et al. 1988; Blakey 2003). Evaporite minerals, chiefly gypsum, crystallized in coastal and/or continental sabkha environments, and as eolian conditions waned at the end of the Esplanade, fluvial systems spread westward into the Grand Canyon region (McKee 1982; Blakey 2003).

Poor exposures, a fine-grained texture, and general lack of interesting features make the overlying, slope-forming Hermit Shale (**Ph**) one of the least studied units in the Grand Canyon. Ledges of silty, faintly ripple-laminated sandstone represent sluggish, shallow stream deposits. The sandstone alternates with layers of slope-forming mudstone deposited in floodplains (Blakey 2003). However, the alternating cycles of sandstone and mudstone may also indicate a transition from a deltaic sequence in the eastern part of the park to a thicker, shoreline sequence in western Grand Canyon (Billingsley and Wellmeyer 2004). Mudcracks at the top of the Hermit Formation indicate a period of exposure and erosion prior to the deposition of the overlying Coconino Sandstone.

The high-angle, sweeping cross-stratification (table 6) and trace fossils (table 12) in the Coconino Sandstone record the southerly advance of very extensive, Sahara-like eolian dunes (Middleton et al. 2003). The dune field in the Grand Canyon area is part of an enormous Permian desert that extended south from Montana and is correlative with the Weber Sandstone in Utah and the Tensleep Sandstone in Wyoming and Montana. Some of the cross-beds in the Coconino Sandstone are as thick as 20 m (66 ft).

In the Grand Canyon region, the Coconino Sandstone is overlain by, or intertongues with, the Toroweap Formation, which records repeated cycles of sea

level rise and fall. The undivided Brady Canyon and Seligman Members (**Ptb**) document an incursion of the sea into the area. Evaporite and tidal flat sediments (Seligman Member) are overlain by a thick, deeper water carbonate sequence (Brady Canyon Member). Mudcracks at the top of the sequence signal a period of subaerial exposure (Turner 2003). Cyclic sedimentation of carbonate, evaporite, and eolian sandstones in the Woods Ranch Member (**Ptw**) indicate another transgressive-regressive episode. Evaporite deposits extended as far west as Nevada and probably denote restricted circulation brought on by sea level fall across the broad shelf. East of the dominantly marine carbonate-evaporite sedimentation, tidal-flat, sabkha, and eolian depositional environments persisted throughout Toroweap time (Turner 2003).

The Kaibab Formation (**Pk**) is the youngest Paleozoic rock unit on the southern Colorado Plateau and represents an ancient seaway that spread over most of the Grand Canyon region about 260 million years ago (Hopkins and Thompson 2003). This last of the Paleozoic epicontinental seas transgressed over a mixed carbonate-siliciclastic ramp that extended across northern Arizona and into southern Nevada. At times this ramp was more than 125 km (200 mi) wide (Hopkins and Thompson, 2003).

The Fossil Mountain Member (**Pkf**) of the Kaibab Formation forms a prominent cliff that weathers into distinctive pinnacles, or “hoodoos”, below the rim of the canyon. Its lithology, mineralogy, and faunal constituents change from west to east. In western Grand Canyon, the member is characterized by cherty, fossiliferous limestone with an abundant and diverse normal-marine fauna (table 12). To the east, the Fossil Mountain Member becomes increasingly siliciclastic (Hopkins and Thompson 2003).

The Harrisburg Member (**Pkh**) forms the uppermost cliffs and receding ledges along both rims of the Grand Canyon. The member thickens to the west and northwest of Kanab Creek and is thickest in northwestern Arizona, southwestern Utah, and southern Nevada. Gypsum becomes a considerable portion of the unit in southern Nevada and is mined at Blue Diamond Hill, west of Las Vegas, Nevada. Faunal assemblages (table 12) include a variety of pelecypods and gastropods, faunal types that represent hardy individuals tolerant of a greater range of environmental conditions. Normal-marine organisms, such as brachiopods, bryozoans, and crinoids, are rare, occurring as small fragments. The fauna, gypsum deposits, and silicified evaporite nodules indicate partially to highly restricted, shallow-marine environments (Hopkins and Thompson 2003).

The interbedded carbonate and siliciclastic sediments record a complex depositional history for the Kaibab Formation. The cyclic nature of these deposits document repeated shifts of subtidal, shallow-marine environments during pulsed transgressions and regressions of the sea into the region. The Fossil Mountain Member records an overall west-to-east transgressive phase of sedimentation punctuated by repeated regressive events of varying regional extent. The alternation between carbonate, siliciclastic, and evaporite deposits in the Harrisburg Member document restricted marine environments that formed during cyclic, overall westward retreat of the Kaibab Sea (Hopkins and Thompson 2003).

The Pennsylvanian and Permian Periods were times of great tectonic upheaval around the globe. All the major landmasses were coming together to form one supercontinent, Pangea. Many organisms went extinct at the end of the Paleozoic, including the once-prolific trilobites, rugose corals, and thousands of species of insects, reptiles, amphibians, and fish. Fossils in Grand Canyon National Park document the presence of many of these Paleozoic animals that are now extinct. Five million years later, at the dawn of the Mesozoic Era, the chemistry of modern oceans began to evolve towards modernity, and the first mammals and dinosaurs appeared on land.

Mesozoic Era (252 million–66 million years ago): Disassembling Pangea, Ergs, and an Inland Sea

Triassic Period

In the Early Triassic, the supercontinent Pangea reached its greatest areal extent. All the continents converged to form a single landmass, but relatively soon after Pangea was assembled, the supercontinent began to split apart (Dubiel 1994).

In the Early Triassic (251 million to 245 million years ago), Pangea was located symmetrically about the equator (fig. 85; Dubiel 1994). To the west, explosive volcanoes arose from the sea and formed a north-south trending arc of islands along the present-day border of California and Nevada (Christiansen et al. 1994; Dubiel 1994; Lawton 1994). The western Colorado Plateau region consisted of a broad continental shelf that accumulated shallow marine to coastal marine sediments while a fluvial and floodplain system developed in the eastern part of the Colorado Plateau from the erosion of Colorado’s Ancestral Rocky Mountains. These deposits became the Moenkopi Formation (**TRm**, **TRmhm**, **TRms**, **TRmw**, **TRmlm**) (Stewart et al. 1972a; Christiansen et al. 1994; Doelling 2010; Anderson et al. 2010; Huntoon et al. 2010). Plant

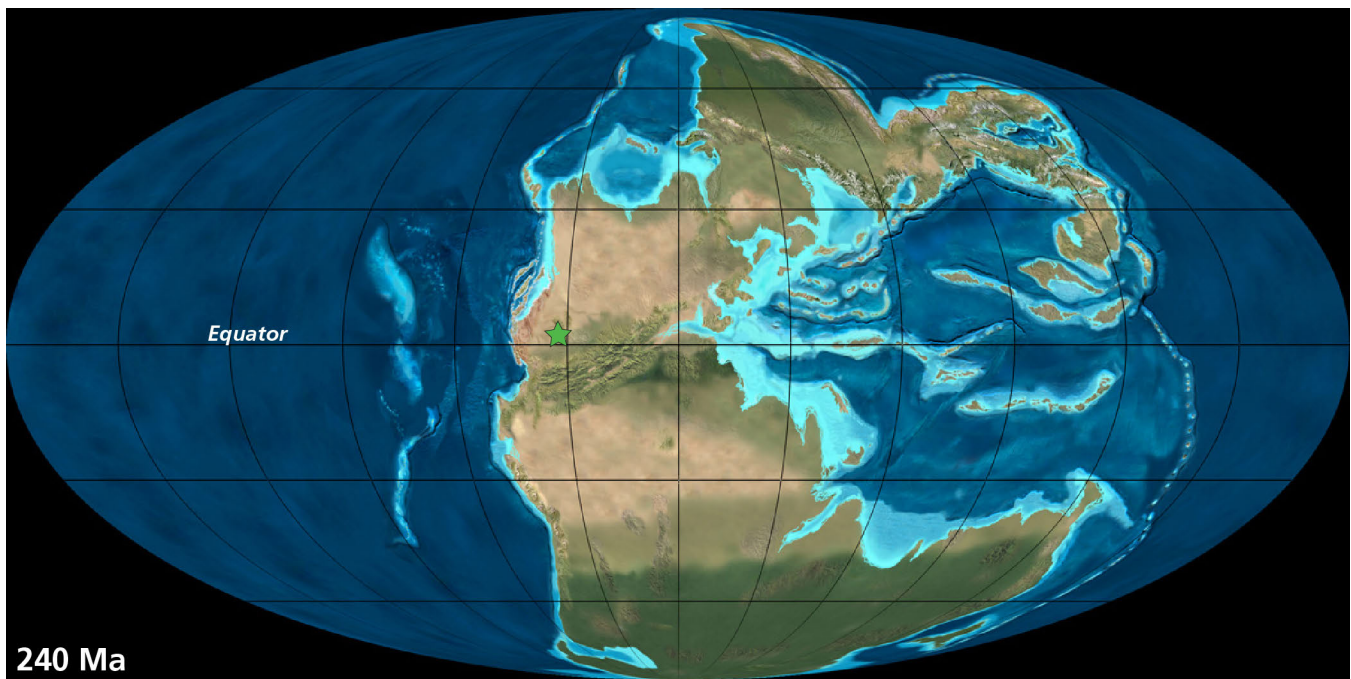


Figure 85. Paleogeographic map of Pangea.

By the Early Triassic, the supercontinent Pangea began to rift apart. The green star approximates the location of Grand Canyon National Park. Base paleogeographic map by Colorado Plateau Geosystems Inc, used under license.

and animal fossils in the Moenkopi Formation suggest a shift to a warm tropical climate with likely monsoonal, wet-dry conditions (Stewart et al. 1972a; Huntoon et al. 2010; Morris et al. 2010).

Breccia pipe and mineral emplacement accelerated during the Triassic Period when the region to the south of Grand Canyon was uplifted (Mogollon Highlands). Uplift increased hydraulic gradients within the confined Redwall-Muav aquifer, significantly enhancing groundwater circulation and corresponding dissolution and collapse (Huntoon 1996).

In the Late Triassic (237 million to 201 million years ago), streams cut valleys into the underlying Moenkopi Formation. Paleovalley geometry and channel sandstones suggest that the main trunk river flowed to the northwest, and tributaries drained highlands that had risen to the west, southwest, south, and southeast (Lucas 1993; Dubiel 1994; Lucas et al. 1997; Morris et al. 2010). The complex assemblage of alluvial, marsh, lacustrine, playa, and eolian deposits became the Chinle Formation (**TRc**) (Stewart et al. 1972b; Anderson et al. 2010). Grand Canyon National Park contains exposures of only the Shinarump Member (**TRcs**), which represents fluvial deposits that filled paleovalleys. Beyond the boundaries of the park, the overlying members include layers of bentonite, altered volcanic ash that had blown into the area from volcanic activity

in present-day Arizona and California (Christiansen et al. 1994; Anderson et al. 2010).

East of the South Rim's Desert View overlook, the Kaibab Formation is overlain by the Moenkopi Formation (**TRm**), which is capped by a resistant layer of Cenozoic volcanic rock. Triassic rocks are also preserved on the Marble Platform.

Jurassic Period

Although no Jurassic or Cretaceous rocks are mapped in Grand Canyon National Park, exposures throughout the Colorado Plateau offer an excellent record of the Jurassic and Cretaceous worlds in the southwestern United States (fig. 86). In the Jurassic, catastrophic volcanic eruptions occurred along the western margin of North America, extending from Mexico to Canada. Collision between the Farallon plate and the North American plate caused west-to-east thrusting in Nevada as additional land accreted to the continent. Inland, extensive dune fields developed in western Utah and northern Arizona. These dune fields are preserved in the Navajo Sandstone and Entrada Sandstone. Zion National Park offers excellent exposures of the Navajo Formation, and Cretaceous formations are exposed in Arizona's Navajo National Monument (Graham 2006, 2007).

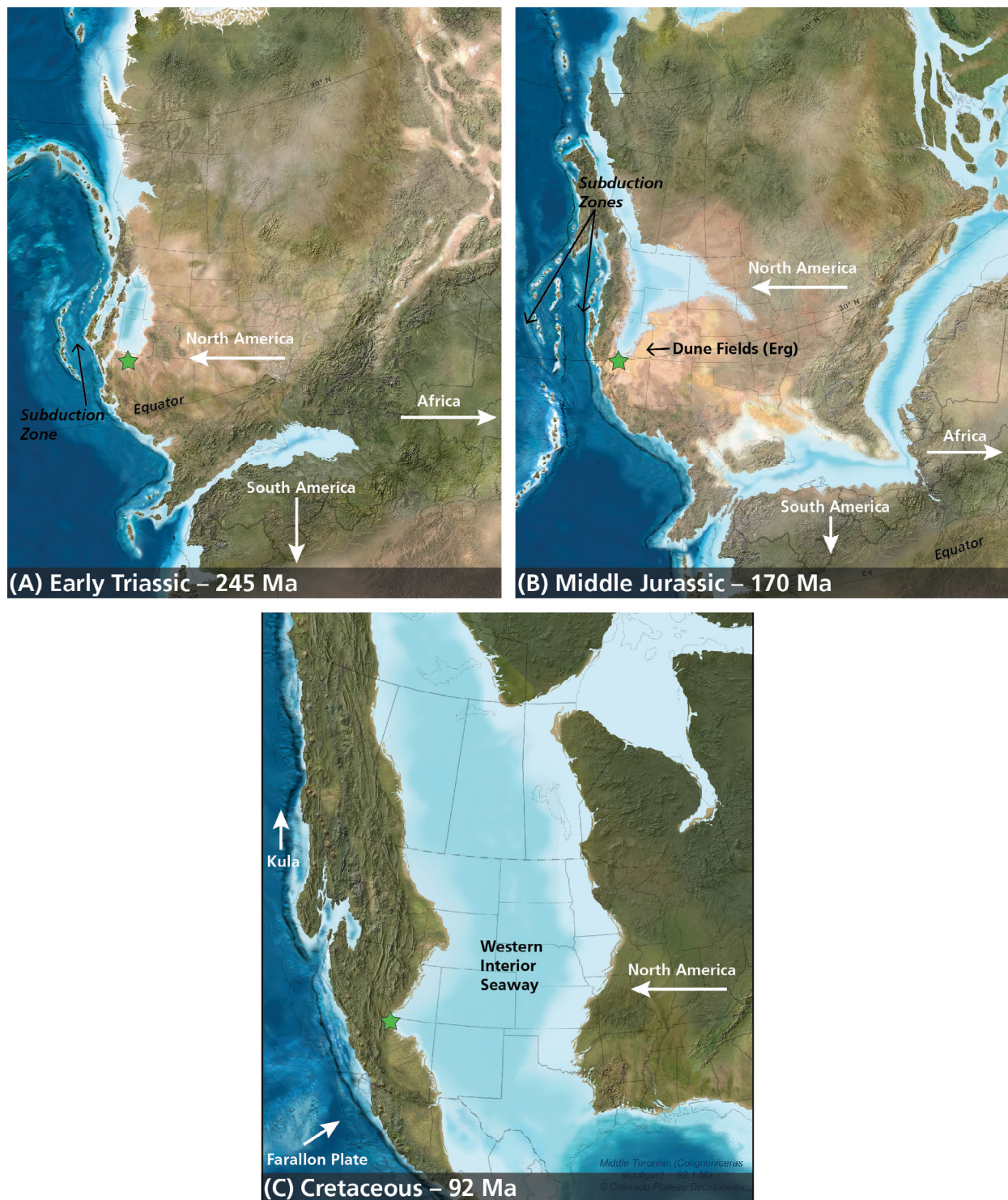


Figure 86. Mesozoic Era paleogeographic maps of North America.

A) In the Triassic, Pangea began to rift apart. Terrestrial deposits of the Moenkopi and Chinle Formations are deposited in the Grand Canyon Region. B) In the Jurassic, a shallow sea and extensive dune fields encroached into the Grand Canyon/Colorado Plateau region from the north. C) The Western Interior Seaway bisected the North American Continent in the Cretaceous (maximum highstand shown here). The darker blue represents deep marine; light blue represents shallow marine; brown is land. White arrows indicate direction of plate movement. The green star approximates the location of Grand Canyon National Park. Base paleogeographic maps are from the "North American Key Time Slices" © 2013 Colorado Plateau Geosystems Inc, used under license.

Cretaceous Period

In the Cretaceous, continued subduction produced the Sevier Orogeny, an orogeny that lasted about 90 million years and which resulted in a north–south-trending belt of folds and thrusts (called the Rocky Mountain fold-and-thrust belt) that extended from the Brooks Range in Alaska to the Sierra Madre Oriental in Mexico (Lageson and Schmitt 1994; DeCelles 2004). The Sevier Orogeny is responsible for the voluminous magma that formed the Sierra Nevada Batholith and emplaced continental-margin plutons from Mexico to the Alaskan peninsula (Oldow et al. 1989; Lawton 1994).

As thrust sheets stacked atop one another, the crust parallel to the fold-and-thrust belt began to subside, creating the Western Interior Seaway. With subsidence, sea water began to fill the basin from the Arctic region and the Gulf of Mexico. Episodic fluctuations in sea level occurred throughout the Cretaceous, culminating in the formation of the most extensive interior seaway ever to bisect the North American continent (fig. 86). The Western Interior Seaway extended from today's Gulf of Mexico to the Arctic Ocean, about 4,800 km (3,000 mi) (Kauffman 1977; Steidtmann 1993). During periods of maximum sea-level rise, the width of the basin reached 1,600 km (1,000 mi).

The seaway receded from the continental interior with the onset of the Laramide Orogeny, which occurred about 70 million to 35 million years ago (Late Cretaceous Period–Eocene Epoch). This orogeny marked a pronounced eastward shift in tectonic activity as the angle of the subducting oceanic plate flattened and compressive forces were felt far inland, east of the Grand Canyon region (fig. 87). Rather than generating volcanic mountain ranges on the west coast as in previous orogenies, the Laramide Orogeny displaced deeply buried Precambrian plutonic and metamorphic rocks that form the core of the Rocky Mountains.

The Laramide Orogeny uplifted the entire Colorado Plateau, reactivated Precambrian faults, and horizontally shortened the region across northerly trending thrust faults (Marshak et al. 2000; Billingsley and Wellmeyer 2004; Huntoon 2003). Primarily east-dipping monoclines formed in Paleozoic and Mesozoic strata and overlie deep-seated, west-dipping reverse faults. The Supai Monocline is the only southwest-dipping monocline in the Grand Canyon area (Billingsley 2000b). Monoclines in the Grand Canyon, particularly the East Kaibab and Meriwhitica monoclines, provide the finest cross sections through monoclines found on the Colorado Plateau (Huntoon 2003). Intervening blocks between faults were gently warped into broad, north-trending arches and basins.

Hanging valleys west of the Toroweap monocline and south of the Colorado River represent preserved remnants of the Laramide drainage system (Young 1999; Huntoon 2003). Meandering patterns of the oldest paleovalleys reveal that original gradients were gentle. Erosion removed all but the upper part of the Muav Limestone and beveled the Meriwhitica monocline on the Hualapai Plateau to very low relief (Huntoon 2003).

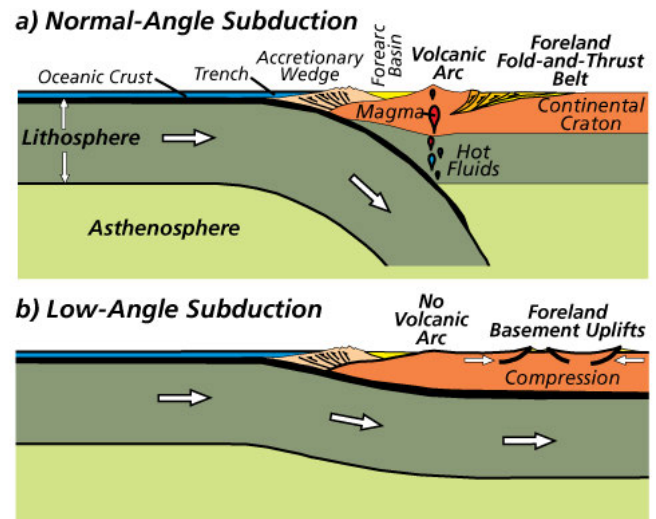


Figure 87. Schematic contrasting the subduction angles of the Sevier Orogeny and Laramide Orogeny. (A) A relatively steep subduction angle caused the Sevier Orogeny, and this steeper angle is typical of most subduction zones. A volcanic arc usually occurs above the subduction zone. (B) The subduction angle flattened out in the Late Cretaceous, causing compressive forces to be felt far inland and causing the Laramide Orogeny and subsequent rise of the Rocky Mountains. Schematic courtesy of Lillie (2005, figure 10.29).

Cenozoic Era (66 million years–present day): Crustal Extension and Carving the Grand Canyon

Renewed uplift in the Eocene cut off meanders and incised ancient valleys. Incision in the vicinity of the Hurricane fault zone carved the Peach Springs paleovalley over 500 m (1,600 ft) below the Laramide surface (Huntoon 2003).

About 45 million years ago (Eocene Epoch), oceanic crustal subduction along the west coast slowed, the descent angle for the descending oceanic slab steepened under the North American plate, and deformation ceased in the Grand Canyon region (Dickinson 1981; Huntoon 2003).

Nearly all the Cenozoic and Mesozoic sedimentary rocks have been removed by erosion from the Grand Canyon area. Incision of the Colorado River has exposed about 1.6 km (1 mi) of strata, but during the Mesozoic Era, a comparable thickness of terrestrial and marine rock layers buried the Kaibab Formation and covered the entire southwestern portion of the Colorado Plateau (Billingsley 1989; Morales 2003). When the Laramide Orogeny uplifted the southwestern Colorado Plateau, erosion removed these Mesozoic sediments from the Grand Canyon region (Lucchitta 2003).

Another 0.8 km (0.5 mi) or more of terrestrial sediments and volcanics were removed when the region was uplifted in the Oligocene epoch (Elston and Young 1989; Morales 2003). The Miocene intrusive (**Ti**) and volcanic rocks of the Hualapai Plateau (**Tv**) are the oldest Cenozoic rocks mapped in the park. Timing of the Miocene volcanics coincided with crustal extension that resulted in the Basin and Range Province. About 5–6 million years ago, in the Pliocene Epoch of the Neogene Period, the Colorado River began carving the Grand Canyon. Incision of sedimentary rocks, especially limestone, and the wet climate that accompanied the Pleistocene ice ages in the Quaternary Period influenced cave formation in Grand Canyon National Park (fig. 88).

Neogene Period and Extensional Tectonics

Complex plate tectonic interactions occurred along the western continental margin in Late Oligocene time, following the Laramide Orogeny. The first significant extension of the upper crust to affect the surface since late Precambrian time occurred in the Miocene (23.3 million–5.3 million years ago) (Huntoon, 2003). The Pacific-Farallon and North American plates obliquely converged upon each other, resulting in right-lateral transform faulting (which would eventually become the San Andreas Fault in the Pliocene) and crustal extension in present-day Basin and Range in Nevada (Dickinson 1981; Huntoon 2003).

Island arc volcanism southwest of the Colorado Plateau produced early Miocene basalt flows that overlie undated gravel deposits of the Buck and Doe Conglomerate, mapped southwest of Grand Canyon National Park (Young 1999). The 18.5-million-year-old (early Miocene) Peach Springs Tuff, a welded rhyolitic ash-flow tuff mapped with the volcanic rocks of the Hualapai Plateau (**Tv**), occupies valleys formed in the Paleogene Period and overlies basalt flows in Milkweed and Peach Springs Canyons (Young and Brennan 1974; Huntoon 2003).

The earliest normal faulting in the Grand Canyon area occurred along the Grand Wash Fault in the Middle–

Late Miocene (Faulds et al. 1997; Huntoon 2003). Normal faulting migrated eastward onto the Colorado Plateau, initially offsetting strata along the Hurricane Fault approximately 5 million years ago in the early Pliocene. Extension continued into the Pleistocene, offsetting strata along the Toroweap Fault about 1.5 million years ago (fig. 88; Billingsley 2000a; Billingsley 2000b; Billingsley and Wellmeyer 2004; Fenton et al. 2001a; Huntoon 2003). Reverse drag along the fault caused strata on the hanging wall to dip inward toward the fault plane and increased the displacement along the faults.

The Hurricane and Toroweap Faults offer the most complete records of Pliocene and younger faulting in the Grand Canyon region. For example, rocks deposited across the Hurricane Fault near Whitmore Wash display a minimum of four faulting events that have occurred since the Pliocene (Fenton 1998; Fenton et al. 2001a, 2001b; Huntoon 2003). All the faults on the Uinkaret Plateau may have become active 3.5 million to 2 million years ago (Billingsley and Workman 2000). Scarps in the alluvium along the Aubrey, Toroweap, and Hurricane faults indicate continued Quaternary activity in the western Grand Canyon region, as well (Huntoon 2003).

The west-facing Grand Wash Fault scarp marks the western margin of the Colorado Plateau from the area north of the Utah state line southward around the entire Hualapai Plateau to a terminus south of the Cottonwood Mountains. Displacement along the fault was enough to sever the northward flow of streams across the Colorado Plateau boundary by late Early Miocene time. In addition to the fault, two other processes worked to further disrupt streams from crossing onto the Colorado Plateau: 1) extensional subsidence and fragmentation of the headlands in the Basin and Range Province, and 2) partial burial of the southern plateau margins by Miocene volcanics (Huntoon 2003).

From Late Miocene and into the Holocene, basalts erupted through vents on the plateaus (Best and Brimhall 1970; Billingsley and Wellmeyer 2004; Huntoon 2003). Regional structure appears to have influenced volcanism. Igneous dikes intruded along fractures that parallel nearby normal faults, for example. A shift in fault activity from the Grand Wash to the Hurricane–Toroweap zones coincided with an eastward shift in volcanism. However, although volcanic cones on the Uinkaret Plateau align parallel to faults, they occur in the areas between the faults (Dutton 1882; Koons 1945; Huntoon 2003). The dikes and vents tended to localize on extended fractures in the Paleozoic section near the surface. Late Cenozoic extension either created or opened the fractures through which the magma flowed.

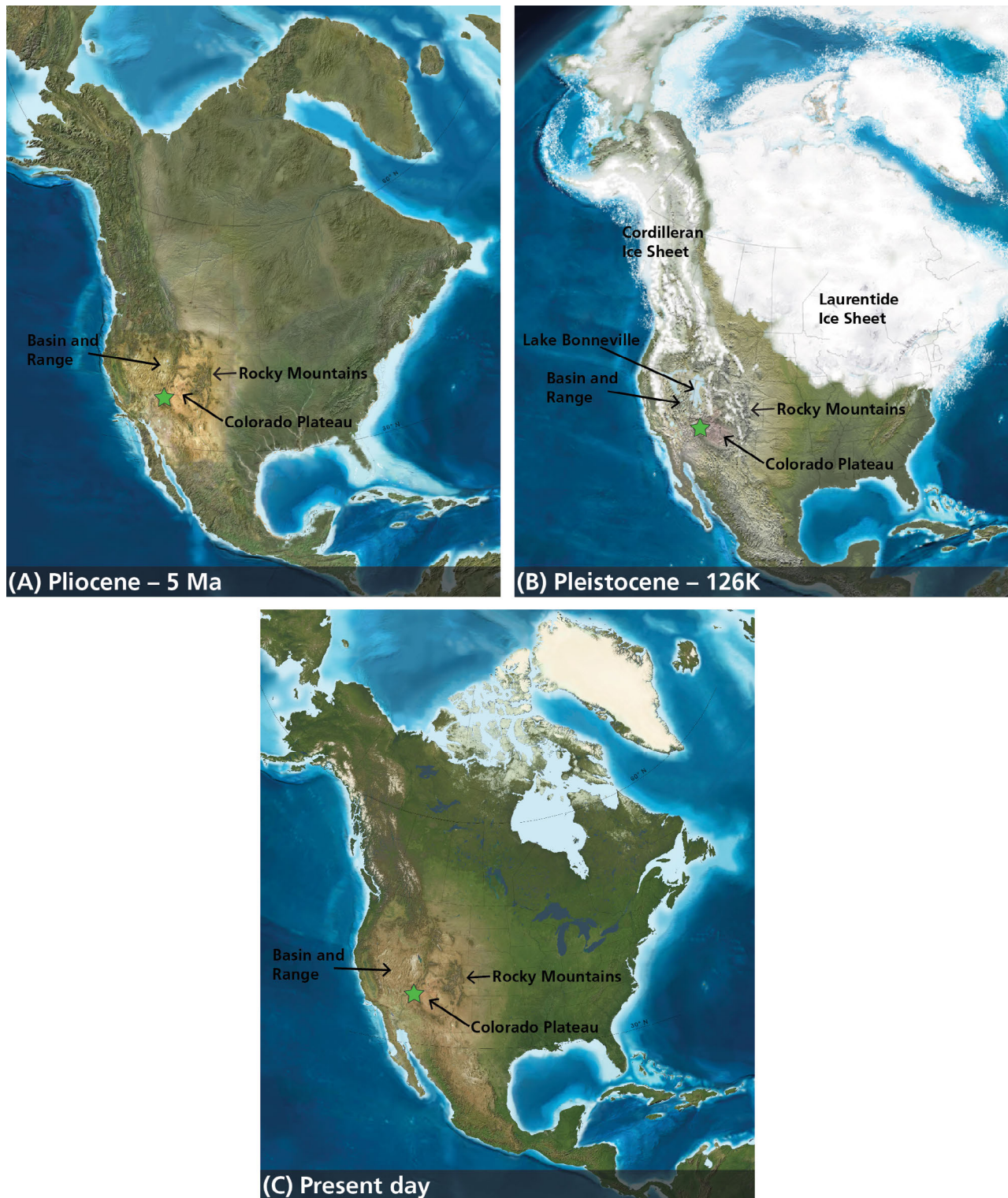


Figure 88. Cenozoic Era paleogeographic and present-day maps of North America. (A) By the Pliocene Epoch, crustal extension had established the Basin and Range and Colorado Plateau Provinces. (B) During the Pleistocene Epoch ice ages, the climate became wetter than during the Holocene, influencing cave formation in the Redwall Limestone. (C) Present day Grand Canyon region. The Grand Canyon has been carved within the last 6 million years. The darker blue represents deep marine; light blue represents shallow marine; brown is land. White arrows indicate direction of plate movement. The green star approximates the location of Grand Canyon National Park. Base paleogeographic maps are from the “North American Key Time Slices” © 2013 Colorado Plateau Geosystems Inc, used under license.

**Quaternary Period (the past 2.6 million years):
Continued Evolution of the Colorado River and
Grand Canyon**

The Colorado River traverses two contrasting landscapes in Arizona: canyon country and plateau country. Highly dissected terrain, usually with substantial topographical relief, characterizes the canyon country, typified by the Grand Canyon. On the other hand, the plateau country, typified by the Navajo and Hopi reservations, features low relief, wide mature valleys, and scarps that develop on beds of contrasting resistance. The younger canyon country encroaches upon the older plateau country.

John Wesley Powell believed that the Colorado River had a simple history, one that began with uplift and subsequent canyon cutting in the Eocene. In this view, the river was part of an integrated drainage system since its inception, and the course of the river has not changed over time. Since erosion of the plateau country is pervasive, early geologists inferred that denudation, canyon cutting, and the uplift ultimately responsible for both must have occurred a long time ago (Lucchitta 2003).

In the 1930s and 1940s, geologists studying the Basin and Range Province found that the Colorado River appeared younger than the Miocene and Pliocene deposits it had eroded. Miocene drainage systems did not resemble the present Colorado River system. Field studies could not find any evidence supporting the hypothesis that the Colorado River flowed through the interior basins of the Basin and Range Province during Miocene deformation (Young 1966; Lucchitta 1967, 2003; Hunt 1969, 1976).

In 1967, McKee et al. proposed that the Colorado River had undergone a multiphase history. Rather than flowing west into the Basin and Range, they suggested that the ancestral Colorado River flowed southeastward along the course of the Little Colorado River and Rio Grande to the Gulf of Mexico. They believed that headward erosion of a Pliocene river that emptied into the Gulf of California captured the ancestral Colorado

River somewhere in eastern Grand Canyon, thus establishing the present course and initiating incision of the Grand Canyon. Their hypothesis suggested that drainage systems evolved continually, chiefly through headward erosion in response to tectonic movements. However, evidence was not found to support an ancient river flowing through the western Grand Canyon region, into the Basin and Range Province, and emptying into the Gulf of California or southeastward drainage along the Little Colorado and Rio Grande Rivers. These early field studies initiated a lively and vigorous debate on the origin and evolution of the Colorado River and the excavation of the Grand Canyon that continues today. Most research agrees that much of the canyon was carved in the past 6 million years.

By early Pleistocene time, the Colorado River had excavated the Grand Canyon to within 15 m (50 ft) of its present depth, but incision rates were not uniform throughout the canyon (McKee et al. 1967; Huntoon 2003). Incision rates based on displacement rates on the Toroweap and Hurricane faults, Quaternary basalts, uplift of the Colorado Plateau, and other criteria indicate higher incision rates for eastern Grand Canyon compared to western Grand Canyon (Lucchitta et al. 2001; Fenton et al. 2001a, 2001b; Pederson et al. 2002b, 2013). In eastern Grand Canyon, downcutting rates of 400 m/million years (1,300 ft/m.y.) were at least double the 70–160 m/m.y. (230–520 ft/m.y.) rates measured west of the Hurricane and Toroweap faults (Fenton et al. 2001a; Pederson et al. 2002b). Incision rates at Lees Ferry and farther upstream were even higher (Pederson et al. 2013). Incision rates over the last 1 million years also contrast sharply between western Grand Canyon and eastern Grand Canyon (table 21). Rather than a uniform gradient and incision rates controlled by the base level of the lower Colorado River, the Colorado River and its tributaries appear to respond quickly to local base level changes and to incise and readjust their channels soon after equilibrium has been disrupted (Willis and Biek 2001).

Table 21. Incision rates of the Colorado River over the last 1 million years.

Calculations are recorded in meters per thousand years (m/ka).

River	West Grand Canyon (m/ka)	East Grand Canyon (m/ka)	Reference
Colorado	0.12	0.4	Davis et al. 2001
Colorado	0.09–0.16	0.31–0.50	Lucchitta et al. 2001
Colorado	Not reported in reference	0.5	Hanks et al. 2001
Virgin	0.06–0.15	0.35–0.40	Willis and Biek 2001

U-Pb age dates from mammillaries from Grand Canyon caves also indicate that the confined caves get progressively younger from west to east in Grand Canyon (Polyak et al. 2008). For example, mammillaries in the Grand Wash Cliffs grew approximately 8 million years ago while mammillaries in Shinumo Creek Cave in Marble Canyon are only 3.5 million years old. Assuming the water table declined at rates equivalent to incision rates, mammillary growth data record faster incision rates for eastern Grand Canyon than for western Grand Canyon. However, incision rates based on speleothem growth do not directly correspond to incision rates mentioned in the previous paragraph. Mammillary growth suggests that incision rates for western Grand Canyon ranged from 3.2 m (1.0 ft) to 7.2 m (2.2 ft) per million years over the past 17 million years, and eastern Grand Canyon incision rates varied from 166 m (51 ft) to 411 m (125 ft) per million years (Polyak et al. 2008).

Although the age of the Colorado River and its incision rates can be constrained by various methods, the interpretation of age dates and the processes by which the Colorado River developed its present course remains open to speculation. Hypotheses include headward erosion by the lower Colorado River, Cenozoic uplift, and multiple lake-overflow events (Lucchitta 2003; Spencer and Pearthree 2001; Meek and Douglas 2001). Active research continues to test these hypotheses.

Gravity Slides and Canyon Widening

Extreme topographic relief creates tremendous stress gradients within the Grand Canyon walls. Associated failure of the rocks yields valley anticlines, high-angle gravity faults, and rotational landslides that are unrelated to deep-seated processes. These gravity slides are responsible for widening the Grand Canyon to its present width. If the Grand Canyon had formed solely by channel incision, the vertical gorge would be only 60–75 m (200–250 ft) wide, the average width of the Colorado River channel (Hamblin 2003). Instead, the Inner Gorge at the level of Temple Butte Limestone is currently about 600 m (2,000 ft) wide. Clearly, slope retreat, not downcutting by the Colorado River, widened most of the Inner Gorge (Hamblin, 2003).

Valley anticlines formed when the saturated mudstone layers of the Cambrian Muav Limestone (**Cm**) and underlying Bright Angel Shale (**Cba**) flowed laterally from under the canyon walls (Huntoon and Elston 1980; Huntoon 2003). The lithostatic load under 640-m (2,100-ft) canyon walls drives the flowage, and the floor of the canyon arches up in response to the compression across it. A valley anticline with an axis parallel to the Colorado River occurs between Fishtail and Parashant

Canyons. Kanab, Tuckup, and other tributary canyons also contain valley anticlines.

Cliff failure occurs because oversteepened slopes collapse. When the Colorado River or its tributaries erode into shale, the buttressing support fails, and blocks of rocks calve off the canyon wall until the slope on the shale is wide enough to support the weight of the overlying rocks. Brittle failure of rocks overlying the Bright Angel Shale triggers high-angle gravity faults, which occur across narrow ridges between deep canyons in which the Bright Angel Shale is exposed. The faults do not penetrate the rocks below the Bright Angel Shale. Once gravity faults form, erosion constructs a chain of buttes in place of the former ridge separating two canyons. Continued erosion isolates the buttes and the faults vanish (Huntoon 2003).

Rotational slides significantly contribute to canyon widening and displace the Colorado River channel. In a rotational slide, massive blocks detach from the canyon wall and glide into the canyon. The block detaches along an upward-facing concave normal fault, and as it does, it rotates backward against the curved fault surface. The largest failures in Grand Canyon involve the section of strata from the Cambrian Bright Angel Shale (**Cba**) upward through the Permian Esplanade Sandstone (**Pe**), a section as much as 490 m (1,600 ft) thick (Huntoon 2003). Smaller rotational slides involve the Cambrian Tapeats Sandstone (**Ct**) that detaches above the ductile Precambrian Galeros Formation (**Zg**) in eastern Grand Canyon.

Progressive rotational sliding above the Galeros Formation caused the large setback of the North Rim along the east side of the Walhalla Plateau in eastern Grand Canyon National Park. Relatively young rotational slides occur along the Colorado River between Deer and Fishtail Canyons and downstream from Whitmore Wash. A 1.9-km-(1.2-mi-)long slide blocked the Colorado River near 205-Mile Canyon and displaced the river eastward (Huntoon 2003).

An older rotational slide off the south side of Cogswell Butte blocked the Colorado River halfway between Deer and Tapeats Canyons. The river bypassed the slide and now the old channel lies 70 m (210 ft) above the modern channel (Huntoon 2003). The oldest slides occur in Surprise Valley. Two or more rows of huge rotational blocks have displaced the mouth of the Tapeats Canyon to the east. Remnants of a paleochannel buried by rotational slides occur about 290 m (900 ft) above the present Colorado River (Huntoon 2003) and suggest a Neogene date for the slide (23 million to 2.6 million years ago).

Carbon Butte contains the farthest traveled rotational slide block in the Grand Canyon. Following the south-plunging axis of a Precambrian syncline, the slide block traveled 1.6 km (1 mi) and fell 550 m (1,800 ft) from its starting point (Ford et al. 1970; Huntoon 2003).

Rather than eroding in one continuous, imperceptibly slow, constant rate of slope retreat, the Grand Canyon widened in relation to the style and degree of tectonic uplift. According to Hamblin (2003), widening occurred through a series of small pulses that shifted the slopes back to a state of equilibrium following tectonic disturbance. Long periods of quiescence occur once equilibrium is reached (Hamblin, 2003).

Late Cenozoic Lava Dams

The lava dams described in the “Geologic Features and Processes” section add essential information regarding the history of the Grand Canyon over the last 830,000 years (Crow et al. 2015; see the “Geologic Features and Processes” section). Five episodes of volcanic activity, originating from the Uinkaret volcanic field, resulted in lava dams in the Lava Falls and Whitmore Wash region (table 9).

The lava dams failed in stages (Crow et al. 2015). While the upstream parts of some dams failed quickly, the down-stream distal sections failed gradually, allowing lakes to form that lasted tens to hundreds of years to perhaps millennia.

Recent Geomorphology

The Holocene history of the Colorado River in Grand Canyon includes terraces and related alluvium, tributary debris fans, and sand dunes (Burke et al., 2003). River terraces described by Burke et al. (2003) and in the “Geologic Features and Processes” section of this report can be extensive and may have been floodplains. In a broad sense, alluvial deposits resulted from flood-related aggradation of the river banks. Overbank deposits enriched the floodplains and evidence suggests

that alluvium of Pueblo II age was locally cultivated by Ancestral Puebloans (Burke et al. 2003). The late Holocene alluvia are separated by two major periods of erosion and nondeposition: 1) the oldest, between 300–700 CE, and 2) the youngest, between 1200–1400 CE.

Prehistoric tributary debris fan deposits control the position of the channel. These boulder-filled, roughly fan-shaped deposits resist erosion and are responsible for forming rapids and forcing the river to flow around the fans. High-level terraces occupy areas of low-current velocity that develop around debris fans. Wind shapes the alluvial deposits into dunes, sand sheets, and mounds of wind-blown sand.

Age dates from dissolution pits on carbonate boulders suggest that the oldest surface on a debris fan is 4,700 calendar years before present (CYBP) (Burke et al. 2003). Dissolution pits require several centuries to develop, and the youngest pit formed between 500 and 600 CYBP. In general, 75% of the dated surfaces are younger than 2,800 years ago (Burke et al. 2003).

The present channel system has been out of balance since the construction of Glen Canyon Dam. Prior to the dam, large mainstream floods distributed sediment discharged into the Colorado River by debris flows. Artificial floods from Glen Canyon Dam have replaced these natural flood events.

In approximately 6 million years, a relatively short geological timeframe, a canyon as intricate and immense as the Grand Canyon was carved in some of the oldest rocks on the continent. The evolution of the Grand Canyon illustrates the dynamic processes affecting the landscape. Extensional faulting continues to fragment the plateaus surrounding the Grand Canyon. Erosion continues to bevel the uplifting Colorado Plateau. Whether viewing the canyon from the rim, the river, or along the trails, Grand Canyon offers the visitor a magnificent example of the wonder and power of natural processes to shape an iconic landscape.

Geologic Map Data

A geologic map in GIS format is the principal deliverable of the GRI program. GRI GIS data produced for the park follows the source maps listed here and includes components described in this chapter. Posters display the data over imagery of the park and surrounding area. Complete GIS data are available at the GRI publications website: <http://go.nps.gov/gripubs>.

Geologic Maps

A geologic map is the fundamental tool for depicting the geology of an area. Geologic maps are two-dimensional representations of the three-dimensional geometry of rock and sediment at or beneath the land surface (Evans 2016). Colors and symbols on geologic maps correspond to geologic map units. The unit symbols consist of an uppercase letter indicating the age and lowercase letters indicating the formation's name. Other symbols depict structures such as faults or folds, locations of past geologic hazards that may be susceptible to future activity, and other geologic features. Anthropogenic features such as mines or quarries, as well as observation or collection locations, may be indicated on geologic maps. The American Geosciences Institute website, <http://www.americangeosciences.org/environment/publications/mapping>, provides more information about geologic maps and their uses.

Geologic maps are typically one of two types: surficial or bedrock. Surficial geologic maps typically encompass deposits that are unconsolidated and formed during the past 2.6 million years (the Quaternary Period). Surficial map units are differentiated by geologic process or depositional environment. Bedrock geologic maps encompass older, typically more consolidated sedimentary, metamorphic, and/or igneous rocks. Bedrock map units are differentiated based on age and/or rock type. GRI produced a bedrock map for Grand Canyon National Park.

Source Maps

The GRI team does not conduct original geologic mapping. The team digitizes paper maps and compiles and converts digital data to conform to the GRI GIS data model. The GRI GIS data set includes essential elements of the source maps such as map unit descriptions, a correlation chart of units, a map legend, map notes, cross sections, figures, and references. These items are included in the `grca_geology.pdf`. The GRI team used the following sources to produce the GRI GIS data set for Grand Canyon National Park. These sources also provided information for this report.

- Billingsley, G.H., and Priest, S.S., 2013, Geologic Map of the Glen Canyon Dam 30' x 60' Quadrangle, Coconino County, Arizona, U.S. Geological Survey, Scientific Investigations Map SIM-3268, 1:100,000 scale.
- Billingsley, G.H., Stoffer, P.W., and Priest, S.S., 2012, Geologic Map of the Tuba City 30' x 60' Quadrangle, Coconino County, Arizona, U.S. Geological Survey, Scientific Investigations Map SIM-3227, 1:50,000 scale.
- Billingsley, G.H., Priest, S.S., and Felger, T.J., 2008, Geologic Map of the Fredonia 30' x 60' Quadrangle, Mohave and Coconino Counties, Northern Arizona, U.S. Geological Survey, Scientific Investigations Map SIM-3035, 1:100,000 scale.
- Billingsley, G.H., Priest, S.S., and Felger, T.J., 2007, Geologic Map of the Cameron 30' x 60' Quadrangle, Coconino County, Northern Arizona, U.S. Geological Survey, Scientific Investigations Map SIM-2977, 1:100,000 scale.
- Billingsley, G.H., Block, D.L., and Dyer, H.C., 2006, Geologic Map of the Peach Springs 30' x 60' Quadrangle, Mohave and Coconino Counties, Northwestern Arizona, U.S. Geological Survey, Scientific Investigations Map SIM-2900, 1:100,000 scale.
- Billingsley, G.H., Felger, T.J., and Priest, S.S., 2006, Geologic Map of the Valle 30' x 60' Quadrangle, Coconino County, Northern Arizona, U.S. Geological Survey, Scientific Investigations Map SIM-2895, 1:100,000 scale.
- Billingsley, G.H., and Wellmeyer, J.L., 2004, Geologic Map of the Mount Trumbull 30' X 60' Quadrangle, Mohave and Coconino Counties, Northwestern Arizona, U.S. Geological Survey, Geologic Investigations Series Map I-2766, 1:100,000 scale.
- Billingsley, G.H., and Hampton, H.M., 2000, Geologic Map of the Grand Canyon 30' X 60' Quadrangle, Coconino and Mohave Counties, Northwestern Arizona, U.S. Geological Survey, Geologic Investigations Series Map I-2688, 1:100,000 scale.

GRI GIS Data

The GRI team standardizes map deliverables by using a data model. The GRI GIS data for Grand Canyon National Park was compiled using data model version 2.1, which is available at <http://go.nps.gov/gridatamodel>. This data model dictates GIS data structure, including layer architecture, feature attribution, and relationships within ESRI ArcGIS software. The GRI website (<http://go.nps.gov/gri>) provides more information about the program's products.

GRI GIS data are available on the GRI publications website <http://go.nps.gov/gripubs> and through the NPS Integrated Resource Management Applications (IRMA) Data Store portal <https://irma.nps.gov/DataStore/Search/Quick>. Enter "GRI" as the search text and select a park from the unit list.

The following components are part of the data set:

- A GIS readme file ([grca_gis_readme.pdf](#)) that describes the GRI data formats, naming conventions, extraction instructions, use constraints, and contact information;
- Data in ESRI geodatabase GIS format;
- Layer files with feature symbology (table 22);
- Federal Geographic Data Committee (FGDC)–compliant metadata;
- An ancillary map information document ([grca_geology.pdf](#)) that contains information captured from source maps such as map unit descriptions, geologic unit correlation tables, legends, cross-sections, and figures;
- An ESRI map document ([grca_geology.mxd](#)) that display the GRI GIS data; and
- A version of the data viewable in Google Earth ([grca_geology.kmz](#); table 5). Point data with symbology does not reproduce accurately in Google Earth, therefore point data layers are not included.

GRI Map Posters

Four posters of the GRI GIS draped over shaded relief images of the park and surrounding area are included with this report. Not all GIS feature classes are included on the posters (table 22). Geographic information and selected park features have been added to the posters. Digital elevation data and added geographic information are not included in the GRI GIS data, but are available online from a variety of sources. Contact GRI for assistance locating these data.

Table 22. GRI GIS data layers for Grand Canyon National Park map.

Data Layer	On Poster?	Google Earth Layer?
Geologic Cross Section Lines	No	No
Geologic Attitude and Observation Localities (strike and dip)	No	No
Geologic Point Features (breccia pipes)	No	No
Geologic Measurement Localities (fault displacement amounts)	No	No
Hazard Point Features (sinkholes and collapse structure/features)	No	No
Mine Point Features (NPS access only)	No	No
Volcanic Point Features (volcanic vents)	No	No
Map Symbology (fold and fault symbols)	Yes	No
Linear Dikes (Proterozoic intrusive rocks, Ydi)	Yes	Yes
Geologic Line Features (fractures)	No	No
Volcanic Line Features (basalt flow directions)	Yes	No
Faults	Yes	Yes
Folds	Yes	Yes
Geologic Contacts	No	Yes
Geologic Units	Yes	Yes

Use Constraints

Graphic and written information provided in this report is not a substitute for site-specific investigations. Ground-disturbing activities should neither be permitted nor denied based upon the information provided here. Please contact GRI with any questions.

Minor inaccuracies may exist regarding the locations of geologic features relative to other geologic or geographic features on the poster. Based on the published source map scale (1:50,000 to 1:100,000) and US National Map Accuracy Standards, geologic features represented in the geologic map data are horizontally within 25 m (83 ft) to 51 m (167 ft) of their true locations.

Even though most of the source map citations state 1:100,000 scale, the GIS data received from the source mappers was compiled from 1:24,000 scale data and contained that more detailed data. The result is a very rich dataset that is far more detailed than the source scales suggest.

Literature Cited

These references are cited in this report. Contact the Geologic Resources Division for assistance in obtaining them.

- Allison, L. 2016. Northwest Arizona earthquake swarm March–May 2016. Arizona Geological Survey, Tucson, Arizona. <https://youtu.be/glEkbsqnhQ> (accessed 11 May 2016).
- Anderson, P. B., G. C. Willis, T. C. Chidsey, Jr., and D. A. Sprinkel. 2010. Geology of Glen Canyon National Recreation Area, Utah-Arizona. Pages 309–347 in D. A. Sprinkel, T. C. Chidsey, Jr., and P. B. Anderson, editors. Geology of Utah’s parks and monuments. Publication 28 (third edition). Utah Geological Association, Salt Lake City, Utah.
- Anthony, J. W., S. A. Williams, R. A. Bideaux, and R. W. Grant. 1995. Mineralogy of Arizona. Third edition. University of Arizona Press, Tucson, Arizona.
- Audra, P., L. Mocochain, J. Y. Bigot, and J.-C. Nobecourt. 2009. The association between bubble trails and folia: a morphological and sedimentary indicator of hypogenic speleogenesis by degassing, example from Adaouste Cave (Provence, France). *International Journal of Speleology* 38(2):93–102.
- Babcock, R. S. 1990. Precambrian crystalline core. Pages 11–28 in S. S. Beus and M. Morales, editors. *Grand Canyon geology*. Oxford University Press, New York, New York.
- Baldwin, C. T., E. Rose, P. K. Strother, and J. Beck. 2000. The paleoecology of the Bright Angel Shale in the eastern Grand Canyon. *Geological Society of America Abstracts with Programs* 32:224.
- Ballentine, C. J., D. Porcelli, and R. Wieler. 2001. 300-Myr-old magmatic CO₂ in natural gas reservoirs of the west Texas Permian basin. *Nature* 409:327–331.
- Bates, B. C., Z. W. Kundzewicz, S. Wu and J. P. Palutikof, editors. 2008. *Climate Change and Water*. Technical Paper VI. Intergovernmental Panel on Climate Change, IPCC Secretariat, Geneva, Switzerland. <http://ipcc.ch/pdf/technical-papers/climate-change-water-en.pdf> (accessed 21 September 2015).
- Becker, L., R. J. Poreda, A. G. Hunt, T. E. Bunch, and M. Rampino. 2001. Impact event at the Permian–Triassic boundary: evidence from extraterrestrial noble gases in fullerenes. *Science* 291(5508):1530–1533.
- Beisner, K. R., N. V. Paretto, F. D. Tillman, D. L. Naftz, D. J. Bills, K. Walton-Day, and T. J. Gallegos. 2016. Geochemistry and hydrology of perched groundwater springs: assessing elevated uranium concentrations at Pigeon Spring relative to nearby Pigeon Mine, Arizona (USA). *Hydrogeology Journal* 25:539–556. <https://link.springer.com/content/pdf/10.1007%2Fs10040-016-1494-8.pdf> (accessed 13 April 2018).
- Beus, S. S. 2003a. Temple Butte Formation. Pages 107–114 (Chapter 7) in S. S. Beus and M. Morales, editors. *Grand Canyon geology*. Second edition. Oxford University Press, New York, New York.
- Beus, S.S. 2003b. Redwall Limestone and Surprise Canyon Formation. Pages 115–135 (Chapter 8) in S. S. Beus and M. Morales, editors. *Grand Canyon geology*. Second edition. Oxford University Press, New York, New York.
- Beus, S. S., and M. Morales. 2003. Introducing the Grand Canyon. Pages 1–8 (Chapter 1) in S. S. Beus and M. Morales, editors. *Grand Canyon geology*. Second edition. Oxford University Press, New York, New York.
- Billingsley, G. H. 1974. Mining in Grand Canyon. Pages 170–179 in W. J. Breed and E. C. Roat, editors. *Geology of the Grand Canyon*. Museum of Northern Arizona, Flagstaff, Arizona.
- Billingsley, G. H. 1989. Mesozoic strata at Lees Ferry, Arizona. Pages 67–71 in S. Beus, editor. *Centennial Field Guide Volume 2*. Rocky Mountain Section, Geological Society of America, Boulder, Colorado.
- Billingsley, G. H. 2000a. Volcanic events of the past 20 Ma in the western Grand Canyon region, significance to Grand Canyon erosion. Pages 1–3 in R. A. Young, editor. *Abstracts for a working conference on the Cenozoic geological evolution of the Colorado River system and the erosional chronology of the Grand Canyon region*. Grand Canyon Association, Grand Canyon, Arizona.
- Billingsley, G. H. 2000b. Geologic map of the Grand Canyon 30’x60’ quadrangle, Coconino and Mohave Counties, Northwestern Arizona (scale 1:100,000). *Geologic Investigations Series I-2688*. USGS, Reston, Virginia. <https://pubs.usgs.gov/imap/i-2688/> (accessed 3 August 2015).

- Billingsley, G. H. 2003. Geologic summary. Geologic Investigations Series I-2766 pamphlet to accompany the geologic map of the Mount Trumbull 30' x 60' quadrangle, Mohave and Coconino Counties, northwest Arizona (scale 1:100,000) by G. H. Billingsley and J. L. Wellmeyer, 2003. US Geological Suvery, Reston, Virginia. <https://doi.org/10.3133/i2766>.
- Billingsley, G. H., and S. S. Priest. 2013. Geologic map of the Glen Canyon Dam 30' x 60' quadrangle, Coconino County, Northern Arizona (scale 1:50,000). Scientific Investigations Map 3268. USGS, Reston, Virginia. <https://doi.org/10.3133/sim3268> (accessed 10 August 2015).
- Billingsley, G. H., and J. B. Workman. 2000. Geologic map of the Littlefield 30' x 60' quadrangle, Mohave County, northwestern Arizona (scale 1:100,000). Geologic Investigations Series I-2628. USGS, Reston, Virginia. <https://doi.org/10.3133/i2628> (accessed 3 August 2015).
- Billingsley, G. H., and J. L. Wellmeyer. 2004. Geologic map of the Mount Trumbull 30' x 60' quadrangle, Mohave and Coconino Counties, northwest Arizona (scale 1:100,000). Geologic Investigations Series I-2766. USGS, Reston, Virginia. <https://doi.org/10.3133/i2766> (accessed 3 August 2015).
- Billingsley, G. H., S. S. Beus, and P. Grover. 1999. Stratigraphy of the Surprise Canyon Formation. Pages 9-16 in G.H. Billingsley and S.S. Beus, editors. Geology of the Surprise Canyon Formation of the Grand Canyon, Arizona. Bulletin 61. Museum of Northern Arizona, Flagstaff, Arizona.
- Billingsley, G. H., D. L. Block, and H. C. Dyer. 2006a. Geologic map of the Peach Springs 30' x 60' quadrangle, Mohave and Coconino Counties, northwestern Arizona (scale 1:100,000). Scientific Investigations Map SIM-2900. USGS, Reston, Virginia. <https://doi.org/10.3133/sim2900> (accessed 29 March 2016).
- Billingsley, G. H., T. J. Felger, and S. S. Priest. 2006b. Geologic map of the Valle 30' x 60' quadrangle, Coconino County, northern Arizona (scale 1:100,000). Scientific Investigations Map SIM-2895. USGS, Reston, Virginia. <https://doi.org/10.3133/sim2895> (accessed 29 March 2016).
- Billingsley, G. H., S. S. Priest, and T. J. Felger. 2007. Geologic map of the Cameron 30' x 60' quadrangle, Coconino County, northern Arizona (scale 1:100,000). Scientific Investigations Map SIM-2977. USGS, Reston, Virginia. <https://doi.org/10.3133/sim2977> (accessed 29 March 2016).
- Billingsley, G. H., S. S. Priest, and T. J. Felger. 2008. Geologic map of the Fredonia 30' x 60' quadrangle, Mohave Coconino Counties, northern Arizona (scale 1:100,000). Scientific Investigations Map SIM-3035. USGS, Reston, Virginia. <https://doi.org/10.3133/sim3035> (accessed 29 March 2016).
- Billingsley, G. H., P. W. Stoffer, and S. S. Priest. 2012. Geologic map of the Tuba City 30' x 60' quadrangle, Coconino County, Arizona (scale 1:50,000). Scientific Investigations Map SIM-3227. USGS, Reston, Virginia. <https://doi.org/10.3133/sim3227> (accessed 29 March 2016).
- Bills, D. J. 2012. Potential impacts of legacy and current uranium mining in the Grand Canyon region of northern Arizona. Fall Meeting. American Geophysical Union, Washington, DC. <http://adsabs.harvard.edu/abs/2012AGUFM.H43L..04B> (accessed 14 May 2016).
- Bills, D. J., and M. E. Flynn. 2002. Hydrogeologic Data for the Coconino Plateau and adjacent areas, Coconino and Yavapai Counties, Arizona. Open-File Report 02-265. USGS, Reston, Virginia.
- Bills, D. J., M. Truini, M. E. Flynn, H. A. Pierce, R. D. Catchings, and M. J. Rymer. 2000. Hydrogeology of the regional aquifer near Flagstaff, Arizona, 1994-97. Water-Resources Investigations Report 00-4122. USGS, Reston, Virginia.
- Bills, D. J., F. D. Tillman, D. W. Anning, R. C. Antweiler, and T. F. Kraemer. 2010. Historical and 2009 water chemistry of wells, perennial and intermittent streams, and springs in northern Arizona. Pages 141-282 in A. E. Alpine, editor. Hydrological, geological, and biological site characterization of breccia pipe uranium deposits in northern Arizona. Scientific Investigations Report 2010-5025. USGS, Reston, Virginia. <https://doi.org/10.3133/sir20105025> (accessed 31 March 2018).
- Bills, D. J., K. M. Brown, A. E. Alpine, J. K. Otton, B. S. Van Gosen, J. E. Hinck, and F. D. Tillman. 2011. Breccia-pipe uranium mining in northern Arizona-estimate of resources and assessment of historical effects. Fact Sheet 2010-3050. USGS, Reston, Virginia. <https://doi.org/10.3133/fs20103050> (access 4 April 2018).
- Bills, D. J., M. E. Flynn, and S. A. Monroe. 2016. Hydrogeology of the Coconino Plateau and adjacent areas, Coconino and Yavapai Counties, Arizona. Scientific Investigations Report 2005-5222, Version 1.1. USGS, Reston, Virginia.
- Bjornsson, H., S. Bjornsson, and T. Sigurgeirsson. 1982. Penetration of water into hot rock boundaries of magma at Grimsvotn. *Nature* 295:580-581.

- Blakey, R. C. 1980. Pennsylvanian and Early Permian paleogeography, southern Colorado Plateau and vicinity. Pages 239–257 in T. D. Fouch, and E. R. Magathan, editors. *Paleozoic Paleogeography of West-Central United States*. Rocky Mountain Section, Society of Economic Paleontology and Mineralogy (SEPM), Denver, Colorado.
- Blakey, R. C. 2003. Supai Group and Hermit Formation. Pages 136–162 (Chapter 9) in S. S. Beus and M. Morales, editors. *Grand Canyon geology*. Second edition. Oxford University Press, New York, New York.
- Blakey, R. C., F. Peterson, and G. Kocurek. 1988. Synthesis of Late Paleozoic and Mesozoic eolian deposits of the Western Interior of the United States. *Sedimentary Geology* 56(1–4):3–126.
- Bodenhamer, H. 2012. Bigfork High School Cave Club establishes cave monitoring in Grand Canyon National Park, AZ. *NSS News* 70(12):19–21.
- Braile, L. W. 2009. Seismic monitoring. Pages 229–244 in R. Young, R. and L. Norby, editors. *Geological monitoring*. Geological Society of America, Boulder, Colorado. <http://go.nps.gov/geomonitoring>. (accessed 11 May 2016).
- Brown, C. R. 2010. Physical, chemical, and isotopic analyses of R-aquifer springs, North Rim, Grand Canyon, Arizona. Thesis. Northern Arizona University, Flagstaff, Arizona.
- Brown, C. R., A. Springer, and S. Rice. 2008. Delineation of recharge areas, groundwater flow pathways, and travel times on the Kaibab Plateau, Arizona. *Geological Society of America Abstracts with Programs* 40(6):211. https://gsa.confex.com/gsa/2008AM/finalprogram/abstract_147270.htm (accessed 28 April 2016).
- Brumbaugh, D. S. 2003. Earthquakes and seismicity of the Grand Canyon region. Pages 346–351 (Chapter 18) in S. S. Beus and M. Morales, editors. *Grand Canyon geology*. Second edition. Oxford University Press, New York, New York.
- Burghardt, J. E. 1995. Trip report: Grand Canyon National Park—investigation of Orphan Mine, May 22, 24, and 25, 1995. Memorandum to Chief, Resource Evaluation Branch, Geologic Resources Division.
- Burghardt, J. E. 1996. Effective management of radiological hazards at abandoned radioactive mine and mill sites (4th revision, March 1996). National Park Service Geologic Resources Division, Lakewood, Colorado. <https://www.nps.gov/subjects/abandonedminerallands/publications.htm> (accessed 19 January 2017).
- Burghardt, J. E., E. S. Norby, and H. S. Pranger, II. 2014. Abandoned mineral lands in the National Park System: comprehensive inventory and assessment. Natural Resource Technical Report NPS/NRSS/GRD/NRTR—2014/906. National Park Service, Fort Collins, Colorado. <https://www.nps.gov/subjects/abandonedminerallands/publications.htm> (accessed 13 May 2016).
- Burke, K. J., H. C. Fairley, R. Hereford, and K. S. Thompson. 2003. Holocene terraces, sand dunes, and debris fans along the Colorado River in Grand Canyon. Pages 352–371 (Chapter 19) in S. S. Beus and M. Morales, editors. *Grand Canyon geology*. Second edition. Oxford University Press, New York, New York.
- Carpenter, M. C., and J. I. Mead. 1999. Late Pleistocene vertebrate communities of the lower Grand Canyon: Rampart and Muav caves. *Journal of Vertebrate Paleontology* 19(supplement to 3):36A.
- Cart, J. 2014. National Park Service calls development plans a threat to Grand Canyon. Online information. Los Angeles Times, Los Angeles, California. <http://www.latimes.com/nation/la-na-grand-canyon-20140706-story.html> (accessed 6 May 2016).
- Castor, S. B., and J. E. Faulds. 2001. Post-6 Ma limestone along the southeastern part of the Las Vegas Valley Shear Zone, southern Nevada. Pages 77–80 in R. A. Young and E. E. Spamer, editors. *Colorado River: origin and evolution; proceedings of a symposium held at Grand Canyon National Park in June, 2000*. Monograph 12. Grand Canyon Association, Grand Canyon, Arizona.
- Chenoweth, W. L. 1986. The Orphan Lode Mine, Grand Canyon, Arizona: a case history of a mineralized, collapse-breccia pipe. Open-File Report 86–510. USGS, Reston, Virginia. <https://doi.org/10.3133/ofr86510> (accessed 12 May 2016).
- Christiansen, E. II, B. J. Kowallis, and M. D. Barton. 1994. Temporal and spatial distribution of volcanic ash in Mesozoic sedimentary rocks of the Western Interior: an alternative record of Mesozoic magmatism. Pages 73–94 in M. V. Caputo, J. A. Peterson, and K. J. Franczyk, editors. *Mesozoic systems of the Rocky Mountain region, USA*. SEPM (Society for Sedimentary Geology), Rocky Mountain Section, Denver, Colorado.
- Christensen, N. S., A. W. Wood, N. Voisin, D. P. Lettenmaier and R. N. Palmer. 2004. The effects of climate change on the hydrology and water resources of the Colorado River basin. *Climatic Change* 62(1–3):337–363. <https://link.springer.com/journal/10584> (accessed 21 September 2015).

- Clark, R. 2016. Grand Canyon uranium mine set to re-open. Grand Canyon National Park, Grand Canyon, Arizona. <https://www.grandcanyontrust.org/blog/grand-canyon-uranium-mine-set-re-open> (accessed 29 March 2018).
- Collier, M. P., R. H. Webb, and E. D. Andrews. 1997. Experimental flooding in Grand Canyon. *Scientific American* January 1997: 82–89. https://www.jstor.org/stable/24993568?seq=1#page_scan_tab_contents (accessed 20 April 2016).
- Cook, B. I., T. R. Ault, and J. E. Smerdon. 2015. Unprecedented 21st century drought risk in the American Southwest and Central Plains. *Science Advances* 1(1):1–7. <http://advances.sciencemag.org/content/1/1/e1400082> (accessed 5 May 2015).
- Cook, D. A. 1991. Sedimentology and shale petrology of the Upper Proterozoic Walcott Member, Kwagunt Formation, Chuar Group, Grand Canyon, Arizona. Thesis. Northern Arizona University, Flagstaff, Arizona.
- Cook, T. 2013. Releasing a flood of controversy on the Colorado River. *Earth: The Science behind the Headlines*. <http://www.earthmagazine.org/article/releasing-flood-controversy-colorado-river> (accessed 22 April 2016).
- Conway, M. 2016. News releases in 2016. Arizona Geological Survey, Tucson, Arizona. http://www.azgs.gov/news_releases2016.shtml#may5 (accessed 11 May 2016).
- Crossey, L. J., T. P. Fischer, P. J. Patchett, K. E. Karlstrom, D. R. Hilton, D. L. Newell, P. Huntoon, A. C. Reynolds, and G. A. M. de Leeuw. 2006. Dissected hydrologic system at the Grand Canyon: interaction between deeply derived fluids and plateau aquifer waters in modern springs and travertine. *Geology* 34(1):25–28.
- Crossey, L. J., K. E. Karlstrom, A. E. Springer, D. Newell, D. R. Hilton, and T. Fischer. 2009. Degassing of mantle-derived CO₂ and He from springs in the southern Colorado Plateau region: neotectonic connections and implications for groundwater systems. *GSA Bulletin* 121(7–8):1034–1053.
- Crow, R. S., K. E. Karlstrom, W. C. McIntosh, L. Peters, and N. Dunbar. 2008. History of Quaternary volcanism and lava dams in western Grand Canyon based on lidar analysis, 40Ar/39Ar dating, and field studies: Implications for flow stratigraphy, timing of volcanic events, and lava dams. *Geosphere* 4(1):183.
- Crow, R. S., K. E. Karlstrom, L. J. Crossey, V. J. Polyak, Y. Asmerom, and K. House. 2014. Deciphering the evolution and origin of the lower Colorado River and uplift of the Colorado Plateau: preliminary U–Pb carbonate dating results and future directions. *American Geophysical Union Abstracts with Programs* 2014:1.
- Crow, R. S., K. E. Karlstrom, W. McIntosh, L. Peters, L. Crossey, and A. Eyster. 2015. A new model for Quaternary lava dams in Grand Canyon based on 40Ar/39Ar dating, basalt geochemistry, and field mapping. *Geosphere* 11(5):1305–1342. <https://pubs.geoscienceworld.org/gsa/geosphere/article/11/5/1305-1342/132253> (accessed 20 August 2019).
- Dallage, T. A., M. H. Ort, W. C. McIntosh, and M. E. Perkins. 2001. Age and depositional basin morphology of the Bidahochi Formation and implications for the ancestral upper Colorado River. Pages 47–52 in R. A. Young and E. E. Spamer, editors. *Colorado River: origin and evolution; proceedings of a symposium held at Grand Canyon National Park in June, 2000*. Monograph 12. Grand Canyon Association, Grand Canyon, Arizona.
- Dalrymple, G. B., and W. K. Hamblin. 1998. K–Ar ages of Pleistocene lava dams in the Grand Canyon in Arizona. *Proceedings of the National Academy of Sciences* 95:9744–9749.
- Daneker, T.M. 1974. Sedimentology of the Precambrian Shinumo Quartzite, Grand Canyon, Arizona. *Geological Society of America Abstracts with Programs* 6:438.
- Darton, N. H. 1910. A reconnaissance of parts of northwestern New Mexico and northern Arizona. *Bulletin* 435. USGS, Reston, Virginia.
- Davis, S. W., M. E. Davis, I. Lucchitta, T. C. Hanks, R. C. Finkel, and M. Caffee. 2001. Erosional history of the Colorado River through Glen and Grand Canyons. Pages 135–140 in R. A. Young and E. E. Spamer, editors. *Colorado River: origin and evolution; proceedings of a symposium held at Grand Canyon National Park in June, 2000*. Monograph 12. Grand Canyon Association, Grand Canyon, Arizona.
- DeCelles, P. G. 2004. Late Jurassic to Eocene evolution of the Cordilleran thrust belt and foreland basin system, western U.S.A. *American Journal of Science* 304 (2):105–168.
- Degraff, J. M., P. E. Long, and A. Aydin. 1989. Use of joint-growth directions and rock textures to infer thermal regimes during solidification of basaltic lava flows. *Journal of Volcanology and Geothermal Research* 38:309–324.

- Dehler, C. M., M. Elrick, K. E. Karlstrom, L. J. Crossey, and G. A. Smith. 2000. Cyclostratigraphy of the mid-Neoproterozoic Chuar Group (approximately 800–742 Ma), Grand Canyon: a record of climatic and tectonic transitions into the Sturtian glacial and during Rodinia breakup. *Geological Society of America Abstracts with Programs* 32:375.
- Dehler, C. M., M. Elrick, K. E. Karlstrom, G. A. Smith, L. J. Crossey, and J. M. Timmons. 2001. Neoproterozoic Chuar Group (approximately 800–742 Ma), Grand Canyon: a record of cyclic marine deposition during global cooling and supercontinent rifting. *Sedimentary Geology* 141–142:465–499.
- Dehler, C. M., S. M. Porter, and J. M. Timmons. 2012. The Neoproterozoic Earth system revealed from the Chuar Group of Grand Canyon. Pages 49–72 in J. M. Timmons and K. E. Karlstrom, editors. *Grand Canyon geology: two billion years of Earth's history*. Special Paper 489. Geological Society of America, Boulder, Colorado.
- Dehler, C., G. Gehrels, S. Porter, M. Heizler, K. Karlstrom, G. Cox, L. Crossey, and M. Timmons. 2017. Synthesis of the 780–740 Ma Chuar, Uinta Mountain, and Pahrump (ChUMP) groups, western USA: implications for Laurentia-wide cratonic marine basins. *Geological Society of America Bulletin* 129(5–6):607–624.
- Dickinson, W.R. 1981. Plate tectonic evolution of the southern Cordillera. *Arizona Geological Society Digest* 14:113–135.
- Dickinson, W. R. 2004. Evolution of the North America Cordillera. *Annual Review of Earth and Planetary Sciences* 32:13–45.
- Doelling, H. H. 2010. Geology of Arches National Park, Utah. Pages 11–37 in D. A. Sprinkel, T. C. Chidsey, Jr., and P. B. Anderson, editors. *Geology of Utah's parks and monuments*. Publication 28 (third edition). Utah Geological Association, Salt Lake City, Utah.
- Draut, A. E., and D. M. Rubin. 2006. Measurements of wind, aeolian sand transport, and precipitation in the Colorado River corridor, Grand Canyon, Arizona: January 2005 to January 2006. Open-File Report 2006-1188. USGS, Reston, Virginia.
- Draut, A. E., and D. M. Rubin. 2008. The role of eolian sediment in the preservation of archeologic sites along the Colorado River corridor in Grand Canyon National Park. Professional Paper 1756. USGS, Reston, Virginia. <https://doi.org/10.3133/pp1756> (accessed 24 April 2016).
- Draut, A. E., H. A. Sondossi, J. E. Hazel, Jr., T. Andrews, H. C. Fairley, C. R. Brown, and K. M. Vanaman. 2009. 2008 weather and aeolian sand-transport data from the Colorado River corridor, Grand Canyon, Arizona. Open-File report 2009–1190. USGS, Reston, Virginia. <http://pubs.usgs.gov/of/2009/1190/> (accessed 25 April 2016).
- Draut, A. E., J. E. Hazel, Jr., H. C. Fairley, and C. R. Brown. 2010. Aeolian reworking of sandbars from the March 2008 Glen Canyon Dam high-flow experiment in Grand Canyon. Scientific Investigations Report 2010–5135. USGS, Reston, Virginia. <https://www.usgs.gov/centers/sbsc/gcmrc> (accessed 25 April 2016).
- Dubiel, R. F. 1994. Triassic deposystems, paleogeography, and paleoclimate of the Western Interior. Pages 133–168 in M. V. Caputo, J. A. Peterson, and K. J. Franczyk, editors. *Mesozoic systems of the Rocky Mountain region, USA*. SEPM (Society for Sedimentary Geology), Rocky Mountain Section, Denver, Colorado.
- Dublyansky, Y. V. 2000. Dissolution of carbonates by geothermal waters. Pages 158–159 in A. B. Klimchouk, D. C. Ford, A. N. Palmer, and W. Dreybrodt, editors. *Speleogenesis: Evolution of Karst Aquifers*. National Speleological Society, Huntsville, Alabama.
- Dunham, R. J. 1962. Classification of carbonate rocks according to depositional texture. Pages 108–121 in W. E. Ham, editor. *Classification of carbonate rocks*. Memoir 1. American Association of Petroleum Geologists, Tulsa, Oklahoma.
- Dutton, C. E. 1882. Tertiary history of the Grand Canyon district. Monograph 2. USGS, Reston, Virginia.
- Elston, D. P. 1989. Middle and Late Proterozoic Grand Canyon Supergroup. Pages 94–105 in D. P. Elston, G. H. Billingsley, and R. A. Young, editors. *Geology of the Grand Canyon, Northern Arizona*. 28th International Geological Congress, Field Trip Guidebook T115/315). American Geophysical Union, Washington, DC.
- Elston, D. P., and E. H. McKee. 1982. Age and correlation of the Late Proterozoic Grand Canyon Disturbance, Northern Arizona. *Geological Society of American Bulletin* 93:681–699.
- Elston, D. P., and R. A. Young. 1989. Development of Cenozoic landscape of Central and Northern Arizona: cutting of Grand Canyon. Pages 145–153 in D. Elston, G. Billingsley, and R. Young, editors. *Geology of Grand Canyon, Northern Arizona with Colorado River guides*. American Geophysical Union, Washington, DC.

- Elston, D. P., P. K. Link, D. Winston, and R. J. Horodyski. 1993. Correlations of Middle and Late Proterozoic successions. Pages 468–487 in J. C. Reed, M. E. Bickford, R. S. Houston, P. K. Lind, D. W. Rankin, P. K. Sims, and W. R. Van Schumus, editors. DNAG Precambrian: Conterminous U.S. The Geology of North America volume C-2. Geological Society of America, Boulder Colorado.
- Environmental Protection Agency. 2012. Water recycling and reuse: the environmental benefits. <http://www3.epa.gov/region9/water/recycling/#benefits> (accessed 12 May 2016).
- Evans, T. J. 2016. General standards for geologic maps. Section 3.1 in M. B. Carpenter and C. M. Keane, compilers. The geoscience handbook 2016. AGI Data Sheets, 5th Edition. American Geosciences Institute, Alexandria, Virginia.
- Faulds, J. E., C. Schreiber, S. J. Reynolds, L. A. Gonzales, and D. Okaya. 1997. Origin and paleogeography of an immense, nonmarine Miocene salt deposit in the Basin Range (Western USA). *Journal of Geology* 105:19–36.
- Faulds, J. E., M. A. Wallace, L. A. Gonzales, and M. T. Heizler. 2001. Depositional environment and paleogeographic implications of the Late Miocene Hualapai Limestone, northwestern Arizona and southern Nevada. Pages 81–88 in R. A. Young and E. E. Spamer, editors. Colorado River: origin and evolution; proceedings of a symposium held at Grand Canyon National Park in June, 2000. Monograph 12. Grand Canyon Association, Grand Canyon, Arizona.
- Faulds, J. E., K. A. Howard, and E. M. Duebendorfer. 2008. Cenozoic evolution of the abrupt Colorado Plateau-Basin and Range boundary, northwest Arizona: a tale of three basins, immense lacustrine-evaporite deposits, and the nascent Colorado River. *Geological Society of America Field Guide* 11:119–151.
- Fenton, C. R. 1998. Cosmogenic ³Helium dating of lava dam outburst-floods in western Grand Canyon. Thesis. University of Utah, Salt Lake City, Utah.
- Fenton, C. R., R. H. Webb, P. A. Pearthree, T. E. Cerling, and R. J. Poreda. 2001a. Displacement rates on the Toroweap and Hurricane faults: implications for Quaternary downcutting in the Grand Canyon, Arizona. *Geology* 29 (11):1035–1038.
- Fenton, C. R., R. H. Webb, P. A. Pearthree, T. E. Cerling, R. J. Poreda, and B. P. Nash. 2001b. Cosmogenic ³He dating of Western Grand Canyon basalts: implications for Quaternary incision of the Colorado River. Pages 147–154 in R. A. Young and E. E. Spamer, editors. Colorado River: origin and evolution; proceedings of a symposium held at Grand Canyon National Park in June 2000. Monograph 12. Grand Canyon Association, Grand Canyon, Arizona.
- Fenton, C. R., T. E. Cerling, B. P. Nash, R. H. Webb, and R. J. Poreda. 2002. Cosmogenic ³He ages and geochemical discrimination of lava-dam outburst-flood deposits in western Grand Canyon, Arizona. Pages 191–215 in P. K. House, R. H. Webb, V. R. Baker, and D. R. Levish, editors. Ancient Floods, Modern Hazards. American Geophysical Union, Washington, DC.
- Fenton, C. R., R. J. Poreda, B. P. Nash, R. H. Webb, and T. E. Cerling. 2004. Geochemical discrimination of five Pleistocene lava-dam outburst-flood deposits, western Grand Canyon, Arizona. *Journal of Geology* 112:91–110.
- Fenton, C. R., R. H. Webb, and T. E. Cerling. 2006. Peak discharge of a Pleistocene lava-dam outburst flood in Grand Canyon, Arizona, USA. *Quaternary Research* 65(2):324–335.
- Ferrari, R. 2008. 2001 Lake Mead sedimentation survey. US Bureau of Reclamation report. Technical Service Center, Denver, Colorado. <https://www.usbr.gov/lc/region/g2000/> (accessed 6 December 2017).
- Finch, W. I., H. B. Sutphin, C. T. Pierson, R. B. McCammon, and K. J. Wenrich. 1990. The 1987 estimate of undiscovered uranium endowment in solution-collapse breccia pipes in the Grand Canyon region of northern Arizona and adjacent Utah. Circular 1051. USGS, Reston, Virginia.
- Flynn, M. E., and D. J. Bills. 2002. Investigation of the geology and hydrology of the Coconino Plateau of northern Arizona; a project of the Arizona Rural Watershed Initiative. Fact Sheet 113-02. USGS, Reston, Virginia. <https://doi.org/10.3133/fs11302> (accessed 2 March 2018).
- Flynn, M. E., S. A. Monroe, and D. J. Bills. 2007. Hydrogeology of the Coconino Plateau and adjacent areas, Coconino and Yavapai Counties, Arizona. Scientific Investigations Report 2005-5222. USGS, Reston, Virginia. <https://doi.org/10.3133/sir20055222>.
- Ford, T. D., and W. J. Breed. 1973. Late Precambrian Chuar Group, Grand Canyon, Arizona. *Geological Society of America Bulletin* 84:1243–1260.

- Ford, T. D., and C. M. Dehler. 2003. Grand Canyon Supergroup: Nankoweap Formation, Chuar Group, and Sixtymile Formation. Pages 53–75 (Chapter 4) in S. S. Beus and M. Morales, editors. *Grand Canyon geology*. Second edition. Oxford University Press, New York, New York.
- Ford, D., and P. Williams. 2007. *Karst hydrogeology and geomorphology*. John Wiley, West Sussex, United Kingdom.
- Ford, T. D., W. J. Breed, and J. S. Mitchell. 1970. Carbon Butte, an unusual landslide. *Plateau* 43:9–15.
- Ford, T. D., W. J. Breed, and J. S. Mitchell. 1972. Name and age of Upper Precambrian basalts in the Eastern Grand Canyon. *Geological Society of America Bulletin* 83:223–226.
- Francischini, H., S. G. Lucas, S. Voigt, L. Marchetti, V. L. Santucci, C. L. Knight, and P. Dentzien-Dias. 2018. The first record of *Ichniotherium* in the Cisuralian Coconino Sandstone of the Grand Canyon National Park (Arizona, USA). XI Simpósio Brasileiro de Paleontologia de Vertebrados, *Paleontologia em Destaque*:52.
- Francischini, H., S. G. Lucas, S. Voigt, L. Marchetti, V. L. Santucci, C. L. Knight, J. R. Wood, P. Dentzien-Dias, and C. L. Schultz. 2019. On the presence of *Ichniotherium* in the Coconino Sandstone (Cisuralian) of the Grand Canyon and remarks on the occupation of deserts by non-amniote tetrapods. *Paläontologische Gesellschaft*. <https://doi.org/10.1007/s12542-019-00450-5> (accessed 28 May 2019).
- Gallagher, A. K. 2003. Reconstructing the paleoenvironment of the Bright Angel Shale, Grand Canyon Arizona. *Geological Society of America Abstracts with Programs* 35:12.
- Gallegos, T., and J. K. Otton. 2012. Leachability of uranium ore and mine wastes from the Grand Canyon area, North Rim mining district, northern Arizona. *Geological Society of America Abstracts with Programs* 44(6):77. https://gsa.confex.com/gsa/2012RM/finalprogram/abstract_203760.htm (accessed 14 May 2016).
- Gandee, M. N., C. M. Valle, B. W. Tobin, C. Hoffman, H. Childres, and E. R. Schenk. 2015. Karst groundwater vulnerability mapping; applications of the COP and EPIK methods to the Kaibab Plateau, Grand Canyon National Park. *Geological Society of America Abstracts with Programs* 47(7):263. <https://gsa.confex.com/gsa/2015AM/webprogram/Paper269547.html> (accessed 23 February 2018).
- Ghiglieri, M. P. 1992. *Canyon*. University of Arizona Press, Tucson, Arizona.
- Ghiglieri, M. P., and T. M. Myers. 2001. *Over the edge: death in Grand Canyon*. Puma Press, Flagstaff, Arizona.
- Giegengack, R., E. K. Ralph, and A. M. Gaines. 1979. Havasu Canyon: a natural geochemical laboratory. Pages 719–726 in R. M. Linn, editor. *Proceedings of the First Conference on Scientific Research in the National Parks*, volume II. National Park Service, Washington, DC. <http://www.riversimulator.org/Resources/GCMRC/Hydrology/Giegengack1979.pdf> (accessed 6 May 2016).
- Gilbert, G. K. 1874. On age of the Tonto Sandstone. *Abstract. Philosophical Society of Washington* 1:109.
- Gilbert, G. K. 1875a. The Colorado Plateau province as a field for geological study. *American Journal of Science and Arts* 12(68):85–103.
- Gilbert, G. K. 1875b. Report on the geology of portions of Nevada, Utah, California, and Arizona. *US Geographical and Geological Survey West of the 100th Meridian* 3(1):17–187, 503–567.
- Gilbert, G. K. 1877. *Geology of the Henry Mountains*. USGS report. Government Printing Office, Washington, DC. <https://doi.org/10.3133/70039916> (accessed 11 October 2017).
- Gilmore, C. W. 1926. Fossil footprints from the Grand Canyon. *Smithsonian Miscellaneous Collections* 77(9).
- Gilmore, C. W. 1927. Fossil footprints from the Grand Canyon: second contribution. *Smithsonian Miscellaneous Collections* 80(3).
- Gilmore, C. W. 1928. Fossil footprints from the Grand Canyon: third contribution. *Smithsonian Miscellaneous Collections* 80(8).
- Glen Canyon Dam Adaptive Management Program. 2013. High flow releases at Glen Canyon Dam. <https://www.usbr.gov/uc/rm/gcdHFE/index.html> (accessed 31 October 2019).
- Gonzalez, P., G. M. Garfin, D. D. Breshears, K. M. Brooks, H. E. Brown, E. H. Elias, A. Gunasekara, N. Huntly, J. K. Maldonado, N. J. Mantua, H. G. Margolis, S. McAfee, B. R. Middleton, and B. H. Udall. 2018. Southwest. Pages 1101–1184 (Chapter 25) in D. R. Reidmiller, C. W. Avery, D. R. Easterling, K. E. Kunkel, K. L. M. Lewis, T. K. Maycock, and B. C. Stewart, editors. *Impacts, risks, and adaptation in the United States: Fourth National Climate Assessment, Volume II*. U.S. Global Change Research Program, Washington, DC. <https://nca2018.globalchange.gov/chapter/southwest> (accessed 30 October 2019).

- Graham, J. P. 2005. Mount Rainier National Park Geologic Resource Evaluation Report. Natural Resource Report NPS/NRPC/GRD/NRR—2005/007. National Park Service, Denver, Colorado. <http://go.nps.gov/gripubs>.
- Graham, J. P. 2006. Zion National Park Geologic Resource Evaluation Report. Natural Resource Report NPS/NRPC/GRD/NRR—2006/014. National Park Service, Denver, Colorado. <http://go.nps.gov/gripubs>.
- Graham, J. P. 2007. Navajo National Monument Geologic Resource Evaluation Report. Natural Resource Report. NPS/NRPC/GRD/NRR—2007/005. National Park Service, Denver, Colorado. <http://go.nps.gov/gripubs>.
- Graham, J. P. 2008. Devils Tower National Monument Geologic Resource Evaluation Report. Natural Resource Report NPS/NRPC/GRD/NRR—2008/046. National Park Service, Denver, Colorado. <http://go.nps.gov/gripubs>.
- Graham, J. P. 2009. Devils Postpile National Monument Geologic Resources Inventory Report. Natural Resource Report NPS/NRPC/GRD/NRR—2009/160. National Park Service, Denver, Colorado. <http://go.nps.gov/gripubs>.
- Graham, J. P. 2014. Great Basin National Park: Geologic Resources Inventory Report. Natural Resource Report NPS/NRSS/GRD/NRR—2014/762. National Park Service, Fort Collins, Colorado. <http://go.nps.gov/gripubs>.
- Graham, J. P. 2016. Glen Canyon National Recreation Area: Geologic Resources Inventory Report. Natural Resource Report NPS/NRSS/GRD/NRR—2016/1264. National Park Service, Fort Collins, Colorado. <http://go.nps.gov/gripubs>.
- Grams, P. E. 2013. A sand budget for Marble Canyon, Arizona: implications for long-term monitoring of sand storage change. Fact Sheet 2013–3074. USGS, Reston, Virginia. <http://pubs.usgs.gov/fs/2013/3074/> (accessed 24 April 2016).
- Grams, P. E., D. J. Topping, J. C. Schmidt, J. E. Hazel, and M. Kaplinski. 2013. Linking morphodynamic response with sediment mass balance on the Colorado River in Marble Canyon: issues of scale, geomorphic setting, and sampling design. *Journal of Geophysical Research* 118(2):361–381. <http://onlinelibrary.wiley.com/doi/10.1002/jgrf.20050/abstract> (accessed 26 April 2016).
- Griffiths, P. G., R. H. Webb, and T. C. Melis. 1996. Initiation and frequency of debris flows in Grand Canyon, Arizona. Open-File Report 96–491. USGS, Reston, Virginia.
- Grover, P. W. 1987. Stratigraphy and depositional environment of the Surprise Canyon Formation, an Upper Mississippian carbonate-clastic estuarine deposit, Grand Canyon, Arizona. Thesis. Northern Arizona University, Flagstaff, Arizona.
- Hamblin, W. K. 1994. Late Cenozoic lava dams in the western Grand Canyon. *Memoir 183*. Geological Society of America, Boulder, Colorado.
- Hamblin, W. K. 2003. Late Cenozoic lava dams in the western Grand Canyon. Pages 313–345 (Chapter 17) in S. S. Beus and M. Morales, editors. *Grand Canyon geology*. Second edition. Oxford University Press, New York, New York.
- Hanks, T. C., I. Lucchitta, S. W. Davis, M. E. Davis, R. C. Finkel, S. A. Lefton, and C. D. Garvin. 2001. The Colorado River and the age of Glen Canyon. Pages 129–134 in R. A. Young and E. E. Spamer, editors. *Colorado River: origin and evolution; proceedings of a symposium held at Grand Canyon National Park in June 2000*. Monograph 12. Grand Canyon Association, Grand Canyon, Arizona.
- Hansen, R. M. 1978. Shasta ground sloth food habits, Rampart Cave, Arizona. *Paleobiology* 4(3):302–319.
- Hardee, H. C. 1980. Solidification in Kilauea Iki lava lake. *Journal of Volcanology and Geothermal Research* 7:211–223.
- Hazel, Jr., J. E., P. E. Grams, J. C. Schmidt, and M. Kaplinski. 2010. Sandbar response in Marble and Grand Canyons, Arizona, following the 2008 high-flow experiment on the Colorado River. *Scientific Investigations Report 2010–5015*. USGS, Reston, Virginia. <http://pubs.usgs.gov/sir/2010/5015/> (accessed 24 April 2016).
- Henderek, R. L., B. W. Tobin, J. R. Wood, and E. R. Schenk. 2015. Using photogrammetry to document and monitor cave paleontological and archaeological sites in Grand Canyon National Park. *Geological Society of America Abstracts with Programs* 47(7):516.
- Hendricks, J. D., and G. M. Stevenson. 2003. Grand Canyon Supergroup: Unkar Group. Pages 39–52 (Chapter 3) in S. S. Beus and M. Morales, editors. *Grand Canyon geology*. Second edition. Oxford University Press, New York, New York.
- Hereford, R., and P. W. Huntoon. 1990. Rock movement and mass wastage in the Grand Canyon. Pages 443–460 in S. S. Beus and M. Morales, editors. *Grand Canyon geology*. First edition. Oxford University Press, New York, New York.

- Hereford, R., H. C. Fairley, K. S. Thompson, and J. R. Balsom. 1993. Surficial geology, geomorphology, and erosion of archeological sites along the Colorado River, eastern Grand Canyon, Grand Canyon National Park, Arizona. Open-File Report 93–517. USGS, Washington, D.C.
- Highland, L. M. and P. Bobrowsky. 2008. The landslide handbook—A guide to understanding landslides. USGS, Reston, Virginia. Circular 1325. <http://pubs.usgs.gov/circ/1325/> (accessed 8 May 2016).
- Hill, C. A. 1990. Sulfuric acid speleogenesis of Carlsbad Cavern and its relationship to hydrocarbons, Delaware Basin, New Mexico and Texas. *American Association of Petroleum Geologists Bulletin* 74(11):1685–1694.
- Hill, C. A., and P. Forti. 1997. Cave minerals of the world. Second edition. National Speleological Society, Huntsville, Alabama.
- Hill, C. A., and V. J. Polyak. 2009. The Grand Canyon, Arizona. Pages 249–252 in A. N. Palmer and M. V. Palmer, editors. *Caves and karst of the USA*. National Speleological Society, Huntsville, Alabama.
- Hill, C. A. and V. J. Polyak. 2010. Karst hydrology of Grand Canyon, Arizona, USA. *Journal of Hydrology* 390:169–181.
- Hill, C. A., V. J. Polyak, W. C. McIntosh, and P. P. Provencio. 2001. Preliminary evidence from Grand Canyon caves and mines for the evolution of Grand Canyon and the Colorado River system. Pages 141–145 in R. A. Young and E. E. Spamer, editors. *The Colorado River: Origin and Evolution*. Monograph 12. Grand Canyon Association, Grand Canyon, Arizona.
- Hill, C. A., N. Eberz, and R. H. Buecher. 2008. A karst connection model for Grand Canyon, Arizona, USA. *Geomorphology* 95:316–334.
- Hinck, J. E., G. Linder, S. Finger, E. Little, D. Tillitt, and W. Kuhne. 2010. Biological pathways of exposure and ecotoxicity values for uranium and associated radionuclides. Pages 287–353 in A. E. Alpine, editor. *Hydrological, geological, and biological site characterization of breccia pipe uranium deposits in northern Arizona*. Scientific Investigations Report 2010–5025. USGS, Reston, Virginia. <https://pubs.usgs.gov/sir/2010/5025/> (accessed 31 March 2018).
- Hodnett, J.-P., and D. K. Elliott. 2018. Chondrichthyan assemblages from the Surprise Canyon (Late Mississippian, Serpukhovian) and Watahomigi (latest Mississippian/Early Pennsylvanian Serpukhovian/Bashkirian) Formations of the western Grand Canyon, northern Arizona. *Rocky Mountain Section Abstracts with Programs*. Geological Society of America, Boulder, Colorado.
- Hoffman, C., B. W. Tobin, C. M. Valle, H. Childres, M. N. Gandee, and E. R. Schenk. 2015. Modeling the water supply of Grand Canyon National Park: the effect of climate change on a karstic aquifer. *Geological Society of America Abstracts with Programs* 47(7):116. <https://gsa.confex.com/gsa/2015AM/webprogram/Paper269594.html> (accessed 28 April 2016).
- Hom, M. 1986. Reclamation report, Orphan Mine, Grand Canyon National Park, Arizona. US Bureau of Land Management, Phoenix, Arizona. <https://archive.org/details/reclamationrepor00homm> (accessed 13 May 2016).
- Hopkins, R. L., and K. L. Thompson. 2003. Kaibab Formation. Pages 196–211 (Chapter 12) in S. S. Beus and M. Morales, editors. *Grand Canyon geology*. Second edition. Oxford University Press, New York, New York.
- Howard, B. C. 2016. U.S. Government says ‘no’ to Grand Canyon project. Online information. National Geographic. <http://news.nationalgeographic.com/2016/03/160307-grand-canyon-development-tusayan-monument-uranium-mining/> (accessed 8 May 2016).
- Hunt, C. B. 1969. Geologic history of the Colorado River. Monograph P 0669C. USGS, Reston, Virginia.
- Hunt, C. B. 1976. Grand Canyon and the Colorado River, their geologic history. Pages 129–141 in W. J. Breed and E. C. Roat, editors. *Geology of the Grand Canyon*. Monograph. Museum of Northern Arizona, Flagstaff, Arizona.
- Huntoon, P. W. 1970. The hydro-mechanics of the ground water system in the southern portion of the Kaibab Plateau, Arizona. Dissertation. University of Arizona, Tucson, Arizona.
- Huntoon, P. W. 1974. The karstic groundwater basins of the Kaibab Plateau, Arizona. *Water Resources Research* 10(3): 579–590.
- Huntoon, P. W. 1981. Fault controlled ground-water circulation under the Colorado River, Marble Canyon, Arizona. *Ground Water* 19(1): 20–27.
- Huntoon, P. W. 1995. Is it appropriate to apply porous media groundwater circulation models to karstic aquifers? Pages 339–358 in A. I. El-Kadi, editor. *Groundwater Models for Resources Analysis and Management*. CRC Lewis Publishers, Boca Raton, Florida.
- Huntoon, P. W. 1996. Large-basin ground water circulation and paleoreconstruction of circulation leading to uranium mineralization in Grand Canyon breccia pipes, Arizona. *The Mountain Geologist* 33(3):71–84.

- Huntoon, P. W. 2000a. Karstification associated with groundwater circulation through the Redwall artesian aquifer, Grand Canyon, Arizona, USA. Pages 287–291 in A. B. Klimchouk, D. C. Ford, A. N. Palmer, and W. Dreybrodt, editors. *Speleogenesis: Evolution of Karst Aquifers*. National Speleological Society, Huntsville, Alabama.
- Huntoon, P. W. 2000b. Variability of karstic permeability between unconfined and confined aquifers, Grand Canyon region, Arizona. *Environmental and Engineering Geoscience* 7(2):155–170.
- Huntoon, P. W. 2003. Post-Precambrian tectonism in the Grand Canyon region. Pages 222–259 (Chapter 14) in S. S. Beus and M. Morales, editors. *Grand Canyon geology*. Second edition. Oxford University Press, New York, New York.
- Huntoon, P. W., G. H. Billingsley, J. W. Sears, B. R. Ilg, K. E. Karlstrom, M. L. Williams, and D. Hawkins. 1996. Geologic map of the eastern part of the Grand Canyon National Park, Arizona (scale 1:62,500). Grand Canyon Association, Grand Canyon, Arizona, and Museum of Northern Arizona, Flagstaff, Arizona.
- Huntoon, J. E., J. D. Stanesco, R. F. Dubiel, and J. Dougan. 2010. Geology of Natural Bridges National Monument, Utah. Pages 237–255 in D. A. Sprinkel, T. C. Chidsey, Jr., and P. B. Anderson, editors. *Geology of Utah's parks and monuments*. Publication 28 (third edition). Utah Geological Association, Salt Lake City, Utah.
- Hyndman, D. W. 1972. *Petrology of igneous and metamorphic rocks*. McGraw-Hill, New York, New York.
- Intergovernmental Panel on Climate Change (IPCC). 2014. *Climate change 2014: impacts, adaptation, and vulnerability*. Volume II: North America. <http://www.ipcc.ch/report/ar5/wg2/> (accessed 5 May 2015).
- Jackson, G. 1990. Tectonic geomorphology of the Toroweap fault, Western Grand Canyon, Arizona: implications for transgression of faulting on the Colorado Plateau. Open-File report 90–4. Arizona Geological Survey, Tucson, Arizona.
- Johnson, J. G. 1970. Taghanic onlap and the end of North American Devonian provinciality. *Geological Society of America Bulletin* 81:2077–2105.
- Johnson, J. G., G. Klapper, G., and C. A. Sandberg. 1985. Devonian eustatic fluctuations in Euramerica. *Geological Society of America Bulletin* 96: 567–587.
- Johnson, J. G., and C. A. Sandberg. 1989. Devonian eustatic events in the western United States and their biostratigraphic responses. Pages 171–178 in N. J. McMillan, A. F. Embry, and D. J. Glass, editors. *Devonian of the World*. Memoir 14. Canadian Society of Petroleum Geologists, Calgary, Alberta, Canada.
- Johnson, J. G., C. A. Sandberg, and F. G. Poole. 1991. Devonian lithofacies of western United States. Pages 83–106 in J. D. Cooper and C. H. Stevens, editors. *Paleozoic paleogeography of the western United States – II. Pacific Section*, Society of Economic Paleontologists and Mineralogists, Los Angeles, California, USA.
- Jones, C., A. E. Springer, and B. W. Tobin. 2016a. Spring hydrograph and recession curve analysis of extreme weather for Roaring Springs, in deep karst R-aquifer of the Grand Canyon. *Geological Society of America Abstracts with Programs* 48(7):np. <https://gsa.confex.com/gsa/2016AM/webprogram/Paper280691.html> (accessed 23 February 2018).
- Jones, C., A. E. Springer, B. W. Tobin, S. J. Zappitello, and N. A. Jones. 2017a. Characterization and hydraulic behaviour of the complex karst of the Kaibab Plateau and Grand Canyon National Park, USA. In M. Parise, F. Gabrovsek, G. Kaufmann, and N. Ravbar, editors. *Advances in karst research: theory, fieldwork and application*. Special Publication 466. Geological Society of London, London, England.
- Jones, N. A., B. W. Tobin, and S. J. Zappitello. 2016b. Geospatial analysis of sinkholes to delineate karst catchment, Kaibab Plateau, Grand Canyon National Park. *Geological Society of America Abstracts with Programs* 48(7):np. <https://gsa.confex.com/gsa/2016AM/webprogram/Paper281780.html> (accessed 23 February 2018).
- Jones, N. A., B. W. Tobin, and E. R. Schenk. 2017b. Sinkhole geomorphology and distribution on the Kaibab Plateau, Grand Canyon National Park. *Geological Society of America Abstracts with Programs* 49(6):poster. <https://gsa.confex.com/gsa/2017AM/webprogram/Paper304321.html> (accessed 22 February 2018).
- Karl, T. R., J. M. Melillo, and T. C. Peterson, editors. 2009. *Global climate change impacts in the United States*. Cambridge University Press, Cambridge, United Kingdom. <http://www.globalchange.gov/usimpacts> (accessed 11 June 2014).

- Karlstrom, K. E., S. A. Bowring, C. M. Dehler, A. H. Knoll, S. M. Porter, D. J. D. Marais, A. B. Weil, Z. D. Sharp, J. W. Geissman, M. B. Elrick, J. M. Timmons, L. J. Crossey, and K. L. Davidek. 2000. Chuar Group of the Grand Canyon: record of breakup of Rodinia, associated change in the global carbon cycle, and ecosystem expansion by 740 Ma. *Geology* 28:619–622.
- Karlstrom, K. E., B. R. Ilg, M. L. Williams, D. P. Hawkins, S. A. Bowring, and S. J. Seaman. 2003. Paleoproterozoic Rocks of the Granite Gorges. Pages 9–38 (Chapter 2) in S. S. Beus and M. Morales, editors. *Grand Canyon geology*. Second edition. Oxford University Press, New York, New York.
- Karlstrom, K. E., R. Crow, W. McIntosh, L. Peters, J. Pederson, J. Raucci, L. J. Crossey, P. Umhoefer, and N. Dunbar. 2007. $^{40}\text{Ar}/^{39}\text{Ar}$ and field studies of Quaternary basalts in Grand Canyon and model for carving Grand Canyon: quantifying the interaction of river incision and normal faulting across the western edge of the Colorado Plateau. *Geological Society of America Bulletin* 119:1283–1312.
- Karlstrom, K. E., E., R. Crow, L. J. Crossey, D. Corblentz, and J. van Wijk. 2008. Model for tectonically driven incision of the less than 6 Ma Grand Canyon. *Geology* 36:835–838.
- Karlstrom, K. E., and J. M. Timmons. 2012. Many unconformities make one ‘Great Unconformity.’ Pages 73–81 in J. M. Timmons and K. E. Karlstrom, editors. *Grand Canyon geology: two billion years of Earth’s history*. Special Paper 489. Geological Society of America, Boulder, Colorado.
- Karlstrom, K. E., B. R. Ilg, D. Hawkins, M. L. Williams, G. Dumond, K. Mahan, and S. A. Bowring. 2012a. Vishnu basement rocks of the Upper Granite Gorge: continent formation 1.84 to 1.66 billion years ago. Pages 7–25 in J. M. Timmons and K. E. Karlstrom, editors. *Grand Canyon geology: two billion years of Earth’s history*. Special Paper 489. Geological Society of America, Boulder, Colorado.
- Karlstrom, K. E., D. Corblentz, K. Dueker, W. Ouimet, E. Kirby, J. van Wijk, B. Schmandt, S. Kelley, G. Lazear, L. J. Crossey, R. Crow, A. Asian, A. Darling, R. Aster, J. MacCarthy, S. M. Hansen, J. Stachnik, D. F. Stockli, R. Va. Garcia, M. Hoffman, R. McKeon, J. Feldman, M. Heizler, M.S. Donahue, and the CREST Working Group. 2012b. Mantle-driven dynamic uplift of the Rocky Mountains and Colorado Plateau and its surface response: toward a unified hypothesis. *Lithosphere* 4:3–22.
- Karlstrom, K., J. Hagadorn, G. Gehrels, W. Matthews, M. Schmitz, L. Madronich, J. Mulder, M. Pecha, D. Giesler, and L. Crossey. 2018. Cambrian Sauk transgression in the Grand Canyon region redefined by detrital zircons. *Nature Geoscience* 11:438–443.
- Kauffman, E. G. 1977. Geological and biological overview: Western Interior Cretaceous basin. *Mountain Geologist* 14: 75–99.
- Kearsley, L. H., R. D. Quartaroli, and M. J. C. Kearsley. 1999. Changes in the number and size of campsites as determined by inventories and measurement. Pages 147–160 in R. H. Webb, J. C. Schmidt, G. R. Marzolf, and R. A. Valdez, editors. *The Controlled Flood in Grand Canyon*. Geophysical Monograph 110. American Geophysical Union, Washington, DC.
- Kelkar, K. 2013a. GRCA Summary Slides. Mosaics in Science document, 2013-GRCA. National Park Service, Denver, Colorado.
- Kelkar, K. 2013b. Geohazards evaluation of mass movements in Grand Canyon National Park. Geological Society of America Abstracts with Programs 45(7):279. <https://gsa.confex.com/gsa/2013AM/webprogram/Paper227635.html> (accessed 8 June 2020).
- Kenworthy, J. P., and V. L. Santucci. 2006. A preliminary investigation of National Park Service paleontological resources in cultural context: Part 1, general overview. Pages 70–76 in S. G. Lucas, J. A. Spielmann, P. M. Hester, J. P. Kenworthy, and V. L. Santucci, editors. *America’s antiquities: 100 years of managing fossils on federal lands*. Bulletin 34. New Mexico Museum of Natural History and Science, Albuquerque, New Mexico.
- Kenworthy, J., V. L. Santucci, and K. L. Cole. 2004. An inventory of paleontological resources associated with caves in Grand Canyon National Park. Pages 211–228 in Riper, C. v. III and K. L. Cole, editors. *The Colorado Plateau: cultural, biological, and physical research*. The University of Arizona Press, Tucson, Arizona.
- Keyes, C. 1938. Basement complex of the Grand Canyon. *Pan American Geologist* 20:91–116.
- Kieffer, S. W. 1988. Hydraulic maps of major rapids, Grand Canyon, Arizona. *Miscellaneous Investigations Map Series I-1897A-J*. USGS, Reston, Virginia.
- Kieffer, S. W. 2003. Hydraulics and geomorphology of the Colorado River in the Grand Canyon. Pages 275–313 (Chapter 16) in S. S. Beus and M. Morales, editors. *Grand Canyon geology*. Second edition. Oxford University Press, New York, New York.

- Kimbrough, D. L., M. Grove, G. E. Gehrels, R. J. Dorsey, K. A. Howard, O. Lovera, A. Aslan, P. K. House, and P. A. Pearthree. 2015. Detrital zircon U-Pb provenance of the Colorado River: a 5 m.y. record of incision into cover strata overlying the Colorado Plateau and adjacent regions. *Geosphere* 11(6):1719–1748. doi:10.1130/GES00982.1.
- Klimchouk, A. B. 2007. Hypogene speleogenesis: hydrogeological and morphogenetic perspective. NCKRI Special Paper 1. National Cave and Karst Research Institute, Carlsbad, New Mexico.
- Knowles, N., M. D. Dettinger, and D. R. Cayan. 2006. Trends in snowfall versus rainfall in the western United States. *Journal of Climate* 19:4545–4959.
- Knudsen, T. R., A. I. Hiscock, W. R. Lunc, and S. D. Bowman. 2016. Geologic hazards of the Bullfrog and Wahweap high-use areas of Glen Canyon National Recreation Area, San Juan, Kane, and Garfield counties, Utah, and Coconino County, Arizona. Utah Geological Survey, Salt Lake City, Utah.
- Kofford, M. E. 1969. The Orphan mine. Pages 190–194 in D. L. Baars, editor. *Geology and natural history of the Grand Canyon region*. Four Corners Geological Society, Durango, Colorado.
- Koons, E. D. 1945. Geology of the Uinkaret Plateau, northern Arizona. *Geological Society of America Bulletin* 56:151–180.
- Lageson, D. R., and J. G. Schmitt. 1994. The Sevier orogenic belt of the western United States: recent advances in understanding its structural and sedimentologic framework. Pages 27–65 in M. V. Caputo, J. A. Peterson, and K. J. Franczyk, editors. *Mesozoic systems of the Rocky Mountain region, USA*. Rocky Mountain Section, Society for Sedimentary Geology, Denver, Colorado.
- Lancaster, N. 2009. Aeolian features and processes. Pages 1–25 in R. Young and L. Norby, editors. *Geological monitoring*. Geological Society of America, Boulder, Colorado. <http://go.nps.gov/geomonitoring> (accessed 21 February 2016).
- Land, L., G. Veni, and D. Joop. 2013. Evaluation of cave and karst programs and issues at US national parks. Report of Investigations 4. National Cave and Karst Research Institute, Carlsbad, New Mexico. http://www.nckri.org/about_nckri/nckri_publications.htm (accessed 25 August 2015).
- Landry, A. 2015. Begaye vows to blow up Grand Canyon Escalade deal. Online information. Indian Country. <http://indiancountrytodaymedianetwork.com/2015/05/21/begaye-vows-blow-grand-canyon-escalade-deal-160436> (accessed 8 May 2016).
- Lawton, T. F. 1994. Tectonic setting of Mesozoic sedimentary basins, Rocky Mountain region, United States. Pages 1–26 in M. V. Caputo, J. A. Peterson, and K. J. Franczyk, editors. *Mesozoic systems of the Rocky Mountain region, USA*. Rocky Mountain Section, SEPM (Society for Sedimentary Geology), Denver, Colorado.
- Lillie, R. J. 2005. *Parks and plates: the geology of our national parks, monuments, and seashores*. W. W. Norton and Company, New York, New York.
- Loehman, R. 2009. Understanding the science of climate change: talking points - impacts to western mountains and forests. Natural Resource Report NPS/NRPC/NRR—2009/090. National Park Service, Fort Collins, Colorado.
- Long, P. E., and B. J. Wood. 1986. Structures, textures, and cooling histories of Columbia River basalt flows. *Geological Society of America Bulletin* 97:1144–1155.
- Lucas, S. G. 1993. The Chinle Group – revised stratigraphy and chronology of Upper Triassic nonmarine strata in western United States. *Museum of Northern Arizona Bulletin* 59:27–50.
- Lucas, S. G., A. B. Heckert, J. W. Estep, and O. J. Anderson. 1997. Stratigraphy of the Upper Triassic Chinle Group, Four Corners region. Pages 81–107 in O. J. Anderson, B. S. Kues, and S. G. Lucas, editors. *Mesozoic geology and paleontology of the Four Corners region*. Guidebook for the 48th Field Conference. New Mexico Geological Society, Socorro, New Mexico.
- Lucas, S. G., and G. S. Morgan. 2005. Pleistocene mammals of Arizona: an overview. Pages 153–158 in A. B. Heckert and S. G. Lucas, editors. *Vertebrate paleontology in Arizona*. Bulletin 29. New Mexico Museum of Natural History and Science, Albuquerque, New Mexico.
- Lucchitta, I. 1967. Cenozoic geology of the Upper Lake Mead area adjacent to the Grand Wash Cliffs, Arizona. Dissertation. Pennsylvania State University, University Park, Pennsylvania.
- Lucchitta, I. 1979. Late Cenozoic uplift of the southwestern Colorado River region. *Tectonophysics* 61:53–95.
- Lucchitta, I. 2003. History of the Grand Canyon and of the Colorado River in Arizona. Pages 260–274 (Chapter 15) in S. S. Beus and M. Morales, editors. *Grand Canyon geology*. Second edition. Oxford University Press, New York, New York.

- Lucchitta, I., and R. A. Jeanne. 2001. Geomorphic features and processes of the Shivwits Plateau, Arizona, and their constraints on the age of Western Grand Canyon. Pages 65–70 in R.A. Young and E.E. Spamer, editors. *Colorado River: origin and evolution; proceedings of a symposium held at Grand Canyon National Park in June 2000*. Monograph 12. Grand Canyon Association, Grand Canyon, Arizona.
- Lucchitta, I., G. H. Curtis, M. E. Davis, S. W. Davis, T. C. Hanks, R. C. Finkel, and B. Turrin. 2001. Rates of downcutting of the Colorado River in the Grand Canyon region. Pages 155–158 in R.A. Young and E.E. Spamer, editors. *Colorado River: origin and evolution; proceedings of a symposium held at Grand Canyon National Park in June 2000*. Monograph 12. Grand Canyon Association, Grand Canyon, Arizona.
- Lyle, P. 2000. The eruption environment of multi-tiered columnar basalt lava flows. *Journal of the Geological Society of London* 157(1986):715–722.
- Marchetti, D. W., M. S. Harris, C. M. Bailey, T. E. Cerling, and S. Bergman. 2011. Timing of glaciation and last glacial maximum paleoclimate estimates from the Fish Lake Plateau, Utah. *Quaternary Research* 75(1):183–195.
- Marchetti, L., S. Voigt, S. G. Lucas, H. Francischini, P. Dentzien-Dias, R. Sacchi, M. Mangiacotti, S. Scali, A. Gazzola, A. Ronchi, and A. Millhouse. 2019. Tetrapod ichnotaxonomy in eolian paleoenvironments (Coconino and De Chelly formations, Arizona) and late Cisuralian (Permian) sauropsid radiation. *Earth Science Reviews* 190:148–170.
- Marshak, S., Karlstorm, K., and Timmons, J. M. 2000. Inversion of Proterozoic extensional faults: an explanation for the pattern of Laramide and Ancestral Rockies intracratonic deformation, United States: *Geological Society of America Bulletin* 28:735–738.
- Marvine, A. R. 1874. Gold Hill mining region, its position and general geology. *American Journal of Science* 8(43):29–33.
- Maxson, J. H. 1961. Geologic map of the Bright Angel quadrangle, Grand Canyon National Park, Arizona (scale 1:48,000). Grand Canyon Natural History Association, Grand Canyon, Arizona.
- McKee, E. D. 1932. Some fucoids from the Grand Canyon. *Grand Canyon Nature Notes* 7:77–81.
- McKee, E. D. 1933a. Landslides and their part in widening the Grand Canyon. *Grand Canyon Nature Notes* 8:58–161.
- McKee, E. D. 1933b. The Coconino Sandstone—its history and origin. Washington, DC, Carnegie Institute, Publication 440:77–115.
- McKee, E. D. 1937. Research on Paleozoic stratigraphy in western Grand Canyon. Washington, DC, Carnegie Institute, Yearbook 36:340–343.
- McKee, E. D. 1938. The environment and history of the Toroweap and Kaibab formations of northern Arizona and southern Utah. Publication 492. Carnegie Institution of Washington, Washington, DC.
- McKee, E. D. 1939. Studies on the history of Grand Canyon Paleozoic formations. Washington, DC, Carnegie Institute, Yearbook 38:313–314.
- McKee, E. D. 1944. Tracks that go uphill in Coconino Sandstone, Grand Canyon, Arizona. *Plateau* 16:61–72.
- McKee, E. D. 1945. Small-scale structures in Coconino Sandstone of northern Arizona. *Journal of Geology* 53:313–325.
- McKee, E. D. 1947. Experiments on the development of tracks in fine cross-bedded sand. *Journal of Sedimentary Petrology* 17:23–28.
- McKee, E. D. 1963. Lithologic subdivisions of the Redwall Limestone of northern Arizona: their paleogeographic and economic significance. Professional Paper 400-B. USGS, Reston, Virginia.
- McKee, E. D. 1974. Paleozoic rocks of Grand Canyon. Pages 42–75 in W. J. Breed and E. Roat, editors. *Geology of the Grand Canyon*. Museum of Northern Arizona Press, Flagstaff, Arizona.
- McKee, E. D. 1975. The Supai Group, subdivision and nomenclature. Bulletin 1395-J. USGS, Reston, Virginia.
- McKee, E. D. 1976. Paleozoic rocks of Grand Canyon. Pages 42–64 in W. J. Breed and E. Roat, editors. *Geology of the Grand Canyon*. Museum of Northern Arizona Press, Flagstaff, Arizona.
- McKee, E. D. 1979. Ancient sandstone considered to be eolian. Pages 187–238 in E. D. McKee, editor. *A study of global sand seas*. Professional Paper 1052. USGS, Reston, Virginia.
- McKee, E. D. 1982. The Supai Group of Grand Canyon. Professional Paper 1173. USGS, Reston, Virginia.
- McKee, E. D., and W. Breed. 1969. The Toroweap Formation and Kaibab Limestone. Pages 12–26 in W. K. Summers and F. E. Kottlowski, editors. *The San Andres Limestone, a reservoir for oil and water in New Mexico*. Special Publication 3. New Mexico Geological Society, Socorro, New Mexico.

- McKee, E. D., and R. C. Gutschick. 1969. History of the Redwall Limestone of Northern Arizona. Memoir 114. Geological Society of America, Boulder, Colorado.
- McKee, E. D., and E. H. McKee. 1972. Pliocene uplift of the Grand Canyon region: time of drainage adjustment. *Geological Society of America Bulletin* 83(7):1923–1932.
- McKee, E. D., and D. C. Nobel. 1974. Radiometric ages of diabase sills and basaltic lava flows in the Unkar Group, Grand Canyon. *Geological Society of America Abstracts with Programs* (6):458.
- McKee, E. D., and D. C. Nobel. 1976. Age of the Cardenas Lavas, Grand Canyon, Arizona. *Geological Society of America Bulletin* 87:1188–1190.
- McKee, E. D., and C. E. Resser. 1945. Cambrian history of the Grand Canyon region. Publication 563. Carnegie Institute, Washington, DC.
- McKee, E. D., and E. T. Schenk. 1942. The lower canyon lavas and related features at Toroweap in Grand Canyon. *Journal of Geomorphology* 5:245–273.
- McKee, E. D., J. R. Douglas, and S. Rittenhouse. 1971. Deformation of lee-side laminae in eolian dunes. *Geological Society of America Bulletin* 82:359–378.
- McKee, E. D., W. K. Hamblin, and P. E. Damon. 1968. K-Ar age of lava dam in Grand Canyon. *Geological Society of America Bulletin* 79:133–136.
- McKee, E. D., R. F. Wilson, W. J. Breed, and C. S. Breed. 1967. Evolution of the Colorado River in Arizona. Bulletin 44. Museum of Northern Arizona, Flagstaff, Arizona.
- McKenney, D., C. M. Dehler, and L. J. Crossey. 2001. Petrographic analysis of the Carbon Canyon and Carbon Butte members of the Chuar Group, eastern Grand Canyon: possible provenance changes. *Geological Society of America Abstracts with Programs* 33:43.
- Meek, N., and J. Douglass. 2001. Lake overflow: an alternative hypothesis for Grand Canyon incision and development of the Colorado River. Pages 199–206 in R. A. Young and E. E. Spamer, editors. *Colorado River: origin and evolution; proceedings of a symposium held at Grand Canyon National Park in June, 2000*. Monograph 12. Grand Canyon Association, Grand Canyon, Arizona.
- Melillo, J. M., T. C. Richmond, and G. W. Yohe, editors. 2014. *Climate change impacts in the United States: the third national climate assessment*. US Global Change Research Program, Washington, DC. <http://nca2014.globalchange.gov/> (accessed 11 June 2014).
- Melis, T. S. 1997. *Geomorphology of debris flows and alluvial fans in Grand Canyon National Park and their influences on the Colorado River below Glen Canyon Dam, Arizona*. Dissertation. University of Arizona, Tucson, Arizona.
- Melis, T. S., R. H. Webb, P. G. Griffiths, and T. J. Wise. 1994. Magnitude and frequency data for historic debris flows in Grand Canyon National Park and vicinity, Arizona. *Water Resources Investigations Report 94–4214*. USGS, Reston, Virginia.
- Melis, T. S., R. H. Webb, and P. G. Griffiths. 1997. Debris flow in Grand Canyon National Park: peak discharges, flow transformations, and hydrographs. Pages 727–736 in C. Chen, editor. *Debris-flow hazards and mitigation: mechanics, prediction, and assessment*. Proceedings of First International Conference. American Society of Civil Engineers, New York, New York.
- Middleton, L. T., and D. K. Elliot. 2003. Tonto Group. Pages 90–106 (Chapter 6) in S. S. Beus and M. Morales, editors. *Grand Canyon geology*. Second edition. Oxford University Press, New York, New York.
- Middleton, L. T., D. K. Elliot, and M. Morales. 2003. Coconino Sandstone. Pages 163–179 (Chapter 10) in S. S. Beus and M. Morales, editors. *Grand Canyon geology*. Second edition. Oxford University Press, New York, New York.
- Mindat.org. 2016a. Talmessite. Online information. <http://www.mindat.org/min-3876.html> (accessed 5 May 2016).
- Mindat.org. 2016b. Grand View Mine (Last Chance Mine). Online information. <http://www.mindat.org/loc-3338.html> (accessed 12 May 2016).
- Morales, M. 2003. Mesozoic and Cenozoic strata of the Colorado Plateau near the Grand Canyon. Pages 212–221 (Chapter 13) in S. S. Beus and M. Morales, editors. *Grand Canyon geology*. Second edition. Oxford University Press, New York, New York.
- Morris, T. H., V. W. Manning, and S. M. Ritter. 2010. Geology of Capitol Reef National Park, Utah. Pages 85–109 in D. A. Sprinkel, T. C. Chidsey, Jr., and P. B. Anderson, editors. *Geology of Utah's parks and monuments*. Publication 28 (third edition). Utah Geological Association, Salt Lake City, Utah.
- Mueller, E. R., P. E. Grams, J. E. Hazel Jr., and J. C. Schmidt. 2018. Variability in eddy sandbar dynamics during two decades of controlled flooding of the Colorado River in the Grand Canyon. *Sedimentary Geology* 363:181–199.
- Muir, J. 1912. *The Yosemite*. The Century Company, New York, New York, USA. Sierra Club Reprint, 1988, by Houghton Mifflin, Boston, Massachusetts.

- Mylroie, J. E., and J. R. Mylroie. 2009. Diagnostic features of hypogenic karst: is confined flow necessary? Pages 12–26 in K. W. Stafford, L. Land, and G. Veni, editors. *Advances in hypogene karst studies*. NCKRI Symposium 1. National Cave and Karst Research Institute, Carlsbad, New Mexico.
- National Park Service. 2001. Grand Canyon NP GRI Workshop June 26, 2001. Online information. Grand Canyon National Park, Grand Canyon, Arizona. <http://go.nps.gov/gripubs>.
- National Park Service. 2010. Grand Canyon National Park foundation statement. Grand Canyon National Park, Grand Canyon, Arizona. <https://www.nps.gov/grca/learn/management/upload/grca-foundation20100414.pdf>.
- National Park Service. 2011. Bigfork High School Cave Club completes inventory and impact mapping of caves in Grand Canyon National Park. Online information. Grand Canyon National Park, Grand Canyon, Arizona. <https://home.nps.gov/grca/learn/news/bigfork-high-school-cave-club-completes-inventory-and-impact-mapping-of-caves-in-grand-canyon-national-park.htm> (access 3 May 2016).
- National Park Service. 2012. Climate change action plan 2012–2014. Online information. Grand Canyon National Park, Grand Canyon, Arizona. <https://www.nps.gov/subjects/climatechange/index.htm> (accessed 27 May 2016).
- National Park Service. 2014. November 2014 high-flow experiment. Online information. Grand Canyon National Park, Grand Canyon, Arizona. <https://www.nps.gov/grca/learn/nature/hfe.htm> (accessed 23 April 2016).
- National Park Service. 2015a. A study of springs and seeps. Online information. Grand Canyon National Park, Grand Canyon, Arizona. <https://www.nps.gov/grca/learn/nature/seepspringstudy.htm> (accessed 2 March 2018).
- National Park Service. 2015b. Abandoned mine lands safety projects begin in Grand Canyon National Park. Grand Canyon National Park, Grand Canyon, Arizona. <https://www.nps.gov/grca/learn/news/abandoned-mine-lands-safety-projects-begin-in-grand-canyon-national-park.htm> (accessed 25 March 2018).
- National Park Service. 2016a. Grand Canyon: water quality. Online information. Grand Canyon National Park, Grand Canyon, Arizona. <https://www.nps.gov/grca/learn/nature/waterquality.htm> (accessed 28 May 2016).
- National Park Service. 2016b. Lake Mead: sediment. Online information. Grand Canyon National Park, Grand Canyon, Arizona. <https://www.nps.gov/lake/learn/nature/sediment.htm> (accessed 28 May 2016).
- National Park Service. 2016c. Trans-Canyon Pipeline. Online information. Grand Canyon National Park, Grand Canyon, Arizona. <https://www.nps.gov/grca/learn/photosmultimedia/gcid-06-tcp.htm> (accessed 12 January 2017).
- National Park Service. 2017. Grand Canyon National Park: cave/karst systems. Online information. Grand Canyon National park, Grand Canyon, Arizona. <https://www.nps.gov/grca/learn/nature/cave.htm> (accessed 22 February 2018, last updated 31 March 2017).
- National Park Service. n.d. North Rim development plan. Online information. Grand Canyon National Park, Grand Canyon, Arizona. <https://www.nps.gov/grca/learn/management/nrdevplan06.htm> (accessed 7 May 2016).
- National Park Service and American Geosciences Institute. 2015. America's geologic heritage: An invitation to leadership. NPS 999/129325. National Park Service, Denver, Colorado. <https://www.nps.gov/subjects/geology/americas-geoheritage.htm>.
- National Parks Blog. 2011. Stanton's cave Grand Canyon National Park rafting. Online information. <http://www.nationalparksblog.com/stantons-cave-grand-canyon-national-park-rafting/> (accessed 26 April 2016).
- Nin, A. 1971. *The Diary of Anais Nin: 1944–1947*. Harcourt Brace Jovanovich, Inc. New York, New York.
- Noble, L. F. 1914. The Shinumo quadrangle, Grand Canyon district, Arizona. Bulletin 549. USGS, Reston, Virginia.
- Noble, L. F. 1922. A section of Paleozoic formations of the Grand Canyon at the Bass Trail. Professional Paper 131-B. USGS, Reston, Virginia.
- O'Brien, G. 2002. Oxygen isotope composition of banded Quaternary travertine, Grand Canyon National Park, Arizona. Thesis. Northern Arizona University, Flagstaff, Arizona.
- Oldow, J. S., A. W. Bally, H. G. Ave Lallemand, and W. P. Leeman. 1989. Phanerozoic evolution of the North American Cordillera; United States and Canada. Pages 139–232 in A. W. Bally and A. R. Palmer, editors. *The Geology of North America: An Overview*. Geological Society of America, Boulder, Colorado, USA.

- Onac, B. P., J. W. Hess, and W. B. White. 2007. The relationship between the mineral composition of speleothems and mineralization of breccia pipes: evidence from Corkscrew Cave, Arizona. *Canadian Mineralogist* 45(5):1177–1188.
- Otton, J. K., and B. S. Van Gosen. 2010. Uranium resource availability in breccia pipes in northern Arizona. Pages 23–41 in A. E. Alpine, editor. Hydrological, geological, and biological site characterization of breccia pipe uranium deposits in northern Arizona. Scientific Investigations Report 2010–5025. USGS, Reston, Virginia. <https://pubs.usgs.gov/sir/2010/5025/> (accessed 31 March 2018).
- Otton, J. K., T. J. Gallegos, B. S. Van Gosen, R. H. Johnson, R. A. Zielinski, S. M. Hall, L. R. Arnold, and D. B. Yager. 2010. Effects of 1980s uranium mining in the Kanab Creek area of northern Arizona. Pages 49–133 in A. E. Alpine, editor. Hydrological, geological, and biological site characterization of breccia pipe uranium deposits in northern Arizona. Scientific Investigations Report 2010–5025. USGS, Reston, Virginia. <https://pubs.usgs.gov/sir/2010/5025/> (accessed 31 March 2018).
- Palmer, A. N. 2007. *Cave geology*. Cave Books, Dayton, Ohio.
- Panno, S. V., W. R. Kelly, J. C. Angel, and D. E. Luman. 2013. Hydrogeologic and topographic controls on evolution of karst features in Illinois’ sinkhole plain. *Carbonates and Evaporites* 28:13–21.
- Patchett, P. J., and J. E. Spencer. 2001. Application of Sr isotopes to the hydrology of the Colorado River system waters and potentially related Neogene sedimentary formations. Pages 167–172 in R. A. Young and E. E. Spamer, editors. *Colorado River: origin and evolution; proceedings of a symposium held at Grand Canyon National Park in June 2000*. Monograph 12. Grand Canyon Association, Grand Canyon, Arizona.
- Pate, D. 2011. 2011–Grand Canyon National Park–technical assistance site visit report–recommendations. Geologic Resources Division, National Park Service, Lakewood, Colorado.
- Pate, D. 2016. Review of greater Grand Canyon landscape assessment. Unpublished draft. NPS Geologic Resources Division, Lakewood, Colorado.
- Patterson, B. 2017. Should iconic Lake Powell be drained? *Scientific American*. Online information. *Scientific American*. <https://www.scientificamerican.com/article/should-iconic-lake-powell-be-drained/> (accessed 10 February 2018).
- Pederson, J. L. 2001. Searching for the pre-Grand Canyon Colorado River: the Muddy Creek Formation north of Lake Mead. Pages 71–76 in R. A. Young and E. E. Spamer, editors. *Colorado River: origin and evolution; proceedings of a symposium held at Grand Canyon National Park in June 2000*. Monograph 12. Grand Canyon Association, Grand Canyon, Arizona.
- Pederson, J. 2005. The last-standing hypothesis about the path and integration of the late Miocene Colorado River off the Colorado Plateau. *Geological Society of America Abstracts with Programs* 37(7):109. https://gsa.confex.com/gsa/2005AM/finalprogram/abstract_95550.htm (accessed 5 June 2015).
- Pederson, J., K. Karlstrom, W. Sharp, and W. McIntosh. 2002a. Differential incision of the Grand Canyon related to Quaternary faulting: constraints from U-series and Ar/Ar dating. *Geology* 30 (8):739–742.
- Pederson, J. L., R. D. Mackley, J. L. Eddleman, and B. Lindsay. 2002b. Uplift and erosion of the Colorado Plateau and Grand Canyon: implications of new calculations of large-scale rock uplift, exhumation, and river incision. *Rocky Mountain Section, Geological Society of America Abstracts with Programs* 34:60.
- Pederson, J. L., and C. Tressler. 2012. Colorado River long-profile metrics, knickzones, and their meaning. *Earth and Planetary Science Letters* 345–348:171–179.
- Pederson, J. L., W. S. Cragun, A. J. Hidy, T. M. Rittenour, and J. C. Gosse. 2013. Colorado River chronostratigraphy at Lee’s Ferry, Arizona, and the Colorado Plateau bull’s-eye of incision. *Geology* 41(4):427–430.
- Petersen, P. A., J. L. Pederson, and W. W. McFarlane. 2002. Gully erosion of archaeological sites in Grand Canyon: photogrammetry and GIS used in geomorphic studies. *Geological Society of America Abstracts with Programs* 34:379.
- Phillips, A. M. III. 1984. Shasta ground sloth extinction: fossil packrat midden evidence from the western Grand Canyon. Pages 148–158 in P. S. Martin, and R. G. Klein, editors. *Quaternary extinctions: a prehistoric revolution*. University of Arizona Press, Tucson, Arizona.
- Pimm, S. L., G. J. Russell, J. L. Gittleman, and T. M. Brooks. 1995. The future of biodiversity. *Science* 269:347–350.
- Polyak, V., C. Hill, and Y. Asmerom. 2008. Age and evolution of Grand Canyon revealed by U-Pb dating of water-table-type speleothems. *Science* 319:1377–1380.

- Poole, F. G., and C. A. Sandberg. 1977. Mississippian paleogeography and tectonics of the western United States. Pages 67–85 in J. H. Stewart, C. H. Stevens, and A. E. Fritsche, editors. *Paleozoic paleogeography of the western United States*. Pacific Coast Paleogeography Symposium 1. Society of Economic Paleontologists and Mineralogists, Los Angeles, California.
- Poole, F. G., and C. A. Sandberg. 1991. Mississippian paleogeography and conodonts biostratigraphy of the western United States. Pages 107–136 in J. D. Cooper and C. H. Stevens, editors. *Paleozoic paleogeography of the western United States – II*. Pacific Section, Society of Economic Paleontologists and Mineralogists, Los Angeles, California.
- Potochnik, A. R. 2001. Paleogeomorphic evolution of the Salt River region: implications for Cretaceous–Laramide inheritance for ancestral Colorado River drainage. Pages 17–24 in R. A. Young and E. E. Spamer, editors. *Colorado River: origin and evolution; proceedings of a symposium held at Grand Canyon National Park in June, 2000*. Monograph 12. Grand Canyon Association, Grand Canyon, Arizona.
- Potochnik, A. R., and S. J. Reynolds. 2003. Side canyons of the Colorado River in Grand Canyon. Pages 391–406 (Chapter 21) in S. S. Beus and M. Morales, editors. *Grand Canyon geology*. Second edition. Oxford University Press, New York, New York.
- Powell, J. W. 1875. *Exploration of the Colorado River of the West*. Smithsonian Institution, Washington, DC. <https://doi.org/10.3133/70039238> (accessed 17 November 2017).
- Price, L. G. 1999. *An introduction to Grand Canyon geology*. Grand Canyon Association, Grand Canyon, Arizona.
- Pulwarty, R., K. Jacobs, and R. Dole. 2005. The hardest working river: drought and critical water problems on the Colorado. Pages 249–285 in D. Wilhite, editor. *Drought and Water Crises: Science, Technology and Management*. Taylor and Francis Press, Boca Raton, Florida.
- Raup, D. M. 1991. *Extinction: bad genes or bad luck?* W.W. Norton and Company, New York, New York.
- Rauzi, S. 2012. Arizona oil and gas well location maps and report. Arizona Geological Survey Oil and Gas–12, 32 p., 2 map sheets. http://repository.azgs.gov/uri_gin/azgs/dlio/1463 (accessed 28 May 2016).
- Reed, V.S. 1974. Stratigraphy of the Hakatai Shale, Grand Canyon, Arizona. *Geological Society of America Abstracts with Programs* 6:469.
- Reimondo, A. 2019. Uranium mining in the Grand Canyon region. Grand Canyon Trust, Flagstaff, Arizona. <https://www.grandcanyontrust.org/grand-canyon-uranium> (accessed 30 October 2019).
- Reynolds, M. W., and D. P. Elston. 1986. Stratigraphy and sedimentation of part of the Proterozoic Chuar Group, Grand Canyon, Arizona. *Geological Society of America Abstracts with Programs* 18:405.
- Roberts, D. 2015. Grand Canyon on the edge. *Smithsonian* 45(11):58–69, 92, 94.
- Roosevelt, Theodore. 1905(?). *The works of Theodore Roosevelt: Presidential addresses and state papers*. Executive edition. P. F. Collier and Sons, New York, New York.
- Rosenberg, R. 2013. Preliminary qualitative assessment of geologic hazards on the corridor trail system, Grand Canyon National Park. Geoscientists-In-the-Parks document, 2013-GRCA. National Park Service, Denver, Colorado.
- Saemundsson, K. 1970. Intraglacial lava flows in the lowlands of southern Iceland and the problem of two-tiered columnar jointing. *Jokull* 20:62–77.
- Santucci, V. L., J. Kenworthy, and R. Kerbo. 2001. An inventory of paleontological resources associated with National Park Service caves. Technical Report NPS/NRGRD/GRDTR—01/02. Geologic Resources Division, National Park Service, Lakewood, Colorado. <https://www.nps.gov/subjects/caves/upload/cavepaleo.pdf> (accessed 6 December 2017).
- Santucci, V. L., J. P. Kenworthy, and A. L. Mims. 2009. Monitoring in situ paleontological resources. Pages 189–204 in R. Young and L. Norby, editors. *Geological monitoring*. Geological Society of America, Boulder, Colorado. <http://go.nps.gov/geomonitoring> (accessed 31 April 2016)
- Santucci V. L., and J. S. Tweet, editors. 2020. Grand Canyon National Park: Centennial paleontological resource inventory (non-sensitive version). Natural Resource Report. NPS/GRCA/NRR—2020/2103. National Park Service. Fort Collins, Colorado. <https://irma.nps.gov/DataStore/Reference/Profile/2272500>.
- Schaar, M. A. 2011. Occurrence and mobility of uranium and other elements in the Grand Canyon springs. *Geological Society of America Abstracts with Programs* 43(4):60. https://gsa.confex.com/gsa/2011RM/finalprogram/abstract_187266.htm (accessed 14 May 2015).
- Schmidt, J. C., and J. B. Graf. 1990. Recirculating flow and sedimentation in the Colorado River in Grand Canyon, Arizona. *Journal of Geology* 98:1–74.

- Schott, N. D., J. E. Hazel, Jr., H. C. Fairley, M. Kaplinski, and R. A. Parnell. 2014. Gully monitoring at two locations in the Grand Canyon National Park, Arizona, 1996–2010, with emphasis on documenting effects of the March 2008 high-flow experiment. Open-File Report 2014–1211. USGS, Reston, Virginia. <https://pubs.usgs.gov/of/2014/1211/> (accessed 25 April 2016).
- Schwab, F. L. 2000. The Neoproterozoic breakup of Rodinia; sedimentary and stratigraphic constraints from the western edge of Laurentia. *Geological Society of America Abstracts with Programs* 32:319.
- Sears, J. W. 1973. Structural geology of the Precambrian Grand Canyon series. Thesis. University of Wyoming, Laramie, Wyoming.
- Sears, J. W., and R. A. Price. 1978. The Siberian Connection: a case for the Precambrian separation of the Siberian and North American Cratons. *Geology* 6:267–270.
- Siegel, D. L., K. A. Lesniak, M. Stute, and S. Frape. 2004. Isotopic geochemistry of the Saratoga springs: implications for the origin of solutes and source of carbon dioxide. *Geology* 32:257–260.
- Smith, W. O., C. P. Vetter, G. B. Cummings, and US Bureau of Reclamation. 1960. Comprehensive survey of sedimentation in Lake Mead 1948–49. US Government Printing Office, Washington, DC.
- Sorey, M. L., W. C. Evans, B. M. Kennedy, C. D. Farrar, L. J. Hainsworth, and B. Hausback. 1998. Carbon dioxide and helium emissions from a reservoir of magmatic gas beneath Mammoth Mountain, California. *Journal of Geophysical Research* 103:15, 303–15, 323.
- Sottile, C., and K. Dahlgren. 2015. Grand Canyon development plan sparks dispute among Navajo. Online information. NBC News. <http://www.nbcnews.com/nightly-news/grand-canyon-development-plan-sparks-dispute-among-navajo-n302521> (accessed 7 May 2016).
- Spamer, E. E. 1984. Paleontology in the Grand Canyon of Arizona: 125 years of lessons and enigmas from the late Precambrian to the present. *The Mosasaur* 2:45–128.
- Spamer, E. E. 1992. The Grand Canyon fossil record: a source book in paleontology of the Grand Canyon and vicinity, northwestern Arizona and southeastern Nevada. Microform Publication 24. Geological Society of America, Boulder, Colorado.
- Spence, J. R. 2001. Climate of the central Colorado Plateau, Utah and Arizona: characterization and recent trends. Pages 187–203 in K. Thomas and C. Van Riper III, editors. Proceedings of the Fifth Biennial Conference on Research on the Colorado Plateau. USGS Report Ser. USGSFRESC/COPL/2001/24. <https://www.usgs.gov/centers/sbsc> (accessed 24 January 2016).
- Spencer, J. E., and P. J. Patchett. 1997. Sr isotope evidence for a lacustrine origin for the upper Miocene to Pliocene Bouse Formation, lower Colorado River trough, and implications for timing of Colorado Plateau uplift. *Geological Society of America Bulletin* 109(6):767–778.
- Spencer, J. E., and P. A. Pearthree. 2001. Headward erosion versus closed-basin spillover as alternative causes of the ancestral Colorado River by the Gulf of California. Pages 215–219 in R. A. Young and E. E. Spamer, editors. Colorado River: origin and evolution; proceedings of a symposium held at Grand Canyon National Park in June, 2000. Monograph 12. Grand Canyon Association, Grand Canyon, Arizona.
- Spencer, J. E., and K. Wenrich. 2011. Breccia-pipe uranium mining in the Grand Canyon region and implications for uranium levels in Colorado River water. Open-File Report 11–04. Arizona Geological Survey, Tucson, Arizona. http://repository.azgs.gov/uri_gin/azgs/dlio/1000 (accessed 14 May 2016).
- Spencer, J. E., L. Peters, W. C. McIntosh, and P. J. Patchett. 2001. $^{40}\text{Ar}/^{39}\text{Ar}$ geochronology of the Hualapai Limestone and Bouse Formation and implications for the age of the lower Colorado River. Pages 89–92 in R. A. Young and E. E. Spamer, editors. Colorado River: origin and evolution; proceedings of a symposium held at Grand Canyon National Park in June 2000. Monograph 12. Grand Canyon Association, Grand Canyon, Arizona.
- Springer, A. E., V. J. Aldridge, G. M. Schindel, and B. W. Tobin. 2015. Innovative spatial and temporal measurements of recharge to the deep aquifers of the Grand Canyon region. *Geological Society of America Abstracts with Programs* 47(7):472. <https://gsa.confex.com/gsa/2015AM/webprogram/Paper264357.html> (accessed 28 April 2016).
- Stegner, W. 1954. *Beyond the Hundredth Meridian*. Penguin Books, New York, New York.
- Steidtmann, J. R. 1993. The Cretaceous foreland basin and its sedimentary record. Pages 250–271 in A. W. Snoke, J. R. Steidtmann, and S. M. Roberts, editors. *Memoir 5*. Wyoming State Geological Survey, Laramie, Wyoming, USA.

- Stevenson, G. M., and S. S. Beus. 1982. Stratigraphy and depositional setting of the upper Precambrian Dox Formation in Grand Canyon. *Geological Society of America Bulletin* 93(2):163–173.
- Stewart, J.H., F. G. Poole, and R. F. Wilson. 1972a. Stratigraphy and origin of the Triassic Moenkopi Formation and related strata in the Colorado Plateau region with a section on sedimentary petrology by R. A. Cadigan. Profession Paper 691, USGS, Reston, Virginia.
- Stewart, J.H., F. G. Poole, and R. F. Wilson. 1972b. Stratigraphy and origin of the Chinle Formation and related Upper Triassic strata in the Colorado Plateau region with a section on sedimentary petrology by R.A. Cadigan and on conglomerate studies by W. Thordarson, H. F. Albee, and J. H. Stewart. Professional Paper 690. USGS, Reston, Virginia.
- Stortz, S. D., C. E. Aslan, T. D. Sisk, T.A. Chaudhry, J. M. Rundall, J. Palumbo, L. Zachmann, and B. Dickson. 2018. Natural resource condition assessment: Greater Grand Canyon landscape assessment. Natural Resource Report NPS/GRCA/NRR—2018/1645. National Park Service, Fort Collins, Colorado. <https://irma.nps.gov/DataStore/DownloadFile/601805> (accessed 5 November 2018).
- Swanson, D. A. 1967. Yakima basalt of the Tieton River area, south-central Washington. *Geological Society of America Bulletin* 78(9):1077.
- Szabo, B. 1990. Ages of travertine deposits in eastern Grand Canyon National Park, Arizona. *Quaternary Research* 34:24–32.
- Thornberry-Ehrlich, T. 2005. Bryce Canyon National Park Geologic Resource Evaluation Report. Natural Resource Report NPS/NRPC/GRD/NRR—2005/002. National Park Service, Denver, Colorado. <http://go.nps.gov/gripubs>.
- Timmons, J. M., K. E. Karlstrom, and J. W. Sears. 2003. Geologic structure of the Grand Canyon Supergroup. Pages 76–90 (Chapter 5) in S. S. Beus and M. Morales, editors. *Grand Canyon geology*. Second edition. Oxford University Press, New York, New York.
- Timmons, J. M., K. E. Karlstrom, M. T. Heizler, S. A. Bowring, G. E. Gehrels, and L. J. Crossey. 2005. Tectonic inferences from the ca. 1254–1100 Ma Unkar Group and Nankoweap Formation, Grand Canyon: intracratonic deformation and basin formation during protracted Grenville orogenesis. *Geological Society of America Bulletin* 117:1573–1595.
- Timmons, J. M., J. Bloch, K. Fletcher, K. E. Karlstrom, M. Heizler, and L. J. Crossey. 2012. The Grand Canyon Unkar Group: Mesoproterozoic basin formation in the continental interior during supercontinent assembly. Pages 25–49 in J. M. Timmons and K. E. Karlstrom, editors. *Grand Canyon geology: two billion years of Earth's history*. Special Paper 489. Geological Society of America, Boulder, Colorado.
- Tindall, S. E., and G. H. Davis. 1999. Monocline development by oblique-slip fault-propagation folding: the East Kaibab monocline, Colorado Plateau, Utah. *Journal of Structural Geology* 21:1303–1320. <https://www.sciencedirect.com/science/article/pii/S0191814199000899> (accessed 6 April 2016).
- Tobin, B. W., B. F. Schwartz, A. E. Springer, L. Stevens, J. Ledbetter, C. M. Valle, and E. R. Schenk. 2015. Remote karst spring characterization and grouping to focus long-term monitoring effects in Sequoia, Kings Canyon, and Grand Canyon National Parks. *Geological Society of America Abstracts with Programs* 47(7):262. <https://gsa.confex.com/gsa/2015AM/webprogram/Paper268855.html> (accessed 28 April 2016).
- Tobin, B. W., A. E. Springer, D. K. Kreamer, and E. Schenk. 2018. Review: The distribution, flow, and quality of Grand Canyon Springs, Arizona (USA). *Hydrogeology Journal* 26(3):721–732.
- Toomey, R. S., III. 2009. Geological monitoring of caves and associated landscapes. Pages 27–46 in R. Young and L. Norby, editors. *Geological monitoring*. Geological Society of America, Boulder, Colorado. <https://go.nps.gov/geomonitoring> (accessed 1 April 2016).
- Topping, D. J., D. M. Rubin, and L. E. Vierra. 2000. Colorado River sediment transport–1: natural sediment supply limitation and the influence of Glen Canyon Dam. *Water Resources Research* 36(2):515–542.
- Topping, D. J., D. M. Rubin, P. E. Grams, R. E. Griffiths, T. A. Sabol, N. Voichick, R. B. Tusso, K. M. Vanaman, and R. R. McDonald. 2010. Sediment transport during three controlled-flood experiments on the Colorado River downstream from Glen Canyon Dam, with implications for eddy-sandbar deposition in Grand Canyon National Park. Open-File Report 2010–1128. USGS, Reston, Virginia. <http://pubs.usgs.gov/of/2010/1128/> (accessed 24 April 2016).
- Turner, C. E. 2003. Toroweap Formation. Pages 180–195 (Chapter 11) in S. S. Beus and M. Morales, editors. *Grand Canyon geology*. Second edition. Oxford University Press, New York, New York.

- Tweet, J. S., V. L. Santucci, J. P. Kenworthy, and A. L. Mims. 2009. Paleontological resource inventory and monitoring—Southern Colorado Plateau Network. Natural Resource Technical Report NPS/NRPC/NRTR—2009/245. National Park Service, Fort Collins, Colorado.
- Tweet, J. S., V. L. Santucci, and A. P. Hunt. 2012. An inventory of packrat (*Neotoma* spp.) middens in National Park Service areas. *New Mexico Museum of Natural History and Science*, Albuquerque, New Mexico. *Bulletin* 57:355–368.
- US Department of the Interior (2012) Record of Decision: Northern Arizona withdrawal: Mohave and Coconino counties, Arizona. Online information. USGS, Reston, Virginia. http://www.fwspubs.org/doi/suppl/10.3996/052014-JFWM-039/suppl_file/052014-jfwm-039r1-s08.pdf?code=ufws-site (assessed 13 April 2018).
- US Geological Survey. 1996. Controlled flooding of the Colorado River in Grand Canyon: the rationale and date-collection planned. Fact Sheet FS-089-96. USGS, Reston, Virginia. <http://pubs.usgs.gov/fs/FS-089-96/> (accessed 20 April 2016).
- US Geological Survey. 2015. USGS water data for the nation. Online information. USGS, Reston, Virginia. <https://waterdata.usgs.gov/nwis> (accessed 13 April 2018).
- US Geological Survey. 2016a. USGS surface-water annual statistics for the Nation: USGS 09402500 Colorado River near Grand Canyon, AZ. USGS National Water Information System. Online information. USGS, Reston, Virginia.
- US Geological Survey. 2016b. Arizona seismicity map. Earthquake Hazards Program. Online information. USGS, Reston, Virginia. <https://earthquake.usgs.gov/earthquakes/byregion/arizona.php> (accessed 11 May 2016).
- US Geological Survey. 2016c. USGS assesses baseline conditions prior to uranium mining near Grand Canyon National Park. Online information. USGS, Reston, Virginia. <https://www.usgs.gov/news/usgs-assesses-baseline-conditions-prior-uranium-mining-near-grand-canyon-national-park> (accessed 4 April 2018).
- Valle, C. M., B. W. Tobin, and E. R. Schenk. 2015. A GIS study of sinkhole morphology and distribution in relation to structural features of the Kaibab Plateau as a means of understanding recharge to the Redwall-Muav aquifer of Grand Canyon National Park, Arizona, USA. *Geological Society of America Abstracts with Programs* 47(7):624. <https://gsa.confex.com/gsa/2015AM/webprogram/Paper269517.html> (accessed 23 February 2018).
- Van Gosen, B. S., and K. J. Wenrich. 1989. Ground magnetometer surveys over known and suspected breccia pipes on the Coconino Plateau, northwestern Arizona. *Bulletin* 1683-C. USGS, Reston, Virginia. <https://pubs.er.usgs.gov/> (accessed 5 February 2018).
- Van Gundy, C. E. 1951. Nankoweap Group of the Grand Canyon Algonkian of Arizona. *Geological Society of America Bulletin* 62:953–959.
- Walcott, C. D. 1880. The Permian and other Paleozoic groups of the Kanab Valley, Arizona. *American Journal of Science* 20(3):221–225.
- Walcott, C. D. 1883. Pre-Carboniferous strata in the Grand Canyon of the Colorado, Arizona. *American Journal of Science* 16(3):437–442, 484.
- Walcott, C. D. 1889. A study of a line of displacement in the Grand Canyon of the Colorado in northern Arizona. *Geological Society of America Bulletin* 1:49–64.
- Walcott, C. D. 1890. The fauna of the Lower Cambrian or *Olenellus* Zone. USGS 10th Annual Report:509–760.
- Walcott, C. D. 1892. The North American continent during Cambrian time. Extract from the Twelfth annual report of the director of the USGS, 1890–91, pt. 1:523–568. Government Printing Office, Washington, DC.
- Walcott, C. D. 1894. Precambrian igneous rocks of the Unkar terrane, Grand Canyon of the Colorado. USGS 14th Annual Report for 1892/3, part 2:497–519.
- Walcott, C. D. 1899. Precambrian fossiliferous formations. *Geological Society of America Bulletin* 10:199–244.
- Walcott, C. D. 1910. Cambrian geology and paleontology II: abrupt appearance of the Cambrian fauna on the North American Continent. *Smithsonian Miscellaneous Collection* 57:14.
- Walcott, C. D. 1918. Cambrian geology and paleontology IV: appendages of trilobites. *Smithsonian Miscellaneous Collection* 67(4):115–216.
- Walcott, C. D. 1920. Cambrian geology and paleontology IV: Middle Cambrian spongiae. *Smithsonian Miscellaneous Collection* 67(4):261–364.
- Walker, G. P. L. 1993. Basaltic-volcano systems. Pages 3–38 in H. M. Prichard, T. Alabaster, N. B. W. Harris, and C. R. Naylor, editors. *Magmatic Processes and Plate Tectonics*. Special Publication 76. Geological Society of London, London, Great Britain.

- Wanless, H. R. 1975. Carbonate tidal flats of the Grand Canyon Cambrian. Pages 269–277 in R. N. Ginsburg, editor. *Tidal deposits: a casebook of recent examples and fossil counterparts*. Springer-Verlag, New York, New York.
- Weary, D. J., and D. H. Doctor. 2014. Karst in the United States: A digital map compilation and database. U.S. Geological Survey, Reston, Virginia. Open-File Report 2014–1156. <https://pubs.usgs.gov/of/2014/1156/> (accessed 5 November 2018).
- Webb, R. H., and P. G. Griffiths. 2014. Monitoring of coarse sediment inputs to the Colorado River in Grand Canyon. Fact Sheet 019–01. USGS, Reston, Virginia. <http://pubs.usgs.gov/fs/FS-019-01/> (accessed 19 June 2016).
- Webb, R. H., T. S. Melis, P. G. Griffiths, J. G. Elliott, T. E. Cerling, R. J. Poreda, T. W. Wise, and J. E. Pizzuto. 1997. Lava Falls Rapid in Grand Canyon: effects of Late Holocene debris flows on the Colorado River. Professional Paper 1591. USGS, Reston, Virginia.
- Webb, R. H., T. S. Melis, P. G. Griffiths, and J. G. Elliott. 1999a. Reworking of aggraded debris fans. Pages 37–52 in R. H. Webb, J. C. Schmidt, G. R. Marzolf, and R. A. Valdez, editors. *The Controlled Flood in Grand Canyon*. Geophysical Monograph 110. American Geophysical Union, Washington, DC.
- Webb, R. H., T. S. Melis, P. G. Griffiths, J. G. Elliott, T. E. Cerling, R. J. Poreda, T. W. Wise, and J. E. Pizzuto. 1999b. Lava Falls Rapid in Grand Canyon, effects of late Holocene debris flows on the Colorado River. Professional Paper 1591. USGS, Reston, Virginia. <https://doi.org/10.3133/pp1591> (accessed 13 February 2018).
- Webb, R. H., P. G. Griffiths, T. S. Melis, and D. R. Hartley. 2000. Sediment delivery by ungaged tributaries of the Colorado River in Grand Canyon, Arizona. Water-Resources Investigations Report 00-4055. USGS, Reston, Virginia.
- Webb, R. H., T. S. Melis, and P. G. Griffiths. 2003. Debris flows and the Colorado River. Pages 371–390 (Chapter 20) in S. S. Beus and M. Morales, editors. *Grand Canyon geology*. Second edition. Oxford University Press, New York, New York.
- Weinberger, S. 2005. The Orphan Mine: Grand Canyon National Park once hosted a working uranium mine. *Rock & Gem* 35(5):66–68.
- Wenrich, K. J., and P. W. Huntoon. 1989. Breccia pipes and associated mineralization in the Grand Canyon region, northern Arizona. Pages 212–218 in D. P. Elston, G. H. Billingsley, and R. A. Young, editors. *Geology of Grand Canyon, northern Arizona with Colorado River guides, Lees Ferry to Pierce Ferry, Arizona*. 28th International Geological Congress Field Trips T115/T315 Guidebook. American Geophysical Union, Washington D.C.
- Wenrich, K. J., and H. B. Sutphin. 1994. Grand Canyon caves, breccia pipes and mineral deposits. *Geology Today* 10(3):97–104.
- Wenrich, K. J., G. H. Billingsley, and P. W. Huntoon. 1986. Breccia pipe and geologic map of the northeastern Hualapai Indian Reservation and vicinity, Arizona. Open-File Report. USGS, Reston, Virginia. <https://doi.org/10.3133/i2440> (accessed 5 February 2018).
- Wenrich, K. J., G. H. Billingsley, and B. S. Van Gosen. 1989. The potential for breccia pipes in the National Tank area, Hualapai Indian Reservation, Arizona. Bulletin 1683-B. USGS, Reston, Virginia. <https://doi.org/10.3133/b1683B>
- White, C. D. 1929a. Flora of the Hermit shale, Grand Canyon, Arizona. Publication 405. Carnegie Institution of Washington, Washington, DC.
- White, C. D. 1929b. Study of the fossil floras in the Grand Canyon, Arizona. *Carnegie Institution of Washington Year Book* 28:392–393.
- Wieczorek, G. F. and J. B. Snyder. 2009. Monitoring slope movements. Pages 245–271 in R. Young and L. Norby, editors. *Geological monitoring*. Geological Society of America, Boulder, Colorado. <https://go.nps.gov/geomonitoring> (accessed 12 May 2016).
- Wiley, B. H., S. L. Rauzi, A. D. Cook, H. E. Clifton, K. Lung-Chaun, and A. J. Moser. 1998. Geologic description, sampling, petroleum potential, and depositional environment of the Chuar Group, Grand Canyon, Arizona. Open File Report, OFR-98-17. Arizona Geological Survey, Tucson, Arizona. http://repository.azgs.gov/uri_gin/azgs/dlio/822 (accessed 2 May 2016).
- Wiley, B. H., C. M. Dehler, S. A. Ghazi, L. Kuo, and S. L. Rauzi. 2002. Geologic description, sampling, and petroleum source rock potential of the Awatubi and Walcott Members, Kwagunt Formation Chuar Group of the Sixtymile Canyon Section, Grand Canyon, Arizona. Open File Report, OFR-02-01. Arizona Geological Survey, Tucson, Arizona. http://repository.azgs.gov/uri_gin/azgs/dlio/138 (accessed 2 May 2016).

- Willis, G. C., and R. F. Biek. 2001. Quaternary incision rates of the Colorado River and major tributaries in the Colorado Plateau, Utah. Pages 119–124 in R. A. Young and E. E. Spamer, editors. *Colorado River: origin and evolution; proceedings of a symposium held at Grand Canyon National Park in June 2000*. Monograph 12. Grand Canyon Association, Grand Canyon, Arizona.
- Wilmarth, M. G. 1957. *Lexicon of geologic names of the United States*. Bulletin 896. USGS, Reston, Virginia.
- World Health Organization. 2006. *Guidelines for the safe use of wastewater, excreta, and greywater*. Volumes 1 and 2. World Health Organization, Geneva, Switzerland.
- Wright, S. A., T. S. Melis, D. J. topping, and D. M. Rubin. 2005. Influence of Glen Canyon Dam operations on downstream sand resources of the Colorado River in Grand Canyon. Pages 17–31 in S. P. Gloss, J. E. Lovich, and T. S. Melis, editors. *The state of the Colorado River ecosystem in Grand Canyon*. Circular 1282. USGS, Reston, Virginia. <http://pubs.usgs.gov/circ/1282> (accessed 25 April 2016).
- Wu, X., J. L. Conkle, F. Ernst, and J. J. Gan. 2014. Treated wastewater irrigation: uptake of pharmaceutical and personal care products by common vegetables under field conditions. *Environmental Science and Technology* 48(19): 11286–11293.
- Young, R. A. 1966. *Cenozoic geology along the edge of the Colorado Plateau in Northwestern Arizona*. Dissertation. Washington University, St. Louis, Missouri.
- Young, R. A. 1999. Nomenclature and ages of Late Cretaceous (?)–Tertiary strata in the Hualapai Plateau region, northwestern Arizona. Pages 21–50 in G. H. Billingsley, K. J. Wenrich, P. W. Huntoon, and R. A. Young, editors. *Breccia-pipe and geologic map of the southwestern part of the Hualapai Indian Reservation and vicinity, Arizona*. Miscellaneous Investigations Series map I-2554. USGS, Reston, Virginia.
- Young, R. A., and W. J. Brennan. 1974. Peach Springs Tuff, its bearing on structural evolution of the Colorado Plateau and development of Cenozoic drainage in Mohave County, Arizona. *Geological Society of America Bulletin* 85:83–90.
- Young, R. A., and E. E. Spamer, editors. 2001. *Colorado River: origin and evolution; proceedings of a symposium held at Grand Canyon National Park in June 2000*. Monograph 12. Grand Canyon Association, Grand Canyon, Arizona.
- Young, R. and L. Norby, editors. 2009. *Geological monitoring*. Geological Society of America, Boulder, Colorado. <https://go.nps.gov/geomonitoring>.
- Zappitello, S., B. W. Tobin, and N. Jones. 2016. Aquifer structure revealed by caves and dye trace, Grand Canyon National Park. *Geological Society of America Abstracts with Programs* 48(7): np. <https://gsa.confex.com/gsa/2016AM/webprogram/Paper281571.html> (accessed 23 February 2018).
- Zappitello S., R. Henderek, and B. Tobin. 2017. Geoscientists in the Park caves: Grand Canyon National Park. Pages 12–15 in D. Bunnell, editor. *NSS news*. May 2017. National Speleological Society, Huntsville, Alabama.

Additional References

These references, resources, and websites may be of use to resource managers. Refer to Appendix B for laws, regulations, and policies that apply to NPS geologic resources.

Geology of National Park Service Areas

- NPS Geologic Resources Division (Lakewood, Colorado) Energy and Minerals; Active Processes and Hazards; Geologic Heritage: <http://go.nps.gov/grd>
- NPS Geodiversity Atlas: http://go.nps.gov/geodiversity_atlas
- NPS Geologic Resources Division Education Website: <http://go.nps.gov/geoeducation>
- NPS Geologic Resources Inventory: <http://go.nps.gov/gri>
- NPS Geoscientist-In-the-Parks (GIP) internship and guest scientist program: <http://go.nps.gov/gip>
- NPS Mosaics In Science (MIS) internship program: <http://go.nps.gov/mosaics>

NPS Resource Management Guidance and Documents

- Management Policies 2006 (Chapter 4: Natural resource management): <http://www.nps.gov/policy/mp/policies.html>
- 1998 National parks omnibus management act: <http://www.gpo.gov/fdsys/pkg/PLAW-105publ391/pdf/PLAW-105publ391.pdf>
- NPS-75: Natural resource inventory and monitoring guideline: <https://irma.nps.gov/DataStore/Reference/Profile/622933>
- NPS Natural resource management reference manual #77: <https://irma.nps.gov/DataStore/Reference/Profile/572379>
- Geologic monitoring manual (Young, R., and L. Norby, editors. 2009. Geological monitoring. Geological Society of America, Boulder, Colorado): <http://go.nps.gov/geomonitoring>
- NPS Technical Information Center (TIC) (Denver, Colorado; repository for technical documents): <https://www.nps.gov/dsc/technicalinfocenter.htm>

Climate Change Resources

- NPS Climate Change Response Program Resources: <http://www.nps.gov/subjects/climatechange/resources.htm>
- US Global Change Research Program: <http://www.globalchange.gov/home>
- Intergovernmental Panel on Climate Change: <http://www.ipcc.ch/>

Geological Surveys and Societies

- Arizona Geological Survey: <https://azgs.arizona.edu/>
- US Geological Survey: <http://www.usgs.gov/>
- Geological Society of America: <http://www.geosociety.org/>
- American Geophysical Union: <http://sites.agu.org/>
- American Geosciences Institute: <http://www.americangeosciences.org/>
- Association of American State Geologists: <http://www.stategeologists.org/>

US Geological Survey Reference Tools

- National geologic map database (NGMDB): http://ngmdb.usgs.gov/ngmdb/ngmdb_home.html
- Geologic names lexicon (GEOLEX; geologic unit nomenclature and summary): <http://ngmdb.usgs.gov/Geolex/search>
- Geographic names information system (GNIS; official listing of place names and geographic features): <http://gnis.usgs.gov/>
- GeoPDFs (download PDFs of any topographic map in the United States): <http://store.usgs.gov> (click on “Map Locator”)
- Publications warehouse (many publications available online): <http://pubs.er.usgs.gov>
- Tapestry of time and terrain (descriptions of physiographic provinces): <http://pubs.usgs.gov/imap/i2720/>

Appendix A: Scoping Participants

The following people attended the GRI scoping meeting, held on 26 June 2001, or the follow-up report writing conference call, held on 12 November 2015. Discussions during these meetings supplied a foundation for this GRI report. The scoping summary document is available on the GRI publications website: <http://go.nps.gov/gripubs>.

2001 Scoping Meeting Participants

Name	Affiliation	Position
George Billingsley	USGS	Geologist, retired
Debra Block	USGS	Not recorded
Tim Connors	NPS, Geologic Resources Division	Geologist, GRI map coordinator
Tracey Felger	NPS, Grand Canyon National Park	GIS specialist
John Graham	Colorado State University	Geologist, GRI report author
Scott Graham	USGS	Not recorded
Sherrie Landon	Navajo National Monument	Not recorded
Allyson Mathis	NPS, Grand Canyon National Park	Ranger, Interpretation
John Rihs	NPS, Grand Canyon National Park	Hydrologist
Della Snyder	NPS, Grand Canyon National Park	Not recorded
Jessica Wellmeyer	USGS	Geologist

2015 Conference Call Participants

Name	Affiliation	Position
George Billingsley	USGS	Geologist, retired
Tim Connors	NPS, Geologic Resources Division	Geologist
John Graham	Colorado State University	Geologist, GRI report author
Jason Kenworthy	NPS Geologic Resources Division	Geologist, GRI reports coordinator
Dale Pate	NPS Geologic Resources Division	Cave and Karst Program Coordinator
Hal Pranger	NPS Geologic Resources Division	Chief, Geologic Features and Systems Branch
Vincent Santucci	NPS, Geologic Resources Division	Paleontologist, Washington Liaison
Ed Schenk	NPS, Grand Canyon National Park	Physical Science Program Manager
Justin Tweet	NPS, Geologic Resources Division	Paleontologist
Jack Wood	NPS, Geologic Resources Division	Guest Scientist, Photogrammetry
Ben Tobin	NPS, Grand Canyon National Park	Hydrologist

Appendix B: Geologic Resource Laws, Regulations, and Policies

The NPS Geologic Resources Division developed this table to summarize laws, regulations, and policies that specifically apply to NPS minerals and geologic resources. The table does not include laws of general application (e.g., Endangered Species Act, Clean Water Act, Wilderness Act, National Environmental Policy Act, or National Historic Preservation Act). The table does include the NPS Organic Act when it serves as the main authority for protection of a particular resource or when other, more specific laws are not available. Information is current as of December 2019. Contact the NPS Geologic Resources Division for detailed guidance.

Resource	Resource-specific Laws	Resource-specific Regulations	2006 Management Policies
<p>Caves and Karst Systems</p>	<p>Federal Cave Resources Protection Act of 1988, 16 USC §§ 4301 – 4309 requires Interior/Agriculture to identify “significant caves” on Federal lands, regulate/restrict use of those caves as appropriate, and include significant caves in land management planning efforts. Imposes civil and criminal penalties for harming a cave or cave resources. Authorizes Secretaries to withhold information about specific location of a significant cave from a Freedom of Information Act (FOIA) requester.</p> <p>National Parks Omnibus Management Act of 1998, 54 USC § 100701 protects the confidentiality of the nature and specific location of cave and karst resources.</p> <p>Lechuguilla Cave Protection Act of 1993, Public Law 103-169 created a cave protection zone (CPZ) around Lechuguilla Cave in Carlsbad Caverns National Park. Within the CPZ, access and the removal of cave resources may be limited or prohibited; existing leases may be cancelled with appropriate compensation; and lands are withdrawn from mineral entry.</p>	<p>36 CFR § 2.1 prohibits possessing/destroying/disturbing...cave resources...in park units.</p> <p>43 CFR Part 37 states that all NPS caves are “significant” and sets forth procedures for determining/releasing confidential information about specific cave locations to a FOIA requester.</p>	<p>Section 4.8.1.2 requires NPS to maintain karst integrity, minimize impacts.</p> <p>Section 4.8.2 requires NPS to protect geologic features from adverse effects of human activity.</p> <p>Section 4.8.2.2 requires NPS to protect caves, allow new development in or on caves if it will not impact cave environment, and to remove existing developments if they impair caves.</p> <p>Section 6.3.11.2 explains how to manage caves in/adjacent to wilderness.</p>

Resource	Resource-specific Laws	Resource-specific Regulations	2006 Management Policies
<p>Paleontology</p>	<p>National Parks Omnibus Management Act of 1998, 54 USC § 100701 protects the confidentiality of the nature and specific location of paleontological resources and objects.</p> <p>Paleontological Resources Preservation Act of 2009, 16 USC § 470aaa et seq. provides for the management and protection of paleontological resources on federal lands.</p> <p>Archaeological Resources Protection Act of 1979, 16 USC §§ 470aa – mm Section 3 (1) Archaeological Resource—nonfossilized and fossilized paleontological specimens, or any portion or piece thereof, shall not be considered archaeological resources, under the regulations of this paragraph, unless found in an archaeological context. Therefore, fossils in an archaeological context are covered under this law.</p> <p>Federal Cave Resources Protection Act of 1988, 16 USC §§ 4301 – 4309 Section 3 (5) Cave Resource—the term “cave resource” includes any material or substance occurring naturally in caves on Federal lands, such as animal life, plant life, paleontological deposits, sediments, minerals, speleogens, and speleothems. Therefore, every reference to cave resource in the law applies to paleontological resources.</p>	<p>36 CFR § 2.1(a)(1)(iii) prohibits destroying, injuring, defacing, removing, digging or disturbing paleontological specimens or parts thereof.</p> <p>Prohibition in 36 CFR § 13.35 applies even in Alaska parks, where the surface collection of other geologic resources is permitted.</p> <p>43 CFR Part 49 (in development) will contain the DOI regulations implementing the Paleontological Resources Preservation Act.</p>	<p>Section 4.8.2 requires NPS to protect geologic features from adverse effects of human activity.</p> <p>Section 4.8.2.1 emphasizes Inventory and Monitoring, encourages scientific research, directs parks to maintain confidentiality of paleontological information, and allows parks to buy fossils only in accordance with certain criteria.</p>
<p>Recreational Collection of Rocks Minerals</p>	<p>NPS Organic Act, 54 USC. § 100101 et seq. directs the NPS to conserve all resources in parks (which includes rock and mineral resources) unless otherwise authorized by law.</p> <p>Exception: 16 USC. § 445c (c) Pipestone National Monument enabling statute. Authorizes American Indian collection of catlinite (red pipestone).</p>	<p>36 C.F.R. § 2.1 prohibits possessing, destroying, disturbing mineral resources...in park units.</p> <p>Exception: 36 C.F.R. § 7.91 allows limited gold panning in Whiskeytown.</p> <p>Exception: 36 C.F.R. § 13.35 allows some surface collection of rocks and minerals in some Alaska parks (not Klondike Gold Rush, Sitka, Denali, Glacier Bay, and Katmai) by non-disturbing methods (e.g., no pickaxes), which can be stopped by superintendent if collection causes significant adverse effects on park resources and visitor enjoyment.</p>	<p>Section 4.8.2 requires NPS to protect geologic features from adverse effects of human activity.</p>

Resource	Resource-specific Laws	Resource-specific Regulations	2006 Management Policies
<p>Geothermal</p>	<p>Geothermal Steam Act of 1970, 30 USC. § 1001 et seq. as amended in 1988, states</p> <ul style="list-style-type: none"> • No geothermal leasing is allowed in parks. • “Significant” thermal features exist in 16 park units (the features listed by the NPS at 52 Fed. Reg. 28793-28800 (August 3, 1987), plus the thermal features in Crater Lake, Big Bend, and Lake Mead). • NPS is required to monitor those features. • Based on scientific evidence, Secretary of Interior must protect significant NPS thermal features from leasing effects. <p>Geothermal Steam Act Amendments of 1988, Public Law 100--443 prohibits geothermal leasing in the Island Park known geothermal resource area near Yellowstone and outside 16 designated NPS units if subsequent geothermal development would significantly adversely affect identified thermal features.</p>	<p>None applicable.</p>	<p>Section 4.8.2.3 requires NPS to</p> <ul style="list-style-type: none"> • Preserve/maintain integrity of all thermal resources in parks. • Work closely with outside agencies. • Monitor significant thermal features.
<p>Mining Claims (Locatable Minerals)</p>	<p>Mining in the Parks Act of 1976, 54 USC § 100731 et seq. authorizes NPS to regulate all activities resulting from exercise of mineral rights, on patented and unpatented mining claims in all areas of the System, in order to preserve and manage those areas.</p> <p>General Mining Law of 1872, 30 USC § 21 et seq. allows US citizens to locate mining claims on Federal lands. Imposes administrative and economic validity requirements for “unpatented” claims (the right to extract Federally-owned locatable minerals). Imposes additional requirements for the processing of “patenting” claims (claimant owns surface and subsurface). Use of patented mining claims may be limited in Wild and Scenic Rivers and OLYM, GLBA, CORO, ORPI, and DEVA.</p> <p>Surface Uses Resources Act of 1955, 30 USC § 612 restricts surface use of unpatented mining claims to mineral activities.</p>	<p>36 CFR § 5.14 prohibits prospecting, mining, and the location of mining claims under the general mining laws in park areas except as authorized by law.</p> <p>36 CFR Part 6 regulates solid waste disposal sites in park units.</p> <p>36 CFR Part 9, Subpart A requires the owners/operators of mining claims to demonstrate bona fide title to mining claim; submit a plan of operations to NPS describing where, when, and how; prepare/submit a reclamation plan; and submit a bond to cover reclamation and potential liability.</p> <p>43 CFR Part 36 governs access to mining claims located in, or adjacent to, National Park System units in Alaska.</p>	<p>Section 6.4.9 requires NPS to seek to remove or extinguish valid mining claims in wilderness through authorized processes, including purchasing valid rights. Where rights are left outstanding, NPS policy is to manage mineral-related activities in NPS wilderness in accordance with the regulations at 36 CFR Parts 6 and 9A.</p> <p>Section 8.7.1 prohibits location of new mining claims in parks; requires validity examination prior to operations on unpatented claims; and confines operations to claim boundaries.</p>

Resource	Resource-specific Laws	Resource-specific Regulations	2006 Management Policies
<p>Nonfederal Oil and Gas</p>	<p>NPS Organic Act, 54 USC § 100751 et seq. authorizes the NPS to promulgate regulations to protect park resources and values (from, for example, the exercise of mining and mineral rights).</p> <p>Individual Park Enabling Statutes:</p> <ul style="list-style-type: none"> ● 16 USC § 230a (Jean Lafitte NHP & Pres.) ● 16 USC § 450kk (Fort Union NM), ● 16 USC § 459d-3 (Padre Island NS), ● 16 USC § 459h-3 (Gulf Islands NS), ● 16 USC § 460ee (Big South Fork NRR), ● 16 USC § 460cc-2(i) (Gateway NRA), ● 16 USC § 460m (Ozark NSR), ● 16 USC § 698c (Big Thicket N Pres.), ● 16 USC § 698f (Big Cypress N Pres.) 	<p>36 CFR Part 6 regulates solid waste disposal sites in park units.</p> <p>36 CFR Part 9, Subpart B requires the owners/operators of nonfederally owned oil and gas rights outside of Alaska to</p> <ul style="list-style-type: none"> ● demonstrate bona fide title to mineral rights; ● submit an Operations Permit Application to NPS describing where, when, how they intend to conduct operations; ● prepare/submit a reclamation plan; and ● submit a bond to cover reclamation and potential liability. <p>43 CFR Part 36 governs access to nonfederal oil and gas rights located in, or adjacent to, National Park System units in Alaska.</p>	<p>Section 8.7.3 requires operators to comply with 9B regulations.</p>

Resource	Resource-specific Laws	Resource-specific Regulations	2006 Management Policies
<p>Federal Mineral Leasing (Oil, Gas, and Solid Minerals)</p>	<p>The Mineral Leasing Act, 30 USC § 181 et seq., and the Mineral Leasing Act for Acquired Lands, 30 USC § 351 et seq. do not authorize the BLM to lease federally owned minerals in NPS units.</p> <p>Combined Hydrocarbon Leasing Act, 30 USC §181, allowed owners of oil and gas leases or placer oil claims in Special Tar Sand Areas (STSA) to convert those leases or claims to combined hydrocarbon leases, and allowed for competitive tar sands leasing. This act did not modify the general prohibition on leasing in park units but did allow for lease conversion in GLCA, which is the only park unit that contains a STSA.</p> <p>Exceptions: Glen Canyon NRA (16 USC § 460dd et seq.), Lake Mead NRA (16 USC § 460n et seq.), and Whiskeytown-Shasta-Trinity NRA (16 USC § 460q et seq.) authorizes the BLM to issue federal mineral leases in these units provided that the BLM obtains NPS consent. Such consent must be predicated on an NPS finding of no significant adverse effect on park resources and/or administration.</p> <p>American Indian Lands Within NPS Boundaries Under the Indian Allottee Leasing Act of 1909, 25 USC §396, and the Indian Leasing Act of 1938, 25 USC §396a, §398 and §399, and Indian Mineral Development Act of 1982, 25 USCS §§2101-2108, all minerals on American Indian trust lands within NPS units are subject to leasing.</p> <p>Federal Coal Leasing Amendments Act of 1975, 30 USC § 201 prohibits coal leasing in National Park System units.</p>	<p>36 CFR § 5.14 states prospecting, mining, and...leasing under the mineral leasing laws [is] prohibited in park areas except as authorized by law.</p> <p>BLM regulations at 43 CFR Parts 3100, 3400, and 3500 govern Federal mineral leasing.</p> <p>43 CFR Part 3160 governs onshore oil and gas operations, which are overseen by the BLM.</p> <p>Regulations re: Native American Lands within NPS Units:</p> <ul style="list-style-type: none"> • 25 CFR Part 211 governs leasing of tribal lands for mineral development. • 25 CFR Part 212 governs leasing of allotted lands for mineral development. • 25 CFR Part 216 governs surface exploration, mining, and reclamation of lands during mineral development. • 25 CFR Part 224 governs tribal energy resource agreements. • 25 CFR Part 225 governs mineral agreements for the development of Indian-owned minerals entered into pursuant to the Indian Mineral Development Act of 1982, Pub. L. No. 97-382, 96 Stat. 1938 (codified at 25 USC §§ 2101-2108). • 30 CFR §§ 1202.100-1202.101 governs royalties on oil produced from Indian leases. • 30 CFR §§ 1202.550-1202.558 governs royalties on gas production from Indian leases. • 30 CFR §§ 1206.50-1206.62 and §§ 1206.170-1206.176 governs product valuation for mineral resources produced from Indian oil and gas leases. • 30 CFR § 1206.450 governs the valuation coal from Indian Tribal and Allotted leases. • 43 CFR Part 3160 governs onshore oil and gas operations, which are overseen by the BLM. 	<p>Section 8.7.2 states that all NPS units are closed to new federal mineral leasing except Glen Canyon, Lake Mead and Whiskeytown-Shasta-Trinity NRAs.</p>

Resource	Resource-specific Laws	Resource-specific Regulations	2006 Management Policies
<p>Nonfederal minerals other than oil and gas</p>	<p>NPS Organic Act, 54 USC §§ 100101 and 100751</p>	<p>NPS regulations at 36 CFR Parts 1, 5, and 6 require the owners/operators of other types of mineral rights to obtain a special use permit from the NPS as a § 5.3 business operation, and § 5.7 – Construction of buildings or other facilities, and to comply with the solid waste regulations at Part 6.</p>	<p>Section 8.7.3 states that operators exercising rights in a park unit must comply with 36 CFR Parts 1 and 5.</p>
<p>Coal</p>	<p>Surface Mining Control and Reclamation Act of 1977, 30 USC § 1201 et. seq. prohibits surface coal mining operations on any lands within the boundaries of a NPS unit, subject to valid existing rights.</p>	<p>SMCRA Regulations at 30 CFR Chapter VII govern surface mining operations on Federal lands and Indian lands by requiring permits, bonding, insurance, reclamation, and employee protection. Part 7 of the regulations states that National Park System lands are unsuitable for surface mining.</p>	<p>None applicable.</p>
<p>Uranium</p>	<p>Atomic Energy Act of 1954 Allows Secretary of Energy to issue leases or permits for uranium on BLM lands; may issue leases or permits in NPS areas only if president declares a national emergency.</p>	<p>None applicable.</p>	<p>None applicable.</p>
<p>Common Variety Mineral Materials (Sand, Gravel, Pumice, etc.)</p>	<p>Materials Act of 1947, 30 USC § 601 does not authorize the NPS to dispose of mineral materials outside of park units.</p> <p>Reclamation Act of 1939, 43 USC §387, authorizes removal of common variety mineral materials from federal lands in federal reclamation projects. This act is cited in the enabling statutes for Glen Canyon and Whiskeytown National Recreation Areas, which provide that the Secretary of the Interior may permit the removal of federally owned nonleasable minerals such as sand, gravel, and building materials from the NRAs under appropriate regulations. Because regulations have not yet been promulgated, the National Park Service may not permit removal of these materials from these National Recreation Areas.</p> <p>16 USC §90c-1(b) authorizes sand, rock and gravel to be available for sale to the residents of Stehekin from the non-wilderness portion of Lake Chelan National Recreation Area, for local use as long as the sale and disposal does not have significant adverse effects on the administration of the national recreation area.</p>	<p>None applicable.</p>	<p>Section 9.1.3.3 clarifies that only the NPS or its agent can extract park-owned common variety minerals (e.g., sand and gravel), and:</p> <ul style="list-style-type: none"> • only for park administrative uses; • after compliance with NEPA and other federal, state, and local laws, and a finding of non-impairment; • after finding the use is park’s most reasonable alternative based on environment and economics; • parks should use existing pits and create new pits only in accordance with park-wide borrow management plan; • spoil areas must comply with Part 6 standards; and • NPS must evaluate use of external quarries. <p>Any deviation from this policy requires a written waiver from the Secretary, Assistant Secretary, or Director.</p>

Resource	Resource-specific Laws	Resource-specific Regulations	2006 Management Policies
<p style="text-align: center;">Coastal Features and Processes</p>	<p>NPS Organic Act, 54 USC § 100751 et. seq. authorizes the NPS to promulgate regulations to protect park resources and values (from, for example, the exercise of mining and mineral rights).</p> <p>Coastal Zone Management Act, 16 USC § 1451 et. seq. requires Federal agencies to prepare a consistency determination for every Federal agency activity in or outside of the coastal zone that affects land or water use of the coastal zone.</p> <p>Clean Water Act, 33 USC § 1342/ Rivers and Harbors Act, 33 USC 403 require that dredge and fill actions comply with a Corps of Engineers Section 404 permit.</p> <p>Executive Order 13089 (coral reefs) (1998) calls for reduction of impacts to coral reefs.</p> <p>Executive Order 13158 (marine protected areas) (2000) requires every federal agency, to the extent permitted by law and the maximum extent practicable, to avoid harming marine protected areas.</p> <p><i>See also "Climate Change"</i></p>	<p>36 CFR § 1.2(a)(3) applies NPS regulations to activities occurring within waters subject to the jurisdiction of the US located within the boundaries of a unit, including navigable water and areas within their ordinary reach, below the mean high water mark (or OHW line) without regard to ownership of submerged lands, tidelands, or lowlands.</p> <p>36 CFR § 5.7 requires NPS authorization prior to constructing a building or other structure (including boat docks) upon, across, over, through, or under any park area.</p> <p><i>See also "Climate Change"</i></p>	<p>Section 4.1.5 directs the NPS to re-establish natural functions and processes in human-disturbed components of natural systems in parks unless directed otherwise by Congress.</p> <p>Section 4.4.2.4 directs the NPS to allow natural recovery of landscapes disturbed by natural phenomena, unless manipulation of the landscape is necessary to protect park development or human safety.</p> <p>Section 4.8.1 requires NPS to allow natural geologic processes to proceed unimpeded. NPS can intervene in these processes only when required by Congress, when necessary for saving human lives, or when there is no other feasible way to protect other natural resources/ park facilities/ historic properties.</p> <p>Section 4.8.1.1 requires NPS to:</p> <ul style="list-style-type: none"> • Allow natural processes to continue without interference, • Investigate alternatives for mitigating the effects of human alterations of natural processes and restoring natural conditions, • Study impacts of cultural resource protection proposals on natural resources, • Use the most effective and natural-looking erosion control methods available, and avoid new developments in areas subject to natural shoreline processes unless certain factors are present. <p><i>See also "Climate Change"</i></p>

Resource	Resource-specific Laws	Resource-specific Regulations	2006 Management Policies
Climate Change	<p>Secretarial Order 3289 (Addressing the Impacts of Climate Change on America's Water, Land, and Other Natural and Cultural Resources) (2009) requires DOI bureaus and offices to incorporate climate change impacts into long-range planning; and establishes DOI regional climate change response centers and Landscape Conservation Cooperatives to better integrate science and management to address climate change and other landscape scale issues.</p> <p>Executive Order 13693 (Planning for Federal Sustainability in the Next Decade) (2015) established to maintain Federal leadership in sustainability and greenhouse gas emission reductions.</p>	<p><i>No applicable regulations, although the following NPS guidance should be considered:</i></p> <p>Coastal Adaptation Strategies Handbook (Beavers et al. 2016) provides strategies and decision-making frameworks to support adaptation of natural and cultural resources to climate change.</p> <p>Climate Change Facility Adaptation Planning and Implementation Framework: The NPS Sustainable Operations and Climate Change Branch is developing a plan to incorporate vulnerability to climate change (Beavers et al. 2016b).</p> <p>NPS Climate Change Response Strategy (2010) describes goals and objectives to guide NPS actions under four integrated components: science, adaptation, mitigation, and communication.</p> <p>Policy Memo 12-02 (Applying National Park Service Management Policies in the Context of Climate Change) (2012) applies considerations of climate change to the impairment prohibition and to maintaining "natural conditions".</p> <p>Policy Memo 14-02 (Climate Change and Stewardship of Cultural Resources) (2014) provides guidance and direction regarding the stewardship of cultural resources in relation to climate change.</p> <p>Policy Memo 15-01 (Climate Change and Natural Hazards for Facilities) (2015) provides guidance on the design of facilities to incorporate impacts of climate change adaptation and natural hazards when making decisions in national parks.</p> <p><i>Continued in 2006 Management Policies column</i></p>	<p>Section 4.1 requires NPS to investigate the possibility to restore natural ecosystem functioning that has been disrupted by past or ongoing human activities. This would include climate change, as put forth by Beavers et al. (2016).</p> <p><i>NPS guidance, continued:</i></p> <p>DOI Manual Part 523, Chapter 1 establishes policy and provides guidance for addressing climate change impacts upon the Department's mission, programs, operations, and personnel.</p> <p>Revisiting Leopold: Resource Stewardship in the National Parks (2012) will guide US National Park natural and cultural resource management into a second century of continuous change, including climate change.</p> <p>Climate Change Action Plan (2012) articulates a set of high-priority no-regrets actions the NPS will undertake over the next few years</p> <p>Green Parks Plan (2013) is a long-term strategic plan for sustainable management of NPS operations.</p>

Resource	Resource-specific Laws	Resource-specific Regulations	2006 Management Policies
<p style="text-align: center;">Upland and Fluvial Processes</p>	<p>Rivers and Harbors Appropriation Act of 1899, 33 USC § 403 prohibits the construction of any obstruction on the waters of the United States not authorized by congress or approved by the USACE.</p> <p>Clean Water Act 33 USC § 1342 requires a permit from the USACE prior to any discharge of dredged or fill material into navigable waters (waters of the US [including streams]).</p> <p>Executive Order 11988 requires federal agencies to avoid adverse impacts to floodplains. (see also D.O. 77-2)</p> <p>Executive Order 11990 requires plans for potentially affected wetlands (including riparian wetlands). (see also D.O. 77-1)</p>	<p>None applicable.</p> <p><i>2006 Management Policies, continued:</i></p> <p>Section 4.6.6 directs the NPS to manage watersheds as complete hydrologic systems and minimize human-caused disturbance to the natural upland processes that deliver water, sediment, and woody debris to streams.</p> <p>Section 4.8.1 directs the NPS to allow natural geologic processes to proceed unimpeded. Geologic processes...include...erosion and sedimentation...processes.</p> <p>Section 4.8.2 directs the NPS to protect geologic features from the unacceptable impacts of human activity while allowing natural processes to continue.</p>	<p>Section 4.1 requires NPS to manage natural resources to preserve fundamental physical and biological processes, as well as individual species, features, and plant and animal communities; maintain all components and processes of naturally evolving park ecosystems.</p> <p>Section 4.1.5 directs the NPS to re-establish natural functions and processes in human-disturbed components of natural systems in parks, unless directed otherwise by Congress.</p> <p>Section 4.4.2.4 directs the NPS to allow natural recovery of landscapes disturbed by natural phenomena, unless manipulation of the landscape is necessary to protect park development or human safety.</p> <p>Section 4.6.4 directs the NPS to (1) manage for the preservation of floodplain values; [and] (2) minimize potentially hazardous conditions associated with flooding.</p> <p><i>continued in Regulations column</i></p>

Resource	Resource-specific Laws	Resource-specific Regulations	2006 Management Policies
Soils	<p>Soil and Water Resources Conservation Act, 16 USC §§ 2011–2009 provides for the collection and analysis of soil and related resource data and the appraisal of the status, condition, and trends for these resources.</p> <p>Farmland Protection Policy Act, 7 USC § 4201 et. seq. requires NPS to identify and take into account the adverse effects of Federal programs on the preservation of farmland; consider alternative actions, and assure that such Federal programs are compatible with State, unit of local government, and private programs and policies to protect farmland. NPS actions are subject to the FPPA if they may irreversibly convert farmland (directly or indirectly) to nonagricultural use and are completed by a Federal agency or with assistance from a Federal agency. Applicable projects require coordination with the Department of Agriculture’s Natural Resources Conservation Service (NRCS).</p>	<p>7 CFR Parts 610 and 611 are the US Department of Agriculture regulations for the Natural Resources Conservation Service. Part 610 governs the NRCS technical assistance program, soil erosion predictions, and the conservation of private grazing land. Part 611 governs soil surveys and cartographic operations. The NRCS works with the NPS through cooperative arrangements.</p>	<p>Section 4.8.2.4 requires NPS to</p> <ul style="list-style-type: none"> • prevent unnatural erosion, removal, and contamination; • conduct soil surveys; • minimize unavoidable excavation; and • develop/follow written prescriptions (instructions).

The Department of the Interior protects and manages the nation's natural resources and cultural heritage; provides scientific and other information about those resources; and honors its special responsibilities to American Indians, Alaska Natives, and affiliated Island Communities.

NPS 113/173858, November 2020

National Park Service
U.S. Department of the Interior



Natural Resources Stewardship and Science
1201 Oak Ridge Drive, Suite 150
Fort Collins, Colorado 80525

<https://www.nps.gov/nature/index.htm>

EXPERIENCE YOUR AMERICA™